DIAGENETIC HISTORY OF THE WAULSORTIAN CARBONATE BUILDUPS,

(DINANTIAN), CRAVEN BASIN, NW ENGLAND

DOUGLAS GILLIES

Doctor of Philosophy

University of Edinburgh
1987

EX BIBL. UNIV. EDINBURGH

DECLARATION.

The work in this thesis is my own. Where the work of others has been used, this is specifically stated in the text.

Douglas Gillies.

ABSTRACT

The Waulsortian carbonate buildups, Craven Basin, NW England (lower Dinantian age), contain significant volumes of void-filling cements, making them ideal for a detailed diagenetic study .

A range of integrated petrographic and geochemical techniques are used and a cement stratigraphy comprising Stages A-N is identified, which can confidently be correlated throughout the basin. The cement stratigraphy framework allows the relative timing of other diagenetic events such as fracturing, stylolitisation, mineralisation, hydrocarbon migration, dolomitisation and calcitisation. Trends in diagenetic environments and porosity evolution are identified, leading to a proposed burial/diagenetic history for the buildups from Chadian times to the present day. A three-fold heirarchical subdivision for cements is proposed comprising; Stage, Substage, Zone.

Diagenesis occurred in three general environments: sea floor to shallow burial marine; deep burial; and moderate burial to near-surface meteoric.

In the marine environment, two periods of dissolution produced large volumes of secondary porosity prior to the first recogniseable cements (Stage A) in the buildups. These dissolution episodes, and Stage A, are exclusive to the bank facies. Stage A comprises isopachous inclusion-rich centripetal layers with strong palimpsest fibrous textures reflecting a fibrous calcite pre-cursor. The term "Crypto-fibrous calcite (CFC) is proposed for these cements, which are interpreted as products of neomorphism. Immediately following CFC are non-ferroan scalenohedral calcites (Stages B,C and D) with a characteristic 'black-bright-dull' CL sequence, They reflect progressive burial through oxic to suboxic and sulphate reduction zones in the shallow subsurface, and are diachronous. Neptunian dykes formed throughout early diagenesis, contributing significantly to redistribution of unconsolidated sediment within the buildups. Early pyrite/marcasite mineralisation occurred during shallow burial. Deep burial cements are fracture-fed, comprising calcite Stages E-I, dolomite Stages J-L, kaolinite, Stage M and calcite Stage N. Other local vein-filling cements could not be integrated with the cement stratigraphy.

The latest vein-fed cements were shallower burial meteoric. The final episode in the diagenetic history, meteoric calcitisation of dolomite, is occurring at the present day surface.

A burial curve, constructed from the $\delta^{18}O$ trend of Stages A-N, is related to lithostratigraphy tectonic episodes indicates: 1) progressive burial through Dinantian-Westphalian times; 2) Stephanian uplift and the development of the Ribblesdale fold Belt; 3) post-Permo-Trias burial and mineralisation; 4) uplift through the Tertiary to the present-day surface.

Pore-occlusion in the buildups was almost complete before the migration of hydrocarbons, hence the buildups have no reservoir potential.

TABLE OF CONTENTS

		Page
Abstract		
Table of contents		
CHAPTER 1	INTRODUCTION	1
1.1	Objectives	1
1.2	Regional setting	2
1.3	Litho-stratigraphy	4
1.4	Structure and basin development	8
1.5	Waulsortian buildups	11
1.6	Waulsortian diagenesis	15
1.7	Exposure and scope of sampling	20
CHAPTER 2	MATERIALS AND METHODS	22
2.1	Materials	22
2.2	Methods	24
CHAPTER 3	TERMINOLOGY AND DEFINITIONS	32
3.1	Diagenesis	32
3.2	Diagenetic history	32
3.3	Cement stratigraphy	34
3.4	Basis of proposed nomenclature	37
3.5	Geochemical heterogeneity in cements	40
	DIAGENESIS PART ONE SEA FLOOR TO SHALLOW BURIAL	45
CHAPTER 4	BUILDUP SEDIMENTS AND ORIGINAL POROSITY	46
4.1	Sediments	46
4.2	Original porosity	50
4.3	Additional remarks	58

Page

CHAPTER 5 EARLY CEMENTATION AND DISSOLUTION 59

5.1 Early lithification of M1 sediment 59
5.2 Early dissolution episodes 62
5.3 Facies control on early diagenesis 64

CHAPTER 6 STAGE A: INCLUSION-RICH ISOPACHOUS CALCITE 70

6.1 Crystal morphology of Stage A cements 70
6.2 Composition of Stage A cements 72
6.3 Inclusion patterns 78
6.4 Crystal growth mechanisms 82
6.5 Distribution of Stage A cements 90
6.6 Discussion 90

CHAPTER 7 STAGES B-D: NON-FERROAN SCALENOHEDRAL CALCITE 106

7.1 Stage B Non-luminescent scalenohedral calcite 107
7.2 Stage C Brightly luminescent scalenohedral calcite 114
7.3 Stage D Moderate to dull luminescent scalenohedral calcite 115
7.4 Textural development of Stage B-D cements 116
7.5 Distribution of non-ferroan scalenohedral calcites 122
7.6 Pyrite 123
7.7 Origin of Stage B-D cements 124
7.8 Interpretation 124
7.9 Origin of micro-zonation in Stage B 133
7.10 Discussion 137
7.11 Diagenetic environments and origin of pore fluids 139
7.12 Relative timing of CFC and Stage B-D cements 143

CHAPTER 8 FISSURES AND NEPTUNIAN DYKES 147

8.1 Fissures 148
8.2 Neptunian dykes 149
8.3 Discussion 153
8.4 Subsequent diagenesis 161
8.5 Previous work 161
8.6 Concluding remarks 163

Page

DIAGENESIS PART TWO
DEEP BURIAL DIAGENESIS 166

CHAPTER 9 CEMENT STAGES E-I: FRACTURE-FED BLOCKY CALCITE 171
9.1 Stage E: Ferroan calcite 173
9.2 Stage F: Ferroan calcite 174
9.3 Stage G: Non-ferroan calcite 179
9.4 Stage H: Ferroan calcite 184
9.5 Stage I: Ferroan calcite 186
9.6 Crystal aggregates 189

CHAPTER 10 STYLOLITISATION 197
10.1 Stylolites in Craven samples 198
10.2 Timing of stylolitisation 205
10.3 Organic matter associated with stylolites 206

CHAPTER 11 STAGE J-L DOLOMITE 209
11.1 Introduction 209
11.2 Dolomite types in the Waulsortian buildups of the Craven basin 212
11.3 Dolomite cements 212
11.4 Replacive dolomite (dolomitisation) 213
11.5 Dolomite composition 232
11.6 Timing and distribution of dolomite types 242
11.7 Discussion 249
11.8 A model for dolomitisation of the Waulsortian buildups 257

CHAPTER 12 POST DOLOMOITE DIAGENETIC STRATIGRAPHY 262
12.3 Hydrocarbon migration 264
12.2 Stage M: Kaolinite 264
12.3 Stage N: Late calcite cement 265
12.4 Other post-dolomite cements 273

Page

CHAPTER 13 MINERALISATION 279
13.1 Early diagenetic mineralisation 284
13.2 Late diagenetic hydrothermal mineralisation 296
13.3 Other authigenic minerals 302

DIAGENESIS PART THREE
METEORIC DIAGENESIS 302

CHAPTER 14 LATE FRACTURE - FILLING CEMENTS 303

CHAPTER 15 CALCITISATION OF DOLOMITE 307
15.1 Petrography 307
15.2 Geochemistry 309
15.3 Discussion 317

DIAGENESIS PART FOUR

CHAPTER 16 FRACTURES AND VEINS 319
16.1 Early diagenetic fractures 320
16.2 Late diagenetic (tectonic) fractures 321
16.3 Field relationships of veins 328
16.4 Association of fractures with stylolites 328
16.5 Significance of fractures in the Waulsortian 329

CHAPTER 17 NEOMORPHISM 331
17.1 Recrystallisation in the Waulsortian buildups 333
17.2 Timing and order of recrystallisation 348
17.3 Implications of neomorphism for cement stratig--raphy 351

SYNTHESIS & CONCLUSIONS

CHAPTER 18 SYNTHESIS 356
18.1 Burial history and diagenetic environments 356
18.2 Porosity evolution 364

Page

CHAPTER 19 CONCLUSIONS AND FUTURE WORK 376

19.1 Cementation and diagenetic history 377

19.2 Burial history and porosity evolution 387

19.3 Limitations of cement stratigraphies 391

19.4 Problems in environmental interpretations from cements 395

ACKNOWLEDGMENTS 397

REFERENCES 399

APPENDICES 419

CHAPTER 1
INTRODUCTION

The Craven Basin in Northwest England contains a thick Dinantian sequence including a series of Waulsortian carbonate buildups (or mud mounds) of Chadian age.

Waulsortian buildups also occur in the Dinantian of Belgium, France, Ireland, Derbyshire and the U.S.A. Apart from intrinsic interest in their origins and depositional settings, in recent years they have attracted much attention because of their hosting of economic deposits, notably base metals in Ireland. The spectacular Waulsortian mounds in the Sacramento Mountains of New Mexico and their enveloping rocks also formed the material for a pioneering study of diagenesis by Meyers (1978), where the concept of cement stratigraphy was developed, and geochemical changes in regionally extensive formation waters were documented with the aid of cathodoluminescence.

Within the Craven Basin there are a large number of buildups, which contain significant volumes of void-filling cements, making them ideal for establishing a cement stratigraphy and for detailed diagenetic histories. No previous work has been done on diagenetic histories in the area, and opportunity was taken in the present study to contribute a diagenetic input to on-going reassessment of the structural and sedimentological history of the basin by other workers.

1.1 OBJECTIVES

This study involved the use of a variety of petrographic and geochemical techniques in an integrated approach, so as to achieve four main objectives:

1. To identify a stratigraphy within the void-filling cement sequence, and to investigate the extent to which this cement stratigraphy could be mapped (either in part or in total)

throughout the numerous Waulsortian buildups which outcrop across the Craven Basin.

2. To relate the crystal texture, trace element and stable isotope characteristics of individual units within the cement stratigraphy to the nature of the fluids from which they precipitated, and thus ascertain the diagenetic environments in which the cements formed.

3. To use the cement stratigraphy as a framework into which the relative timing of other processes (such as mineralisation, hydrocarbon migration, neomorphism, stylolitisation and fracturing) could be integrated, and if possible, to extend this overall diagenetic history to other parts of the Dinantian sequence in the Craven Basin.

4. To identify a burial trend for the Dinantian sequence from changes in stable isotope and trace-element compositions through the cement stratigraphy, and to relate this to the changes in sedimentation and tectonics which affected basin development. Further, to identify from this trend the history of pore occlusion in the buildups.

1.2 REGIONAL SETTING

The Waulsortian buildups mainly outcrop along two linear NE-SW trends of the Ribblesdale Fold Belt within the central part of the Craven (Bowland) Basin in Northwest England (Fig. 1.1). The main town in the area is Clitheroe, which is situated some 22 miles (35 km) SW of Lancaster and 17 miles (25km) NE of Preston in the county of Lancashire. The outcrops of the Waulsortian are largely confined to the two main river valleys in the area; the River Hodder in the north, and River Ribble in the south. Many of the buildups form prominent topographic features accentuated by glaciation, and are reasonably well exposed. Several buildups have been extensively quarried for their very pure limestone, giving access to their bases and cores.

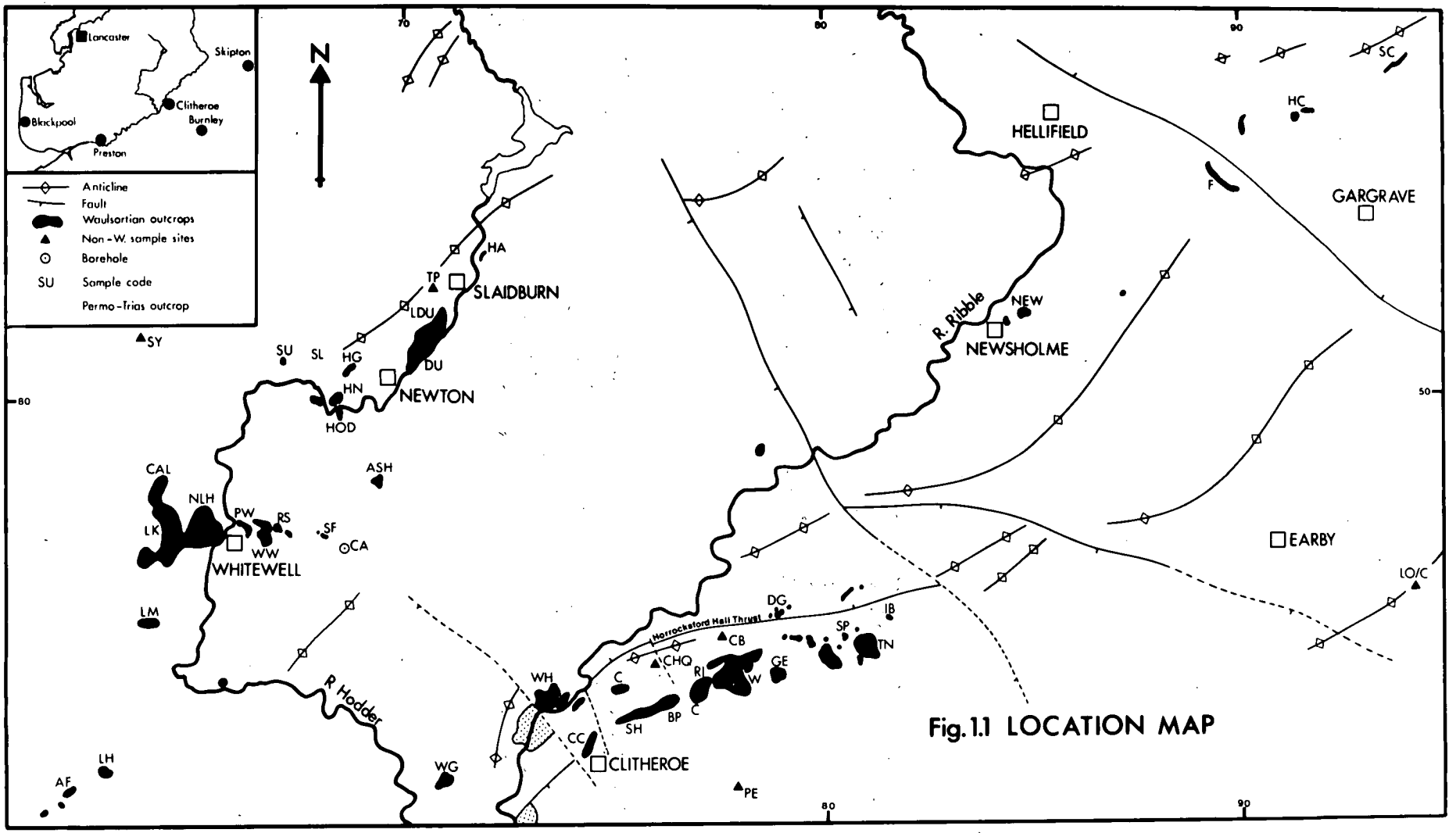

Fig. 1.1 LOCATION MAP

SAMPLE LOCALITY CODES FROM FIG.1.1

WAULSORTIAN BUILDUPS

CODE	LOCALITY	GR:	CODE	LOCALITY	GR:
AF	Arbour Farm	620,408	LK	Long Knots	643,468
ASH	Ashnott	793,480	LM	Leagram Quarries	638,448
BP	Bellmanpark Quarry	760,427	NEW	Dobbers Quarry, Newsholme	847,519
C	Coplow Quarry	752,432	NLH	New Laund Hill	651,468
CA	Cow Ark borehole (BGS)	683,465	PW	Porters Wood	660,471
CAL	Old Calamine Mines	642,477	RI	The Ridge	774,432
CC	Clitheroe Castle	743,418	RS	Raven Scar Plantation	669,469
CH	Crow Hill road cut	767,431	SC	Scarnber	938,578
DG	Downham Green	788,449	SF	Crimpton pit, Spire Farm	679,468
Du-LDU	Dunnow-Little Dunnow	702,514	SH	Salthill Quarry	755,426
F	Fogger	895,553	SP	Springs	804,443
GE	Gerna	788,435	SU	Sugarloaf Quarry	688,508
HA	Hammerton Hall	718,532	TN	Twiston Mill Quarry	808,443
HC	Haw Crag	914,565	W	Worsaw Hill	776,436
HG	Heaning	687,506	WG	Withgill Quarry	709,410
HN-HOD	Knoll Wood	684,502	WH	Waddow Hall	735,429
IB	Ings Beck	815,448	WW	Hall Hill Qy., Whitewell	667,467
LH	Leach House Quarry	628,412			

PERI-WAULSORTIAN and OTHER FACIES

CODE	LOCALITY	GR:
CB	Clitheroe By-pass (A59) Chadian stratotype. Partly interbank	775,445
CHQ	Chatburn Quarries, Clitheroe. Chatburn Lst. Fm.	760,440
LO/C	Raygill Quarry, Lothersdale. Mineralised Embsay Lst., Worston Shales Fm. (Harrison 1982, p24)	942,453
PE	Stream section, Pendle Hill. Holkerian-Namurian	775,408
TP	Townfield Plantation, Slaidburn. Interbank facies	706,526
SL	Interbank Facies near Sugarloaf buildup	675,510
SY	Sykes Quarries. Turbiditic shelf slope carbonates of Gawthorpe (1986)	628,519

1.3 LITHO-STRATIGRAPHY

1.3.1 General succession of the Craven Basin

No pre-Carboniferous rocks are known within the Craven Basin (Fig.1.2). The oldest rocks are lower Dinantian (Tournaisian) in age and although the base of the Dinantian sequence is not seen, over 2km of carbonates and terrigenous mudstones with rare sandstones, have been proven from outcrop and borehole material (Earp et al. 1961; Charsley 1984).

Namurian marine and fluvio-deltaic beds dominate the post-Dinantian sequence in the Craven Basin, reaching a maximum thickness of 1.8km (Earp et al. 1961). Only the lower Namurian rocks (Pendleian) of the upper Bowland Shales and Pendle Grit outcrop in the study area. The Namurian beds were succeeded by Lower Coal Measures, the original thickness of which is unknown because of uplift in Upper Carboniferous (Stephanian) times, which was followed by deep erosion. This erosion reached the level of mid-Dinantian sediments in some parts of the basin, prior to the deposition of Permo-Triassic sandstones and marls (Earp et al. 1961). Only three thin outliers of Permo-Trias remain in the region following Tertiary - Quaternary erosion, but a more extensive former development is indicated by widespread reddening of the Carboniferous rocks across the Craven Basin (Earp et al. 1961 p.208).

1.3.2 Stratigraphy of the Study Area

The rocks in the area of the present study range from Chadian (mid-Dinantian) to Pendleian (lower Namurian) in age.

Several stratigraphic schemes have been suggested for all or part of the Dinantian sequence in the Craven Basin (Parkinson 1926; Earp et al. 1961; Miller & Grayson 1972; Fewtrell & Smith 1980), and revisions are currently being prepared by the British Geological Survey among others. The scheme used in this study is based on Miller and Grayson (1972) and Fewtrell and Smith (1980) (Fig. 1.2).

FIG. 1.2 GENERALISED STRATIGRAPHY OF THE CLITHEROE AREA, CRAVEN BASIN

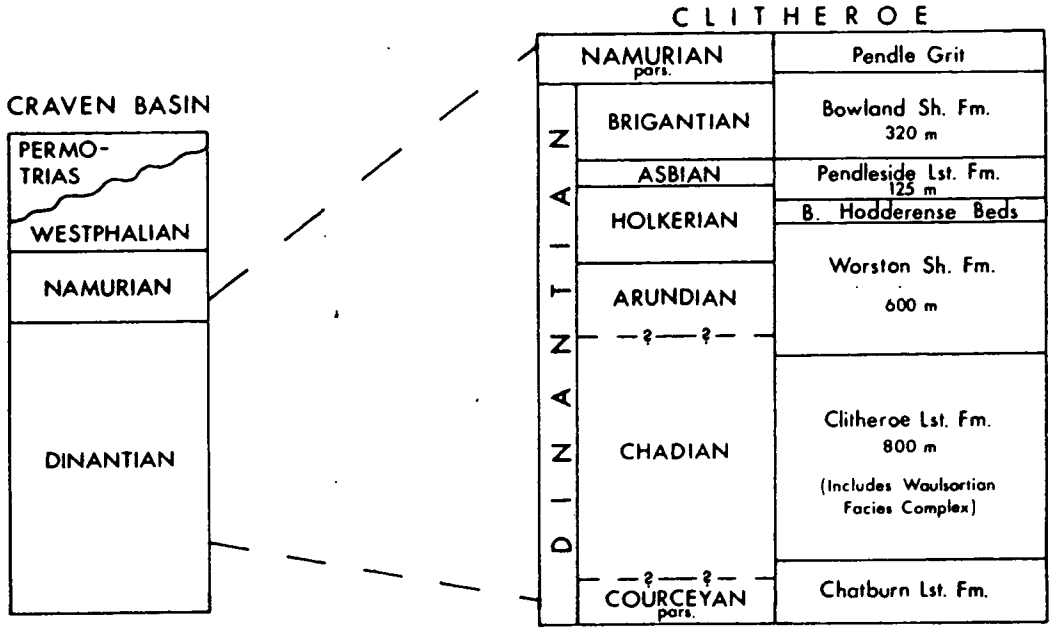

FIG 1.3 SCHEMATIC CROSS SECTION THROUGH THE CLITHEROE LIMESTONE FORMATION

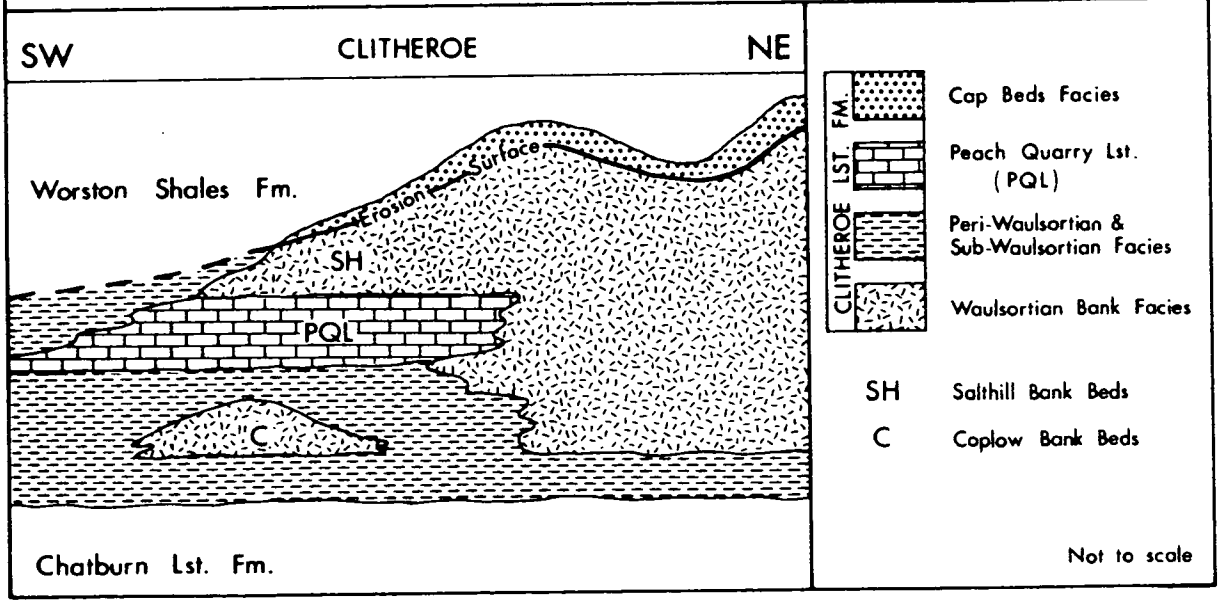

The exposed Dinantian sequence can be divided into five litho-stratigraphic formations (in stratigraphical order); the Chatburn Limestone, Clitheroe Limestone, Worston Shale, Pendleside, and Bowland Shale Formations (after Fewtrell & Smith, 1980).

The oldest rocks comprise the Chatburn Limestone Formation (mainly Chadian age) and are predominantly dark grey, well-bedded, sometimes pyritous, limestones interbedded with subsidiary beds of dark grey shales. They are strongly redolent of bitumen. The base of the Chatburn Limestone Formation is not seen although at least 690m of sediments have been proved (Fewtrell & Smith 1980).

The overlying Clitheroe Limestone Formation (also Chadian) varies in thickness between 300m and 1500m, and contains the Waulsortian buildups and a range of other facies which are often laterally impersistent. Lack of precise biostratigraphical control within this part of the sequence means that the stratigraphy has been based on litho-types and the complexity of the facies mosaic makes correlation within the formation difficult.

The Clitheroe Limestone Formation is only well exposed in the vicinity of Clitheroe itself, where several abandoned quarries and road cuts allowed Miller and Grayson (1972) to recognise a litho-stratigraphic sequence in which the Waulsortian buildups occur at two stratigraphic horizons characterised by the (lower) Coplow Bank beds and the (upper) Salthill Bank beds, but several km northeast of Clitheroe these two horizons of bank facies merge into a single buildup development. There are suggestions from macro-faunal evidence that the buildups in the Hodder valley may also have developed at two horizons equivalent to the Coplow and Salthill Bank beds. The evidence, however, is tenuous and there is no reliable way to correlate buildups at all precisely within the Craven Basin. The section at Clitheroe is best known, and appears to be typical for the area, so it is described in some detail below.

The base of the Clitheroe Limestone Formation begins with a sequence of dark shales which pass up into dark bituminous, often highly bioclastic limestones with shaley partings. These bioclastic lime wackestones and packstones outcrop beneath the Waulsortian buildup in Coplow quarry. They form part of what are referred to in this study as sub-Waulsortian facies (Fig. 1.3) and are partial equivalents of the Lower Coplow Shales of Miller and Grayson (1972).

The Waulsortian buildups themselves consist of very pure limestone with a dominant micrite (strictly, microspar) component. They contain a range of microfacies and have characteristic sparry fabrics. The Waulsortian buildups occur within an envelope of peri-Waulsortian facies (sensu Miller 1986) which are mainly crinoidal wackestones and packstones interbedded with thin shales. These peri-Waulsortian facies may be called sub-bank (sub-Waulsortian) or interbank, depending on their relationship to the enclosed buildups.

In the area of the Clitheroe Anticline (Fig. 1.3), the two stratigraphic levels of Waulsortian buildups are separated by the algal-rich packstones, wackestones and rare grainstones of the Peach Quarry Limestone (PQL) (Earp et al. 1961; Miller & Grayson 1972). The PQL is succeeded by the Salthill buildup (Salthill Bank beds of Miller & Grayson op cit.). Several erosion surfaces, associated with the development of boulder beds, occur at the top of the Salthill buildup, and are interpreted as the product of localised, often severe submarine erosion (Miller & Grayson 1982).

Draping the erosion surfaces and boulder beds are the Salthill Cap Beds, which are well-bedded and consist predominantly of poorly-sorted, unabraded crinoidal grainstones. They are interpreted as a current-swept lag deposit (Miller & Grayson 1972). The thickness of these beds varies over short distances from zero up to a maximum of 45m (Miller & Grayson 1972). The Salthill Cap Beds facies marks the top of the Clitheroe Limestone Formation, which is placed, with some uncertainty, just below the Chadian/Arundian boundary.

The Clitheroe Limestone Formation is overlain by the predominantly shaley lithologies of the Worston Shale Formation (upper Chadian to Holkerian), marking an abrupt change from the previously carbonate-dominated succession

A band of characteristically blotched calcareous mudstones and shales occurs above the Worston Shales in the study area. Named the Bollandoceras hodderense Beds after the goniatite which often occurs within them, they have not been consistently assigned to one or other of the adjacent formations (see Fewtrell & Smith 1980 p44), but they are a distinctive basin-wide marker horizon.

Above the B. hodderense Beds are the dominantly turbiditic lime-grainstones and packstones of the Pendleside Limestone Formation (Holkerian to Asbian), and these represent debris from the break-up of the Holkerian - Asbian apron reef to the north. The top of the Dinantian sequence consists of the black pyritic shales of the Bowland Shale Formation, which span the Dinantian - Namurian boundary in the area. The lowest Namurian (Pendleian) marine-turbidites and fluvio-deltaic sandstones of the Pendle Grit (Earp et al. 1961) form the top of the stratigraphic sequence in the study area, apart from a thin Permo-Triassic outlier near Clitheroe.

The maximum thickness of post-Waulsortian Dinantian sediments in the Craven area is 1045m (from Fewtrell & Smith 1980), while the Namurian sediments are up to 460m in thickness (Earp et al. 1961).

1.4 STRUCTURE AND BASIN DEVELOPMENT

1.4.1 Structure

The Craven Basin is one of several rift basins within a Dinantian rift province, developed during the Hercynian orogeny, which extended across much of central and northern Britain (Anderton et al. 1979; Arthurton 1983).

Structurally, the Craven Basin consists of a series of NE-SW trending anticlines and broad synclines, NW-SE trending faults and fault zones, and NE-SW-trending thrust faults, which form part of the Ribblesdale Fold Belt.

In the study area, the main structures are the Slaidburn and Clitheroe anticlines which underlie the valleys of the rivers Hodder and Ribble respectively (Fig. 1.1). The two linear trends of Waulsortian buildups approximately parallel the axial trends of these anticlines, but this is complicated somewhat by the two major fault zones, the Clitheroe Fault and Knotts Fault, which transect the area in a NW-SE to NNW-SSE direction (Earp et al. 1961; Harrison 1982) and displace the anticlinal axes in what appears to have been a phase of dextral transcurrent movement (Gawthorpe 1987). A series of minor normal faults parallel these two major fault zones.

The other major structural feature in the study area is the NE-SW trending Horrocksford Hall Thrust. The Clitheroe Anticline is situated in the hanging wall of this thrust. The Slaidburn anticline to the northwest, also occurs in the hanging wall of a NE-SW-trending thrust.

1.4.2 Basin development

The 'block and basin' hypothesis was traditionally used to explain thickness variations in the Dinantian rocks of Britain. The basins were supposedly areas of rapid subsidence which developed thick Dinantian sequences, while the more stable blocks were areas of slower subsidence where the Dinantian sequence was condensed.

The 'block and basin' hypothesis has been found to be an inadequate model for much of the Dinantian of Northern Britain, in particular the Craven Basin, and so an alternative hypothesis, the 'Tilt Block hypothesis', was invoked to explain the thickness and facies variations encountered (Miller & Grayson 1982; Grayson & Oldham 1987).

Tilt blocks are essentially half-graben structures which present a gradually deepening depositional 'floor' (sensu Grayson & Oldham op. cit.) developed as a result of differential subsidence of a basement block.

In the Craven Basin, the rates of subsidence in the Dinantian were controlled by movements along a complex series of strike slip faults which defined the tilt block margins. As parts of the tilt blocks subsided at greater rates than others, progressively deepening ramps developed (cf. Ahr 1973). In the early Dinantian of the study area, sedimentation and subsidence were able to keep pace, resulting in a thick sequence of relatively shallow water carbonates, the Chatburn Limestone Formation. Later in the Chadian, the rate of subsidence had greatly increased, resulting in the development of a deeper water situation ("Deep" of Grayson & Oldham op cit.) which persisted throughout the remainder of the Dinantian and into the Namurian.

The Waulsortian buildups developed along broad linear trends which coincided with a favourable range of water depths (see Lees & Miller 1985) on the distal portion of carbonate ramps (Lees 1982; Miller & Grayson 1982).

Gawthorpe (1986) suggested that the Craven Basin as a whole evolved as a carbonate ramp in Courceyan (Ivorian) to Chadian times. Tectonism during Chadian times then developed small-scale sea floor topography which effected a structural control on the development of the Waulsortian buildups, i.e. producing their linear trends. Two further periods of extension in late Chadian to Arundian and late Asbian to early Brigantian times are indicated by the development of boulder beds, submarine erosion, debris-flow horizons and sedimentary slides in the NW of the basin. During the former tectonic episode, the basin evolved from a carbonate ramp to a carbonate slope situation with major intra-basin topography marked by changes in facies and thickness and the development of the submarine erosion of the Waulsortian complex at Clitheroe. The latter tectonic episode broke-up the northern reefal rim of the basin, producing the turbiditic carbonate facies of the Pendleside Limestone Fm., and introducing terrigenous clastic sedimentation, concluding major carbonate production in the basin.

Movement on the basement faults was probably continuous throughout and after the Carboniferous. Several late phases of reactivation along these fault zones are indicated (Gawthorpe 1987).

A period of uplift occurred in the late Carboniferous (Westphalian to Stephanian times). This was probably related to transpression on the major fault zones. Transpression of this kind was probably also responsible for the development of the Horrocksford Hall Thrust (cf. Arthurton 1983).

Severe erosion pre-dated the deposition of Permo-Triassic sandstones and marls.

Earp et al. (1961 p215) indicate a period of further fault movements in post-Permo-Triassic times related to mineralisation of the Clitheroe faults. This may have resulted from reactivation of Hercynian structures (Ineson et al. 1972, p.140).

Earp et al.(op. cit.) also suggested that the area underwent a period of tension in Tertiary times.

1.5 WAULSORTIAN BUILDUPS

Waulsortian buildups were first described as fenestellid-rich lime-mud and spar mounds from the upper Tournaisian and lower Visean of southern Belgium by Dupont (1863). They were also reported from Eire (Lees 1964), the southwestern USA (Pray 1958; Meyers 1974) and Montana (Cotter 1966; Stone 1972), and the Craven Basin (Lees & Miller 1985). The Craven buildups (or "knoll-reefs") were described in a series of papers by Parkinson (1926,1950,1957,1967), Black (1958), Earp et al. (1961) and Miller and Grayson (1972). But because of differences between them and the type Waulsortian facies in Belgium, none of these authors specifically refered to the Craven buildups as 'Waulsortian'. Recently, however, Lees and Miller (1985) have demonstrated that the Belgian Waulsortian facies encompasses a range of lithotypes, and that the Craven buildups are comparable to part of that range, thus justifying their appelation as 'Waulsortian'. All buildups of Waulsortian type are Dinantian in age, and though superficially similar buildups have been identified elsewhere in the Palaeozoic, the term Waulsortian is best reserved for the Dinantian examples. The Waulsortian buildups characteristically occur within an envelope of associated facies, forming a facies mosaic often referred to as a "Waulsortian complex".

1.5.1 Facies (Fig. 1.4)

A range of facies have been defined from Waulsortian complexes (sensu Miller & Grayson 1982) by Lees (1964), Miller and Grayson (1972) and Miller (1986).

a). Bank Facies (also referred to as Waulsortian facies).

This facies comprises the buildup rocks themselves and consists of very pure lime-mud with varying contents of bryozoan, mollusc, brachiopod, ostracod and crinoid debris. Abundant cavities (now mainly spar-filled) may occur and these may have digitate roofs with smooth geopetal floors of internal sediments. Cavity shapes are usually complex, and there may be several generations of internal sediments. The sediments which comprise the bank facies are complex

Figure 1.4 Facies within the Waulsortian Complex

A Hall Hill buildup: View towards NW, showing white, poorly-bedded bank facies with bank beds dipping off the bank core (A), overlying thin-bedded argillaceous sub-Waulsortian facies (B). Hall Hill Quarry, near Whitewell.

B Interdigitation of dark argillaceous interbank facies and lighter crinoidal flank facies. Salthill Quarry, Clitheroe.

C Negative print of a thin section showing a sharp transition between sub-Waulsortian crinoidal wackestones and micritic, sparry bank facies. Stylolites (s) are common in the sub-bank material (appears as anastomosing white line in negative print). Shape of the complex sparry areas in the bank facies (black areas) are largely controlled by fronds of fenestellid bryozoans (F) which appear as lines of white elliptical zooecia in the negative. Coplow Quarry, Clitheroe.

D Discrete lenticular masses of micrite (arrowed) in toe facies which amalgamate into larger masses approaching the bank towards the right of the picture. Hall Hill Quarry, near Whitewell.

E Small cross-laminated dune bedforms in the sub-Waulsortian facies at Hall Hill quarry (arrowed). Notice concentration of coarse crinoidal grains overlying one of the bedforms, showing that current activity in this case may have been quite strong. Coin for scale is 1p; diameter = 2cm.

F Biosparite facies of the Cap Beds. Unabraded crinoid fragments are abundant in these well-bedded and jointed limestones. Coin for scale is 5p; diameter = 2.3cm. Bellmanpark Quarry.

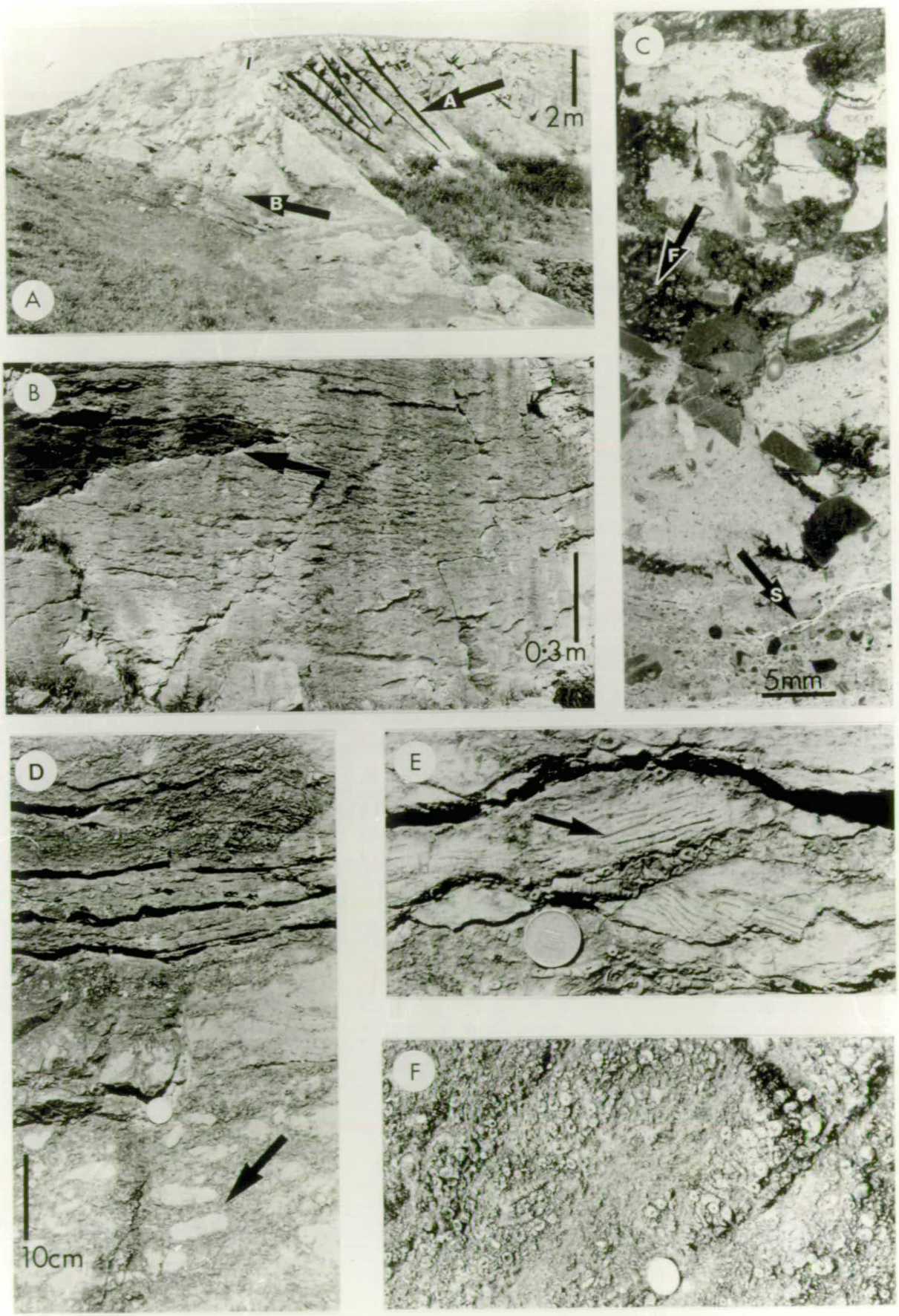
A
2m
B
C
F
S
5mm
B
0·3m
D
10cm
E
F

and multi-generational (polymuds of Lees 1964). In the Craven Basin, they typically contain a high proportion of small skeletal grains (or moulds thereof) and peloids, along with the fine micrite component.

The bank facies are often well-bedded. Individual bank beds (sensu Lees 1964) show rapid increase in thickness towards the bank core. Geopetal internal sediments and other fabrics occurring at often high angles to bedding indicate that the apparent steepening of the bank beds at buildup margins (Fig. 1.4A) represents a true depositional slope up to, or over 30°on a growing sediment pile (Lees 1964).

b). Flank facies.

These are fine-grained limestones with a significant crinoidal content which lie immediately adjacent to buildup margins. They are well-bedded.

Lateral and vertical transitions between flank facies and bank or interbank facies are often rapid, usually occuring within a few metres (Fig. 1.4C). Where bank beds pass into flank facies, the transitional zone is the bank "toe" (Miller 1986), and this region often contains discrete nodular masses of lime-mud which is similar in character to that of the bank facies and presents a pseudo-brecciated appearance(Fig. 1.4D).

c). Interbank facies.

Distal to the buildups, the flank facies pass laterally into interbank facies. Typically, these sediments are thin-bedded, lenticular, dark grey argillaceous limestones alternating with thin calcareous shales. The limestones are bituminous and pyritic, and commonly contain chert flats and nodules. There is a high proportion of disarticulated crinoidal material and comminuted shell fragments. Variation in the bedding style of the interbank may occur as a result of changing percentages of carbonate and shale. Rarely, there are small cross-laminated dune bedforms which consist of purer carbonate than the surrounding sediments (Fig. 1.4E).

The interbank and flank facies can be collectively referred to as off-bank facies.

Miller (1986) described the details of transitions from the bank facies to the interbank. This transition is generally marked by an increase in micrite and sparry fabrics over crinoids and other allochems, and a decrease in evidence for compaction. A similar, and often very abrupt change also occurs at the base of a buildup (Miller 1986) (Fig. 1.4 A&B).

d). Biosparite facies.

These crinoidal packstones are generally restricted to the post-Waulsortian Cap Beds in the Clitheroe area. They are pale grey, well-bedded and jointed limestones consisting primarily of unabraded crinoid fragments which often contain geopetal mud-fills (Fig. 1.4F).

1.5.2 Waulsortian Phases.

Detailed petrographic analyses of Waulsortian buildups from Britain, Europe and the USA have revealed four depth-related Phases: A,B,C and D, which represent a range of marine sedimentary environments, with Phase A being the deepest (probably over 300m), and Phase D forming in the photic zone at depths of about 120m or shallower (Lees et al. 1985; Lees & Miller 1985).

The Waulsortian buildups of the Craven Basin represent only the shallower Phases C and D, with many of the buildups showing characteristics of both phases. Phase D, with cryptalgal coating and micritisation of grains, cavity walls and early cements is particularly well-developed in the Craven Basin (Lees & Miller 1985 p.160). The inference, therefore, is that subsidence of the Craven Deep did not attain water depths much beyond about 120m or so (the likely photic limit), in contrast with some of the Irish and Belgian settings of the Waulsortian.

1.6 WAULSORTIAN DIAGENESIS

Previous studies related to the diagenesis of Waulsortian buildups have focussed upon four topics:

1. Early cementation and consolidation of the sediment
2. Origin of the sparry fabrics
3. Origin of isopachous "fibrous" cements
4. Overall diagenetic history and cement stratigraphy

1.6.1 Early cementation and consolidation.

Waulsortian buildups sometimes developed relief of tens of metres above the penecontemporaneous sea floor, with depositional slopes of 30° or more. Yet they are conspicuously lacking in skeletal frame-builders. Until 1977, explanations of the consolidation of the buildups emphasised the biological nature of accumulation. Crinoids and fenestrate bryozoans were postulated as baffling agents for lime-mud (eg. Wilson 1975), but a simple baffling mechanism is untenable (Lees & Miller 1985; Miller 1986). Other unfossilised organisms have been implicated: plant filaments or sponges (Lees 1964); algae, perhaps stromatolitic (H. Dupont 1969); an unknown benthic invertebrate (Pray 1969); a rigid cryptalgal framework, perhaps blue-green algae (Pratt 1982).

In 1977, Neumann *et al*. reported the discovery of " lithoherms", rocky carbonate mounds at depths of about 700m in the Straits of Florida. These structures apparently consisted of onion-like layers of hardgrounds with softer, uncemented layers between, and prompted re-consideration of the role played by submarine cementation in the origin of the Waulsortian buildups which had originally been proposed by Lees in 1964. Bathurst (1980, 1982) applied the idea of surface-hardened crusts to various Palaeozoic buildups and used them in his explanation of the "stromatactis" spar-filled voids (see below).

Cowan and Meyers (1982) and Miller (1986) were unable to find direct evidence of an early intergranular marine cement in Waulsortian facies, either from isotope or textural data. These authors, however, were in agreement that early lithification had played a key part in slope stabilisation. Using detailed studies of flank-bank facies transitions, Miller (*op. cit.*) adduced evidence for an *in situ* biological origin of primary lime-muds (perhaps by cyanobacteria), and the rapid attainment of a firm gel consistency of these muds, presumably by a syndepositional phase of cementation. Thus the biological nature of the accumulations and their penecontemporaneous cementation were considered together as accounting for buildup accretion.

1.6.2 Origin of sparry fabrics

Early work on the diagenesis of Waulsortian buildups centred upon the common sparry areas with digitate roofs and flat floors referred to as "stromatactis" by Dupont (1881), who suggested that they were cryptic stromatoporoids, formed after dissolution of the skeletal material.

Bathurst (1959) concluded that the sparry calcites had formed by infilling of primary voids, although Ross *et al.* (1975) regarded the spar as a product of recrystallisation of the host carbonate mud, a claim which Bathurst (1977) challenged. In a seminal paper, Lees (1964) agreed that the sparry masses were indeed void-fills, but indicated that "stromatactis" had developed as a result of collapse of the primary sediment perhaps following decay of organic baffles and the development of mechanical bridges by larger grains which roofed the cavities. The shape of the cavities was often complex and angular as a result of the occurrence of fenestellid bryozoan fronds in the sediment which formed the roof support for many cavities after sediment collapse (see Fig. 1.4C). The complex distribution of the multi-component sediments (polymuds of Lees & Miller 1985) was also seen as a control on the shape of some stromatactis cavities, as well as the attitude of the bed which, if steep enough, caused down-stepping of the sparry fabric. Lees (*op. cit.*) also identified other sheet-form cavities, or "sheet spars" which occurred in unsupported mud and also had geopetal floors but did not share a common origin with "stromatactis." Sheet spars (*sensu* Lees 1964) often showed a marked resemblance between upper and lower surfaces which could be re-fitted and, therefore, suggested cavity formation by shear-failure and a pull-apart mechanism. Therefore, features exhibiting similar form, but of entirely different origin fell within the scope of "stromatactis".

Lees also identified other sparry fabrics which were simple void-fills in shells and bryozoan meshworks. Bathurst (1980,1982) sought a common origin for "stromatactis" fabrics in a variety of Phanerozoic lime-mud buildups by postulating the partial removal of unconsolidated sediment between successive surface-hardened crusts, with marine cements centripetally filling the resulting void.

Bathurst was unable to suggest a plausible mechanism whereby the loose sediment was selectively removed, and his hypothesis fails to explain the wide variety in the size and shape of spar-filled voids in the Waulsortian, or their tendency to occur in repeated patterns ranging from simple sheet-spars to complex irregular types in each Waulsortian bank bed (J. Miller pers. com.).

Recently, Miller (1986) has shown that significant modification of Waulsortian cavity systems occurred prior to the precipitation of the earliest recognisable void-filling cements as a result of two early dissolution episodes, firstly of siliceous hyalosteliid sponge spicules, and secondly of carbonate sediment. This helps to explain how spars may account for up to 50% of the rock volume in some buildups, and also indicates that little of the spar-filled cavities represent the primary porosity network. Clearly, with these considerations, the "stromatactis" concept has little value and should be abandoned. However, the non-genetic term "stromatactoid" may be usefully retained to describe a void with a digitate roof and smooth undulating floor.

1.6.3 Origin of Isopachous "Fibrous" Cements

The first obvious void-filling cement to form in Waulsortian buildups generally consisted of thick isopachous rims of spar with a distinctly dusty, fibrous appearance. These inclusion-rich calcites may exhibit centripetal banding comparable with modern acicular cement layers.

Many examples exhibit the characteristic fabrics of radiaxial fibrous calcite first described by Bathurst (1959), and subsequently by numerous authors, particularly Kendall and Tucker (1973), Lohmann and Meyers (1975), and Kendall (1985). Some disagreement as to the origin of these spars has arisen. Originally, Bathurst (1959) invoked recrystallisation of a fibrous pre-cursor, and this mechanism was developed by Kendall and Tucker (1973). Lohmann and Meyers identified microdolomite inclusions in radiaxial spars with CL and suggested, therefore, that the precursor was high-Mg calcite which was recrystallised by meteoric fluids. More recently, Kendall (1985) has suggested that all of the characteristic radiaxial fibrous

calcite textures can be explained in terms of a primary precipitate, and Sandberg (1985) has suggested that they are primary low Mg-calcite precipitates.

In the Waulsortian buildups of the Craven Basin, these early diagenetic spars account for over 50% of the the total spar-volume, therefore, an understanding of their origin was a prime concern of this study.

1.6.4 Diagenetic History and Cement Stratigraphy

The first detailed diagenetic study of Waulsortian buildups was from the Mississippian Lodgepole Limestone Formation in Montana by Cotter (1966). His detailed textural and mineralogical investigation recognised several phases of cementation, dissolution, fracturing and replacement, which he linked to periods of emergence and submergence during the burial history of the rocks. Subsequently, Stone (1972) confirmed many of Cotter's observations and also related the relative timing of "diagenetic events", including porosity elimination, to the eogenetic, mesogenetic and telogenetic burial realms of Choquette and Pray (1970).

The pioneering work on carbonate cement stratigraphy employing cathodoluminescence (Meyers 1974), used material from Waulsortian buildups and associated facies of New Mexico to identify regionally extensive cement "zones" which could be mapped over several hundreds of square kilometres.

Subsequently, King (1984) applied the same principles to the spars of the Waulsortian buildups of the Irish Midlands, and identified seven luminescent cement zones in cavity and vein-filling sequences. He used the cement stratigraphy as a framework within which he placed the timing of fracturing episodes, stylolitisation, dolomitisation, silicification, and mineralisation. In an integrated approach, using staining, microprobe trace-element and isotopic analyses King (op. cit.) was able to construct a model for the burial history and pore-fluid evolution of the buildups in his study.

Cowan (1980) in a further study of the Sacremento Mountains buildups, using cathodoluminescence and stable isotope analysis, investigated the timing and mechanisms of initial cementation in

Waulsortian lime-mud and associated stromatactoid cavities to determine their role in sediment stabilisation. She identified early, non-luminescent marine cementation and later luminescent cementation thought to be associated with the influx of meteoric fluids.

Recently, Miller (1986) has identified variations in the development of cements between Waulsortian bank facies and the adjacent flank and interbank facies. He noticed that the isopachous fibrous calcite marine cements common to the bank facies were absent from toe, flank and interbank facies, indicating that the environs of the buildups encouraged early marine cementation, either by biogenic activity or favourable physico-chemical conditions, while the off-bank environments did not. Miller (op. cit.) also recognised early dissolution phases which pre-dated the marine cements in the banks and significantly modified the primary porosity (see above). The development of early diagenetic crumbly fractures in the bank facies was also recognised and used to indicate the consistency of the substrate as a firm gel. This study was important in showing that the early diagenesis of the Waulsortian buildups was not a simple case of progressive lithification of the lime-muds, but also involved other processes such as dissolution and fracturing.

While concentrating on the early stages of diagenesis, Miller also recognised a simplified 6-stage cement stratigraphy which included fracture-related calcite, dolomite and silica cements from later burial stages, of a buildup from Hill 707, Co. Galway, Ireland.

1.7 EXPOSURE AND SCOPE OF SAMPLING

Exposures of the Waulsortian facies in the Craven area are largely confined to abandoned quarries which occur in most buildups, and occasional road cuts and stream sections. The quality of the exposure is good, facilitating extensive sampling of cement-filled cavities and veins which are ideally suited to cement stratigraphy studies. Over 30 buildups were sampled (Fig. 1.1), and cores from a B.G.S. borehole at Cow Ark were also examined. These samples thus represent virtually all of the buildups exposed in the Craven Basin. Outwith the Waulsortian buildups, the peri-Waulsortian beds are less well exposed and only occur in occasional abandoned quarries or stream sections.

The thick basinal limestones of the Chatburn Limestone Formation which underlie the Waulsortian buildups are also poorly exposed, with the exception of the extensive working quarries at Clitheroe (run by the Ribblesdale Cement Co.) and the A59 road cut (Fig. 1.1) NE of Clitheroe, which contains the Chadian stratotype section. The Chatburn Limestones were sampled in order to detect which cement stages were developed subsequently to those in the overlying Waulsortian, i.e. from basin-wide formation waters during deep burial. For this reason, special attention was paid to veins and other fracture-fills.

Samples were also collected from a stream section through the Pendleside Limestone on Pendle Hill, 3 km SE of Clitheroe, to see if the Waulsortian cement stratigraphy could be related to younger (Holkerian-Asbian) rocks in the Dinantian sequence, in an attempt to constrain the timing of at least part of the cementation history.

Comparative material was collected from the Waulsortian in Eire, where the opportunity was taken to view the classic material described by Lees (1964), including lateral facies changes, fabric development and neptunian dykes.

Full details of sampling strategies and locations are given in Chapter 2.

CHAPTER 2:
MATERIALS AND METHODS

2.1 MATERIALS (Sampling strategies and localities)

Field sampling was carried out with 4 main objectives:

1. To sample areas of rocks which were likely to give most extensive development of cements in order to establish cement stratigraphy. There was, therefore, a deliberate biasing towards large spar-filled cavities and fractures.

2. To sample as many of the large number of Waulsortian buildups at outcrop in order to identify basin-wide patterns in the cement stratigraphy.

3. To sample lateral and vertical facies transitions from bank to peri-Waulsortian facies, and the wide range of microfacies within buildups themselves, to compare diagenetic styles and determine their distribution within the Waulsortian complex.

4. To sample from older and younger beds in the stratigraphic succession of the study area in an attempt to put better constraints on timing of individual diagenetic episodes.

Some 33 Waulsortian buildups and complexes were sampled at outcrop, including the vast majority of known bank facies exposures across the Craven Basin. Supplementary samples from a number of mounds were supplied by Dr J Miller; and a suite of thin sections from Haw Crag buildup were supplied by Prof. A. Lees (Fig. 1.1). A detailed breakdown of localities and facies sampled is given in Appendix 1. Detailed sampling of facies transitions was carried out at several localities (mainly larger abandoned quarries) where exposure was uninterrupted.

Lateral toe-bank facies transitions were sampled from individual bank beds at Sugarloaf, Hall Hill, Newsholme, Dunnow and New Laund Hill localities. Vertical facies transitions from sub-bank to bank facies were sampled at Hall Hill, Coplow, Dunnow and Newsholme buildups. Limited sampling of core material was also carried out from BGS Cow Ark Number 9 borehole at SD:6832,4647 which contained a vertical section through Waulsortian and enclosing facies.

Sediment-filled neptunian dykes are a common feature in many of the buildups. Although detailed field study of these structures was not undertaken, samples of dyke material, associated sediments and internal sediments in cavity-fills were collected from Crow Hill, Porters Wood, Leagram, Bellmanpark and New Laund Hill.

Peri-Waulsortian facies were collected in the vicinity of Sugarloaf, Heaning, Waddow Hall, Little Dunnow, Coplow and Ings Beck buildups and from the Crow Hill road cut.

A few samples of mineralised Waulsortian facies were collected from Withgill, Bellmanpark and Hammerton buildups as well as the Chatburn Lst. Fm. near Ings Beck. A single sample of galena came from the Cow Ark No 9 borehole. Supplementary samples of mineralised material from Waulsortian and other facies across the Craven Basin were supplied by Mr L. Oldham.

In an attempt to determine the extent of the cement stratigraphy outwith the Waulsortian buildups, samples of the older Chatburn Lst. Fm. were collected from the Ribblesdale Cement Co. quarry at Clitheroe, including samples of vein-fills from the vicinity of the Horrocksford Hall Thrust, and from the Chadian stratotype section in the A59 road cut near Clitheroe. The biosparite facies of the Salthill Cap Beds was sampled in Salthill and Bellmanpark quarries. Peach Quarry itself being no longer accessible, samples from this horizon between the Coplow and Salthill Bank beds were supplied by Dr J. Miller. Samples containing calcite-filled veins were collected from lower Arundian sandstones (Buck Banks Sandstone) some 120m west of Leagram buildup under the guidance of Dr N. Riley of the BGS. Spicular calcareous mudstones from the Worston Shales near Worsaw buildup was also collected at Worsaw End (SD:7782,4310). Other

samples of turbiditic shelf-slope carbonates associated with slump horizons of late Chadian/Arundian age were collected from Sykes quarries in the Trough of Bowland under the guidance of Mr R. Gawthorpe.

A stream section on Pendle Hill near Mearly Hall (SD:768,408), 3km SE of Clitheroe, through turbiditic carbonates of the Pendleside Lst Fm. and overlying shales, sandstones and limestones of the Bowland Shale Formation, and Namurian sandstones from the Pendle Grit, was also sampled at selected horizons. Finally, vein material was collected from the B. hodderense Beds near the River Hodder at Mitton-le-Main under the guidance of Messrs R.F. Grayson and L. Oldham.

2.2 METHODS

2.2.1 Cathodoluminescence (CL)

Cathodoluminescence petrography was carried out using a Nuclide Corporation ELM-2B Luminoscope. Ideal operating conditions used beam voltage of 10-16kV at a beam current of 0.5-1.0mA. Vacuum was maintained at 0.55-0.75 millitorr.

An Olympus monocular microscope and OM2-n camera with microscope adaptor was used for photomicrographs. An Olympus 50mm macro-lens with extension tubes was also used to photograph large areas of thin sections and rock plaquettes up to 5cm across under CL.

The Camebax microprobe instrument (see 2.2.5) has the facility for de-focussing the electron beam so that areas of samples can be viewed under CL. This was of great assistance in identifying areas of particular CL characteristics for microprobe analysis. Unfortunately this facility only became available towards the end of the tenure of this study and was, therefore, only used in confirmation of results obtained from the Microscan-5 instrument.

Preparations

Thin sections of two sizes (48 x 25mm and 48 x 75mm) were used for cathodoluminescence, staining and microprobe analysis. All

sections were double polished as described by Miller (1987). Thin rock plaquettes with maximum dimensions of 50 x 75 x 5 mm were surfaced and ground up to 1000-grade carborundum grit, and finally polished with Al_2O_3 powder for use in CL, and in preparation for isotope sampling.

Principles of Cathodoluminescence

The emission of light resulting from the bombardment of a phosphor by electrons or cathode rays, is termed cathodoluminescence (CL). Excitation induced in a phosphor raises electrons to a higher energy state which then "jump" to a lower state releasing photons. For a detailed explanation of the solid state physics of CL see Walker 1985.

Luminescence is caused by physical defect centres in the crystal lattice (intrinsic centres) or the presence of impurity ions (extrinsic centres). Two main types of extrinsic luminescence centre may be induced by the presence of impurity ions:-

1. Activator

Relatively low energy levels are necessary to raise electrons to an excited state and, therefore, light-emission is easily produced.

2. Quencher

Even with high energy levels, excitation is not sufficient to raise electrons to the necessary energy state, and energy is absorbed, thus quenching luminescence.

In carbonate minerals, the main luminescence activator is Mn^{2+} while Fe^{2+} is the most effective quencher, and luminescence of carbonates has been usually expressed in terms of these two ionic species. Suggested limits for calcite and dolomite CL in terms of Fe and Mn concentrations show significant variation (Pierson 1981; Frank et al. 1982; Amieux 1982; Fairchild 1983; Machel 1985). Many of the studies used electron microprobe analysis for determination of trace element concentrations, but the detection limits and precision of

such instruments is not sufficient for accurate determinations at low concentrations (Table 2.1). In a study of CL in experimentally grown calcites, ten Have and Heijnen (1985) have shown that changes in concentration of a few ppm may be sufficient to cause large scale variation in CL. In that study, atomic absorption spectrometry was used to determine trace element levels and this is considerably more accurate than microprobe analysis.

Recently, Machel (1985) has reviewed evidence that a range of transition metal and REE ions may act as sensitisors to activator centres in a carbonate crystal lattice. This, therefore, indicated to him that concentrations of Mn^{2+} and Fe^{2+} alone could be misleading when interpreting CL. However, Meyers and Grams (in press) concluded that transition metal and REE sensitsors have no significant effect on CL in natural carbonates, and therefore reaffirmed that luminescence in most carbonates can be explained by their Fe and Mn contents. No attempt was made in my study to determine the presence of trace quantities of possible sensitisors.

2.2.2 Staining

Staining with a mixture of acid-based solutions of alizarin red-S (ARS), and potassium ferricyanide (PF) was carried out in accordance with the method of Dickson (1965, 1966), with the exception that the stain solutions were kept in a water bath which was maintained at a temperature of 20-25°C. This achieved a better stain quality than at ambient room temperature and reduced the residence time of CO_2 bubbles on the surface of samples, as these inhibit staining and so give a blotchy appearance. Immersion times for different samples in the stain solutions varied by $\pm$30 secs. The aim was to enhance contrasts between the cements rather than to use the staining process quantitatively.

Duplicate thin sections were cut from each sample so that comparisons between staining and CL characteristics could be made. Stained thin-sections may not be used for CL because the electron beam fades the stain, and the uneven surface produced by the acid etch causes inconsistency in luminescence properties due to sample surface effects.

Acetate peels were prepared from over 50% of the samples, after grinding to 1000-grade carborundum to increase definition. All acetate peels were from stained samples. They were primarily useful in study of fabrics, porosity evolution and veining relationships on a larger scale than possible with thin sections.

2.2.3 Scanning Electron Microscopy (SEM)

SEM work was carried out using a Cambridge Mark 4 Stereoscan at operating voltages between 20-30kV. Samples consisted of broken rock chips. Some were left fresh while others were surfaced and etched in a saturated solution of EDTA after the method of Miller and Clarkson (1980). Gold sputter-coating was used.

2.2.4 X-RAY DIFFRACTION (XRD)

X-ray diffraction was employed in various aspects of the study including:

a) Non-carbonate mineral identification, especially with respect to samples of mineralised material and dolomite alteration products.
b) Check for purity in carbonate and sulphur isotope samples.
c) Determination of calcite/dolomite ratios in calcitised dolomites. In these cases, the instrument was calibrated empirically against calcite/dolomite mixtures of known proportions (see Chapter 11).

Powdered samples were run on a Philips system powder diffractometer using nickel-filtered copper K-alpha radiation at 40 kV and 20mA. Mineral identification traces were run at a scan rate of 1°2θ/min. Calcite-dolomite ratios were calculated from traces run at a scan rate of 0.25° 2θ/min.

2.2.5 Electron Microprobe

Major and trace-element quantitative wavelength dispersive analysis (WDS) was carried out on two microprobe instruments at Edinburgh University.

A Cambridge Instruments Microscan-5 was used for over 85% of microprobe analyses in this study, at operating conditions of 20kV beam voltage and 30mA beam current (WDS). Typical detection limits and precisions for elements analysed are given in Table 2.1. Electron dispersive system (EDS) was also employed in a qualitative mode for non-carbonate phase identification.

Carbon-coated double polished thin sections of 25 x 48 and 75 x 48mm size were used. Negative prints of thin sections were used as photo-maps, with detailed maps of areas of interest photographed in PPL and CL on the Luminoscope.

In the final year of this study, the newly acquired Cameca Camebax microprobe came on-line at Edinburgh. WDS and quantitative scans were run at 15kV beam voltage and 5mA beam current. This instrument has the facility to de-focus the beam in order to view samples under CL, which makes detailed photo-maps redundant for CL purposes, and allows precise positioning of analysis points in specific cement stages revealed only by their CL.

2.2.6 Back Scattered Electron Imagery (BEI)

This facility was available on the Camebax microprobe and was used primarily to detect and map variations in Fe and Mg in dolomites (Chapter 11).

2.2.7 Stable Isotope Analysis

Stable isotope analyses were carried out at the Scottish Universities Research and Reactor Centre (SURRC) at East Kilbride. Carbon and oxygen isotopes from carbonates, and a small suite of sulphur isotopes from iron sulphide minerals were investigated.

2.1.7.1 Carbon and Oxygen

Within the limits imposed by sampling difficulties it was intended to analyse individual cement stages and some sediment components within the Waulsortian buildups. Staining and CL were employed to identify suitable samples after their surfaces had been

Table 2.1 Precision and Detection Limits for Microprobe analyses

Averages of 5 calcite and 5 dolomite analyses from microprobe instruments used in this study.

Detection limit and 2σ precisions calculated using the formulae:

Detection limit $= 3/m \times (Rb/Tb)^{0.5}$

Precision $\sigma = 100/T_p^{0.5} \times 1/(R_p^{0.5})-(Rb^{0.5})\%$

Where
- m = counts sec^{-1}% $oxide^{-1}$
- Rb = background counts sec^{-1}
- Tb = time on background (secs)
- Rp = peak counts sec^{-1}
- Tp = time on peak (secs)

Instrument: MICROSCAN-5 Count time: 10 secs (4 peak 2 background)

Calcite

Oxide	wt%	± 2σ	Detection limit (% oxide)
CaO	53.25	± 0.25	0.03
MgO	0.37	± 0.03	0.02
MnO	0.12	± 0.06	0.01
FeO	0.07	± 0.03	0.01
SiO_2	0.09	± 0.04	0.03

Dolomite

CaO	28.63	± 0.19	0.03
MgO	17.01	± 0.14	0.02
MnO	0.27	± 0.03	0.02
FeO	6.25	± 0.10	0.03
SiO_2	0.02	± 0.04	0.03

Instrument: CAMEBAX Count time: 10 secs (2 peak 2 background)

Calcite

Oxide	wt%	± 2σ	Detection limit (% oxide)
CaO	55.85	± 0.57	0.04
MgO	0.31	± 0.07	0.03
MnO	0.16	± 0.11	0.04
FeO	0.08	± 0.10	0.02

Dolomite

CaO	31.07	± 0.45	0.04
MgO	18.28	± 0.34	0.04
MnO	0.13	± 0.10	0.03
FeO	4.12	± 0.25	0.05

cut and prepared to 1000-grade carborundum grit. Most cement stages could be identified from their staining response and were therefore sampled directly from stained blocks or plaquettes. Other cement stages could only be delineated with CL, and in these cases a more complex sampling technique was employed.

Thin rock plaquettes (maximum 75 x 50 x 5mm in size) were prepared with 1000-grade carborundum and then polished with Al_2O_3 powder. Dried samples were then etched with a rough 2 x 2mm grid using a diamond-tipped scriber. The sample was then photographed in CL using macrophotography attachments, and the grid and photo-map were later used as a guide for locating the sample regions. Samples were drilled from these blocks using a diamond-tipped dentist's drill-bit.

Certain samples thought to contain organic matter which might affect the carbon isotope ratio were roasted under vacuum at 450°C for 2hrs in an attempt to remove this interference.

Samples weighing a minimum of 5mg and up to 20mg were reacted in sealed, evacuated vessels, at 25°C with concentrated phosphoric acid. The evolved gas was extracted by passing it through two low-temperature traps in order to remove impurities; the first consisting of a "slush" of dry-ice and acetone to remove any water vapour; the second consisting of liquid nitrogen which freezes the CO_2 and allows non-condensible gasses to be pumped away. Raw d45 and d46 isotope ratios were obtained from a VG-903 mass spectrometer and these were computer-refined to give $\delta^{18}O$ and $\delta^{13}C$ values.

International standards NBS-19 and NBS-20 were run in parallel with samples at the beginning of each analytical session for calibration purposes.

Some dolomite samples were wholly or partially calcitised, and others consisted of small rhombs which could not be isolated from surrounding calcites. In these cases, the proportions of calcite to dolomite were calculated from calibrated XRD traces (see Chapters 11 and 15).

2.1.7.2 Sulphur isotopes

A small suite of iron sulphides (3 samples) were analysed by Dr A. Boyce at SURRC. Samples consisted of pyrite and pyrite/marcasite mixtures. Sample weights were in excess of 20mg, and were also

obtained using a diamond drill-bit. Any carbonate contamination was removed prior to analysis with conc. HCL, which does not react with pyrite and marcasite.

CHAPTER 3
TERMINOLOGY AND DEFINITIONS

3.1 DIAGENESIS

The concept of diagenesis was originally introduced by Von Gumbel (1868) to define processes which act on sediments after deposition, including all of the textural and mineralogical development of a sediment between the time of its deposition and the onset of metamorphism.

Diagenetic processes such as cementation, dissolution, pressure solution, mineral stability transformations, neomorphism, dolomitisation, organic matter degradation, compaction, replacement, mineralisation and fracturing can affect a sediment to such an extent that the resulting rock is as much a product of diagenesis as it is one of deposition.

Limestones are texturally and chemically heterogeneous, and thus particularly susceptible to develop complex diagenetic histories. During diagenesis, a carbonate rock may be subjected to a variety of diagenetic environments, each developing characteristic fabrics and cements and to a certain extent overprinting products of earlier diagenesis. The result is a sequence of textures and cement stages which record changing diagenetic environments through the burial history of a rock, and can be used to determine the geographical extent and effects of diagenetic episodes, and their relative timing. Such information is vital when attempting to reconstruct fluid movements, cementation patterns, tectonic episodes and palaeoaquifer distributions within a basin.

3.2 DIAGENETIC HISTORY

Documenting the diagenetic history of carbonate rocks began with petrographic descriptions of cement fabrics and mineralogies (Sorby 1879; Cullis 1904).

A voluminous literature on carbonate rocks and their diagenetic

fabrics has followed which is too vast to receive full attention here. Reviews and works of major importance include those on cementation (Bricker 1971; Bathurst 1975; and Schneidermann & Harris 1985), porosity (Choquette & Pray 1970), dolomitisation (Zenger et al. 1980), recrystallisation (Folk 1965; Bathurst 1964, 1983), stylolitisation and pressure solution (Wanless 1979; Bathurst 1983; Logan & Semeniuk 1976) and veinlet formation (Misik 1971; Durney & Ramsay 1973).

The increasing knowledge of diagenetic fabrics in limestones led to better understanding of diagenetic processes and environments. Dixon (1966) recognised that the sequential distribution of ferrous and non-ferrous iron in sparry calcite cements provided a key for solving some of the problems of diagenetic carbonate genesis. Evamy (1969) used staining techniques to identify compositional zonation in carbonate cements and so deduce their precipitational environments. This developed into a broad concept of diagenetic environments, first suggested by Friedman (1968) and further refined by Matthews (1968, 1974), Land (1970, 1971), Folk (1973, 1974) and Bathurst (1975). In a review, Longman (1980) identified four major near-surface diagenetic environments; the marine phreatic, mixed marine-freshwater phreatic, freshwater phreatic and freshwater vadose zones. He emphasised the spatial distribution of diagenetic environments in a rock body and how this could be used to predict porosity trends. Longman's paper also showed how successive diagenetic episodes in changing diagenetic environments could have a marked effect on styles of lithification and pore occlusion. Other notable works include two papers by James and Choquette (1983, 1984) on marine and meteoric diagenesis in limestones.

The role of deep burial diagenesis was evaluated by Scholle and Halley (1985), and they concluded that the part played by deep burial diagenetic processes in the development of porosity had been greatly underestimated. The effects of burial diagenesis were similarly emphasised by Prezbindowski (1985) and Woronick & Land (1985).

The nature of ancient pore fluids has been recognised as an important factor in the definition of diagenetic environments, and several techniques have been employed to detect former pore fluid compositions and environments. Electron microprobe analysis (Lohmann & Meyers 1977; Frank et al. 1982; Fairchild 1980), cathodoluminescence (Sippel & Glover 1965; Sommer 1972; Meyers 1974,1978; Meyers & Lohmann 1980,1985; Amieux 1982; Grover & Read 1983; Given & Lohmann 1985,1986) and stable isotope ratios (Allan & Matthews 1977,1982; Hudson 1977; Irwin et al. 1977; Meyers 1978; Coleman et al. 1979; Walls et al. 1979; Dickson & Coleman 1980; Marshall & Ashton 1980; Moore & Druckmann 1981; Marshall 1982; Meyers & Lohmann 1985; Czerniakowski et al. 1984; Prezbindowski 1985; Woronick & Land 1985; and several papers in Schroeder & Purser 1986) have improved our knowledge of the source and composition of diagenetic fluids, and how these can change during diagenesis.

3.3 CEMENT STRATIGRAPHY: Description and nomenclature

Apart from establishing a time sequence of diagenetic processes, a further development of cement studies involved study of the spatial distribution of carbonate cements within lithological units or whole basins of sedimentation. Sippel and Glover (1965) were the first to use cathodoluminescence in this context. They found luminescent bands in cements which could be correlated "from grain to grain and in some cases from different thin sections".

Evamy (1969) concluded that the apparent variations in iron content of carbonate cements, indicated by staining, represented diagenetic time horizons, and that these could be used for correlation and other stratigraphic purposes in elucidating the trend of porosity occlusion in limestones. Meyers (1974) successfully applied this principle, which he termed cement stratigraphy, in a spectacular demonstration. Compositional zonation in carbonate cements was mapped over tens of kilometres through the Mississippian Lake Valley Formation of New Mexico. Alizarin red S/potassium ferricyanide staining helped differentiate the cements, but their most detailed characterisation came from using cathodoluminescence (CL).

Cement stratigraphy, as a powerful new tool for documenting the diagenetic environments through which limestones had passed, was taken up and developed further (e.g. Meyers 1978; Fairchild 1980; Frank et al 1982; Grover and Read 1983; King 1984; Walkden & Berry 1984b; Meyers & Lohmann 1985; Miller 1986). Some of these studies went beyond regional correlation of carbonate cements and diagnosis of precipitational environments. Using a variety of techniques including CL microscopy, staining, geochemical analysis and stable isotope determinations, very detailed diagenetic histories were produced, including other non-cementation events such as dissolution phases, silicification, pyrite formation, dolomitisation, replacement and mineralisation. The original concept of cement stratigraphy has now, therefore, become part of a broader approach to studies of complete diagenetic histories.

Stratigraphers have long been aware of the value of a standardised nomenclature for lithostratigraphic descriptions. Various committees, both national and international, have published Stratigraphic Codes which divide the rock column hierarchically into units such as Formations, Members, beds etc. Use of the recommended nomenclature provides a sound basis for objectivity in recording stratigraphic data, and more importantly, facilitates communication and understanding of this data. Examination of the literature on cement stratigraphy (see below) reveals considerable variability in the terms employed to describe cement sequences in limestones. Not only do the terms differ markedly between authors, but there are cases where the ones chosen are not even consistently employed within a particular report.

3.3.1 Previous usage (Table 3.1)

Pre-dating the use of CL characters in cement stratigraphy, Dickson (1966) demonstrated his application of artificial staining on a Lower Carboniferous cement sequence and distinguished "stages" of ferroan calcite cement which often showed "zones" depicted by bands of similar staining. Mirsal and Zankl (1979), also without using CL, divided a sequence of Triassic reef cements into several "generations", some of which had internal layers characterised by

different inclusion densities; these were referred to as "sub-generations".

In his seminal paper on cement stratigraphy, Meyers (1974) distinguished six compositional "zones" within cements from the Mississippian Lake Valley Formation on the basis of their CL properties. He described "complex subzoning" as sets of thin bright and dark luminescing bands within the zones. Additionally, he used the term "stage" to indicate variation in Fe content of syntaxial rim cements. In his 1978 paper, he clearly separated descriptions of cements based on morphology, substrate selectivity and inclusion content from the compositional zones based on CL. He also referred to "generations" of cement.

Amieux (1982) (Table 3.1) used the term "CL Facies" to embrace all the luminescence and geochemical characters of carbonate crystal aggregates, be they cements or neomorphic replacements. Considering cements alone, Amieux distinguished "CL zones" (op cit. p.455), and introduced the notion of cement "sequences" as indicating the progressive evolution of cementation environments in terms of groundwater chemistry, redox potential and temperature. In a later paper, Amieux et al. (1983) divided a cement sequence in some septarian nodules into "layers" (couches), three of calcite and one of dolomite, on the basis of staining properties and crystal morphology. Some of the cements contained compositionally distinct "zones". Luminescence properties of the cement layers were described in terms of two CL Facies, determined by their distinctive emission spectrographic signatures and relative intensities.

In their important study of regional diagenesis in the Middle Ordovician of Virginia, Grover and Read (1983) used the term "zone" indiscriminately. For example, they referred to "crystal growth zones" (apparently the equivalent of Meyers' "sub-zones"), "cement zones" (the equivalent of Meyers' zones and the layers of Amieux et al.), and "cement zone sequences" to denote precipitation from progressively reducing pore waters. Under cathodoluminescence, some cements were further said to be "subzoned", whereas (paradoxically) other cement zones were "nonzoned". Several zones showed "luminescent laminae" - a fine and subtle form of subzoning.

Walkden and Berry (1984b) utilized a scheme similar to that of Meyers (1974) in describing Lower Carboniferous limestone diagenesis in central England. They reported four "zones" of cement, mainly on the basis of luminescence properties and crystal morphology, with some zones showing complex "subzoning". The term "growth zonation" was also applied, referring to changes in crystal habit throughout growth. Walkden and Berry also used the term "generation", apparently interchangeably with zone. Progressive development of the cement zones was described in terms of a series of diagenetic "stages" which included both dissolution and precipitation phases following changing groundwater conditions.

The above review indicates the confusing extent of variation and internal inconsistency in the terminology applied to carbonate cements. Authors have not explicitly defined the terms they used, nor have most of them stated the criteria by which they identified the boundaries used to subdivide the cement sequence.

3.4 BASIS OF PROPOSED NOMENCLATURE

Cements, like rock units, often occur in natural groupings as they may derive from sequentially connected processes. An hierarchical nomenclature is thus required, as clearly realised by Meyers and others. However, the term 'zone' is too limited for this purpose, as it can only be subdivided once into subzone. The Shorter Oxford English Dictionary defines the crystallographic sense of zone as "a series of faces extending round a crystal and having their lines of intersection parallel" and this corresponds best to growth banding shown by CL (referred to as subzoning by some authors), rather than to the usage for discrete layers of cement separated by unconformities envisaged by Meyers (1974, 1978). While the terms "layer" and "generation" have also been used to describe these major subdivisions of a cement sequence, I have preferred the terms stage and substage for these broader divisions. Together with zone, they have a consistent and common usage in a stratigraphic sense, and are broadly the terms used by Dickson (1966) and Fairchild (1980).

Units within cement stratigraphies can be subdivided on a hierarchical basis reflecting the correlateable extent of individual

Table 3.1 Nomenclature of cement stratigraphies from various studies.

This study	Stage	Substage	Zone
Miller (1986)	Stage	-------	Zone
Walkden & Berry (1984)	Zone / Generation	-------	Subzone
Grover & Read (1983)	Zone	Subzone	Laminae
Amieux et al. (1983)	Layers	-------	Zone
Amieux (1982)	Facies	-------	Zone
Frank et al. (1982)	Zone	Zone	Subzone
Fairchild (1980)	Stage	Substage	Zone
Meyers (1974,1978) ____ & Lohmann (1980,1985)	Zone / Generation	-------	Subzone
Dickson (1966)	Stage	-------	Zone

subdivisions, in a similar way to those of standard stratigraphy. The classification given below utilizes some of the terms in previous work but the definitions are intrinsic to this study.

3.4.1 Stratigraphical classification

The following hierarchy will be used throughout this study and each term is defined below:

Stage	(Denoted by upper case letter e.g. Stage A)
Substage	(Denoted numerically e.g. Substage A1, A2)
Zone	(Denoted by lower case letter e.g. Zone A1a)

A **Stage** is the primary unit of cement stratigraphy. It should have some degree of internal mineralogical homogeneity or distinctive geochemical features that separate it from adjacent cements. Stages are usually bounded by major textural hiatuses analogous to unconformities or discontinuities. Above all, a stage should be correlateable over large enough areas to allow comparisons to be drawn between most samples in a particular study.

A **Substage** is part of a Stage identified by some distinctive compositional characteristic(s). Substages are conformable cement units which are locally correlateable, i.e. within one facies, but are often discontinuous on a basinwide scale. Internal heterogeneity is common and may be reflected as a gradational change or sharp zonation.

A **Zone** is the smallest individual unit normally observable, and may only be correlateable within one cavity or even a single crystal. Zones are conformable and essentially homogeneous, the exception being where crystals exhibit compositional sector zonation (See below and Reeder & Prosky 1986).

3.4.2 Correlation of CL and staining in cement unit determination

Using CL on stained thin sections is unadvisable because the stain colour tends to burn-out under the electron beam. However, a

limited trial was attempted to establish if the cement unit boundaries identified by the two techniques occurred at the same place, and in general it was found that they were directly coincident.

Staining, however, is a less subtle technique than CL. Consequently, some cement stages, substages and zones identified by CL may not be visible with staining. This is particularly the case with non-ferroan calcites and dolomites which usually tend to stain homogeneously. In ferroan calcites, although many more zones may be visible in CL, the positions of stage and substage boundaries can usually be identified by both techniques.

In strongly ferroan calcites and all ferroan dolomites, the quenching effect of Fe^{2+} on CL often means that compositional variation is only identified with staining.

While chemical reasons for the staining response are well known, the levels of activator and quencher ions which effect CL in carbonates are poorly understood (see Chapter 19). Cements which have visibly indistinguishable CL characteristics may be chemically quite distinct. Examples occur within this study where adjacent ferroan and non-ferroan cement stages are only separable with difficulty on the basis of their luminescence alone. These cases demonstrate the necessity of using both staining and CL techniques in cement stratigraphy studies.

3.5 GEOCHEMICAL HETEROGENEITY IN CEMENTS

Three styles of compositional zonation occur in the cements of this study as identified with CL and staining (Fig 3.1).

a) Concentric zonation: homogeneous units
b) Concentric zonation: gradational units
c) Crystallographic sector zonation.

a) Concentric zonation: homogeneous units

All zones within the cement sequence, the majority of substages and some stages,are chemically homogeneous. The boundaries of these units are sharp as identified by CL, staining and BEI techniques.

Compositional variation in trace element levels across boundaries are usually detectable in microprobe analyses, sometimes in the order of hundreds of ppm.

b) Concentric zonation: gradational units

Occasionally units, usually substages, within the cement sequence show a gradational internal variation in CL or staining characteristics. Unit boundaries are often difficult to identify (see Frank et al. 1982, Fig. 1D). Although petrographically visible, the gradational variation is not significantly detectable in microprobe analyses. Close examination with BEI and transmission electron microscopy (Reeder & Prosky 1986) indicates that microzonation on a scale below the optical limits of petrographic microscopes is common, and may well be the cause of the gradational change in luminescence and staining characteristics seen in these units.

c) Crystallographic sector zonation

Using CL, compositional difference within sectors of calcite cement crystals that are independent of any concentric zonation can be identified. Sectors usually have sharp but often irregular boundaries. Under CL, sectors appear as areas of cement crystals where individual concentric cement units have consistently duller or brighter luminescence than their correlative in neighbouring sectors. Trace element variations across sector boundaries were not investigated in this study. No sector zonation was detected in dolomite crystals.

Discussion

Large-scale concentric variations in crystal chemistry are generally thought to result from changes in pore water chemistry and precipitational environments (Evamy 1969; Meyers 1974; Grover & Read 1983; Walkden & Berry 1984b). However, there is evidence that some chemical variations within cement crystals are also controlled by crystal growth mechanisms. An experimental study by ten Have and

Fig. 3.1 Cement stratigraphical nomenclature and styles of geochemical heterogeneity in cements.

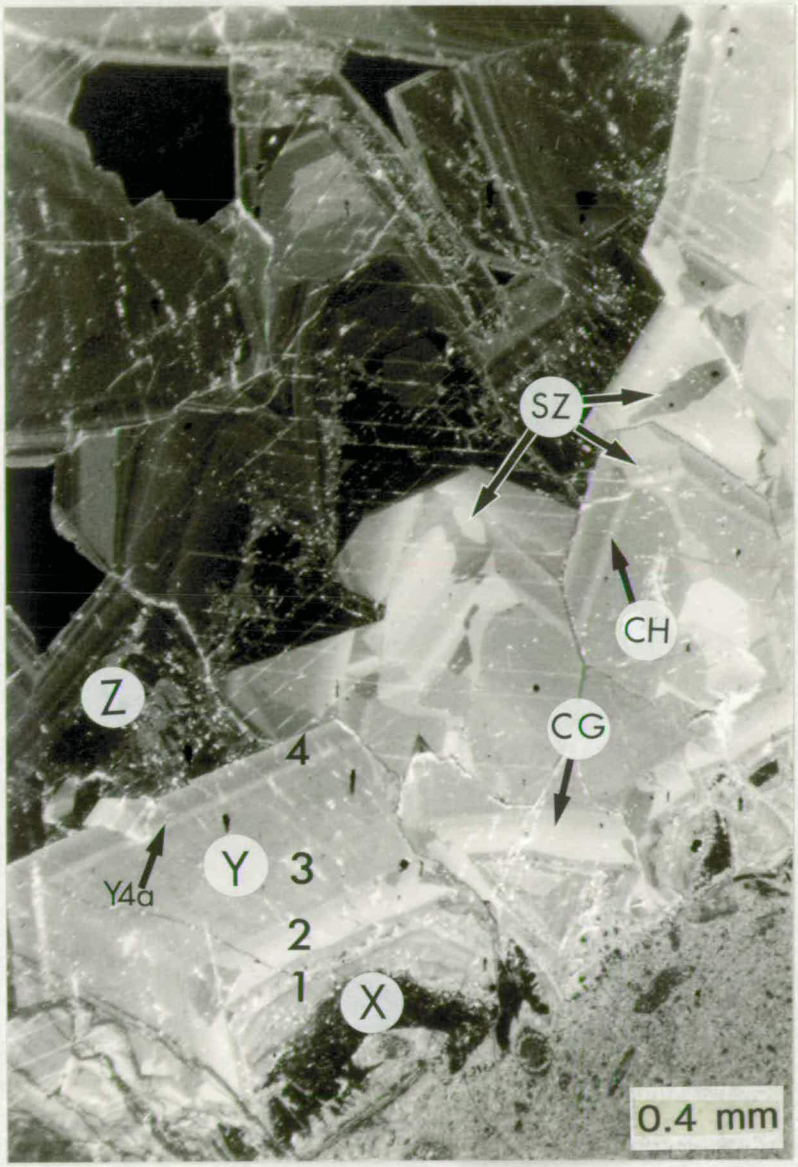

This CL photomicrograph illustrates the use of the proposed hierarchical terminology for cement stratigraphy. X,Y and Z are used for the stage designations to avoid confusion with the Craven cement sequence described in this thesis. N.B. this is a simplified view, as staining techniques reveal further stages which are not visible in CL alone. The three cement stages (X,Y and Z) are separated by textural and/or geochemical hiatuses. The X-Y boundary is irregular, as a result of dissolution, while the Y-Z boundary in this example is planar, and largely a product of geochemical variation. Stage Y comprises Substages Y1-Y4, the latter of which has a relatively bright early Zone Y4a.

Styles of geochemical heterogeneity in cements are also shown:

CH = Concentric homogeneous zonation.
CG = Concentric gradational zonation.
SZ = Compositional sector zonation.

Heijnen (1985) reported the production of compositional zonation in artificial calcites grown in fluids of constant chemical composition, and so they invoked crystal growth rate as the controlling mechanism.

An important consideration is the level of trace element variation induced by the different processes. The difference in Fe^{2+} occuring across a boundary between non-ferroan and ferroan calcite units, as identified by staining, is in the order of several hundreds to thousands of ppm (Dickson 1966; Oldershaw & Scoffin 1967; Lindholm & Finkelman 1971). The majority of microprobe analyses taken across major luminescent boundaries (stages and substages) in this study reflect variations of similar magnitude. Variations in crystal chemistry of this order are unlikely to be the result of crystal growth rate mechanisms. However, it is likely that many zones reflect a combination of crystal growth mechanisms (cf. Reeder & Prosky 1986) and pore fluid compositional changes .

The degree of homogeneity of cement units is probably related to the stability of pore fluid composition and crystal growth rates during precipitation. Chemically homogeneous units reflect stability in all aspects of crystal growth. The chemically gradational units, on the other hand, reflect a degree of change. This could have been a gradual change in crystal growth rate, or the gradual depletion of dissolved impurity ions during precipitation from a chemically closed-system pore fluid.

The development of compositional sector zoning is common in high temperature minerals but has recently also been reported in dolomite (Reeder & Prosky 1986). It is thought to be the product of metastable crystallisation resulting in the preferential uptake of impurity ions on different crystallographic growth surfaces. This is effected by variable atomic configurations, in the form of partialy formed cation sites (Reeder & Prosky 1986).

3.5.1 Origins of hiatuses in the cement sequence.

The major textural hiatuses defining stage boundaries in the cement sequence reflect important changes in pore fluids, the pore system, or tectonic processes. Changes in crystal habit may develop

in response to a variety of factors such as salinity, reduced pore fluid flow rates, restriction and pore occlusion from burial and cementation, or porosity increase resulting from dissolution or fracturing.

Not all stage boundaries are marked by a change in crystal habit. Irregular surfaces, as defined by CL and staining, record periods of crystal growth interupted by some degree of solution of earlier cement (Meyers 1974; Frank et al. 1982; Walkden and Berry 1984a). Carbonate minerals are especially susceptible to dissolution as a result of changing diagenetic environments. The dissolution kinetics of carbonates are very complex (see Berner & Morse 1974; Sjoberg & Rickard 1984) with the main controlling factors being pH, pCO_2, ionic strength, degree of carbonate saturation and temperature (Plummer 1975).

In early diagenesis, that is within the first few centimetres to tens of metres of the sediment-water interface, organisms may be responsible for some of the pore fluid changes which effect dissolution (Curtis 1978; Berner 1981; Birnbaum & Wireman 1984).

In burial situations, with the exception of pressure solution, most dissolution in carbonate rocks results from the influx of an undersaturated or aggressive fluid. Other prerequisites for solution of carbonate minerals include; significant volumes of aggressive fluid; a method of fluid transport through the rock i.e. efficient fluid pathways; significant throughput of fluid for widescale dissolution, and the presence of metastable mineralogy (Giles & Marshall 1986). Possible mechanisms for subsurface dissolution in carbonates as reviewed by Giles & Marshall (1986) include:

1. Meteoric water penetration
2. Mixing corrosion (Bögli 1964; Plummer 1975)
3. Acidic fluids generated from CO_2 as a product of thermal maturation of organic matter (Schmidt & McDonald 1979).
4. Carboxylic acids generated during the thermal maturation of organic matter (Surdam et al. 1984).
5. Acidic fluids generated by clay mineral reactions (Bjørlykke 1981).

Other mechanisms which could control carbonate dissolution are: the influx of warm subsurface brines or hydrothermal fluids, and temperature change resulting from increased burial.

DIAGENESIS

PART ONE

DIAGENESIS PART ONE

SEA FLOOR TO SHALLOW BURIAL

Introduction.

Significant diagenetic modification of the Craven Waulsortian occurred contemporaneously with buildup accretion on the sea floor and continued into the shallow burial realm.

Strong circumstantial evidence suggests that several extensive diagenetic episodes took place before the precipitation of the first recognisable cements in the pore space.

The cements themselves are highly distinctive in terms of their fabrics, textures and geochemistry, and notably, in the case of Stage A, because of the sheer volume of cement that was precipitated into the complex void network of the bank facies.

These early cements are commonly interbedded with marine internal sediments and may also contain marine bioclasts included within their layers, thus indicating precipitation from sea water.

Petrographic, geochemical and stable isotopic analysis show that the cements which developed during the early part of the diagenetic history of the buildups can be related to changes in pore fluid circulation and composition during progressive (shallow) burial in the marine phreatic realm.

CHAPTER 4.

BUILDUP SEDIMENTS AND ORIGINAL POROSITY

4.1 SEDIMENTS

The nature and arrangement of sediment within the Waulsortian bank facies is extremely complex. The importance of the sediments to this study was mainly in their relationship with spar fabrics. Detailed research into the sediments themselves was not undertaken, but the work of Lees (1964) is directly applicable to the Craven Basin Waulsortian, and is used as a basis for the brief outline of buildup sediments given below.

There are five major components in Waulsortian sediments (Lees 1964):-

1. Calcite mudstone (lime-mud and peloids)
2. Coarser calcite mosaics (from aggrading neomorphism or primary spar growth)
3. In situ bryozoan meshworks
4. Skeletal debris
5. Entire fossils other than in situ bryozoans.

The primary sediment (M1) consists mainly of lime mud, with varying proportions of other components, particularly skeletal debris. After the deposition of M1, several stages of further remobilisation of the sediment resulting from mechanical collapse and dewatering, led to the development of an inhomogeneous, multicomponent sediment (polymuds of Lees & Miller 1985; Miller 1986) in which the boundaries between sediment generations (designated M2 et seq.) are often highly irregular and diffuse.

The M1 sediment itself "occurs as 'floculent' masses or isolated patches up to a few centimetres across" and is "generally surrounded by later generations of geopetal mud and spar" (Lees 1964, p 515). Commonly M1 accounts for much less than 50% of the sediment volume. In most cases, the volume of M1 sediment in the rocks would not have been sufficient to have supported itself, even if it had formed a

continuous framework. Such frameworks of M1 do not exist, and therefore the redistribution of that early sediment must have occurred *in situ* with the M2 (etc.) sediments supporting the original M1 masses, indicating that sedimentation was largely internal, i.e. remobilisation occurred within the bank. The M1 sediment is therefore the only generation which is truly primary. The rest are strictly secondary.

The origin of the M1 micrite is a long-standing problem. The lack of a consistently-developed skeletal or supporting framework in the buildups indicate that sediment baffling only played a minor part in buildup development. Although evidence of bio-erosion occurs in Phase C and D buildups, it is rarely abundant and this also is unlikely to have produced such large quantities of fine-grained sediment. Lees and Miller (1985) noted the presence of presumed cyanobacterial filaments in M1 from Waulsortian Phases B,C and D. However, the absence of such filaments from Phase A bank facies precludes those particular organisms from being responsible for the generation of M1. In the Phase C and D buildups of the Craven Basin, these and other filaments including *Girvanella* are very common, and they undoubtedly played a significant part in stabilisation of M1 muds. Considering all this evidence, together with the characteristic way in which M1 nodules are developed in proximal flank facies, and merge in the toe beds and developed fully Waulsortian bank facies at the periphery of the buildups, Miller (1986) proposed that the M1 was biogenic, formed *in situ* by cyanobacterial populations. These populations were also considered to have influenced the early stages of interparticle cementation in the buildups.

4.1.1 Sediments associated with spar-filled cavities

The majority of cavities (now mainly spar- and sediment-filled) within the bank facies contain geopetal sediment, often laminated, which may be of more than one generation and which may pre-date, be interbedded with, or post-date early diagenetic cements in the cavities (see below Chapter 8 and Fig. 4.1).

There are four common grain constituents of internal sediments:

a) Lime mud
b) Peloids
c) Lithic intraclasts
d) Skeletal grains

a) Lime Mud

Lime mud, which is mainly micrite (<4 μm, Folk 1959) may occur either as a major constituent or as a minor interstitial component of internal sediments (Fig. 4.1A). Laminations are particularly well-developed in lime mud internal sediments.

b) Peloids

Peloidal grains vary widely in shape and size. They may be round or ellipsoidal, cylindrical, rectangular or square. Dimensions are up to hundreds of microns. The majority of peloids are micritic. Some have associated organic matter and authigenic pyrite. Interstitial material in peloidal sediments is either lime mud or microspar. The considerable range in shape and size of peloids suggests polygenetic origins. The four most probable sources are:

i) Sediment trapped within or filling the framework of living or dead organisms. Peloids were freed either by fall-out or the break-up or dissolution of the skeleton.

ii) Faecal pellets. This applied mainly to rounded and ellipsoidal peloids (Bathurst 1975, p 85; Brown 1964), although none observed in the present study contained internal layering or other textures attributed to undoubted faecal pellets (see Illing 1954).

iii) Calcified algal sheaths, either filled by micrite or microspar, when broken and re-distributed, may form a variety of peloidal grains, mainly ellipsoidal, and ranging from a few to tens of microns. Coniglio and James (1985) suggested that such grains were major contributors to Palaeozoic carbonate buildup sediments. Peloids which could be assigned to this origin are common in the Waulsortian buildups of the Craven Basin.

iv) Direct precipitation. MacIntyre (1977) suggested that some peloids in Recent sediments may be direct precipitates, i.e. they are cements. However, SEM examination of peloids in this study show no evidence of the kind of crystal textures usually associated with direct precipitation and a direct cement origin is considered highly unlikely.

The origin of many peloids still remains uncertain. Some irregularly-shaped varieties were probably derived from the reworking of partially lithified primary and secondary sediments supporting the interconnected cavity system.

Peloidal internal sediments are particularly common prior to or interlaminated with early diagenetic isopachous marine (fibrous) calcite cements, and are particularly well-developed in Phase D buildups.

c) Lithic intraclasts (see Chapter 8, Fig. 8.1)

These are irregular grains composed of fragments of lithified sediments which were reworked from the M1 sediment either by collapse or dewatering processes. They usually have rounded edges while some also have protruding particles ("grapestones" of Illing 1954). Size varies between 0.05 and 2.00mm. The majority of intraclasts are peloidal, but a variety of different microfabrics occur which reflect the inhomogeneity of the sediment mass from which they were derived.

Some intraclasts are coated with dense cryptalgal micrite whereas others have thin rinds of cement on their outer edges, and, rarely, on grains contained within them.

d) Skeletal grains

Skeletal grains are relatively uncommon in geopetal internal sediments. Most are finely comminuted grains of often indeterminate fossil origin, although small fragments of most Waulsortian fossil groups may occur. One notable exception is that siliceous sponge spicules, or moulds thereof, are rarely found in internal sediments of spar-filled cavities.

4.1.2 Origin of internal sediments

Most, if not all, internal sediments were derived from within the bank facies itself. Peri-Waulsortian facies are considerably more argillaceous than the bank facies and therefore if bank sediment had been externally derived, perhaps by currents re-working off-bank facies and then accessing the Waulsortian pore system, then clay-rich internal sediments would be expected; this is not the case.

Internal reworking of the bank facies probably occurred by stoping and collapse of the sediment shortly after burial (see below, 4.2).

Significant localised influx of internal sediment into the developing void network was associated with the development of neptunian dykes in the buildups (see below Chapter 8). On many occasions, the dykes broke into and enlarged original pore systems while injecting mobile sediment (usually fine grained lime-mud) into the cavities.

4.2 ORIGINAL POROSITY

The original porosity of the bank facies (now almost totally spar-filled) was dominated by large, irregular interconnected cavities up to several tens of centimetres across which invariably contained layers of geopetal sediment forming a flat floor, with often very complex roofs. The term "stromatactis" (Dupont 1881) was suggested because similar features in Belgian upper Devonian mud-mounds were considered to be replaced stromatoporoids. The name unfortunately became entrenched in the literature and came to be applied to a variety of features with similar appearance but whose origins were dissimilar. The term "stromatactoid" (cavity) is used in this study as a general term for this type of structure without inferring any process or mechanism. Other porosity types occurred in Waulsortian banks which are common to many carbonate buildups throughout the geological record (cf. Harris 1983).

Figure 4.1 Internal sediments

A Photomicrograph of stromatactoid cavity in bank facies, containing laminated micrite (m) and peloidal (p) internal sediments. The interstices of the peloidal sediment consist of inclusion-rich microspar. The outlined area (arrowed) is representative of the material shown in B and C below: Hall Hill buildup.

B SEM photograph of similar pelsparite geopetal sediment from Knoll Wood buildup. Very fine grained, granular peloids (p) are contained within an irregular mosaic of inclusion-rich microspar (s). White box represents area of C. Sample surfaced and etched using EDTA, after Miller and Clarkson (1980).

C High magnification, split-screen SEM image of boxed area in B, showing the boundary between peloid (p) and microspar (s). Microspar contains many equant to irregular inclusions (arrowed) which have been preferentially etched by the EDTA.

UNIV. EDINBURGH EX BIBL.

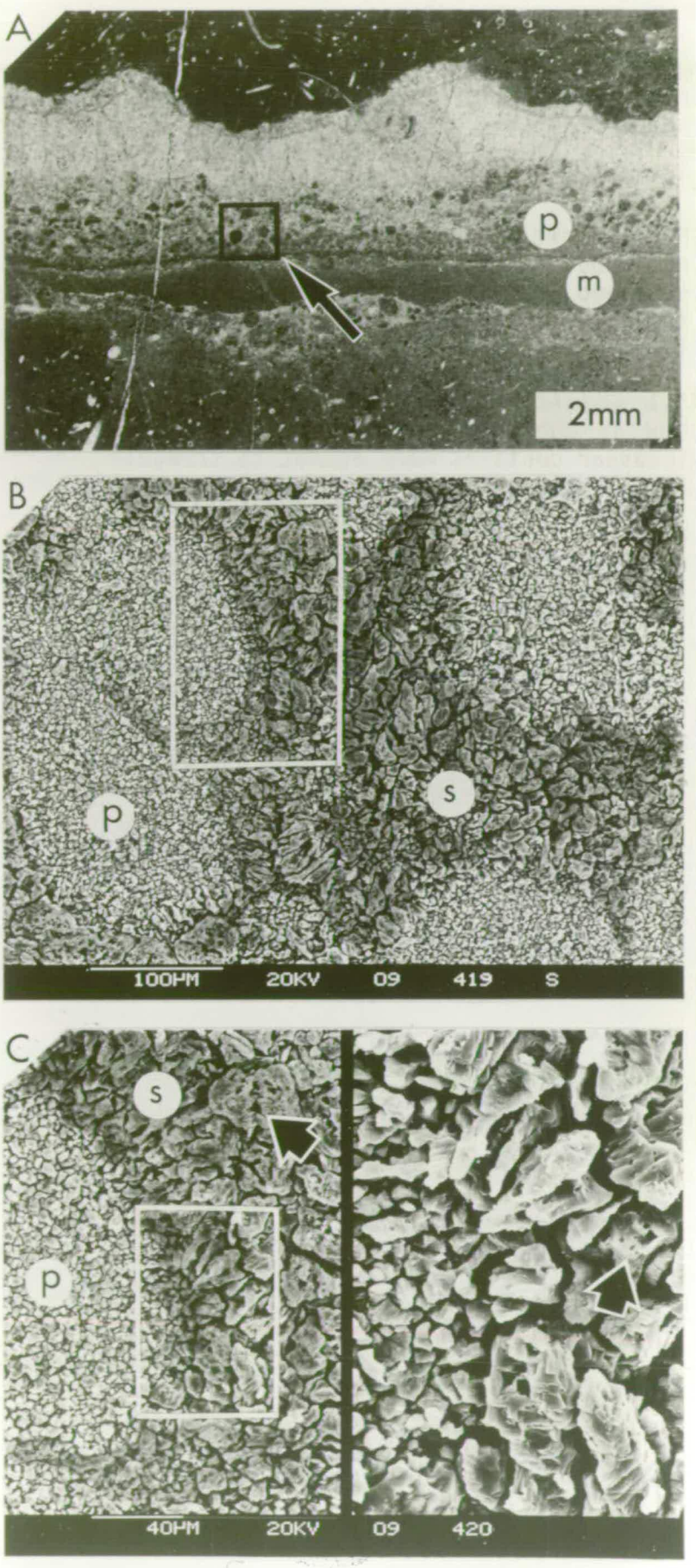
A
p
m
2mm
B
p
s
100μM 20KV 09 419 S
C
s
p
40μM 20KV 09 420

Figure 4.2 Original Porosity in the bank facies.

Negative prints from thin sections.

A. Showing a stromatactoid cavity developed within polymuds (p). The shape of the cavity is controlled by the presence of fenestellid bryozoan fronds (F) which acted as reinforcements in the sediment. An early isopachous cement (S1) was followed by the influx of internal sediment (m), and later clean blocky spar (black areas in negative). Ings Beck buildup.

B. Showing sheet spars developed in micritic, bioclastic M1 sediment. The sheet-like cavities have secondary floors of laminated peloidal and micritic geopetal sediments (M2). These are partially interlaminated with inclusion-rich, subisopachous S1 cements which are followed by clear, blocky spar (S2). The primary floors of the voids are very difficult to trace without etching. Hall Hill buildup.

C. Showing intraskeletal porosity (i) in a brachiopod which is seen in growth position in a laminated sediment, filling a cavity which was probably open to the bank surface (note the abundant hyalosteliid rod-bundle spicules, seen as block dots). Subsequent sediment layers draped over the brachiopod shell. Hall Hill buildup.

D. Showing spar-filled porosity within a meshwork of fenestellid bryozoans (F). The earliest spar (S1) is isopachous and inclusion-rich, with substrate-parallel inclusion bounding, and fills the majority of the void space. Some later blocky spar (S2) also occurs. New Laund Hill buildup.

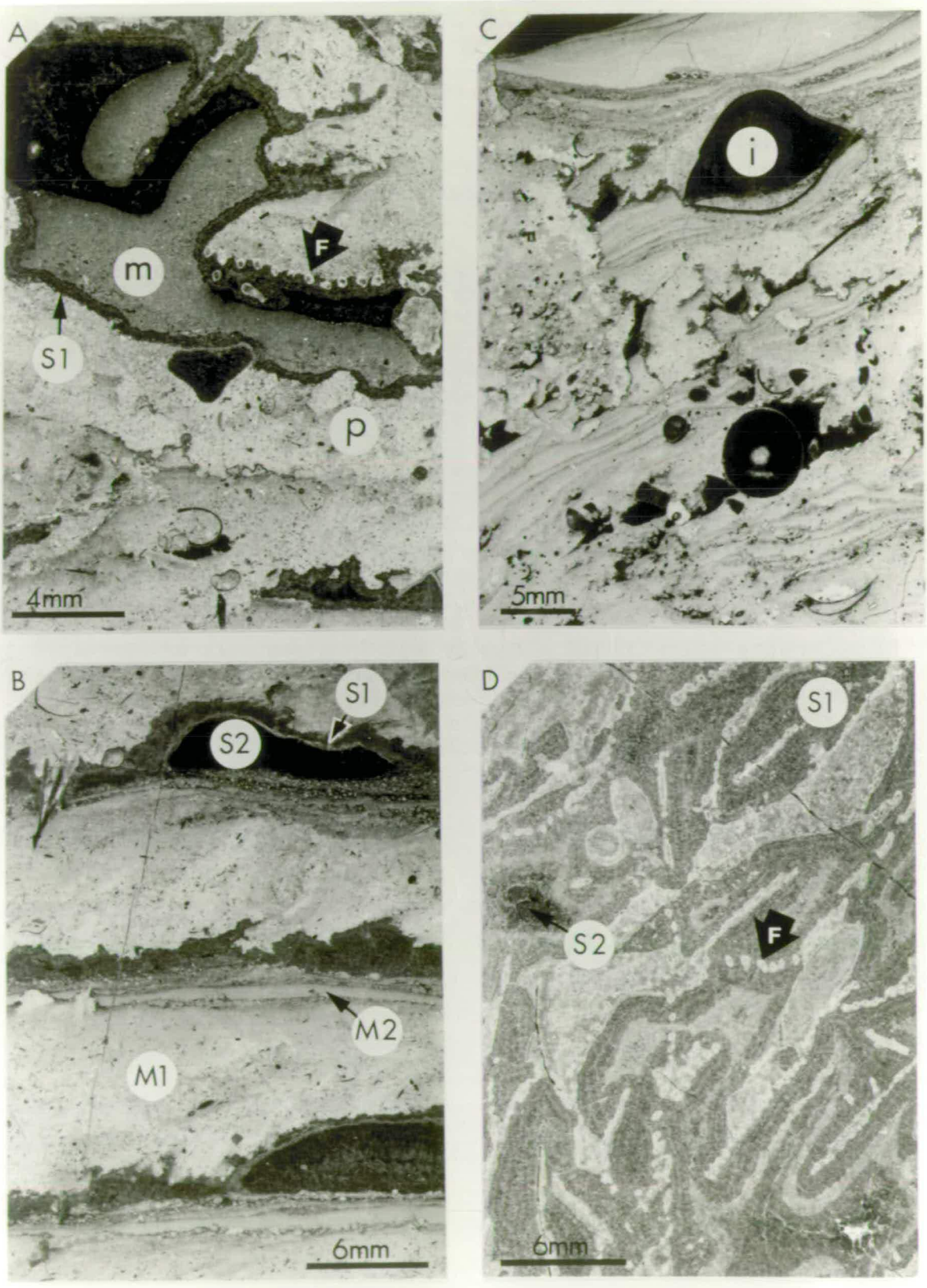
A
m
F
S1
p
4mm
C
i
5mm
B
S1
S2
M2
M1
6mm
D
S1
S2
F
6mm

The main types of original porosity were (Fig 4.2):

1. Stromatactoid cavities
2. Porosity within meshworks of fenestellid bryozoans
3. Intraskeletal porosity in shells of other fossil groups
4. Intergranular porosity between sedimentary grains.

4.2.1 Stromatactoid cavities

Lees (1964) has described in detail the development of stromatactoid cavities in Waulsortian buildups. He showed that there are two main forms:

a) "Stromatactis" cavities (Fig. 4.2 A&B)

These have irregularly embayed, undulating or digitate upper surfaces with flattish though often stepped floors, which consist of a layer or layers of internal sediment. They range in size from a few mm to tens of cm across and are generally parallel to bedding. It was discovered that a variety of factors affected the morphology of "stromatactis" including bedding attitude, the presence of bryozoan fronds in the sediment (and other large grains or collections thereof) or other sediment inhomogeneity (see Lees 1964, Figs 22 and 31).

The vast majority of stromatactoid cavities in the Craven Basin Waulsortian are of this type. With only rare exceptions, a degree of skeletal control on the morphology of these cavities can usually be identified. The main supporting fossil grains are fenestellid fronds and hyalosteliid sponge spicules from the basal rod-bundles, (now spar-filled moulds) with brachiopod, gastropod and ostracod shells being locally important.

b) Sheet spars

Less common are undulating sheet-like masses (sheet spars) which may extend laterally up to several metres but are usually less than 1cm thick. These flat cavities were considered by Bathurst (1982) as "stromatactis" even though not included in Dupont's (op. cit.) original definition. The upper and lower surfaces of the sheet-like cavities (after allowing for internal sediment), although often denticulate, are commonly parallel and would lock together if brought into juxtaposition. They generally formed in the more homogeneous

regions of the lime mud sediment where large skeletal grains are absent (Fig. 4.2B).

The sheet spar type of stromatactoid cavity is very rare in the Phase C and D Waulsortian of the Craven Basin because large areas of homogeneous lime-mud are not as common as in Phase A and B buildups.

4.2.1.1 Origin of stromatactoid cavities

"Stromatactis" and sheet spars developed by two completely different processes.

In the case of "stromatactis", Lees (1964) showed that the cavities and polymuds developed at the same time.

Initially, the M1 micrite was probably both produced and stabilized by micro-organisms, possibly filamentous algae (Pray 1958; Lees 1964; Miller 1986). Growth of the buildups resulted in burial and decay of the binding organic matter, releasing sediment, some of which was in the form of "lumps" which were sufficiently cohesive and competent to form mechanical bridges which then became the support under which cavities opened by collapse of unconsolidated material below. These supports were probably strengthened in some cases by patchy incipient cementation (see below, Chapter 5). Bridging supports were also provided by fenestellid fronds and hyalosteliid rod bundles, both acting much like reinforcing mats in concrete. The remobilisation of the M1 sediment resulted in development of the complex polymuds, some early voids being completely filled by secondary collapse, giving the characteristic mottled appearance.

The "collapse hypothesis" proposed by Lees (op. cit.) can therefore explain the development of "stromatactis" cavities and polymuds, and indicates that these two most characteristic textural features of the Waulsortian facies were synchronous.

Sheet spars formed without the influence of mechanical bridges; indeed they only developed in sediments from which skeletal meshworks such as fenestellids and hyalosteliid rod bundles are conspicuously absent. Their often parallel, refitable margins indicate formation by parting along cracks, i.e. they are pull-apart structures. Lees (1964) suggests that such pull-apart was rapid, and resulted from shear-failure of the de-watering and shrinking mud.

4.2.2 Bryozoan meshwork porosity

Intricate meshworks consisting of mats of fenestellid bryozoan fronds, some in growth position, occur only patchily in the Craven Basin Waulsortian . These meshworks were sufficiently rigid to maintain open void-space and so allow cements to precipitate (Fig. 4.2). Without exception, these structures were cemented by isopachous layers of fibrous marine cements. Although the fenestellid meshwork was rigid, it was not totally sealed, and secondary internal sediments, consisting mainly of peloids and lime mud, filtered into the meshwork and often became interbedded with the developing layers of cement.

4.2.3 Intraskeletal porosity

This includes internal space within skeletons of brachiopods (Fig. 4.2C), molluscs, ostracods, foraminifera and the rare solitary rugose coral (Amplexus). During early stages of burial, most intraskeletal pore space was isolated from the main cavity system and, therefore, very few intraskeletal voids developed linings of early marine fibrous cements. The resistance of the lime mud buildups to compaction helped to preserve this pore space until later periods of fracturing allowed diagenetic fluids to access the voids and precipitate cements.

4.2.4 Intergranular porosity

The extent of original intergranular porosity of the buildup sediments is impossible to gauge. However, estimates from Recent lime-muds suggest that primary intergranular porosity may have been as high as 40-70% (Bathurst 1975, p.415). Subsequent neomorphism removed any indication of original lime-mud porosity in the Waulsortian, but it is apparent that peloidal sediments and occasional crinoid-rich layers may have had significant primary intergranular porosity.

4.3 ADDITIONAL REMARKS

4.3.1 Lack of shelter porosity

Evidence of shelter porosity (created by the sheltering effect of relatively large sedimentary particles which prevent the infill of the underlying pore space by finer particles from suspension cf. Choquette & Pray 1970), is conspicuously absent from the Waulsortian facies. This is seen as evidence supporting the postulation of *in situ* production of lime-mud in the banks (cf. Lees & Miller 1985), as opposed to the baffling of sediment by a skeletal framework, or accretion by suspension fall-out. Additionally, sediment produced *in situ* is still likely to settle and therefore produce shelter voids. The absence of such voids in the Waulsortian sediments suggests that grains may have originally been bound by an organic meshwork (cf. Miller 1986).

4.3.2 Subsequent void modification

The original porosity of the Waulsortian facies was extensively modified by dissolution episodes which occurred during the earliest stage of diagenesis in the banks (see Chapter 5).

CHAPTER 5.
EARLY CEMENTATION AND DISSOLUTION

5.1 EARLY LITHIFICATION OF M1 SEDIMENT

The very fine-grained M1 micrites of the bank facies are difficult to study by standard petrographic means. Furthermore, CL petrography shows evidence of patchy dissolution and neomorphism which has largely overprinted the original sediment textures and left no direct evidence of the earliest phases of their cementation. Nevertheless, circumstantial evidence indicates the presence of an early intergranular cement which stabilized the bank facies sediment, namely:

1. The evident stability of the banks with their steep depositional slopes, in the absence of skeletal frame builders.
2. The lack of compactional features within the bank facies in strong contrast to peri-Waulsortian facies.
3. The occurrence within the bank facies of complex interconnected dissolution-void networks with no apparent cavity supports (see 4.2).
4. The development within the banks of crumbly-edged fractures and microfractures indicative of a firm gel consistency, in some cases formed prior to Stage A marine cements (see Chapter 8).

5.1.1. Distribution of Early Cement

Synsedimentary sediment-filled neptunian fractures, occurring on microscopic and macroscopic scales, are a common feature of the Craven Waulsortian (Chapter 8). While the development of fractures indicates early lithification of the banks, the injection of sediment along these and later neptunian dykes suggests that parts of the buildups remained uncemented throughout early diagenesis, and therefore any early cementation must have been patchy, i.e. non-pervasive. The common development of polymuds (sensu Lees & Miller 1985) in the bank facies is also indicative of mobile sediment in

some areas of the buildups.

Bathurst (1980, 1982) and Pratt (1982) suggested that synsedimentary cementation within mudmounds developed in layers or laminar surface-hardened crusts, Bathurst (op. cit.) invoking physiochemical cementation and Pratt (op. cit.) suggesting biogenic precipitation in association with stromatolitic algal mats. However, there is no evidence in the Craven Waulsortian of any systematic organisation of early cemented areas within the buildups. Miller (1986) in a study of Craven and Irish Waulsortian, identified lateral facies transitions at bank margins comprising small isolated lensoidal masses of bank-type M1 micrite, which showed evidence, in the form of greater resistance to compaction compared with enveloping material, that they had been "firmed-up" by synsedimentary cementation. He found it difficult to reconcile such lensoidal textures with the development of lithified crusts as postulated by Bathurst (op. cit.). Lees (1964), Cowan & Meyers (1982) and Miller (1986) also agreed that early lithification had been important in stabilizing the Waulsortian buildups, although they were unable to show direct evidence. Meyers et al. (1982) did, however, detect a stable isotopic signature indicative of marine cementation in Waulsortian muds from New Mexico.

Early cementation in marine sediments was invoked to explain the consistent lack of compaction features in ancient micritic carbonates (Bathurst 1970). Most studies of Recent sediments concentrated on the shallow marine environment where early lithification was identified in a number of settings (Shinn 1969; Taylor & Illing 1969; Land & Goreau 1970; James et al. 1976). There has been a distinct lack of data concerning the early diagenesis of micritic carbonates, with notable exception of the studies by Choquette (1968) and Steinen (1978). The advent of the DSDP program brought more understanding of the diagenesis of pelagic muds (see various papers in G.J. van der Lingen Ed. 1977) which suggests that early cementation in marine pore waters provides a supportive framework in micritic sediments (Schlanger & Douglas 1974).

5.2 EARLY DISSOLUTION EPISODES

Miller (1986) detected two dissolution phases in Irish Waulsortian facies, which pre-dated the first sparry cement stage. These early dissolution phases are also present in the Craven Waulsortian (Figs. 5.1 & 5.2).

5.2.1 Silica Dissolution (Fig. 5.2B)

Siliceous hyalosteliid sponge spicules were common constituents of the M1 bank sediment and the peri-Waulsortian facies. In the bank facies, they are always represented by calcite-filled moulds whilst in the peri-Waulsortian facies, preservation of hyalosteliids was usually by later calcite replacement which commonly retained the shape of the central canal in cross-section.

Land (1976) reported early dissolution of opaline spicules in Recent coral reefs and noted that the dissolution could occur even in living sponge tissues, possibly suggesting some biological agency. In keeping with this, Friedman et al. (1976) suggested that pH fluctuations caused by algal metabolism were responsible for the early dissolution of quartz in a Recent example.

As Miller (1986) pointed out, the large size and abundance of hyalosteliid rod bundle mats in Phase B and C Waulsortian, requires dissolution and removal of significant volumes of silica at an early stage in diagenesis. This would apparently require alkaline pore waters, and Birnbaum and Wireman (1984) indicate that such conditions could occur during early diagenesis of certain organic substrates.

5.2.2. Carbonate Dissolution (Fig. 5.2C)

Margins of voids within the Waulsortian bank facies consistently show evidence of dissolution, mainly of the fine grained M1 matrix, but also of carbonate skeletal grains, prior to the development of the first recognisable cements in the sequence.

The style of dissolution of skeletal grains was dependent upon the nature of the original fossil structure and mineralogy. Fenestellid bryozoan fronds, and less commonly echinoderms (both origin-

ally HMC), often show evidence of partial dissolution in the form of irregular and embayed surfaces which truncate the primary skeletal structure. Meanwhile, molluscan grains (originally aragonite or a mixture of aragonite and calcite) may be represented by spar-filled moulds.

Dissolution of the M1 micrite was considerably more extensive, often resulting in the development of deeply embayed cavity roofs and walls and producing significant volumes of secondary porosity. Hyalosteliid spicule moulds resulting from prior silica dissolution, often acted as conduits for the aggressive fluids (Miller 1986) resulting in the development of intricate interconnected void networks which extended for significant distances into the M1 matrix beyond the original cavity margins. These networks commonly resemble the clotted micrite and spar textures termed "structure grumeleuse" (Cayeux 1935). It is often difficult to imagine how many of these clotted micrites resisted collapse, unless they had been bound by a precursor intergranular cement.

Changes in pore fluid chemistry brought about by bacterial degradation of certain types of organic matter within the sediments (Birnbaum & Wireman 1984) could have caused early carbonate dissolution. Progressive selective dissolution of mineralogically metastable bioclasts and supersoluble micrite has been identified from DSDP cores (Matter et al. 1975).

5.2.3 Timing of Early Lithification and Dissolution Episodes: Discussion

The relative timing of the early lithification and dissolution episodes can be ascertained by the reconstruction of primary fabrics, and the sequential evolution of the pore space and its contained cement stages (Fig. 5.2).

The original void network of the bank facies was commonly, though not always, supported by fenestellid bryozoan fronds or hyalosteliid spicule bundles, which acted as mechanical bridges after sediment collapse (cf. Lees 1964) (Fig. 5.2,A). Dissolution of siliceous spicules was accompanied by some collapse/stoping of the cavity margins which enlarged the primary pore space and often

produced geopetal internal sediments (Fig. 5.2,B). Many spicule moulds, however, did not collapse, suggesting that they were supported, probably by synsedimentary cement, i.e. the cement pre-dated silica dissolution. Spicule moulds were never observed in these geopetal sediments, while carbonate skeletal debris is not uncommon. This suggests that spicule dissolution pre-dated the development of the geopetal sediment.

Carbonate dissolution then followed (Fig. 5.2,C). Spicule moulds which opened into the void-network were exploited by the aggressive fluids which dissolved the adjacent M1 micrite and thus enhanced their interconnectivity to other moulds in the matrix, often resulting in digitate cavity roofs and clotted micrite textures. Carbonate skeletal grains were also subject to dissolution at this stage, and mouldic voids developed in place of some molluscan material. Further stoping and internal sedimentation occurred.

The final episode in this part of the sequence involved the precipitation of the first recognisable cements in the sequence (Stage A) (Fig. 5.2.D).

From the fact that the carbonate dissolution exploited the sponge spicule moulds to produce the intricate void systems and clotted micrites, it is apparent that silica dissolution must have been prior to that of carbonate.

However, the relative timing of micrite dissolution and that of carbonate skeletals is more difficult to constrain. Certainly, fenestellid and echinoderm grains were dissolved at approximately the same time as micrite. Often, dissolution surfaces truncating micrite and carbonate skeletals are continuous (Fig. 5.1B). However, the timing of development of molluscan moulds is less certain (Fig 5.1 F&G). Especially considering that some modern mollusc shells contain layers of both aragonite and calcite, cementation and/or replacement may have occurred during several episodes. Furthermore, molluscan moulds in the bank facies may have had micrite envelopes (cf. Bathurst 1966, 1975; Flügel 1982, p. 83); features which could support the mouldic voids and form an effective seal so that cementation could not occur except after fracturing, i.e. the cement stages filling the voids may be considerably later than the original dissolution episode. There is, however, some evidence in the bank

facies of molluscan moulds which opened onto the main void network and contain Stage A cements (Fig. 5.1D). Therefore I conclude that some dissolution of molluscs (either aragonite, calcite or both) also occurred prior to the first recognisable cement stage.

In some cases, the fabric which resulted from this sequence of cementation and dissolution phases consisted of up to 60% void space, and probably bore little resemblance to the primary fabric of the bank facies.

The occurrence of early dissolution and cementation at approximately the same time is problematic. It is most likely that dissolution was caused by the setting-up of micro-environments in the sediment associated with bio-degradation of organic matter, while cementation may also have been influenced by micro-organisms and the physico-chemical characteristics of the pore fluids. It is possible that some of the early carbonate dissolution may have been the source of some of the cement.

5.3 FACIES CONTROL ON EARLY DIAGENESIS

The fabrics and textures described in this chapter are specific to the bank facies. No evidence, circumstantial or otherwise, of similar features, occurs in the peri-Waulsortian sediments.

The reason for the facies specificity of these episodes is uncertain. In discussing similar facies control, this time on the development of later marine cements (Stage A equivalents), Miller (1986) concluded that environmental factors such as temperature and pressure were unfavourable for physico-chemical cement precipitation at depths where the Waulsortian formed, and suggested that the Stage A cements specific to the banks, could have been mediated by their specific microbial populations. Thus, the overall (inferred) biological controls on buildup development may also have been the main influence on the facies-specific nature of early diagenetic episodes in the Waulsortian bank facies.

Figure 5.1 Early dissolution episodes

A Showing a complex, digitate stromatactoid cavity roof, developed by early dissolution of micrite in the M1 matrix. The complex network was subsequently filled by inclusion-rich calcites representing the first recognisable cement, Stage A. Small, irregular patches of M1 were left 'floating' in the Stage A spars (arrowed). Thin section, bank facies, Crow Hill buildup.

B Photomicrograph showing an irregular dissolution surface on a micritised cavity floor (arrow). Dissolution of a gastropod (g) left a mouldic void which was subsequently filled by inclusion-rich calcite cements of Stage A (S1) while clotted texture developed as a result of dissolution and cementation in the peloidal sediment matrix (m). Thin section photomicrograph, bank facies, Crow Hill buildup.

C Dissolution of siliceous hyalosteliid sponge spicules leaving elliptical or spindle-shaped moulds. Those in close proximity to the main void network were often exploited and subsequently cemented by inclusion-rich calcites (A) of Stage A (Chapter 6). Those moulds which were isolated within the M1 matrix were filled by later, less turbid cements (B). Thin section, bank facies, Hall Hill buildup.

D Area of white box in C showing spindle-shaped spicule mould filled by inclusion-rich cement which accessed the void from the adjacent stromatactoid cavity (arrowed).

E Preservation of hyalosteliid spicules in peri-Waulsortian facies. Spicules were replaced by ferroan calcite which preserved the central canal structures. This figure shows a longitudinal section (A) and the more characteristic elliptical transverse sections through the spicules (B). Stained thin section, Ings Beck.

F Photomicrograph in PPL of a spar-filled gastropod mould (g) adjacent to a cavity, containing inclusion-rich cements (S1). The mould has a micrite envelope (e) which probably restricted pore fluid circulation sufficiently to prevent S1 cements forming. A later veinlet (v) transects the mould. Thin section, bank facies, Crow Hill buildup.

G Same area as F but under cathodoluminescence (CL). The inclusion rich cements (A) are non-luminescent but have a dusty appearance, and did not enter the gastropod mould. Within the mould (large arrow) the spar sequence comprises non-luminescent Stage (B), and brightly luminescent scalenohedral spars, followed by later dull luminescent burial spars (Stages E and F) which were fed by the veinlet. The timing of gastropod dissolution appears in this case to have been between Stages A and B, but this is complicated by the presence of the protective micrite envelope which may have isolated the mould from the earlier cements.

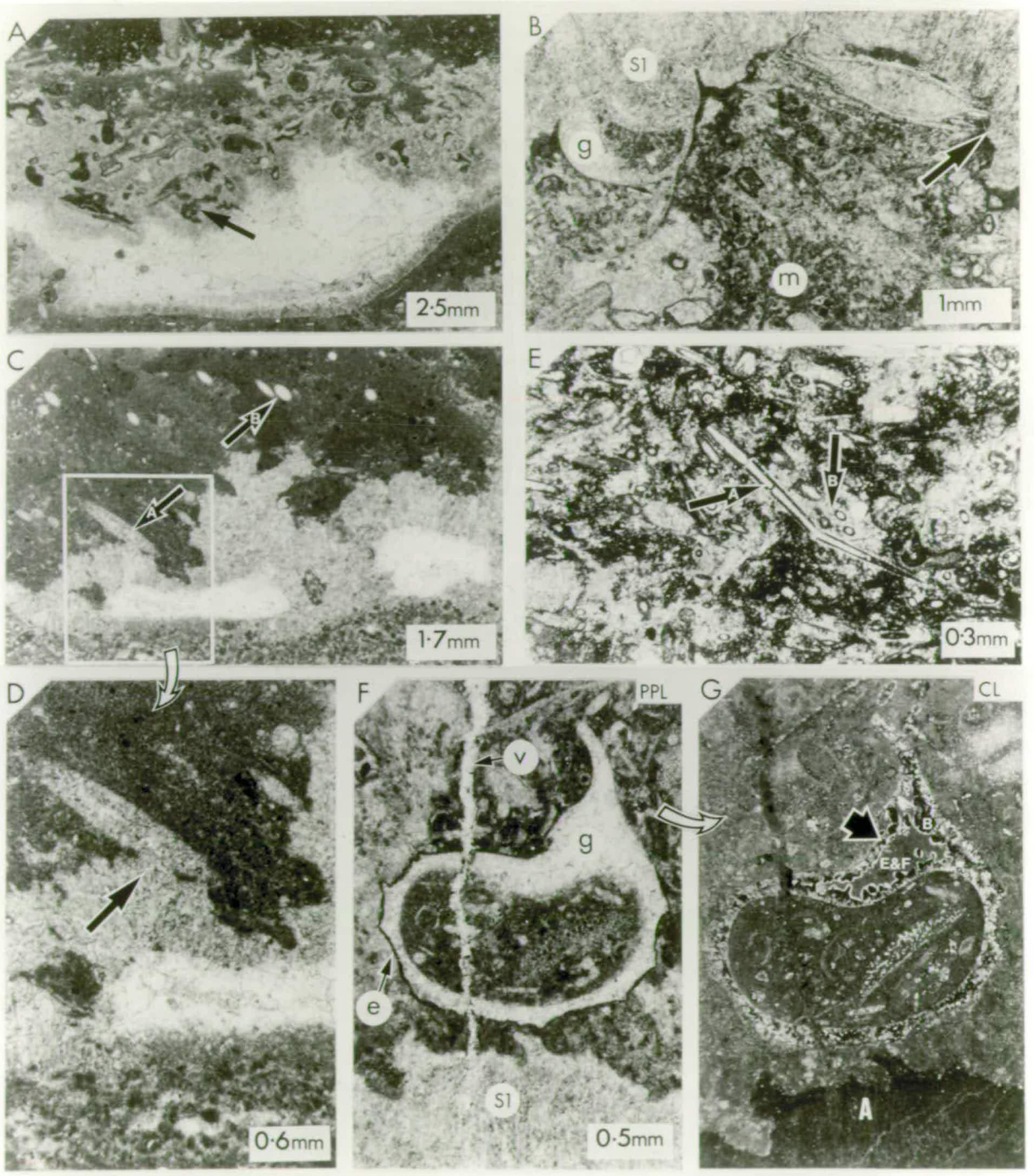
A
2·5mm
B
S1
g
m
1mm
C
A
B
1·7mm
E
A
B
0·3mm
D
0·6mm
F
PPL
v
g
e
S1
0·5mm
G
CL
B
E&F
A

Fig. 5.2 Effects of pre-Stage A dissolution on Waulsortian bank facies.

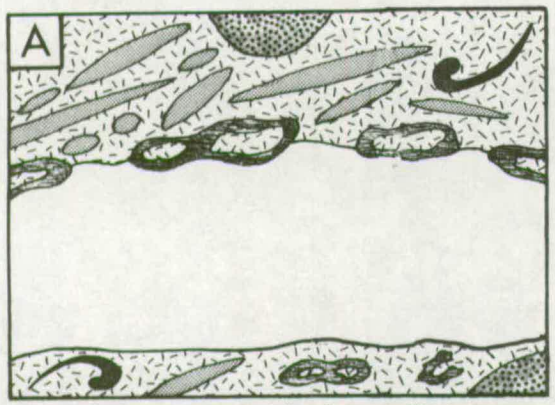

Cavity in M1 supported by fenestellid bryozoan frond and sponge spicules.

SILICA DISSOLUTION

Secondary porosity created

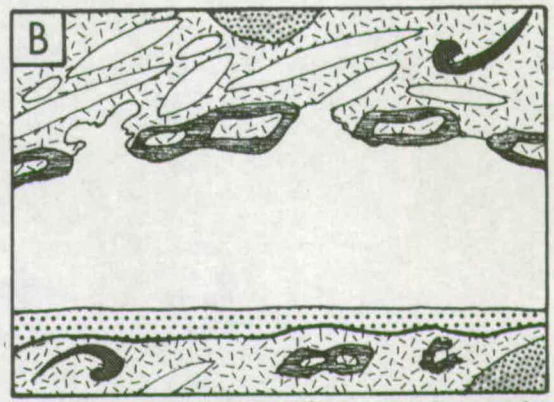

Mouldic void space created. Some collapse of roof forms geopetal M2. Incipient cementation of M1 supports most moulds.

CARBONATE DISSOLUTION

Secondary porosity enlarged

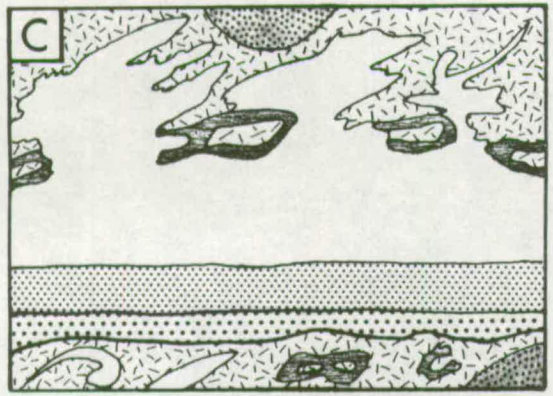

Complex pore network developed by micrite dis--solution and collapse Molluscs and bryozoans dissolved. M3 geopetal.

MARINE CEMENTATION

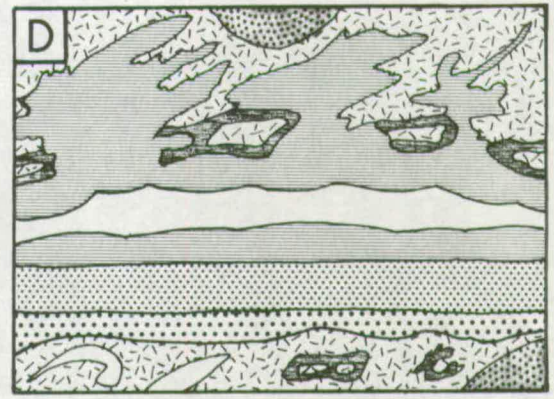

Stage A marine cement precipitated.

KEY

Bioclasts

- Bryozoan
- Siliceous sponge
- Mollusc
- Crinoid

Sediments

- M1 Primary
- M2, M3 Internal

Cement

- Stage A
- Void

CONCLUSIONS

1. Significant diagenetic modification of the Waulsortian bank facies occurred prior to the development of the first recognisable cements in the pore space. Three main episodes were identified from direct and circumstantial evidence (in order of occurrence):-
   i) Synsedimentary precipitation of intergranular cement
   ii) Silica dissolution
   iii) Carbonate dissolution.

2. The presence of a non-pervasive intergranular synsedimentary cement is inferred from several lines of evidence:-
   i) Bank facies sediments show no signs of early compaction in contrast with peri-Waulsortian facies.
   ii) The banks were able to maintain steep depositional slopes, without slumping, despite the absence of skeletal frame builders.
   iii) Synsedimentary sediment-filled fractures occasionally developed before the first recognisable cements in the bank facies indicating that the sediment was already partially lithified. However, significant volumes of sediment must have remained uncemented in order to fill these fractures, i.e. the synsedimentary cements were non-pervasive. The development of polymuds is further evidence of the patchy distribution of these cements.
   iv) No evidence of layered cement crusts of the kind postulated by previous authors occurs within the Craven Waulsortian. Furthermore, the development of lenticular lumps of firm bank-type M1 sediment in bank-margin facies transitions indicates a highly locallised cement distribution (cf. Miller 1986).

3. Dissolution of siliceous hyalosteliid sponge spicules, leading to the development of mouldic voids, is ubiquitous in the bank facies. In many cases, mouldic voids remained open, probably

supported by synsedimentary cement. In others, silica dissolution resulted in collapse of the primary sedimentary fabric, and the development of digitate cavity margins and internal sediment layers.

4. Carbonate dissolution, primarily of M1 micrite but also skeletal carbonate grains, resulted in the development of extensive secondary porosity and extended by the aggressive fluids to form complex clotted micrite and spar textures in the vicinity of the original cavity margins. In some cases, the resultant fabric was up to 60% void space, and must have been supported, at least in part, by the synsedimentary cements. The exploitation of the spicule moulds during this dissolution phase is evidence that silica dissolution was prior to carbonate dissolution.

5. The changes in pore fluid pH necessary to produce both dissolution episodes could have resulted from bio-degradation of different types of organic matter (cf. Birnbaum & Wireman 1984).

6. Although evidence of synsedimentary cementation and silica and carbonate dissolution is ubiquitous in the bank facies, similar episodes apparently did not occur in the peri-Waulsortian facies. All are most probably related to the biological controls which seem to have resulted in buildup accretion.

CHAPTER 6
STAGE A: INCLUSION-RICH ISOPACHOUS CALCITE CEMENTS

Isopachous to sub-isopachous layers of inclusion-rich calcite are the first directly observable sparry cements in the solution-modified primary porespace of the bank facies, and also in some of the original primary porosity which was unaffected by the early dissolution episodes.

Stage A cements are commonly interbedded with internal sediments containing marine bioclasts, and some are microbored and/or micritised. They are further characterised by closely-spaced substrate-normal or distally divergent inclusion trails along with substrate-parallel zones of varying inclusion density (Fig 6.1E).

Cement layers are composed of crystal mosaics which exhibit four different crystal habits. Mosaics may be transitional from one crystal habit to another.

6.1 CRYSTAL MORPHOLOGY OF STAGE A CEMENTS*

The main characteristics common to all varieties are their patterns of substrate-parallel and substrate-normal or divergent inclusions, which cross-cut intercrystal boundaries and have a strong resemblance to textures observed in modern fibrous cements. Fibrous crystals themselves are not observed. Four distinct crystal habits occur:-

a). Botryoidal mosaic (Fig 6.1 A&B; Fig.6.3; Fig6.6)

Botryoidal mosaics are thin sequential, sub-isopachous, centripetal layers consisting of a series of small coalescing botryoidal crystals which show sweeping undulose extinction and contain distally divergent trails of inclusions.

Botryoid surfaces are smooth and distally convex giving a scalloped appearance to the centripetal layers. Some regions of the mosaics may have areas where the distal surface becomes irregular

* Subsequently termed 'crypto-fibrous calcite' (CFC). See p. 92

and appears degraded. Boundaries between individual botryoids are often infiltrated by dense micrite which otherwise forms a concentric crust on the distal surface of the cement layer. Apart from micrite crusts, successive cement layers may also be separated by geopetal sediments. (Fig 6.3).

Botryoidal mosaics are always covered by a micrite crust or layer of internal sediment, and where present, are always the first recognisable cement in the sequence.

b). Bladed mosaic (Fig 6.1 C&D)

The commonest form of Stage A cement layers are centripetal rinds consisting of a mosaic of bladed calcite. Crystals contain closely-spaced inclusion trails which may be divergent near the substrate, tending distally towards substrate normal. There are also substrate-parallel inclusion-rich zones which cut intercrystalline boundaries within the mosaic and have scalloped, convex distal margins. The intercrystalline boundaries are often very irregular and are least well-defined in those examples with the highest inclusion density.

Bladed crystals are length-fast with sweeping undulose extinction. The dimensions of crystals are in the order of hundreds of microns in the c-axis direction, reaching a maximum of 2mm, with maximum crystal width of 0.7mm.

c). Irregular mosaic (Fig 6.1 E&F)

Restricted and often laterally impersistent, the crystal habits within these mosaics are obscure and irregular. Sweeping extinction is observed and is occasionally substrate-parallel. Intercrystalline boundaries are very irregular. These cements are often substrate selective on bioclasts protruding into voids, and are volumetrically insignificant.

Relict fibrous textures in the form of centripetal inclusion banding and substrate-normal to slightly divergent inclusion trails are strongly developed within irregular mosaics. Distal surfaces of

irregular mosaic layers appear superficially smooth, but close examination reveals a microscopically jagged surface suggesting the presence of composite crystals (cf. Sandberg 1985, Fig. 11).

d). Radiaxial calcites (Figs. 6.1 G&H; Fig. 6.5)

(Radiaxial fibrous calcite, RFC of, Bathurst 1971; Kendall & Tucker 1973; Kendall 1985).

Radiaxial calcites form a mosaic of length-fast bladed crystals, which may be composed of several distally divergent sub-crystals with distally convergent fast vibration directions. Cleavage and twin planes are distally concave. Sweeping extinction is observed under crossed polars but tends to be more uniform within individual sub-crystals.

Radiaxial calcites contain noticeably fewer inclusions than any other Stage A cements.

Inclusion patterns are identical to those in the bladed mosaic type (see above) occur although less well-developed. Aditionally, inclusions may be concentrated along cleavage and twin planes (cf. Kendall & Tucker 1973).

Radiaxial calcites account for only a small proportion of all Stage A cements in the Craven Waulsortian, although they are very much more common in comparative material from the Irish Waulsortian. With the exception of coalescing botryoids, lateral transitions between different crystal types within single cement layers are common (Fig. 6.5). In most cases, these transitions are independent of changes in crystal substrate.

6.2 COMPOSITION OF STAGE A CEMENTS

6.2.1 Major and trace elements

The mean composition of Stage A cements is given in Table 6.1. Microprobe analyses of clear radiaxial calcite and other more turbid Stage A cements were compared with those of non-luminescent crinoid ossicles (Table 6.2). Such crinoid allochems were used for

comparison as they are believed to have had an original high-Mg calcite (HMC) mineralogy (Lowenstam 1961), and non-luminescent grains are typical of least diagenetically altered marine carbonate (cf. Given & Lohmann 1986).

The analyses in Table 6.2 show that the magnesium content is related to the amount of inclusions in the cements. Turbid Stage A cements have similar levels of magnesium to crinoid ossicles whereas clearer cements, particularly radiaxial calcites, have much lower levels of magnesium.

Microprobe studies show that all the Stage A cements are non-ferroan and non-manganoan (FeO<0.01 wt%; MnO<0.01 wt%). This is supported by their pink colour after staining, and non-luminescence.

Botryoidal mosaics are alone in containing detectable silica, and their associated micrite crusts have even higher SiO_2 values (Table 6.4). The source of the silica is uncertain, but the fact that it is not detectable in other Stage A cements suggests that it is not diagenetic. Most likely the silica resides in traces of detrital clay minerals incorporated into the cement during growth in voids open to the buildup surface.

6.2.2 Stable Isotopes

Stable carbon and oxygen isotope composition was determined in three samples of inclusion rich isopachous calcites (Table 6.3). Care was taken to sample only from those (rare) areas of Stage A which were diagenetically uncontaminated as indicated by their non-luminescence.

6.2.3 Cathodoluminescence

Stage A cements are particularly susceptable to diagenetic alteration. Those areas of the crystal mosaics which have undergone the least diagenetic alteration are non-luminescent or very rarely may have a slightly blotchy luminescence. Individual crystal boundaries are thus rarely identifiable in unaltered Stage A cements when viewed with CL. However, centripetal inclusion patterns which cut across crystal boundaries are commonly visible. The four

Figure 6.1 Crypto-fibrous calcite types

A and B; Botryoidal mosaic

A Photomicrograph showing a thin isopachous layer of botryoidal mosaic (arrow 1). A micrite crust coats the botryoidal mosaic, but is discontinuous (arrow 2) indicating a biogenic rather than a direct-precipitation origin. Thin section, bank facies, Coplow buildup:

B SEM photograph showing botryoidal crystal habit (white box). Substrate again is a fenestellid bryozoan which, in this case, is coated with extremely fine-grained micrite.

C and D; Bladed Mosaic

C PPL photomicrograph showing inclusion-rich exhibiting bladed mosaic crystal morphology. Thin section, Sugarloaf buildup:

D Bladed mosaic under crossed polars. Area outlined in white corresponds with the black box in C, and shows gradational sweeping extinction across the bladed crystal.

E and F; Irregular mosaic

E PPL photomicrograph showing strong centripetal inclusion banding in a CFC cement layer (arrowed), which is nucleated on a fenestellid fragment:

F XPL photomicrograph showing irregular CFC crystals and inter-crystalline boundaries (arrow 1). The irregular mosaic is succeeded by a layer of scalenohedral calcite of Stages B-D, showing palisade texture (arrow 2); bank facies, Bellmanpark buildup.

G and H; Radiaxial calcite

G PPL photomicrograph showing bladed crystal morphology with characteristic curved cleavage and twin planes (arrowed). Crystals are less turbid than other CFC types:

H XPL of same area showing greater extinction uniformity and strong sub-crystal boundaries (arrow) which are in contrast with other CFC types. Substrate is recrystallised M1 mudstone. Thin section, Bellmanpark buildup.

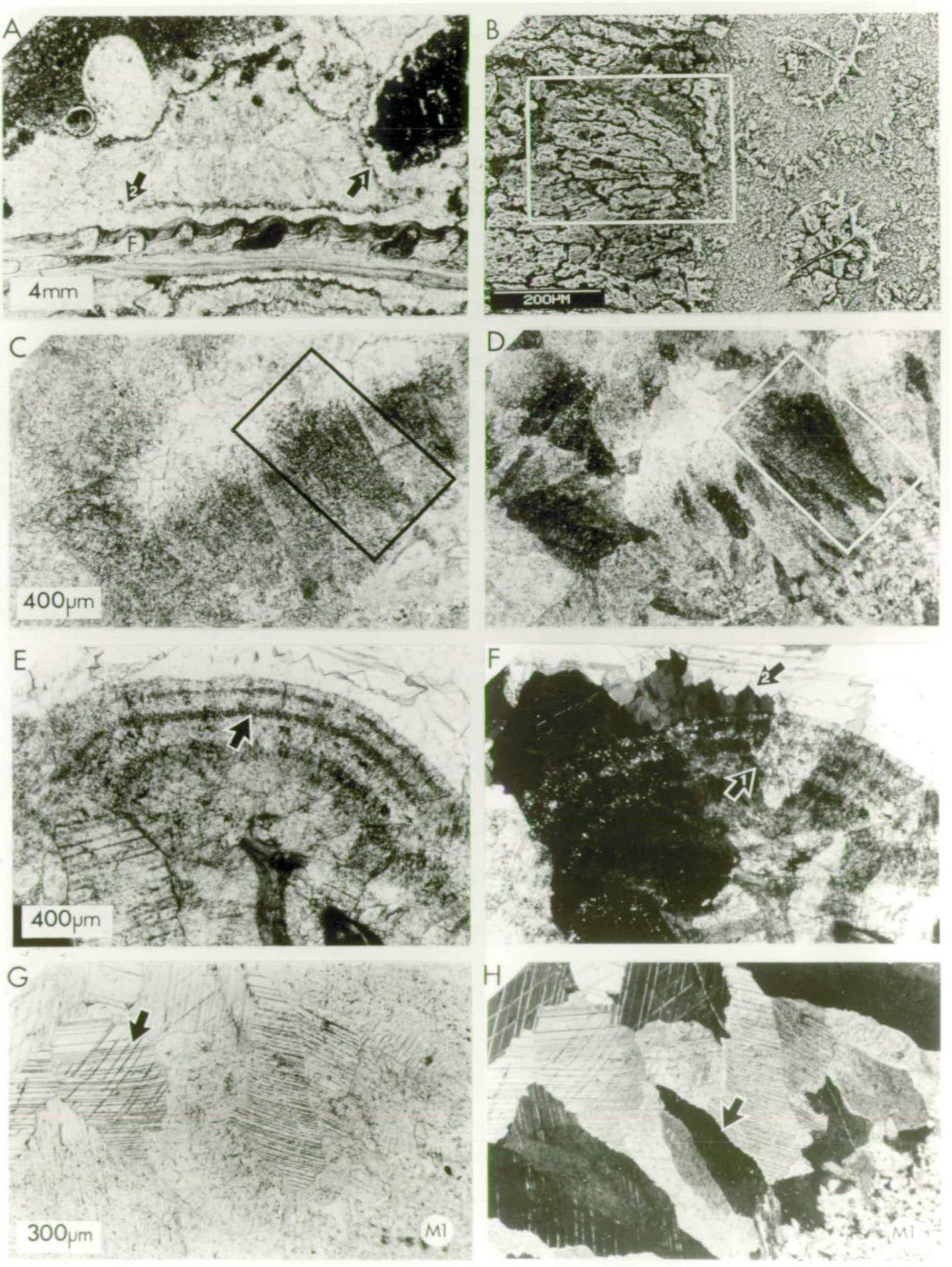
A
4mm
B
200μm
C
400μm
D
E
400μm
F
G
300μm
M1
H
M1

Table 6.1 Mean composition of Stage A cements.

Oxide	Mean wt%	S.D.	C.V.	n=18
CaO	55.36	1.11	0.02	
MgO	0.34	0.13	0.37	
FeO	0.02	0.03	1.36	
MnO	0.02	0.02	1.12	
SiO_2	0.02	0.03	1.77	

18 analyses from 7 buildups

S.D. = Standard deviation @ 95% confidence level
C.V. = Coefficient of variation

Table 6.2. Variation in MgO with inclusion density, Stage A, Crypto-fibrous calcite.

Sample	Turbid crystals MgO wt%	Sample	Clear crystals MgO wt%	Sample	Crinoid MgO wt%
SH37 (15)	0.37	WG3 (3)	0.21	NEW4 (13)	0.57
" (16)	0.50	NLH13 (38)	0.27	RI1 (16)	0.66
WG3 (2)	0.51	" (39)	0.16		
" (4)	0.59	" (40)	0.21		
" (6)	0.39	" (41)	0.22		
" (8)	0.39				
CP8 (5)	0.40				
mean	0.44±.08	mean	0.21±.03	mean	0.62±.05

different mosaic types described above are not distinguishable with CL alone, even where transitions between crystal types occur.

Table 6.3 Isotopic composition of non-luminescent Stage A cements.

Sample*	$\delta^{13}C$	$\delta^{18}O$
C 28	3.22	-2.23
GE 01	3.69	-1.23
NLH 19	3.30	-2.41
mean	3.40 $\pm$0.2	-1.96 $\pm$0.5

Analyses quoted in per mil versus PDB standard.
* Sample locality codes given in Appendix 2

6.3 INCLUSION PATTERNS

All Stage A cements characteristically display substrate-parallel zones of varying inclusion density together with substrate normal or distally divergent inclusion trails, although the development of these fabrics varies greatly from sample to sample. The substrate-parallel inclusion zones characteristically cut across cement crystal boundaries, whereas the substrate-normal and distally divergent inclusion trails stop at intercrystal boundaries. Inclusions of solid and liquid phases occur in Stage A cements.

6.3.1 Solid inclusions

Three kinds of solid inclusion have been identified:-

a) Mainly equant or tabular crystals with regular to irregular faces. Diffraction and internal reflections give these transparent crystals a pink tinge under PPL. They have high relief over the

surrounding cement crystal, and although "twinkling" occurs on rotation of the microscope stage, it is not strong enough to cause pseudopleochroism. Individual inclusions are from 4-5μm in diameter and 6-10μm in length. Long axes of tabular crystals are often aligned parallel to inclusion trails (Fig 6.2B).

b) Irregular, often dendritic inclusions 10-30μm in size. These are usually optically dense and may have a brown colouration. Some are aggregates of smaller crystals whereas others appear amorphous (Fig 6.2 B&C).

c) Rhombic inclusions; the least common inclusion type are transparent rhombic crystals up to 10μm in size (Fig 6.2C). They have high relief over the surrounding cement crystal.

The brown colouration and amorphous nature of the irregular inclusions may indicate the presence of organic matter. Kendall and Tucker (1973) found that the turbidity of similar cements disappeared or was considerably lessened after treatment with a strong oxidising agent such as H_2O_2, and suggested that this was due to the presence of organic matter. I conducted a similar experiment and found that the density of inclusions did indeed appear to decrease on application of H_2O_2 to the sample surface. However, no reaction was observed, and when the sample surface began to dry out, the inclusion density gradually increased to its former level, i.e. it appears that the apparent loss of inclusions in my experiment was purely a refractive index phenomena, with the addition of the thin film of liquid rendering some of the inclusions invisible.

The most turbid crystals have higher Mg levels (Table 6.?1), suggesting either that the inclusions contain significantly higher magnesium than the rest of the crystal, or that inclusion-rich calcites themselves contain more Mg.

It is possible that the rhombic inclusions are microdolomite similar to those described by Lohmann and Meyers (1977), although no analytical facility was available on the SEM used in this study to allow confirmation of mineralogy. However, micron-sized orange-red

Figure 6.2 Inclusions in crypto-fibrous calcite (CFC)

A Photomicrograph of bladed CFC radiaxial mosaic with characteristic curved cleavage and twin planes, showing trails of inclusions (arrowed) which are slightly divergent away from the M1 substrate and sub-parallel to the C-axis direction: PPL, thin section, Bellmanpark Quarry.

B High magnification photomicrograph of inclusions in radiaxial calcite shown in A. Different types of inclusions are arrowed:

1. Equant to tabular solid inclusions aligned sub-parallel to the C-axis.
2. Dense, amorphous, irregular inclusions.
3. Rounded fluid inclusions.

C SEM photograph of CFC showing rhombic inclusions (R) which may be microdolomites. Other inclusions have been differentially etched during preparation with EDTA and include:

2. Irregular, composite inclusions.
3. Sub-rounded ?fluid inclusions.

Strong lineament parallel to the C-axis is only visible in acid-etched preparations, and most probably reflects a relict fibrous texture. Knoll Wood buildup.

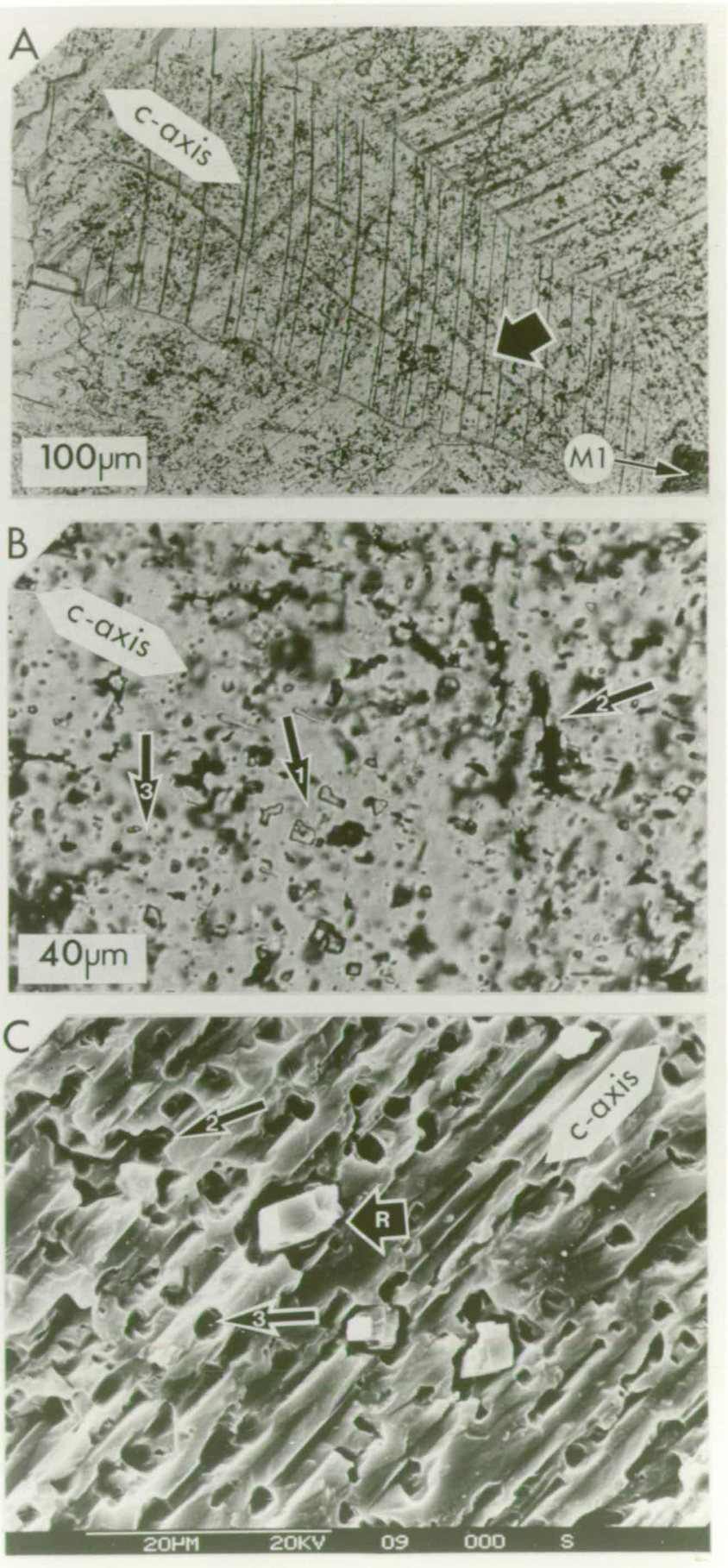
A
c-axis
100μm
M1
B
c-axis
3
1
2
40μm
C
2
c-axis
R
3
20HM 20KV 09 000 S

luminescent inclusions which could be microdolomites do occur in some Stage A cements. These were far less common than the microdolomites in the material described by Lohmann and Meyers (op. cit.).

6.3.2 Fluid inclusions

Petrographically, many inclusions are rounded and have low relief compared to the enclosing crystal. In both lightly etched and fractured SEM preparations, many sub-spherical pores are seen (Fig 6.2C), which are likely to have been fluid incluusions.

Kendall (1985) suggested that the majority of inclusions in similar cements from his study were fluid filled. This concurs with observations on equivalent cements in Irish Waulsortian buildups (Miller 1986: and my own observations on comparative material). However, Chafetz and Folk (1984) reported abundant short rod-like inclusions in comparable cement from Waulsortian mounds in Montana, which they compared with cyanobacteria present in recent travertine calcites. No convincing evidence of bacterial moulds has been found in Stage A cements in the present study.

6.4 CRYSTAL GROWTH MECHANISMS: Association of Stage A cements with micrite crusts and internal sediments

Stage A cements are commonly associated with micritisation and internal sediments. The inter-relationship of cement and micrite crusts can give information about crystal growth mechanisms and can help to explain the range in crystal morphologies developed in Stage A.

6.4.1 Micrite crusts

Crusts of optically dense micrite commonly coat the distal surfaces of botyoidal mosaic, and occasionally bladed mosaic, Stage A cements. Coating not only involves cement layers, but often also the cavity wall (Fig. 6.1A; Fig. 6.3D).

Micrite-coated cements are always the earliest recognisable cements in the sequence, though they often pass centripetally into non-crusted mosaics of other Stage A cements.

The crusts are usually irregularly spaced, although within this irregular distribution it is noticeable that they generally become less frequent towards cavity centres.

In CL, the micrite usually luminesces, often quite brightly, in stark contrast with the non-luminescent Stage A cements. Such micrite is characteristic of Phase D (photic zone) buildups (Lees & Miller 1985).

The distribution of micrite crusts within a void is often patchy and laterally discontinuous. They are usually irregularly spaced. Thickness is inconsistent, even within a single layer, and may reach a maximum of 0.3mm.

The micrite crusts also often form prominent bands which are irregularly inter-layered with poorly-developed botryoidal mosaics on a microscopic scale, giving the impression of a meshwork texture (Fig. 6.1A). Distal surfaces of micritised cement crystals are usually irregular in shape, often with sharp embayments (Fig. 6.3D).

Within the buildups, micrite crusts are best developed in large interconnected void networks such as those supported by fenestrate bryozoans. However, not all such cavities necessarily contain micrite-coated cements.

6.4.1.1 Interpretation of micrite crusts

Great difficulties are experienced in distinguishing sedimentary or particulate micrite from physico-chemically precipitated micrite (Mountjoy & Riding 1981; James et al. 1976), especially in situations such as the present study where subsequent diagenetic alteration of the micrites is commonplace.

Micrite crusts have three potential origins:-

a) suspension fallout mud

b) Cryptocrystalline cement (Macintyre 1984; Friedman 1985)

c) Biogenic micritisation

a) Suspension fallout mud

Although often laterally discontinuous, the micrite crusts are developed equally on cavity walls and roofs as well as floors, indicating a lack of gravitational influence on their development. This would tend to argue against a suspension fallout origin as sediment films would be expected to develop preferentially on cavity floors. However, relatively abundant trace-element silica was detected in the micrite crusts (in common with the M1 mud), suggesting that some particulate silicate minerals may have been present. Silica was also detected, although at lower concentrations, in botryoidal mosaics (Table 6.4), while being absent in other Stage A cements which are not coated by micrite. No direct evidence of any finely particulate silicate minerals occurs, and while the SiO_2 may reflect suspension fallout, it may just as easily have been of authigenic origin.

b) Cryptocrystalline cement

Friedman (1985) reviewed the problems of classifying fine-grained carbonate components as cements. These stem largely from the grain size of the material which is usually so small that it prevents observation of individual crystals. Centripetal layers of micrite similar to those in this study have been reported by Macintyre (1984) and recently by Enos (1986). In both cases, the layers were generally isopachous and continuous (Enos used the term, "isopachous mud"). This is seen as being indicative of cementation in water-saturated pores (Enos op. cit.). However, the micrite crusts in this study, although generally developed on an essentially uniform substrate of Stage A cement, are characteristically discontinuous and patchy (Fig. 6.1A), and it therefore seems unlikely that they originated from physico-chemical precipitation.

c) Biogenic micritisation

Micritisation of carbonate grains to produce centripetal replacements or envelopes is a common feature of modern and ancient

Table 6.4. MgO and SiO_2 content of Botryoidal mosaic and associated micrite crusts.

Botryoidal cements				Micrite crusts			
Sample		MgO wt%	SiO_2 wt%	Sample		MgO wt%	SiO_2 wt%
CP	(1)	0.36	0.07	CP1	(3)	0.34	0.10
"	(4)	0.46	-	"	(5)	0.26	0.13
"	(6)	0.46	0.08	"	(7)	0.40	0.07
"	(8)	0.58	0.05	HN300	(24)	0.20	-
"	(9)	0.39	0.08	SU11	(13)	0.41	0.31
HN300	(11)	0.23	-	HN300	(8)	0.24	0.01
"	(19)	0.34	-	"	(9)	0.21	-
"	(22)	0.36	-	SU11	(9)	0.29	0.67
"	(23)	0.30	-	WG3	(5)	0.27	0.46
SU11	(12)	0.49	0.01	WG3	(7)	0.42	-
mean		0.40	0.03	mean		0.30	0.18

sediments and is generally attributed to the activity of micro organisms, particularly algae (Taylor & Illing 1969; Bathurst 1975).

Four reasons suggest that the micrite crusts in the Stage A cements were also of biogenic origin:

i) Micrite layers and algal encrustation appear together, and only in Phase D Waulsortian facies, the only phase considered to be entirely in the photic zone (Lees & Miller 1985). Micritised grains also occur in the matrix, and these often exhibit tube-shaped microborings (cf. Bathurst 1975, p. 381-388).

ii) The irregular interface which commonly occurs between the micrite and underlying botryoidal mosaics is suggestive of micritisation (cf. Enos 1986, Fig. 6c).

iii) Micrite crusts tend to become less common towards cavity centres, indicating that progressive restriction of the pore system with Stage A cementation may have limited and eventually suppressed the activity of micritising organisms.

iv) The micrite layers are encrustations as opposed to sediment coverings or cement accretions. The irregularly interlayerd cement and micrite "meshworks" are interpreted as a result of intermittent micritisation during pauses in precipitation of botryoidal mosaics.

6.4.1.2 Subsequent diagenesis of Micrite Crusts

Micrite crusts generally exhibit brighter luminescence than the Stage A cements and matrix grains with which they are associated. The luminescence is, however, patchy and variable in colour and intensity, and may extend in a diffuse manner, into the adjacent Stage A cements. Furthermore, these diffuse luminescent layers may be transgressive across micrite crusts and cements alike. They are interpreted as neomorphic products (see Chapter 17) and indicate that very few, if any, of the micrite crusts have retained their primary fabrics and mineralogy. In SEM, the micrite crusts consist of an irregular mosaic of interlocking, anhedral microspar crystals,

Figure 6.3 CFC cements associated with internal sediments. All PPL photomicrographs.

A Photomicrograph showing a thick sequence of laminated geopetal sediment interbedded with thin layers of CFC botryoidal mosaic in a large cavity. The cavity walls are coated with sub-isopachous CFC cement (s) which exhibits strong substrate-parallel inclusion patterns. White box depicts the area of B. Stained thin section, bank facies, Sugarloaf buildup.

B Layers of botryoidal in same sample mosaic mark the successive levels of the cavity floor during episodic influx of internal sediments. Successive layers of botryoidal mosaic coalesce at the cavity walls to form thicker CFC layers (arrow) with inclusion-rich bands between which correlate with the episodes of sediment influx.

C Thin layers of botryoidal mosaic (B) cements in the same cavity-fill as A and B above. Cement layers often contain clotted micrite and peloids (P).

D Micrite crusts developed on botryoidal mosaic cements. Arrows show:
1. Irregular surface underlying a micrite crust, indicative of micritisation by micro organisms.
2. Irregular interlayering of micrite crusts with poorly developed botryoidal mosaic crystals forming a meshwork texture.

Bank facies, Knoll Wood buildup.

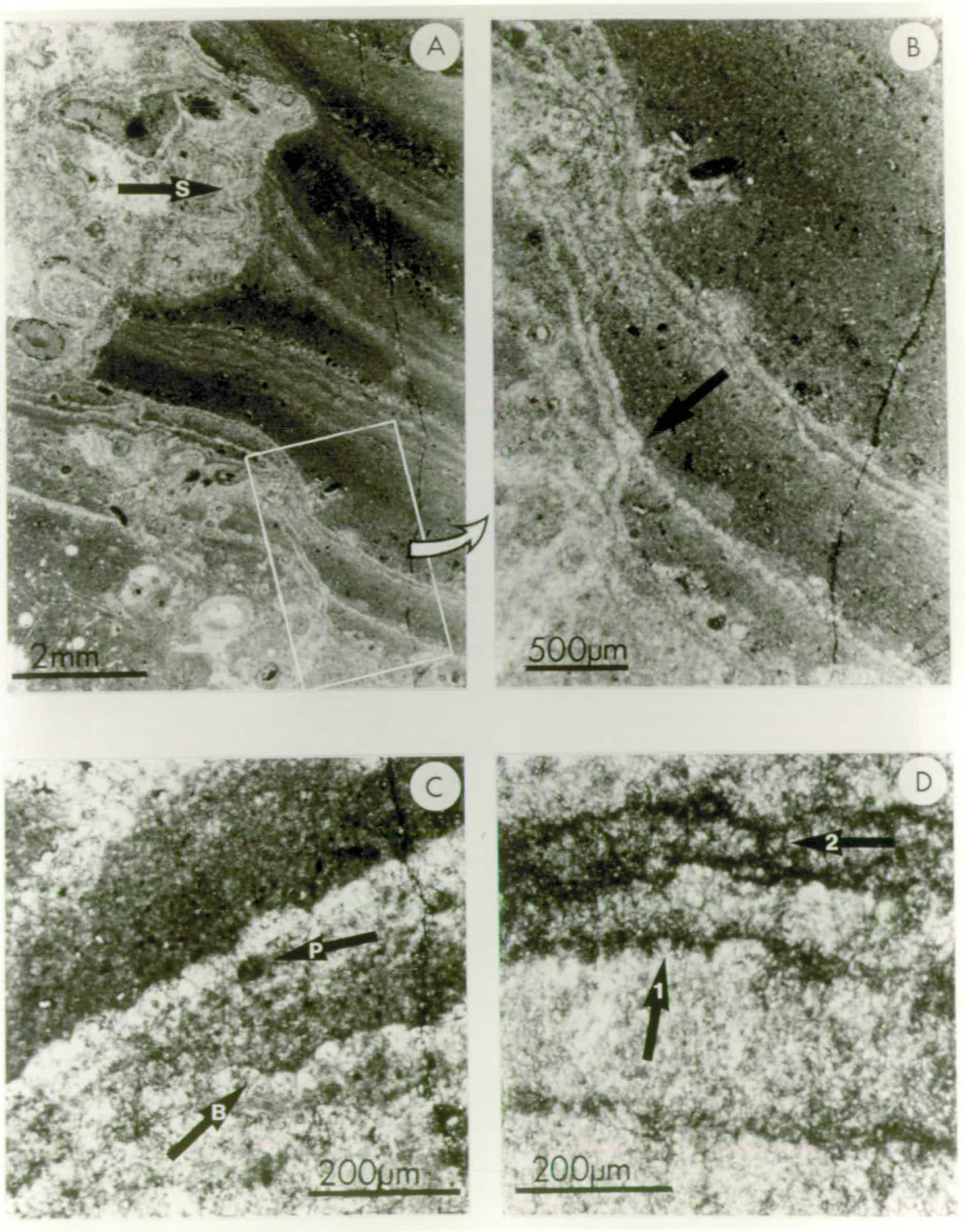
A
S
2mm
B
500µm
C
P
B
200µm
D
2
1
200µm

characteristic of neomorphism. The micrite crusts must therefore have been selectively replaced by later diagenetic phases.

6.4.2 Internal Sediment Interlayered with Botryoidal Mosaic

The relationships of geopetal sediment and Stage A cement can be used to shed light on some aspects of growth mechanisms and cement fabrics in Stage A.

In Fig. 6.3, a thick sequence of laminated internal sediment was interbedded with thin centripetal layers of Stage A botryoidal mosaic cements.

Development of the thin centripetal cement layers was periodically interupted by sediment influx. Successive cement layers mark the changing position of the cavity floor as it was progressively raised by new generations of internal sediment. At the cavity walls, in areas which lay above the geopetal sediments, continuous cementation occurred, developing a single, thin sub-isopachous cement layer of bladed to irregular Stage A mosaic (S in Fig. 6.3A). Strong centripetal inclusion banding occurs within this cement, and the inclusion-rich bands correspond with successive sediment layers (Fig. 6.3B). As a result of the progressive infilling of the cavity, the number of centripetal zones within the sub-isopachous layer S, increases upwards as successive botryoidal mosaic layers coalesced at the cavity walls (Fig. 6.3B).

In this example, botryoidal cements only occur where cement growth was terminated by sediment influx. However, above the level of internal sediment, bladed crystals developed. These contain bands depicted by inclusion zones which correlate with the botryoidal layers. This suggests that the botryoidal crystals represent a restricted early phase in the development of the bladed mosaic.

Similar textures were observed in micritised botryoidal mosaics. Where micrite crusts are absent or less frequent, cement layers are composed of a mosaic of bladed crystals, some of which have divergent inclusion trails near the substrate tending towards substrate-parallel in distal portions of the crystal. The early divergent inclusion trails may represent original botryoids which, being unaffected by micritisation, were able to develop into larger

crystals. Gradual interference from adjacent crystals would tend to favour substrate-normal crystal growth towards the increasingly restricted free porespace at the cavity centre. This could explain the decrease in divergence of inclusion trails in distal portions of the crystals. The restricted size range of botryoidal crystals and the fact that they are only found in close association with micrite crusts and layers of internal sediment lends support to this hypothesis.

6.5 DISTRIBUTION OF STAGE A CEMENTS

With the exception of rare and poorly-developed examples in rare grainstones in the peri-Waulsortian facies and Peach Quarry Limestone (PQL), Stage A cements are confined to the Waulsortian bank facies. No Stage A equivalents occur in the packstones and wackestones of toe, flank and interbank facies, confirming the observations by Miller (1986).

Within the bank facies, Stage A cements are best developed in the large interconnected pores of the complex void network, but also occur in all other porosity types independent of void size. However, many intraskeletal voids and sponge spicule moulds do not contain Stage A cements. Such voids tend to be distant from the main interconnected void network, or in the case of intraskeletal voids, have intact shells or micrite envelopes.

6.6 DISCUSSION

In this discussion it is intended to address three main questions:

1. In what diagenetic environment did Stage A cements precipitate?
2. Which process or processes were responsible for the wide range of textures exhibited by Stage A cements?
3. What were the controls on the distribution of Stage A?

The original descriptions of radiaxial fibrous calcite (and facicular optic calcite) showed bladed, not fibrous crystals. The attribution of fibrous habit arose because these cements possess

textures in the form of extinction and inclusion patterns which are strongly reminiscent of modern fibrous cements. However, fibrous crystal boundaries are not directly observed in the ancient examples, only a palimpsest fibrous texture, indicated by inclusions which presumably reflect the primary fabric.

In view of the palimpsest nature of the fibrous origin of these cements, and their forming a family or spectrum of related mosaic types, a generic name to cover the entire family would be useful. I propose crypto-fibrous calcite (CFC) for this purpose.

Although four crystal types were identified in this study, it is possible that others exist elsewhere, and the term crypto-fibrous calcite need not be confined to these cases.

6.6.1 Interpretation of Stage A cement environment

6.6.1.1 Previous Work

Inclusion-rich calcite cements forming isopachous layers composed of crystals with undulose extinction, are a common occurrence in depositional or early diagenetic cavities in ancient reefs and other carbonate buildups (Bathurst 1959, 1982; Pray 1965; Krebs 1969; Kendall & Tucker 1973; Ross et al. 1975; Davies 1977; Walls et al. 1979; King 1984; Walls & Burrowes 1985; Prezbindowski 1985; Miller 1986; and numerous papers in Schroeder & Purser 1986). The occurrence of such cements in close association with encrusting blue-green algae and internal sediments has been invoked as evidence of a marine origin by Krebs (1969). Folk (1974) attributed the development of inclusion-rich bladed and fibrous calcite to precipitation from solutions of high ionic strength, such as seawater. Similar cements have been identified from Cenozoic and Recent marine environments (see Friedman et al. 1974; Schneidermann & Harris 1985; Aissaoui et al. 1986a, 1986b: Schroeder 1986).

Four common cement types have been identified in previous work based on extinction patterns and crystal morphology:

a). Botryoidal calcite (Davies 1977): hemispheroidal masses, up to tens of centimetres in radius, composed of radially orientated fibrous crystals with concentric zones of inclusions. These are interpreted as neomorphosed aragonite cements (Davies 1977; Sandberg 1983, 1985).

b). Radial fibrous calcite (Bathurst 1975; Davies 1977; Mazzullo 1980): a fabric of crystal fibres arranged with their long axes radiating from a centre.

c). Radiaxial fibrous calcite (RFC): first described by Bathurst (1959), is identified as crystals containing sub-crystals that diverge away from the substrate but have distally convergent fast-vibration directions and corresponding curvatures of cleavage, twin lamellae and glide planes.

d). Fascicular-optic calcite (FOC) (Kendall 1977): similar to radiaxial calcite but has distally divergent fast-vibration directions which coincide with that of the sub-crystals. RFC and FOC commonly occur together in the same cavity (Kendall 1977; Chafetz 1979; Marshall 1981).

6.6.1.2 Interpretation of Stage A diagenetic environment

The cements of this study consist of a sequence of inter-related calcites which include radiaxial calcites and equivalents of radial fibrous calcites. FOC, and botryoidal calcite as a replacement of former aragonite, were not observed herein.

The following petrographic, geochemical and isotopic data collected in this study indicate that Stage A cements were precipitated from oxic pore-waters in the marine phreatic environment:-

a). Stage A cements are often interlayered with geopetal sediments which contain marine bioclasts.

b). Some Stage A cements (as well as sediment grains) are micritised or micro-bored, probably by micro-organisms. Such features are common in modern and ancient marine carbonate sediments. (Fig 6.3 D).

c). Isopachous to sub-isopachous layering of CFC cements is indicative of a phreatic environment.

d). Prior to any subsequent diagenetic alteration, the Stage A cement crystals were fibrous to bladed and inclusion-rich. This crystal form is ascribed to precipitation from solutions of high ionic strength such as sea water (Folk 1974).

e). Similar cements have been identified from Recent marine environments (see Friedman et al. 1974 for discussion).

f). The low levels of Fe^{2+} and Mn^{2+} as indicated by CL, staining and microprobe analyses can be attributed to precipitation from oxidised waters (Curtis 1978; Meyers 1978; Grover & Read 1983; Czerniakowski et al. 1984; Walkden & Berry 1984a).

g). Levels of magnesium in the cements are similar to those in crinoid ossicles which were originally composed of high-Mg calcite (HMC). This carbonate species is precipitated from normal marine to hypersaline solutions (Folk 1974). There are no signs of aragonite cements. Sandberg (1983) has indicated that the Lower Carboniferous was a period during which aragonite cements were less likely to precipitate in the marine environment.

h). The isotopic composition of Stage A cements is consistent with values for Lower Carboniferous marine calcites (Veizer & Hoefs 1976). The values are comparable with other ancient examples of marine cements and sediments, including inclusion-rich, isopachous radiaxial fibrous calcite cements from the Waulsortian of the Sacramento Mountains (Meyers & Lohmann 1985) and Eire (King 1984). They are also comparable with Holocene submarine HMC cements and sediments from Jamaica (Land & Goreau 1970). The $\delta^{13}C$ values of Stage A lie

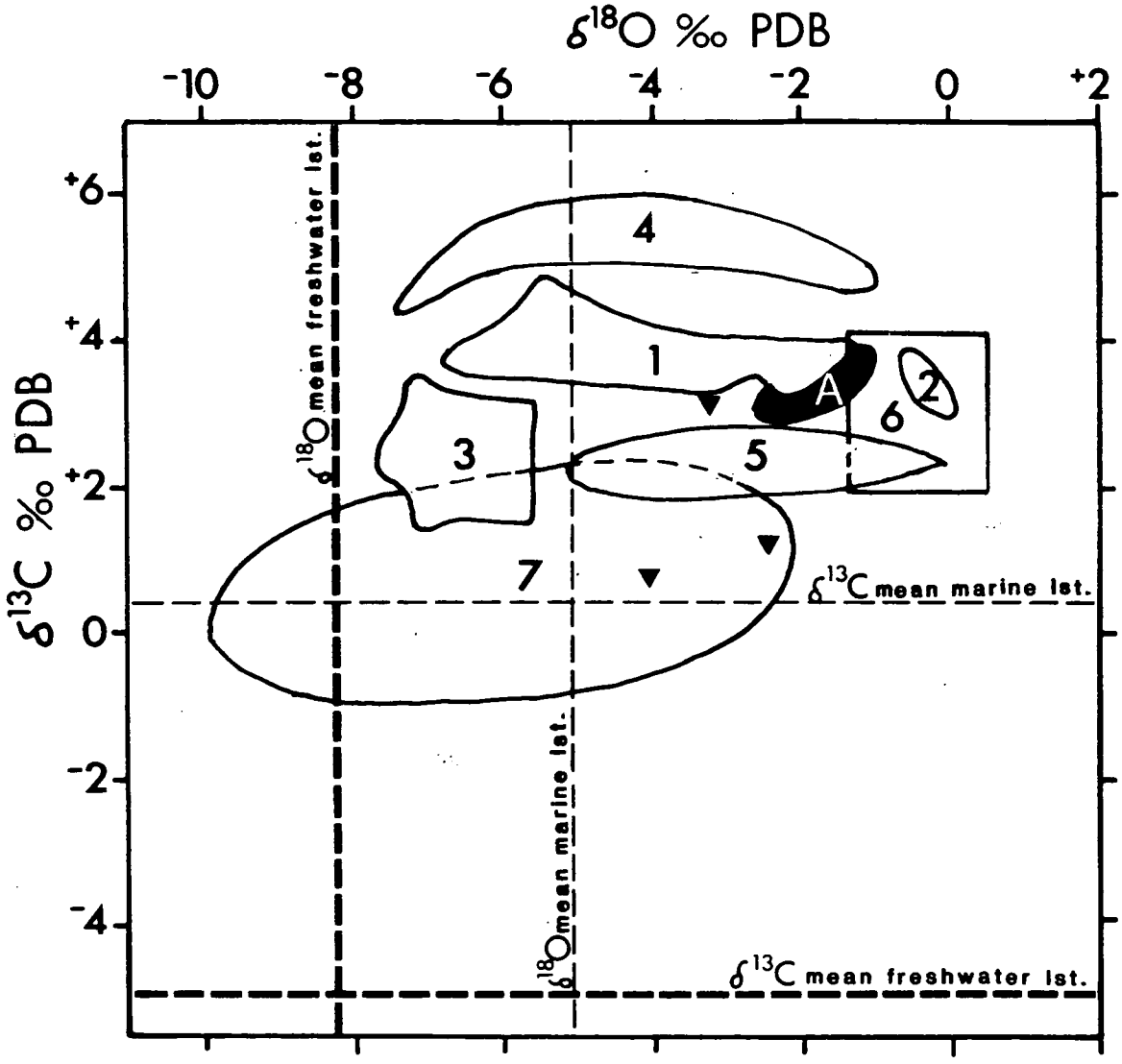

Figure 6.4. Plot of $S^{13}C°/_{oo}$ and $S^{18}O°/_{oo}$ for Stage A marine cements of this study compared with marine cements and mean limestone values from other studies. (A) CFC marine cements from this study; (1) Marine radiaxial calcite, Waulsortian buildups, New Mexico. Meyers & Lohmann 1985; (2) Waulsortian marine isopachous cement, Eire. King 1984; (3) Marine radiaxial calcite, internal sediments and bioclasts, Devonian reefs, Canada. Walls et al. 1979; (4) Submarine cements and internal sediments, Pennsylvanian-Permian reef, Canada. Davies 1979; (5) Marine radiaxial calcite, mid-Cretaceous rudist reefs, Mexico. Enos 1986; (6) Holocene submarine Mg-calcite cements and sediments, Jamaica. Land & Goreau 1970; (7) Average marine limestones, Hudson 1977; ▼Submarine cement, Mississippian, Illinois. Choquette 1968; Fresh and marine-water mean isotopic values from Keith & Weber 1964. Redrawn with additions from Walls et al. 1979 and Meyers & Lohmann 1985.

within the range of submarine cements in modern reefs ($^{+}2.0$ to $^{+}4.5$ $\delta^{13}C$°/₀₀ PDB, Davies 1977).

A comparison between the isotopic composition of Stage A and those of other marine cements from the literature is shown in Fig. 6.4. Notably, the Stage A values are significantly different to the mean freshwater limestone isotopic composition indicated by Keith and Weber (1964) shown in Fig. 6.4.

6.6.2 Origin of CFC

6.6.2.1. Previous Work

a) Origin of textures

Within the CFC group of cements, only radiaxial calcites have received much attention in the literature, mainly because their crystal textures are so distinctive that they could not be simply assigned with other 'fibrous' calcites.

In his original description, Bathurst (1959) suggested a neomorphic origin for radiaxial fibrous calcite after acicular carbonate cement. This hypothesis was later developed by Kendall and Tucker (1973). Strong relict fibrous textures, patterns of inclusions and neomorphic textures such as irregular, sutured crystal boundaries, were cited as evidence of replacement of a precursor acicular cement. These same textures were later re-interpreted as primary by Kendall (1985) who invoked a process of split crystal growth to explain the characteristic optical properties. Sandberg (1985) also favoured a primary origin to explain the optical characteristics of radiaxial calcites.

Ross et al. (1975) believed that RFC could also develop by replacement of primary calcilutite and skeletal grains, but this suggestion was refuted by Bathurst (1977) on the grounds that the hypothesis proposed by Ross et al. had ignored substantial evidence of the cavity-filling nature of the cements and associated geopetal sediments which were occasionally cross-laminated.

b) Mineralogy of CFC cements

Bathurst (1959) believed that radiaxial fibrous calcite had initially been an acicular cement, probably aragonite. Lohmann and Meyers (1977) identified microdolomite inclusions in the low magnesium calcite (LMC) crystals using CL and microprobe techniques. They suggested that the RFC had originally been HMC and that the microdolomite inclusions were the product of a neomorphic transition to LMC. In a Recent fibrous calcite example, Videtich (1985) identified a probable HMC precursor to RFC.

Davies (1977) used trace element levels of magnesium and strontium to identify precursor HMC in similar cements.

6.6.2.2 Interpretation of CFC in this study

The evidence of a transitional series of contemporaneous cements lacking substrate control while sharing palimpsest fibrous textures suggests that the CFC cements in this study represent various stages of a neomorphic transition from a common precursor cement.

The example in Fig. 6.5 shows such a transition from irregular mosaic through bladed mosaic to radiaxial calcite within the same CFC cement layer, with inclusion density decreasing towards the radiaxial calcites. I propose that the crystals with the strongest relict fibrous textures represent the least altered end-members of the transition, with progressive neomorphism culminating in the development of the less turbid radiaxial calcite mosaics.

With this in mind, and assuming that the CFC cements represent an original HMC which has inverted to LMC (Lohmann & Meyers 1977), then it might be possible to relate magnesium levels and inclusion density in CFC cements to the degree of neomorphic alteration of the precursor cement. The magnesium levels in turbid CFC cements (Table 6.2) are higher than those of radiaxial calcites, and closer to the magnesium content of the crinoid control, compatable with the hypothesis that RFC cements are the end-member product of the neomorphic transition from HMC precursor to LMC crypto-fibrous calcites.

Figure 6.5

Photomicrographs in PPL and crossed polars (XPL), of a lateral transition between different CFC crystal types within a single Stage A cement layer. In PPL, the density of inclusions within the Stage A cement decreases away from I towards C, where less turbid CFC crystals show curved cleavage and twin planes, characteristic of radiaxial calcites. In XPL, this decrease in inclusion density is shown to correspond with a transition from irregular mosaic (I) through bladed mosaic (B), to radiaxial calcites with strongly defined sub-crystals (R): Thin section, bank facies, Bellmanpark Quarry.

Fig. 6.5

This conclusion is in agreement with Bathurst (1959) and Kendall and Tucker (1973), but signficantly not with the most recent work by Kendall (1985) and Sandberg (1985) who propose a primary origin for RFC.

It is difficult to accept Kendall's (1985) idea that radiaxial calcite developed as primary crystals by a process of split crystal growth for a number of reasons:

i) It seems unusual that the textures which prompted previous workers to call these cements radiaxial fibrous calcites, namely the patterns of inclusions, are least well developed in the classic radiaxial fibrous calcite spars. These spars are rather unlike any primary fibrous crystals in Recent examples. Sandberg (1985) commented on the lack of characteristic curved twin planes and cleavages in Recent cements which he believed to be primary radiaxial fibrous calcite. The absence of curved cleavage and twin planes in this material is critical, and suggests that such fabrics may develop later, during diagenetic alteration of the primary cement. The similarities between Sandberg's examples and radiaxial calcites from the ancient cannot be coincidental, and I am of the opinion that these younger examples most probably represent the earliest stages in the neomorphic transition.

ii) If radiaxial calcites were HMC cements as suggested by Kendall (1985), then again it seems unusual that the cements which show the best radiaxial calcite fabrics have the lowest levels of magnesium.

*Further discussions of the HMC - LMC transition are given on p.348.

iii) Sweeping extinction is one characteristic of fibrous crystal mosaics. In well-developed radiaxial calcite crystals the sub-crystals exhibit more uniform extinction than in other crypto-fibrous calcites, i.e. they have less in common with the optical properties of fibrous calcites than do other CFC crystals.

iv) Cathodoluminscence is often used to highlight relict primary textures. Under CL, separate Stage A crystal types and the associated lateral transitions are not identified. Instead, continuous

isopachous cement layers are seen. Centripetal inclusion zonation and relict fibrous textures are often highlighted by later diagenetic replacement (Lohmann & Meyers 1977) (see Chapter 17). This evidence suggests that the radiaxial calcite fabrics are not entirely primary. This then begs the question of when the neomorphic transition took place. Geochemical and isotopic signatures accompanied by CL and staining observations indicate an origin from oxidised marine waters. The fact that these characteristics were preserved after the neomorphism of the precursor cement suggests that the neomorphic process took place in equilibrium with marine ambient fluid during early diagenesis.

6.6.2.3 Precursor fabrics of Crypto-fibrous calcite

The original fabric of Stage A cements appears to have been one of isopachous to sub-isopachous layers of fibrous cements composed of interfering bundles of fibres or fibrous palisades (Fig. 6.6). This is supported by the relict textures picked out by CL, and the fact that the distally divergent inclusion trails never cut CFC crystal boundaries. The often irregular shape of intercrystal boundaries in CFC mosaics reflects a combination of the interference of the original fibrous bundles (Kendall 1985), and subsequent modification of these boundaries during neomorphism.

Botryoidal CFC cements in the present study only occur where cementation was interupted by micritisation or internal sedimentation. Crystals rarely exceeded 200μm in diameter. Where cementation occurred in cavities which received periodic influxes of sediment, botryoidal CFC is interlayered with the sediment, while bladed crystals formed in the free space above the goepetal layers. Inclusion patterns in the bladed crystals indicate that botryoids developed into less divergent fibrous bundles as competition for space increased. Zones of dense inclusions in the bladed cements correlate exactly with the layers of sediment in the base of the cavity. This is contrary to the observation of Kendall (1985) who states:
"Internal sediments always overlie inclusion-poor zones and thin layers of this cement type may occur within the internal sediment". This, however, merely implies that clear cement developed between

Fig. 6.6 Development of Crypto-fibrous Calcite crystal types

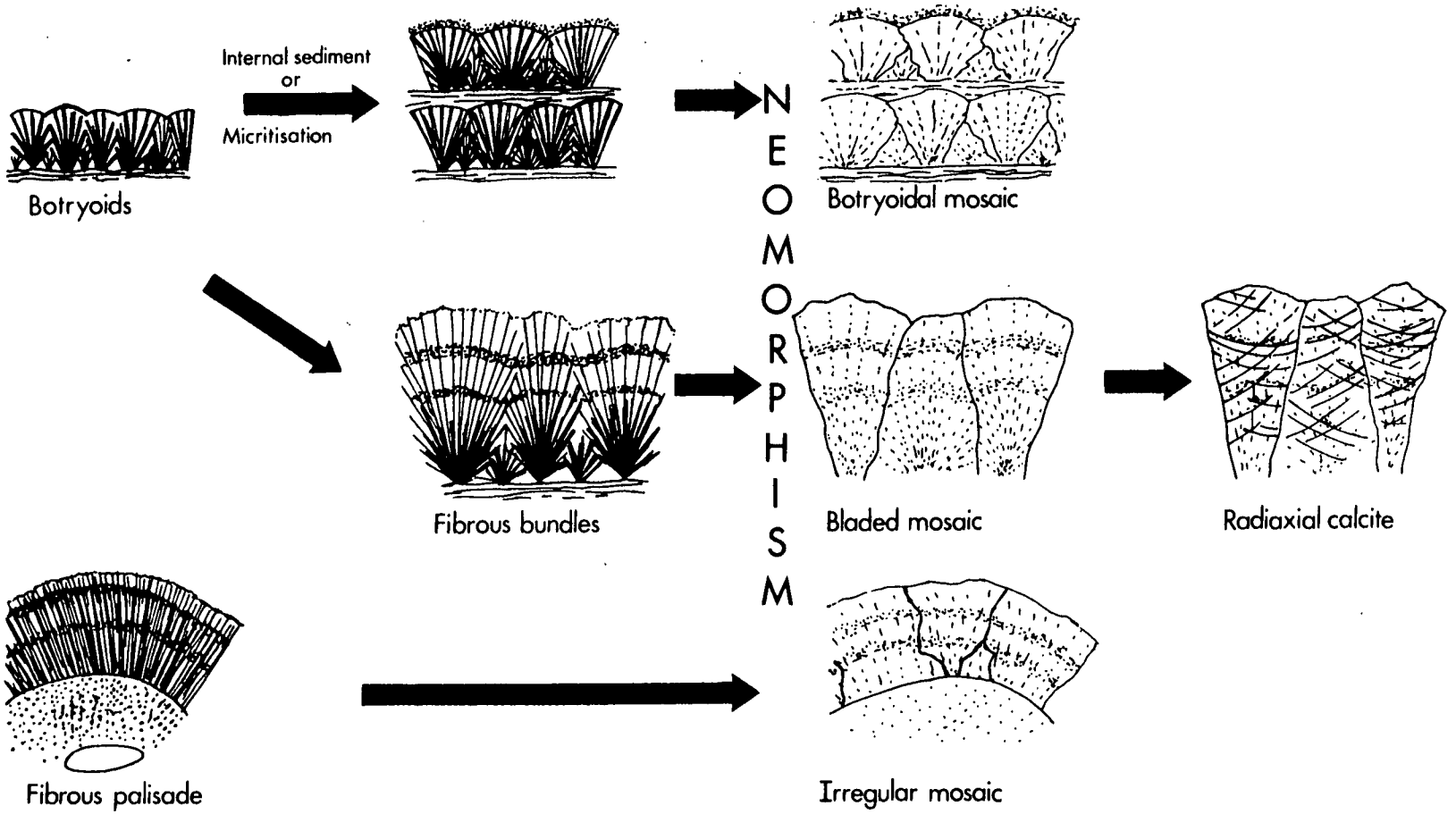

the influx of internal sediment generations, not contemporaneous with it.

6.6.3 Controls on Stage A distribution

Two questions arise from the observed distribution of Stage A cements in this study:

1. Why are Stage A cements confined to the Waulsortian bank facies?
2. Why did CFC develop in parts of the pre-Stage A pore system of the banks, but not in others?

6.6.3.1 Facies control on Stage A cements

Several factors may have influenced the facies-specific distribution of Stage A cements. Miller (1986; and in personal communications) in studying Waulsortian buildups from Eire and Craven observed that while CFC is a marine cement occurring in voids of most sizes in the bank facies, it is absent or extremely rare in peri-Waulsortian facies immediately adjacent to the bank. He therefore concluded that despite the abundance of appropriate substrates in the off-bank, pressure/temperature conditions may not have favoured precipitation of HMC on the seafloor, and since micrite production on the buildups was apparently under biological control, then possibly the CFC in the banks was also influenced thus.

A possible biogenic origin was also suggested by Van Laer and Monty (1984) who identified flabellate microbial filaments within radiaxial calcites. Sandberg (1985) and Videtich (1985) have also suggested that radiaxial fibrous calcite may have originally developed in association with the activity of micro-organisms.

If the biogenic origin postulated for CFC cements is correct, then the micro-organisms involved must have been confined to the Waulsortian bank facies.

Another important consideration is the contrasting pore systems in bank and peri-Waulsortian facies. The resistance of the buildups to compaction helped preserve a complex interconnected void-network which would have allowed circulation of large volumes of pore fluid

through the sediment and thus encouraged cementation. In the off-bank facies, however, early compaction is evident, large interconnected void networks were not developed, and it is likely therefore that pore fluid flow rates were much lower than in the banks. Such restricted pore systems would be less likely to develop thick isopachous layers of fibrous cements. Pressure/temperature controls as suggested by Miller (1986) need not therefore be invoked.

However, the lateral facies transitions which occur at bank margins (Miller 1986) are not simply a reflection of changing sediment and porosity types. Clots of bank-type M1 sediment occur within the toe facies, and some of these contain spar filled voids including stromatactoid type, which are identical to cavities in the banks, and yet Stage A is absent.

I would suggest therefore that the restriction of Stage A cements to the bank facies is a result of the presence of a large interconnected void network which allowed relatively high fluid flow rates and was therefore a favourable environment for micro-organisms which influenced CFC cementation.

6.6.3.2 Distribution of Stage A within the bank facies

Spar-filled cavities within the buildups which do not contain Stage A cements generally appear to have been isolated from the complex interconnected void system (Fig. 5.1). This was either because they occur at positions within the sediment which were not in the vicinity of the main pore network, or because they were effectively sealed by shell walls or micrite envelopes thus preventing circulation of Stage A pore fluids. The non-pervasive distribution of Stage A cements within the banks was independent of porosity type or pore dimensions, suggesting a purely spacial control on cement development. However, because of the continuation of shrinkage, collapse and sediment re-organisation during the shallow burial period, some voids may not have been formed until after Stage A precipitation.

CONCLUSIONS

1. The first major pore-filling cements, Stage A, are exclusive to the bank facies. They are interpreted as marine phreatic cements because they developed isopachous to sub-isopachous layers which are often interlayered with marine internal sediments or may be micritised, and exhibit relict textures which are suggestive of modern marine phreatic fibrous cements.

2. Stage A cements consist of a family of four contemporaneous crystal mosaic types, all of which exhibit palimpsest fibrous textures in the form of patterns of inclusions and sweeping extinction, although actual fibre boundaries are not seen. It is proposed that such spars should be called crypto-fibrous calcite (CFC).

3. The four crystal mosaic types identified are:

i) Botryoidal mosaic
ii) Bladed mosaic
iii) Irregular mosaic
iv) Radiaxial calcite

Lateral transitions between the three latter CFC types often occur within the same layer. These transitions are independent of substrate and often associated with changes in inclusion density. Radiaxial mosaics are the least turbid and have poorly developed palimpsest fibrous textures whereas in the bladed and irregular mosaics, palimpsest textures are strong. Cathodoluminescence highlights the original isopachous cement layers but cannot distinguish between the different mosaic types in lateral transitions. It is suggested therefore that the CFC cements represent the product of neomorphism of a fibrous cement precursor, common to all CFC mosaics in this study.

4. The relative limpidity of radiaxial calcites is associated with the lowest Mg level of all CFC cements. Considering the original HMC precursor mineralogy suggested in previous work, radiaxial calcites appear to have undergone greater diagenetic alteration than other CFC cements. They are therefore considered to be the final end-member

product of the neomorphic transition.

5. Botryoidal mosaics only occur where crystal growth shows evidence of interuption or impedence by influxes of internal sediment or by micritisation. In cavities where crystal growth was only restricted in certain areas, such as cavity floors receiving internal sediment layers, botryoidal mosaics only developed in the areas where cementation had been interupted. Elsewhere in the same cavity, thicker isopachous layers developed, containing lateral growth zones that correspond with the individual botryoidal layers. The botryoidal crystals therefore represent the earliest growth stages of the CFC fibrous precursor and are only preserved where cementation was interupted or short-lived.

6. Geochemical and isotopic data for Stage A are indicative of cements precipitated from oxic marine waters and are comparable with similar cements from the literature. In view of the neomorphic origin of CFC textures, it is therefore presumed that the neomorphic transition was affected in marine pore water during early diagenesis.

7. A combination of two major factors were probably responsible for Stage A cements being restricted to the Waulsortian bank facies:-

i) The resistance of the buildups to early compaction leading to the development of an extensive interconnected void network within the banks which was significantly enlarged by early dissolution episodes, thus encouraging pore fluid circulation and the precipitation of fibrous cements. Compaction and pore restriction in the off-bank facies inhibited fibrous calcite crystal growth.

ii) Micro-organisms exclusive to the banks may have induced precipitation of the fibrous precursor.

8. Within the banks, voids which were isolated from the main void network did not develop Stage A cements, the commonest examples being intraskeletal cavities and sponge spicule moulds.

CHAPTER 7

STAGES B-D: NON-FERROAN SCALENOHEDRAL CALCITE

Cements described in this section immediately post-date the Stage A crypto-fibrous calcite (CFC) marine cements. They were all passive void-fills and pre-dated vein-fed cements and brittle fractures which characterise deep burial diagenesis (Part Two). They occasionally developed within crumbly-edged fractures, which have been related to sediment dewatering during early burial (Miller 1986), and rare brittle fractures, which were probably associated with the development of neptunian dykes (Chapter 8). Generations of internal sediment often pre- and post-date these cements. These internal sediments are mainly micrite but may occasionally contain small bioclasts. Much internal sediment was derived from sediment-filled neptunian dykes which developed within the buildups during this part of the early diagenesis (see below, Chapter 8).

Two significant episodes of dissolution occurred during this period, marking major changes in the nature of the pore-filling cements. The composition of Stage B-D cements can be related to geochemical zonation observed in the shallow subsurface of modern marine sediments.

The first major textural hiatus which can be recognised in the cement sequence of all Waulsortian buildups in this study is marked by a change in crystal habit from CFC (Stage A) to scalenohedral (dog-tooth) calcite spars. In the off-bank facies, Stage A is absent and these dog-tooth calcites are the first recognisable cements, preceeding all pressure dissolution features (with the exception of early compaction seams). The boundary between CFC cements and the scalenohedral spars is usually conformable, although geopetal sediments may occur between Stages A and B.

The dog-tooth spars either exhibit palisade texture or occur as individual scalenohedral prisms. Crystals are length-fast and usually syntaxial with CFC crystals. They show uniform extinction, and are often turbid with inclusions, which are fewer than in Stage A, and apparently distributed randomly in the crystal, i.e. not

indicating palimpsest fibres as in CFC. Crystal size is usually from tens to a few hundreds of microns along the c-axis direction. Larger crystals, up to several hundreds of microns in size, developed as overgrowths, particularly on echinoderm grains.

Under CL, a characteristic 3-stage division is revealed, consisting of a black, or non-luminescent, Stage B, followed by bright luminescent Stage C and, finally, dull luminescent Stage D. This pattern of 'black-bright-dull' CL is common to all Waulsortian and associated facies in this study, and is therefore an important part of the cement stratigraphy (Fig. 7.1).

7.1 STAGE B: Non-luminescent scalenohedral calcite

Stage B cements are identified by their characteristic non-luminescence.

7.1.1 Composition

a). Trace elements

Magnesium concentrations are almost identical to those of Stage A cements (0.44 wt% MgO, Table 7.1), while iron and manganese are often undetectable in microanalysis and are always less than 0.40 wt% oxide. The lack of iron is indicated by pink colour after staining with ARS and PF, while the non-luminescence results from the absence both of CL activator (Mn^{2+}) and quencher (Fe^{2+}) ions (Table 7.1).

b). Stable Isotopes

As with Stage A, Stage B cements were greatly affected by subsequent diagenesis. Infiltration of later cements along crystal boundaries associated with significant dissolution made it difficult to obtain sufficient quantities (5 mg) of pure material for isotope analysis. Furthermore, the fact that all Stage B-D cements are non-ferroan made identification of separate stages impossible with staining alone. Photo mosaics of cements under CL were therefore used as templates for sample drilling (see Chapter 2), but this was only successful for Stages B and C.

Because of these sampling difficulties, only one stable isotope analysis of Stage B was obtained (Fig. 7.5):

$$\delta^{13}C = +3.30°/_{oo} \text{ vs PDB}$$
$$\delta^{18}O = -3.23°/_{oo} \text{ vs PDB}$$

7.1.2 Compositional Variation

Crystals of Stage B cements may contain brightly luminescent zones, varying in number from 1 to 10 or more (Figs. 7.1 & 7.2). Some are very fine hairline zones with moderate intensity orange luminescence, whereas others may be a few um across with very bright orange-yellow luminescence.

The development of these zones is usually restricted to one sample or even to a single crystal. Zones usually reflect euhedral to subhedral crystal growth and may be regularly or irregularly spaced. They are best developed in large syntaxial overgrowths on bioclasts, especially echinoderm grains (Fig. 7.1C).

The development of zoned crystals is in any case rather uncommon, and not consistent within a particular buildup. The example illustrated in Fig. 7.1C, which exhibits the largest number of zones observed in the study, is from the Old Calamine Mines, where the majority of Stage B cements are internally homogeneous. On the other hand, certain buildups (Dunnow, Porter Wood, Hall Hill) consistently have a small number of bright zones in most Stage B crystals.

Difficulties in gaining microprobe analyses of such fine zonation were overcome with the Camebax probe by defocussing the beam and viewing the specimen under cathodoluminescence. After centring on a particular zone, the beam could be refocussed for quantitative analysis (Fig. 7.2). However, the pit caused by beam damage of the sample surface (3 μm in calcite, 1μm in dolomite), controlled the minimum size of zone which could be analysed. Non-luminescent zones have compositions which are consistent with Stage B, whereas the brighter zones have high manganese levels (up to 0.1 wt% MnO) comparable with Stage C (see below), and so the bright zone CL is evidently due to an increase in Mn^{2+} activator.

Figure 7.1 Scalenohedral Stage B-D cements

A Cathodoluminescence photomicrograph showing the characteristic 'black-bright-dull' luminescence sequence of Stages B, C, and D respectively (white circles). The scalenohedral crystals exhibit palisade texture with 'saw-tooth' centripetal growth zonation (arrow X). Polished thin section, bank facies, Bellmanpark Quarry.

B&C Photomicrographs in plane polarised light and CL respectively, of Stage B cement filling a stromatactoid cavity. In B; large syntaxial overgrowths are developed on crinoid fragments (arrowed) which protruded into the cavity. In C; multiple brightly-luminescent zones occur within the non-luminescent Stage B cements. Polished thin section, bank facies, Old Calamine Mines.

D Cathodoluminescence photomicrograph showing crystal development in a Stage B syntaxial overgrowth on a crinoid fragment. Bright-luminescent zones (arrowed) show a decrease in the number of 'dog-tooth' terminations as smaller crystals merged into the larger overgrowth during growth. Polished thin section, bank facies, Hall Hill quarry.

E Cathodoluminescence photomicrograph showing euhedral scalenohedral crystals of Stage B and C (arrowed) developed in hyalosteliid sponge spicule moulds. Polished thin section, bank facies, Coplow Quarry.

A
0·5mm
B
C
D
X
B
PPL
0·35mm
C
CL
D
0·1mm
E
0·2mm

Fig 7.2. Compositional variation within Stage B cements.

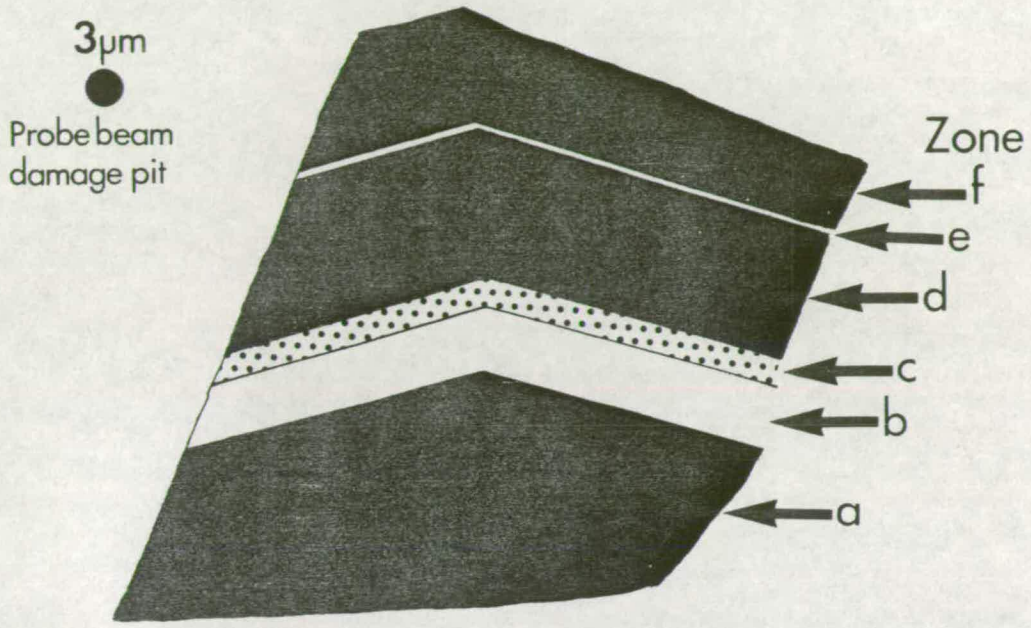

Zone
a = non-luminescent
b = bright yellow-orange luminescence
c = orange luminescence
d = non-luminescent
e = bright orange luminescence
f = non-luminescent

Microprobe analyses (in wt% oxide)

Zone	CaO	MgO	FeO	MnO	Analysis Total
a	56.61	0.25	0	0	56.86
b	55.72	0.52	0.04	0.70	56.96
c		No data			
d	56.44	0.39	0	0	56.93
e		No data			
f	56.30	0.47	0	0	56.77

Table 7.1 Mean composition of Stage B-D cements.

Stage B

Oxide	Mean wt.%	S.D.	C.V.	n=40
CaO	54.80	2.39	0.04	
MgO	0.44	0.21	0.47	
FeO	0.01	0.02	1.73	
MnO	0.01	0.02	1.64	

40 analyses from 6 buildups

Stage C

Oxide	Mean wt.%	S.D.	C.V.	n=14
CaO	56.62	2.30	0.04	
MgO	0.28	0.18	0.65	
FeO	0.03	0.04	1.24	
MnO	0.84	0.96	1.14	

14 analyses from 5 buildups

Stage D

Oxide	Mean wt.%	S.D.	C.V.	n=45
CaO	56.60	2.03	0.04	
MgO	0.29	0.24	0.83	
FeO	0.02	0.03	1.58	
MnO	0.06	0.06	1.08	

45 analyses from 8 buildups

S.D. = Standard deviation @ 95 % confidence level.
C.V. = Coefficient of variation

Table 7.2. Mean composition of substages in Stage C cement from Bellmanpark bank facies.

Substage	C1 (n=2)		C2 (n=4)	
Luminescence:	Very bright		Bright	
Oxide	Mean wt.%	S.D.	Mean wt.%	S.D.
CaO	56.70	0.20	56.95	0.30
MgO	0.15	0.05	0.06	0.01
FeO	0.01	0.02	0.06	0.06
MnO	2.29	0.36	0.62	0.06

n = number of analyses.
S.D. = Standard deviation @ 95% confidence level

7.2 STAGE C: Brightly luminescent scalenohedral calcite

An irregular dissolution surface commonly occurs between Stage B and Stage C cements throughout the Waulsortian buildups of the Craven Basin. The extent of the dissolution was often quite marked, and in many cases only small relict fragments of Stage B can be recognised, indicating that the earlier non-luminescent crystals were almost entirely dissolved. Stage C cements precipitated on the dissolution surface in optical continuity with Stage B cements, 'healing' the irregularities and restoring the scalenohedral habit.

Dissolution often propagated along intercrystalline boundaries of Stage B crystals, and also along cleavage planes. Stage C cements occasionally formed at the edges of early crumbly fractures which post-date Stage B.

A gradual decrease in inclusion density often occurs through Stage C and into the subsequent Stage D.

7.2.1 Composition (Table 7.1).

a). Trace elements and CL

Stage C usually forms a thin homogeneous layer of bright orange-yellow luminescent calcite after the non-luminescent Stage B. In larger crystals, where Stage C is better developed, compositional variation can be recognised.

In an example from Bellmanpark Quarry (Table 7.2), Stage C consists of two substages, C1 and C2, each containing many zones. Both substages exhibit bright orange-yellow luminescence, but the luminescence intensity of substage C1 is greater than that of C2. The bright luminescence reflects a significant increase in Mn over previous cements, with the highest concentration in substage C1 (MnO = 2.29 ± 0.36 wt%) producing the brightest luminescence. The levels of magnesium in Stage C calcites are lower than earlier cement stages (MgO = 0.28 ± 0.18 wt%). A noticeable drop in magnesium content occurs between Substage C1 and C2.

b). Isotopes

A single stable isotope analysis of Stage C indicates a marked change from earlier cements, with depleted values of both $\delta^{13}C$ and $\delta^{18}O$ (Fig.7.5):

$\delta^{13}C$ = +0.61°/₀₀ vs PDB

$\delta^{18}O$ = -4.98°/₀₀ vs PDB

7.3 STAGE D: Moderate to dull luminescent Scalenohedral calcite

As with Stage C, an irregular dissolution surface was often developed within the scalenohedral cements prior to Stage D cementation. In many cases, only small remnants of earlier prismatic cements survived dissolution. In the example shown (Fig.7.3), the highly irregular surface between non-luminescent Stage B and dull luminescent Stage D consists of many straight facets which are generally guided by the cleavage planes of the original crystal. I assume that Stage C was completely removed or did not develop. Deep corrosion in three dimensions is indicated by the development of re-entrant pits in the Stage B crystal which were subsequently filled by Stage D cement.

Stage D cements are recognised by their markedly duller CL intensity compared to Stage C. They exhibit moderate to dull orange luminescence with the exception of a common brightly luminescent final substage. Considerable internal compositional variation occurs, manifested in a number of substages and zones (Table 7.1). This variation is locally inconsistent, sometimes from cavity to cavity in the same sample, although the brightly luminescent final substage (Fig. 7.4, D8) is observed in many buildups.

In common with other non-ferroan scalenohedral calcites, Stage D is only identifiable with CL.

7.3.1 Composition

a). Trace elements

The average trace element composition shows relatively low manganese (MnO = 0.06 ± 0.06 wt%) compared with Stage C. Iron is also

low (FeO = 0.17 ± 0.03 wt%) and magnesium content is comparable with Stage C (MgO = 0.29 ± 0.24 wt%; Table 7.1, Fig. 7.5).

Compositional variation within Stage D is highlighted by an example from Ings Beck (Fig. 7.4). Eight substages, varying in thickness between 10 and 60μm, were identified with CL and their composition was studied in detail.

The results show the complex relationship between luminescence intensity and trace element composition in these non-ferroan calcite cements. It is apparent from this limited study that luminescence cannot be defined solely on the basis of visual estimates of intensity or in terms of activator / quencher concentrations or ratios of those elements analysed in this study.

b). Isotopes

Satisfactory samples for stable isotope determinations were not obtained from Stage D, which is only visible in CL.

7.4 TEXTURAL DEVELOPMENT OF STAGE B-D CEMENTS

Stage B-D cements developed textures which varied in response to substrate and pore geometry. Five fabric types are identifiable, of which four are common:-

7.4.1 Textures of Stage B-D cements

1. Palisade texture

The most common fabric consists of isopachous to sub-isopachous layers of prismatic crystals growing normal to the substrate. Planar compromise boundaries occur between neighbouring crystals, while euhedral "dog-tooth" terminations developed in unrestricted void space. A centripetal "saw-tooth" pattern was developed by consecutive cement stages within these palisade layers (Fig 7.1A).

Substrates were usually either CFC cements, internal or M1 sediments, or skeletal material (brachiopod, mollusc, ostracod, bryozoan). Crystal size within palisade layers is generally consist-

ent, although larger individual crystals occasionally developed as overgrowths on bioclasts (particularly echinoderms), occurring within finer grained Stage B-D substrates.

2. Euhedral scalenohedral crystals

Many smaller intraskeletal and mouldic cavities contain isolated euhedral crystals of Stage B-D cements. Consecutive growth stages follow the euhedral form and are not centripetal (Fig 7.1E). These crystals developed independently of substrate control.

3. Syntaxial overgrowths

Syntaxial overgrowths of prismatic calcites on bioclasts are particularly common in crinoid-rich facies. Figure 7.1D shows how the overgrowth developed. After the initiation of several small prisms, the number of prismatic spires decreased as crystals merged during overgrowth development (cf. Walkden & Berry 1984b, Fig. 1a).

4. Intergranular spar

In peloidal sediments from both bank and off-bank facies, sufficient porosity was maintained during early burial to allow the precipitation of Stage B-D cements. The pore dimensions were usually so small that euhedral crystals could not develop before growth of neighbouring crystals caused interference. The result was an irregular mosaic of microspar. Stage D was rarely developed in these voids, as the majority of pore space had been occluded by Stage B and some Stage C.

5. Solution Corona Overgrowths

These unusual syntaxial overgrowths on echinoderm grains are generally surrounded by micrite (see Walkden & Berry 1984b). Very few examples were found, and these were confined to off-bank crinoidal wackestones and packstones.

Figure 7.3

Cathodoluminescence photomicrograph of a large scalenohedral calcite overgrowth on a crinoid fragment. An irregular dissolution surface occurs between non-luminescent Stage B and zoned, dull-luminescent Stage D (white circles). The dissolution surface comprises short, straight faces (1) which often parallel cleavage planes (depicted by white dashed lines). The complex three-dimensional effects of the dissolution resulted in the development of a re-entrant pit in the Stage B crystal (2), which was subsequently filled by Stage D cement. Coplow Quarry.

Fig. 7.3

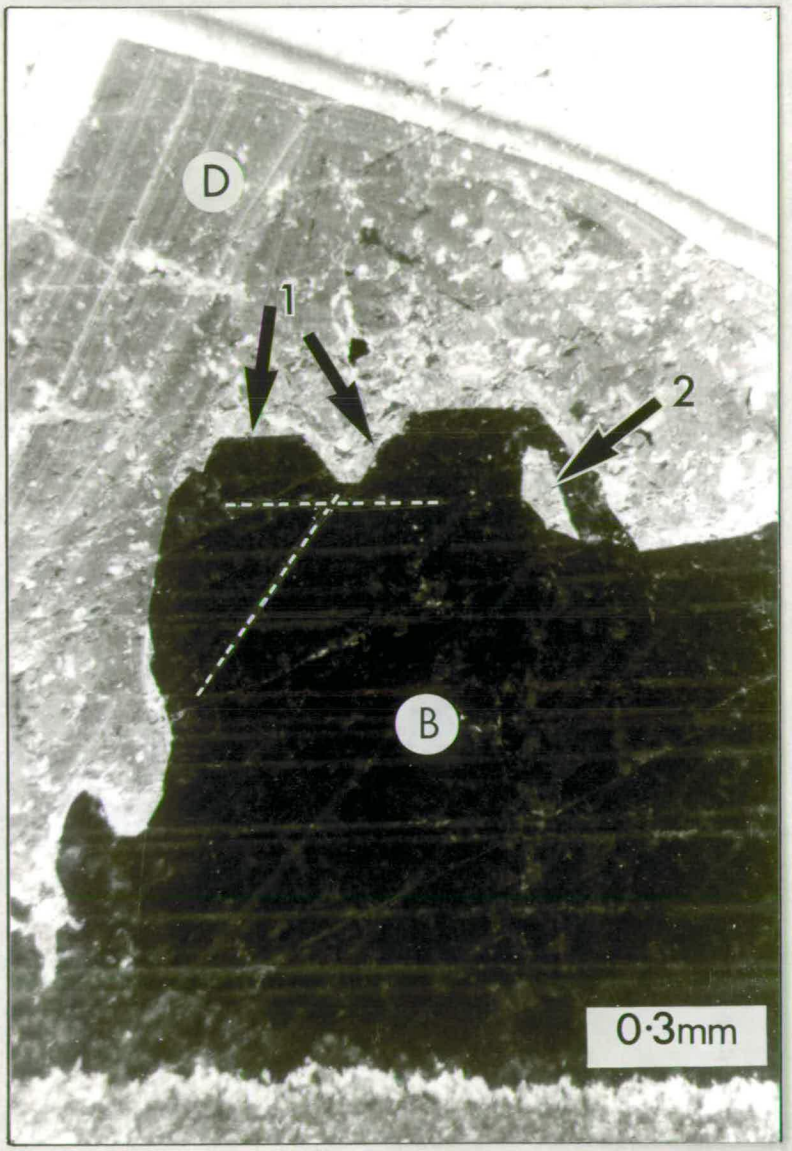

Figure 7.4 Compositional variation within Stage D in an example from Ings Beck buildup.

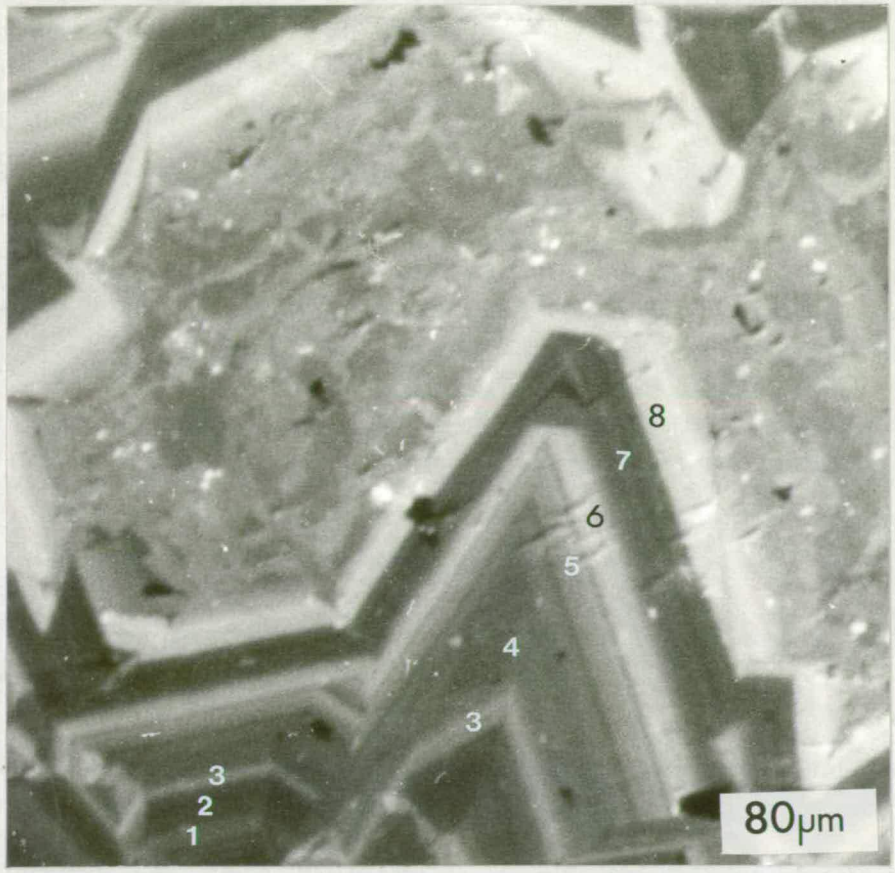

	Wt % oxide				
	CaO	MgO	FeO	MnO	CL intensity
Substage					
D1	59.02	0.44	0	0.11	Moderately Dull
D2	58.22	0.07	0	0.03	Dull
D3	58.24	0.11	0	0.03	Moderate
D4	56.51	0.13	0.02	0.12	Dull
D5	58.80	0.06	0.06	0.20	Moderate
D6	59.00	0.07	0.13	0.21	Moderately Bright
D7	58.03	0.08	0	0	Very Dull
D8	58.08	0.06	0.01	0.26	Bright

7.4.2 Interpretation of prismatic cement fabrics

There is no marked unconformity between Stage A and Stage B, and the boundary is often difficult to define, suggesting that crystal growth may have been continuous. The change of crystal habit that occurred could not have been caused by a change in pore fluid chemistry because the compositions of Stage A and Stage B are so similar. The only other possibility is that a change occurred in the physical controls on cementation, i.e. fluid temperature, pCO_2 or the rate of pore-fluid circulation through the buildups. The similarity in isotopic signatures of Stages A and B suggests that temperature and pCO_2 were essentially the same for both, and therefore the most probable cause for the change in crystal habit would have been variation of the rate of fluid flow through the pore system.

Folk (1974) suggested that fibrous cements were the result of rapid crystal growth from solutions of high ionic strength such as seawater, and he also indicated that pore restriction would inhibit the development of fibrous crystals and reduce inclusion density (Folk 1979). Accordingly, the development of the less turbid scalenohedral calcites after fibrous Stage A, probably reflects a decreased fluid flow and consequently decreased crystal growth rates in the bank facies, as a result of void space restriction by CFC cements.

Palisade texture results from the lateral interference of crystals growing in a void which are not restricted in the direction of the greatest growth vector (g.g.v., term of Dickson 1983), i.e. the c-axis direction. The lateral growth interference of crystals before the onset of Stage C suggests that nucleation sites for such crystals were closely spaced. This texture is commonly developed in large cavities and on favourable, homogeneous substrates. From this I conclude that relatively rapid crystal growth in open cavities with high fluid flow rates, and closely-spaced nucleation sites on homogeneous substrates, combined to develop palisade texture. The size of crystals developed would have depended on their initial nuclear spacing (Dickson 1983).

Euhedral scalenohedral crystals tend to be confined to isolated voids which would probably have had intrinsically low fluid flow

rates. The evident lack of substrate control on their development suggests that slower crystal growth at dispersed nucleation sites controlled this form of crystal development. With the exception of the rare solution corona overgrowths, syntaxial crinoid overgrowths are all interpreted as passive cement fills of primary intergranular pores (Evamy & Shearman 1965, 1969; Freeman 1971; Meyers 1974, 1978).

The solution corona overgrowths themselves are also regarded as passive cement fills, but of dissolution voids, not primary pore space (Walkden & Berry 1984). Walkden and Berry (op. cit.) suggest that solution corona development is a characteristic of meteoric diagenesis, but this does not appear to be the case for the present material.

7.5 DISTRIBUTION of NON-FERROAN SCALENOHEDRAL CALCITES

Scalenohedral, non-ferroan calcites are the first facies-independent cements in the cement stratigraphy. They are common in all deposits of bank and peri-Waulsortian facies, occurring in primary intraskeletal, intergranular and stromatactoid cavities and also in mouldic voids.

A number of factors affected the volumetric development of cements in different facies:

a). Dissolution and void connectivity

The effects of cement dissolution tended to be more significant in the volumetrically large interconnected void system of the bank facies, with best preservation of those cements occurring in protected intraskeletal or mouldic cavities in all facies. Relatively high fluid flow-rates in the interconnected void network of the bank facies probably contributed to the more effective dissolution in those regions.

Limited secondary porosity development occurred as a result of the dissolution episodes which pre-dated Stage C and Stage D, but this was mainly confined to the bank facies. Although dissolution was usually confined to Stage B and C cements, even CFC was occasionally dissolved when protective Stages B-C had not developed or were removed by the dissolution.

b). Void dimensions

In the bank facies, many voids were too large to be completely occluded by non-ferroan scalenohedral calcites. Later diagenetic fluids could therefore develop within the remaining void-space. Stage A-D cements were thus often subject to dissolution by these later fluids. In the peri-Waulsortian facies, however, pre-Stage B compaction greatly reduced the size and volume of primary porosity, and many voids were completely occluded by Stage B-D cements. This reduced the effective permeability of these rocks, and so reduced the amount of their subsequent dissolution by later diagenetic fluids.

c). Early fractures

Early, crumbly-edged, refitable fractures are a common feature of the bank and toe facies. These fractures often contain Stage B-D cements, but may also truncate them. They probably developed in response to sediment dewatering (Miller 1986) and/or the intrusion of neptunian dykes (see below), and provided pathways along which aggressive, later diagenetic fluids could pass, thus effecting the dissolution of existing cements.

7.6 PYRITE

Framboidal pyrite and spheroidal pyrite aggregates commonly formed within Stage D and occasionally Stage C cement layers. They also commonly developed at the Stage B-C boundary, but never within Stage B itself (Fig. 7.8A).

Pyrite was identified by XRD and reflected light microscopy: in some cases it was oxidised to hematite.

Individual pyrite framboids are 10-30 μm in diameter, while the spheroidal aggregates, composed of radially developed dog-tooth crystals, are up to 200 μm in diameter. The two habits of pyrite are often found in close association (Fig 7.8 B&C), indicating a common origin. Occasionally, at cavity margins, framboids developed into dendritic aggregates (Fig 7.8 D&E). Reflected light microscopy revealed irregular centripetal growth zonation within spheroidal

pyrite aggregates, while some of the individual framboids have an unusual cell-like structure, suggestive of organic growth structures.

Pyrite of similar form and habit is commonly found within crusts of marcasite associated with an early mineralisation episode (see Chapter 13).

7.7 ORIGIN of STAGE B-D CEMENTS

The lack of a significant disconformity between Stage A and Stage B, accompanied by the close similarities in the composition of these stages, suggests that no major change had taken place in the diagenetic environment, so that the precipitation of cement had been continuous. Accompanied by the fact that these cements may be truncated by crumbly-edged fractures associated with early sediment dewatering, the indications are that the non-ferroan scalenohedral cements of Stage B-D are the product of continued shallow burial diagenesis. Correspondingly, the isopachous and sparry textures developed by these cements are indeed those characteristic of phreatic conditions.

7.8 INTERPRETATION

The chemistry of modern shallow subsurface diagenetic environments is closely related to the bacterial degradation of organic matter in the sediment. Four main zones have been identified (Irwin et al. 1977; Froelich et al. 1979; Berner 1981; Dymond et al. 1984.), and are listed below in order of increasing depth:

1. Oxic zone: The zone between the sediment/water interface and the disappearance of dissolved O_2. Manganese and iron exist as oxides, hydroxides or complexes. No Mn^{2+} or Fe^{2+} occurs (Czerniakowski et al. 1984).

2. Suboxic zone: The zone between the appearance of dissolved Mn^{2+} and the onset of sulphate reduction (Froelich et al. 1979). Mn^{2+} appears but Fe^{2+} is rare.

3. Sulphate reduction zone: The zone of bacterial conversion of sulphate to sulphide (Coleman et al. 1979; Irwin et al. 1977). Pyrite can form.

4. Fermentation zone: The zone after the effective disappearance of dissolved sulphate. Organic molecules are biogenically degraded to CH_4 and CO_2 among other products. (Irwin et al. 1977; Coleman et al. 1979; Froelich et al. 1979). Iron-rich calcites would precipitate (Curtis 1978).

These diagenetic zones were described from pelagic and hemipelagic sediments where suboxic and reducing conditions are rapidly achieved within the first few centimetres of the sediment / water interface (Curtis 1978; Shimmield & Price 1986). However, the depth at which oxic bacteria can function is controlled by downward diffusion of dissolved O_2 (Coleman et al. 1979), which is related to the rate of sediment accumulation, organic carbon content, and the porosity and permeability of the primary sediments. The porosity and permeability of the Waulsortian bank sediments would have been greater than those of fine grained pelagic sediments because of the voluminous, interconnected void system, and therefore it is possible that the depth of the oxic zone in the buildups was greater than the values quoted for pelagic sediments (cf. Czierniakowski et al. 1984).

7.8.1 Relationship of Diagenetic Zones to Waulsortian Cement Stages.

The characteristic "black-bright-dull" CL pattern exhibited by Stages B-D reflects differences in trace element geochemistry (Fig. 7.5). These in turn can be related to the changing oxidation potential of the pore-fluids as they passed through the diagenetic zones in the shallow subsurface during burial. The sequence of events is outlined in Fig. 7.6.

Stage B

The main activator and quencher of CL in carbonate minerals are the divalent ions of manganese and iron respectively. Previous work has shown that these ions are only freed into pore waters under

reducing conditions (Czerniakowski et al. 1984; Froelich et al. 1979). The non-luminescence of Stage B (and for that matter Stage A) is attributed to a lack of activator (Mn^{2+}) (and Fe^{2+} quencher) ions (Fig.7.5), and so indicates oxic zone diagenesis. The trace element composition of Stage B is almost identical to Stage A, which suggests that pore fluid composition had remained essentially unchanged with respect to redox potential and $Fe^{2+}$and Mn^{2+} concentrations. The lack of any apparent dissolution surface between Stages A and B further suggests that void-fill cement precipitation continued through Stage A until pore restriction slowed crystal growth-rates and induced scalenohedral crystal development (Fig.7.6,1).

Stage C

The dissolution episode preceeding this stage developed an often highly irregular surface on the Stage B cements (Fig. 7.6,2), and reflects a major change in pore fluid chemistry. Stage C cements contain relatively high levels of Mn^{2+} but little Fe^{2+}, reflected in the bright yellow-orange luminescence (Fig. 7.5). The level of Mn^{2+} increased rapidly in Substage C1 and then gradually decreased in Substage C2 (Table 7.2). The appearance of Mn^{2+} and the low levels of Fe^{2+} in the calcite lattice indicates precipitation from suboxic pore fluids.

In modern sediments, the oxidation of organic matter reactions such as:

$$(CH_2O)_{106}(NH_3)_{16}(H_3PO_4) + 236MnO_2 + 472H^+$$
$$236Mn^{2+} + 106CO_2 + N_2 + H_3PO_4 + 366H_2O$$

(Froelich et al. 1979)

where MnO_2 acts as an electron acceptor, cause a rapid increase in dissolved Mn^{2+} at the onset of reducing conditions (Shimmield & Price 1986). The level of dissolved manganese in the pore fluid rapidly reaches a maximum, which is maintained unless Mn^{2+} is used in other reactions such as those which result in the precipitation of carbonate (Pedersen & Price 1982), with Mn^{2+} substituting into Ca^{2+} or Mg^{2+} sites. This would gradually deplete the dissolved manganese in the pore fluids as reflected by the initially high Mn levels of Substage C1, being followed by depleted Mn levels in Substage C2 (Table 7.2).

Fig. 7.5 Geochemistry and Diagenetic Environments of Stage A–D cements

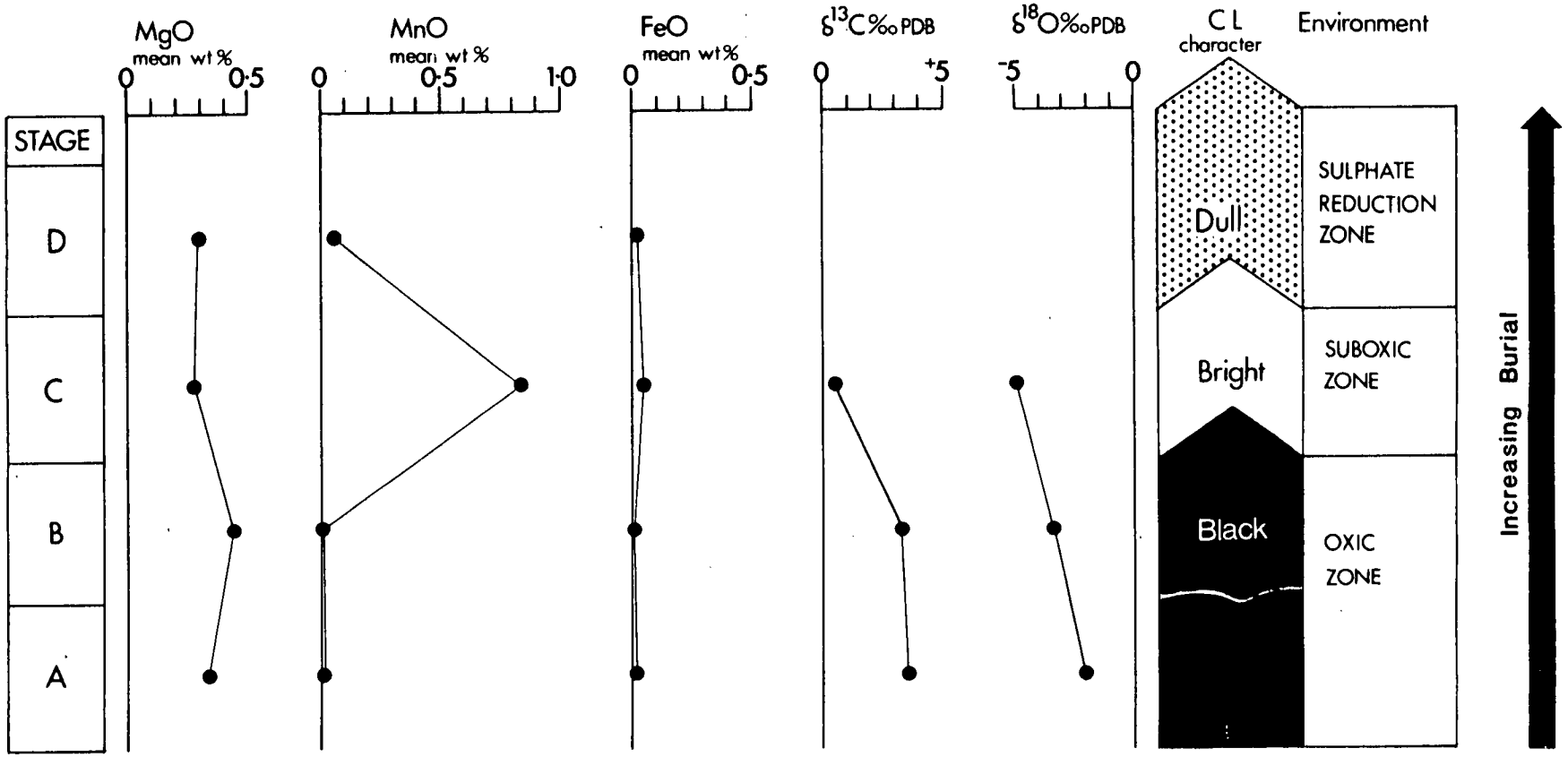

Fig. 7.6 Development of Stage B–D cements with changing diagenetic environments

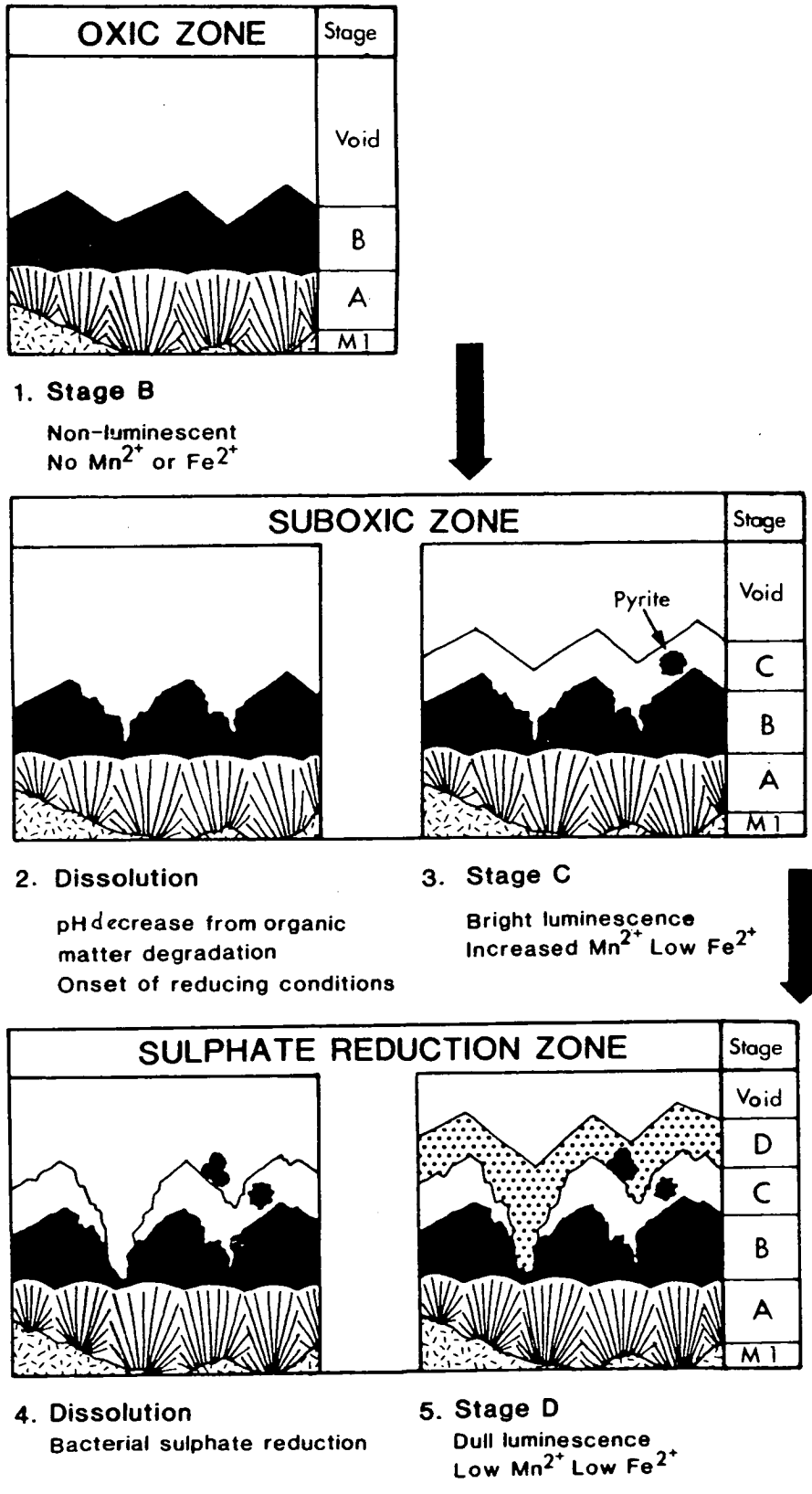

In support of this interpretation, an experimental coprecipitation of manganese with calcite (Bodine et al. 1965), recorded very rapid removal of Mn^{2+} from solution, so that when 40% of the total calcium in solution had been precipitated, less than 1% of the total dissolved manganese remained. A relatively high Mn concentration would be expected in the earliest cements precipitated in this case.

Furthermore, the distribution coefficient of Mn^{2+} in calcite, although a subject of disagreement in the literature (Bodine et al. 1965; Crocket & Winchester 1966; Michard 1968; Ichikuni 1973; Brand & Veizer 1980) is much greater than 1 (Pingitore 1978 suggests a value between 10 and 18). In effect, this means that the Mn^{2+}/Ca^{2+} ratio is greater in the precipitate than the coexisting solution at any given instant and so would tend to favour relative Mn^{2+} enrichment in the solid phase. The distribution coefficient of Fe^{2+} in calcite is approximately 1. Therefore no relative enrichment of iron in the solid phase would occur.

The decrease in magnesium content in Stage C calcites is probably related to depletion of Mg^{2+} in the chemically isolated pore fluids, and substitution of Mn^{2+} into lattice sites which might otherwise have been filled by Mg^{2+}. Also, considering that some of the inclusions in these cements may have had relatively higher levels of magnesium, the decrease in inclusion density which is often seen in the latter stages of scalenohedral calcites may be responsible for the downward trend in Mg^{2+} in the calcite lattice.

Stage D

The duller luminescence of Stage D reflects a combination of depleted Mn^{2+} and quenching by slightly increased Fe^{2+}. Most of the framboidal sulphides found in association with the non-ferroan prismatic cements occur within Stage D. These features together reflect the onset of sulphate reduction in the pore waters. The occurrence of some pyrite in Stage C indicates a degree of overlap between the suboxic and sulphate reduction environments. Significantly, no pyrite occurs in Stage B (oxic zone) cements.

Stage C shows a marked increase in Mn^{2+} in the pore fluids, and therefore indicates the onset of reducing conditions. The stoichiometric equation for steady state organic matter oxidation given

above, predicts that Mn^{2+} will only continue to precipitate with carbonate in proportion to the original amount of MnO_2 in the sediment reduced during suboxic diagenesis, i.e. MnO_2 is limiting. Therefore, the amount of Mn incorporated into the calcite lattice would be expected to decline as MnO_2 reduction continued, and it would appear that the progressive depletion of Mn^{2+} through Stage C and D calcite cements reflects this process.

Bacterial sulphate reduction is characterised by the setting up of micro-environments, suggesting that the complex, and often local compositional variation observed within Stage D was the result of fluctuating rates of bacterial sulphate reduction. The degree of bacterial sulphate reduction would quite probably differ from mound to mound and even cavity to cavity depending on the local conditions affecting organic activity, and such variation is clearly reflected in the sample set.

The wide-spread occurrence of a bright luminescent final substage in Stage D (Fig. 7.4) indicates that the end of Stage D precipitation reflects a development in the pore fluids which was common to most mounds. It does not, however, imply that all Stage D cements were contemporaneous, as they are internally too variable. Trace element analysis of this substage in Fig. 7.4, indicates an almost total absence of Fe^{2+} and a slight increase in Mn^{2+} in the pore fluids. This may mean that dissolved Fe^{2+} had been almost completely removed by reactions producing pyrite, i.e. Fe was limiting because of excess of sulphate in the marine pore waters, and the high solubility of MnS_2, thus leaving an excess of Mn^{2+}.

7.8.2 Interpretation of Stable Isotope data: Origin of Diagenetic Fluids

The carbon isotopic composition of the earliest prismatic cements (Stage B) is comparable with that for the CFC cements of Stage A (Fig. 7.7). While their $\delta^{18}O$ is slightly depleted, cements of both Stage A and B fall within the accepted fields for marine carbonates (Veizer & Hoefs 1976; Hudson 1977; Walls et al. 1979).

The stable isotope ratios of diagenetically unaltered bioclasts in ancient limestones may be used to indicate coeval marine water

isotopic composition (Brand & Veizer 1981). Non-luminescent bioclasts are presumed to be the least diagenetically altered (Popp et al. 1983, 1986), and so these were analysed in this study for comparison with Stage B cements. (Table 7.3; Fig. 7.7).

Isotopic analyses of a non-luminescent crinoid and brachiopod were carried out. The brachiopod contained a non-luminescent geopetal sediment which was also analysed.

Recent and fossil articulate brachiopods have been shown not to display any biological fractionation and, therefore, must have laid down shell carbonate in isotopic equilibrium with the surrounding waters (Lowenstam 1961). Recent crinoids are, as a group, enriched in ^{12}C and ^{16}O (Milliman 1974, p.134). The isotopic composition of the four carbonate components in Table 7.3 are very consistent, suggesting that they represent the nearest approach to the isotopic composition of the marine pore fluids in the Waulsortian.

TABLE 7.3 Isotopic composition of non-luminescent components. Coplow bank facies

	$\delta^{13}C$	$\delta^{18}O$
Cement (Stage B)	3.30	-3.23
Brachiopod	3.80	-3.26
Crinoid	3.35	-3.01
Geopetal sediment	3.56	-3.43

Values in per mil versus PDB Standard

These results are close to values from the Lower Carboniferous obtained in an extensive study of Palaeozoic non-luminescent brachiopods (Popp et al. 1986, Fig.7), and indicate that the Lower Carboniferous seawater was slightly depleted in $\delta^{18}O$ and enriched in $\delta^{13}C$ relative to the present day.

The carbon and oxygen isotopic trends of Stage B cements can be discussed separately.

Fig. 7.7 ISOTOPIC COMPOSITIONS OF NON-LUMINESCENT CEMENTS, BIOCLASTS AND INTERNAL SEDIMENT

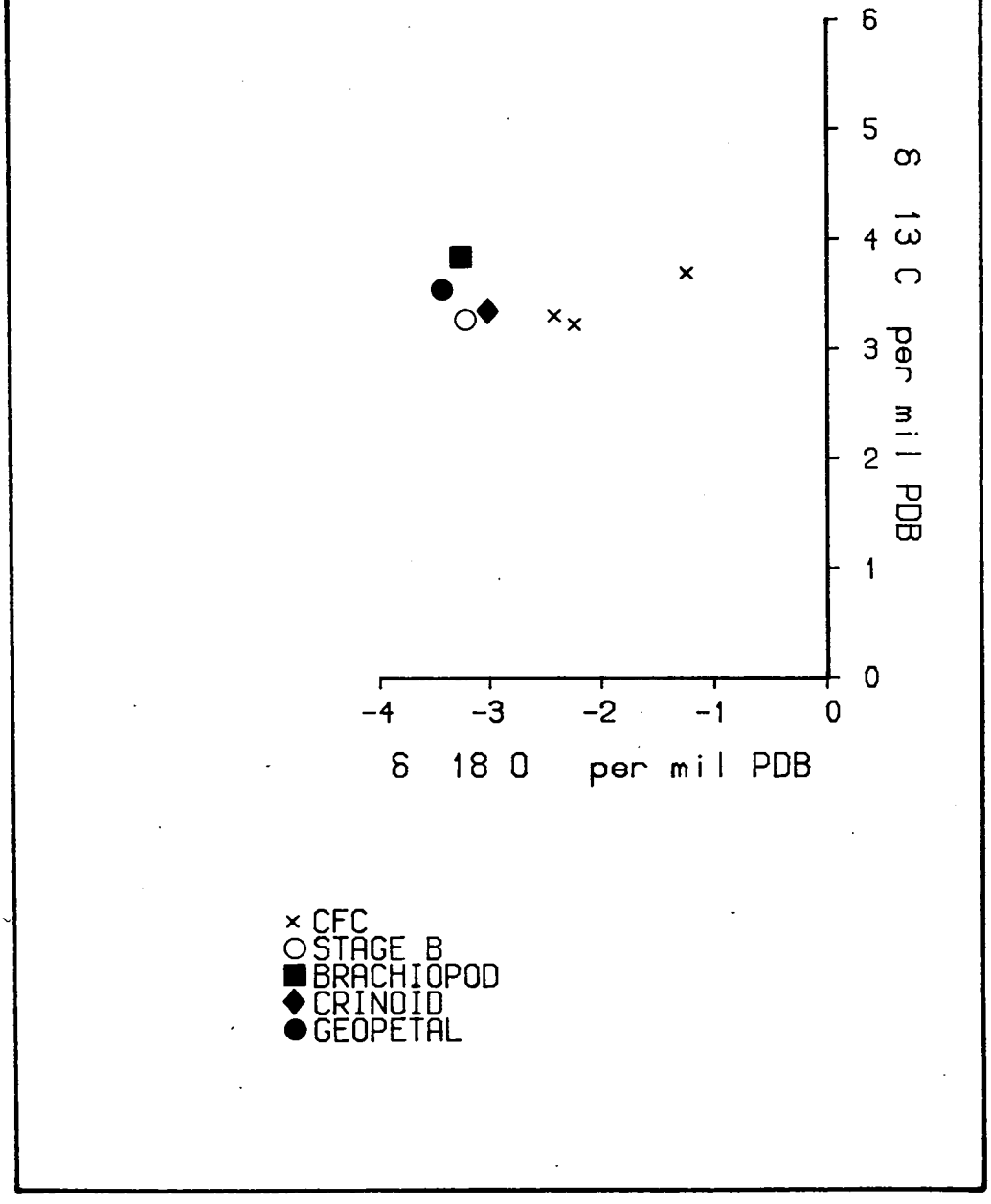

a). Oxygen isotopes

Assuming an original marine pore fluid, the depletion of $\delta^{18}O$ from Stage B to C suggests progressive burial. Potential variables within the system such as porosity, permeability, organic matter content, and type of carbonate, make it impossible to accurately relate the change in $\delta^{18}O$, i.e. the change in pore fluid temperature, to actual burial depths, and it is therefore not possible to delimit the extent of the oxic, suboxic and sulphate reduction zones within the sediment column. The depth over which sulphate reduction occurs in sediments is controlled by the organic carbon content and sediment accumulation rate, and varies from a few tens of centimetres in organic-rich sediments to hundreds of metres in organic-poor sediments (G. Shimmield pers. comm.).

b). Carbon Isotopes

A significant depletion of $\delta^{13}C$ occurs in Stage C. This probably reflects the onset of reducing conditions, although the level of depletion is much lower than would be expected. Irwin et al. (1977) suggest a $\delta^{13}C$ depletion of up to -20°/₀₀ in the zone of bacterial sulphate reduction. The limited depletion of carbon (0.61°/₀₀) could indicate that little carbon of organic origin ($\delta^{13}C$ -20°/₀₀, Degens & Mopper, 1976) was utilised in the Mn-carbonate precipitation reaction. Carbon would, therefore, have been supplied from carbon species diffusing downward from sea water or from dissolution of carbonate grains (Pedersen & Price 1982). The most likely reason for $\delta^{13}C$ values remaining relatively heavy despite being in a reducing environment is that the carbon was buffered by carbonate dissolving out of the rock, as is indicated by the occurrence of dissolution episodes at appropriate points in the cement stratigraphy.

7.9 ORIGIN of MICRO-ZONATION in STAGE B.

The alternating non-luminescent (black) and bright luminescent internal zones have trace element compositions which are comparable to Stage B and Stage C cements respectively. Bearing in mind the

Figure 7.8 Early diagenetic pyrite

A Cathodoluminescence photomicrograph showing aggregates of framboidal pyrite (p) developed within syntaxial overgrowths on crinoid grains. The pyrite occurs on the boundary between non-luminescent Stage B and subsequent non-ferroan calcite Stages C (arrowed) and D. Ferroan calcite Stage E is the latest cement in the sequence. Toe facies, Coplow buildup.

B Photomicrograph showing opaque spheroidal pyrite aggregates associated with framboids, which developed on a geopetal sediment floor. Internal sedimentation and pyrite development were contemporaneous, as is indicated by aggregates buried within the geopetal carbonate(left of picture). The boxed area is shown in detail in 'C'. Thin section, bank facies, Dunnow buildup.

C Photomicrograph of boxed area in 'B' showing a spheroidal pyrite aggregate (s) with dog-tooth crystal terminations, associated with a smaller framboid (f) which exhibits a cellular structure. Dunnow buildup.

D Photomicrograph showing dendritic framboidal aggregates (arrowed) growing preferentially downwards from a cavity roof. A geopetal sediment-fill (dashed) in an ostracod indicates the way-up. The boxed area is shown in detail in 'E' below. Thin section, bank facies, Newsholme buildup.

E Transmitted light photomicrograph of the dendritic framboidal aggregate outlined in 'D'.

Fig. 7.8

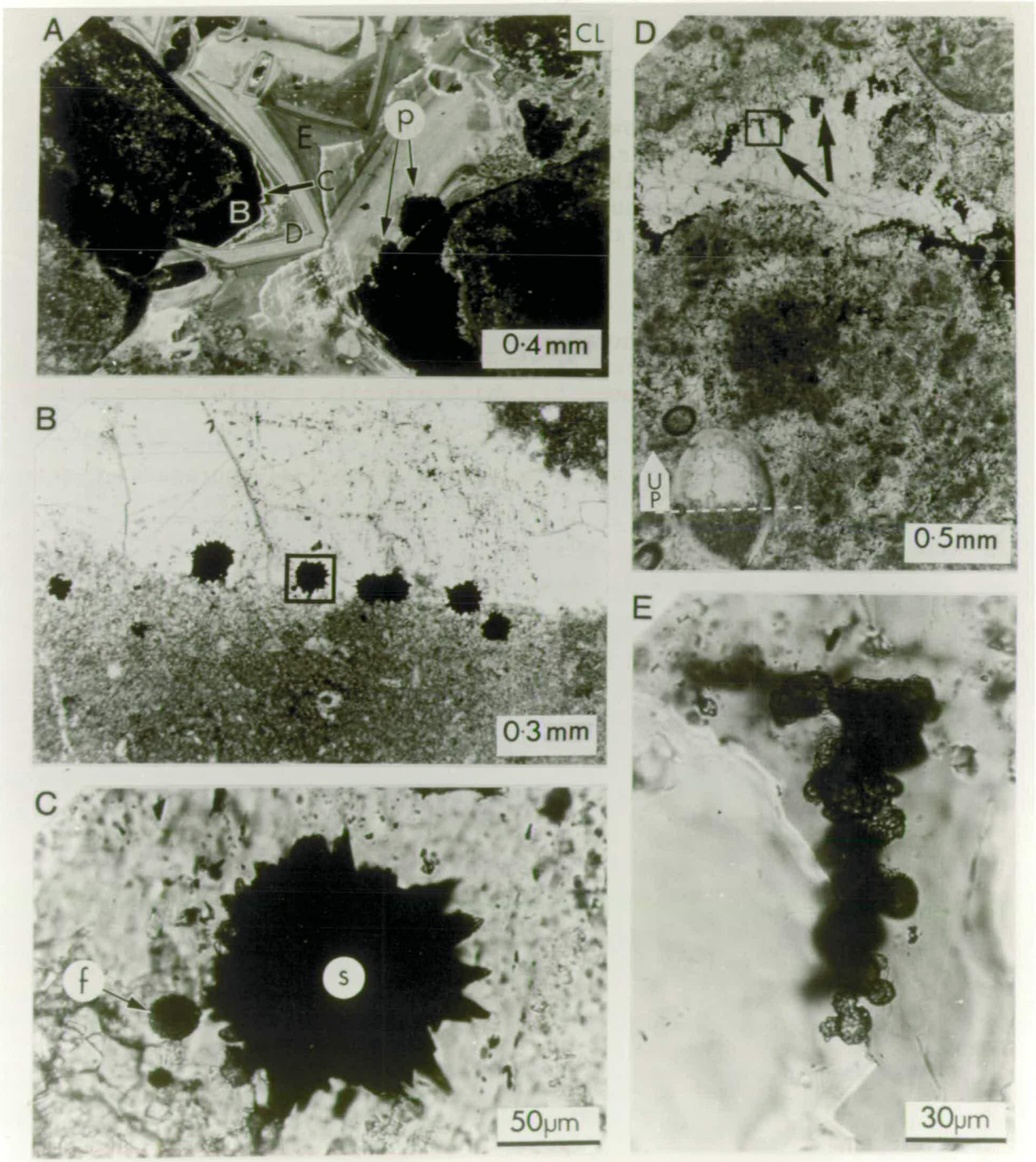

proposed controls on the development of Stage B and C, it remains to suggest a process or processes which could cause localised cyclicity of such cements. Internal zonation of Stage B was not observed in the peri-Waulsortian rocks, but this may purely be a function of the limited sample set for those facies.

In an experimental study, ten Have and Heijnen (1985) showed that micro-zonation could be produced in calcite crystals grown from solutions of constant composition. The zones could only be the product of changes in crystal growth rates. They identified luminescent zones which represented changes in Mn^{2+} within the calcite lattice of a few ppm. However, the differences in chemical composition between the micro-zones in Waulsortian Stage B cements are much greater than a few ppm., and in the ancient cements it is most unlikely that precipitating solutions remained of constant composition for any one of several ionic species in a much more complex parent fluid. Zonation in Stage B cements, therefore, cannot be simply a crystal growth phenomenon. The zones are probably related to a variety of factors including crystal growth rates, substrate nature and availability, changes in activity of organic species affecting the redox potential of pore fluids, and burial rates (cf. Coleman et al. 1979).

Having established the likely relationship of black and bright CL zones to oxic and suboxic diagenesis, it remains to suggest a mechanism whereby these environments could produce internal zonation of Stage B cement crystals.

At times of slow burial, organic matter would spend relatively more time in the oxic surface layers and, therefore, in the presence of aerobic bacteria. This would allow a greater depth of O_2 diffusion downwards. With higher sedimentation rates in the buildups, the residence time of organic matter in the oxic zone would be reduced and so the supply of labile organic matter to the anaerobic bacteria would be increased, although rapid sedimentation would tend to cause relative "dilution" of organic matter within the greater volume of sediment.

The hypothesis that the Stage B-D cement sequence can be related to bacterial degradation of organic matter with progressive burial, suggests that the main control on the development of the micro-

zonation in Stage B was localised cyclicity in the activity of the micro-organic community in the Waulsortian buildups, possibly influenced by changes in sedimentation and/or burial rates.

The occurrence of multiple repetition of bright and non-luminescent zones has been identified in previous studies (Walls & Burrowes 1985; King 1984; Walkden & Berry 1984; Frykman 1986). In the cases cited by Walls and Burrowes (1985), King (1984) and Frykman (1986) the zones are well defined and euhedral as in Waulsortian Stage B cements. In Walkden and Berry's example, however, the bright zones define dissolution horizons within the cement sequence, and may well represent quite a different diagenetic environment than that proposed above.

7.10 DISCUSSION

The characteristic 'black-bright-dull' CL sequence of Stage B-D cements in this study is interpreted as representing the passage of pore waters from oxic through suboxic to sulphate reduction zones, which occurred within the marine pore waters as a result of bacterial degredation of organic matter in the sediment during progressive shallow burial of the Waulsortian buildups.

Stage B-D cements are ubiquitous in all Chadian rocks examined in this study. Their development was associated with a dynamic system of geochemical zones which would have maintained a position at approximately constant depths within the first few tens of metres of the sediment body as sedimentation continued. The depth and lateral extent of these zones at any one time depended mainly upon bacterial activity within the buildups. The thickness of sediment containing these cements is far in excess of the vertical or lateral extent to which individual geochemical zones could have penetrated at any one time, and therefore the cements must be diachronous. The consistency of the pattern of cement stages throughout the entire thickness of the Waulsortian facies in the Craven Basin suggests that the appropriate diagenetic environments were repeatedly developed during a protracted period of burial under marine conditions.

Early diagenetic non-ferroan cement sequences exhibiting similar CL characteristics to those of this study have been identified in rocks ranging from Cambrian (Frank et al. 1982) to Recent (Meyers 1974 p.857). Although an example has been recorded from Cretaceous sediments (Stow & Miller 1984), most examples are of Palaeozoic age (Freeman 1971; Meyers 1974, 1978; Meyers & Lohmann 1980, 1985; Cowan 1982; Grover & Read 1983; King 1984; Walkden & Berry 1984; Walls & Burrowes 1985; Miller 1986; Kerans et al. 1986; Frykman 1986).

These "black-bright-dull" cements are reported from a range of carbonate facies, including subtidal-shelf (Freeman 1971; Walkden & Berry 1984; Meyers 1974, 1978; Meyers & Lohmann 1980, 1985; Grover & Read 1983), restricted bays (Frank et al. 1982), reefs (Walls & Burrowes 1985; Kerans et al. 1986) and Waulsortian buildups (Cowan 1982; King 1984; Miller 1986).

The relationship between CL and trace element geochemistry has been investigated by many workers (Table 7.4) and shows a high degree of consistency, leaving little doubt that the "black-bright-dull" sequences have a common origin, despite the divergence in their reported habitats.

Fewer isotope analyses have been reported, but they include examples from the Lower Carboniferous, one from the Waulsortian facies from Eire (King 1984) and another from skeletal calcarenites associated with Waulsortian buildups in the Sacramento Mts, U.S.A (Meyers & Lohmann 1985). Table 7.5 shows some similarities in isotopic composition between cements in this study and other Waulsortian examples, for non-luminescent Stage B equivalents. The $\delta^{13}C$ values are comparable, but there is some difference in the $\delta^{18}O$ ratios. However, this variation, which could be partly due to the effects of subsequent diagenetic alteration, primary sea water composition, or variability in the burial depth at which each example formed, is still within the reported ranges for Lower Carboniferous marine calcites (cf. Fig.6.4; and Meyers & Lohmann 1985).

TABLE 7.4 TRACE ELEMENT COMPOSITION & CL CHARACTERISTICS OF STAGE B-D COMPARATIVES FROM OTHER STUDIES.

AUTHOR(S)	STAGE/ZONE	FeO wt%	MnO wt%	MgO wt%	LUMINESCENCE
Freeman (1971)*	-----	Trace	0.26	----	Luminescent
	-----	Trace	0.13	----	Dull luminescent
	-----	Trace	<0.13	----	Non-luminescent
Oglesby (1976)*	1	<0.03	0.11	----	Very bright
	2	0.10 ±0.01	0.26 ±0.03	----	Bright to very bright
	3	0.10 ±0.01	0.23 ±0.04	----	" " " "
	4	0.09 ±0.01	0.17 ±0.02	----	" " " "
	5	0.10 ±0.01	0.17 ±0.02	----	" " " "
	6	0.11 ±0.01	0.20 ±0.03	----	" " " "
	7	0.14 ±0.01	0.10 ±0.01	----	Dull
	8	0.14 ±0.01	0.06 ±0.01	----	"
	9	0.08 ±0.01	0.03 ±0.01	----	"
	10	<0.03	<0.03	----	Non-luminescent
Frank et al. (1982)*	1	<0.03	<0.03	0.14 ±0.09	None..thin bright subzones
	2	<0.03	0.15 ±0.05	0.18 ±0.05	Very bright, faintly subzoned
	3	0.05 ±0.04	<0.03	0.43 ±0.22	Very weak, slightly subzoned
	4	0.04 ±0.03	0.30 ±0.04	0.55 ±0.07	Very bright
	5A	0.35 ±0.06	0.12 ±0.03	0.54 ±0.10	Very weak
	5B	0.18 ±0.03	0.13 ±0.02	0.65 ±0.09	Moderate, faintly subzoned
	6	0.03 ±0.02	0.03 ±0.02	0.99 ±0.22	Moderate, numerous subzones
Grover & Read (1983)*	"Oldest"	0.03	0.01	0.23	Non-luminescent
		0.04	0.42	0.17	Brightly luminescent
		0.10	0.04	0.19	Dull luminescent
	"Youngest"	0.02	0.12	0.20	Very dull luminescent
Walkden & Berry (1984b)**	1	Non-ferroan	----	----	Non-luminescent
	2	Non-ferroan	----	----	Bright luminescent
	3	Non-ferroan	----	----	Dull luminescent
Meyers & Lohmann (1985)	1	0.007 ±0.002	0.01 ±0.004	0.17 ±0.020	Non-luminescent
	2	0.070 ±0.01	0.08 ±0.02	0.14 ±0.01	Brightly luminescent
(Meyers 1974)	3	0.010 ±0.003	0.02 ±0.009	0.06 ±0.008	Non-luminescent
	5	0.240 ±0.050	0.06 ±0.006	0.19 ±0.020	Dull luminescence

* Recalculated to wt. % oxide from mole % carbonate or wt. % element.
** Staining and CL characteristics only.

Table 7.5 Comparison of Stage B (non-luminescent) and Stage C (brightly luminescent) isotopic signatures with similar non-ferroan cements from other Waulsortian studies.

(Analyses given in °/₀₀ vs PDB standard)

	Stage B (Non-luminescent)		Stage C (Bright Luminescence)	
	$\delta^{13}C$	$\delta^{18}O$	$\delta^{13}C$	$\delta^{18}O$
This study	+3.30	-3.23	+0.61	-4.98
King (1984)	+3.30	-2.60	-	-
Meyers & Lohmann (1985)	+3.70	-1.30	+2.40	-2.80

7.11 DIAGENETIC ENVIRONMENTS AND ORIGIN OF PORE FLUIDS

On the basis of the CL and trace element data, most authors agree that the characteristic 'black-bright-dull' sequence of cements reflects the change from oxic to reducing pore fluids (Oglesby 1976; Frank et al. 1982; Grover & Read 1983; Walkden & Berry 1984; Meyers 1978; Meyers & Lohmann 1980, 1985; King 1984; Miller 1986). However, a range of interpretations have been suggested for the origin of these pore fluids. These include; vadose (Freeman 1971), meteoric vadose to shallow phreatic (Grover & Read 1983), meteoric phreatic (Meyers 1974, 1978; Meyers & Lohmann 1985; Cowan 1982; King 1984; Walkden & Berry 1984) and marine phreatic environments (Miller 1986).

Significantly, Meyers (1974), Grover and Read (1983) and King (1984) conclude that these cements precipitated from regionally extensive lenses of meteoric water. For a variety of reasons, this interpretation does not fit the evidence from the Waulsortian

buildups in this study. The interpretation of the isotopic and trace element data in the above mentioned studies is questionable, casting doubt upon the proposed involvement of regionally extensive palaeo-aquifer systems in the development of this type of cement.

The consistency of CL, stable isotope and trace element characteristics of the unequivocally marine Stage A cements and the earliest scalenohedral (Stage B) calcites in the Craven Waulsortian, accompanied by the lack of any dissolution surface between them, shows that there was no major change in pore fluid characteristics during that part of the early diagenesis, excluding the possibility of any influx of meteoric fluids.

The presence of marine bioclasts in some internal sediments which post-date Stage B-D could also be invoked as evidence of marine diagenesis. However, many of these sediments were fed by neptunian dykes which often re-worked the buildup sediments (see below Chapter 8), and re-worked sediments do not carry any characteristic environmental indications, so this evidence remains equivocal.

The studies of bioclast assemblages in the Waulsortian buildups of the Craven Basin (Lees & Miller 1985) suggest that they formed below wave base in relatively deep water on a carbonate ramp. No evidence of contemporaneous emergence is seen in the Chadian rocks of the Craven basin,and the cement stratigraphy records progressive burial (see Chapter 17). It is therefore unlikely that meteoric fluids could have gained access to the buildups during early diagenesis. For them to have done so, one would have to postulate that all voids in the bank facies remained uncemented after CFC production, and that no cements at all were developed in peri-Waulsortian facies, until a basin-wide meteoric regime was established. This is contrary to all the petrographic, geochemical and geological evidence.

Similar 'black-bright-dull' cement sequences occur in the Irish (King 1984; Miller 1986) and the Belgian Waulsortian (A. Lees pers. com.). King (1984) admitted uncertainty as to the source and mechanism for the ingress of meteoric water into the Waulsortian deposits of the Central Irish Basin from which, he suggests, the comparable cements in his study originated. Having proved that all the cementation and mineralisation of those Irish Waulsortian buildups was completed by the end of the Chadian, he had to propose

some structural devices whereby fresh water could be introduced into the basinal rocks which were palaeogeographically implausable. Precipitation from a marine pore fluid seems more likely in this case also.

Significantly, Stow & Miller (1984) reported the 'black-bright-dull' cement sequence from deep fan turbidite Cretaceous carbonates in D.S.D.P. cores in the SE Atlantic, which could not have been affected by meteoric diagenesis. In this case a marine origin for the cement is unequivocal.

Meyers (1974, 1978) and Meyers and Lohmann (1980, 1985) suggested meteoric diagenesis for the formation of their early diagenetic non-ferroan cements in Waulsortian and associated facies of New Mexico. In this case, the bioherms were cut by several major regional unconformities which would have allowed for the influx of meteoric fluids. However, the interpretation of isotopic data for their Zone 1-3 cements must be re-examined (see below).

The isotopic data cited by Meyers and Lohmann (1985) for their early diagenetic cements lies outside the fields for meteoric fluids and cements defined in the literature (Walls et al. 1979; Hudson 1977), but is much closer to the fields of average marine limestones (same refs.) and modern day ocean water values (Shackleton & Kennet 1975), and within the range for Lower Carboniferous non-luminescent brachiopods (Popp et al. 1986). With the possible effects of secular variation of $\delta^{18}O$ through time (Veizer & Hoefs 1976) and the error involved in calculations of ancient seawater compositions from carbonate components (Brand 1982) it is possible that at least the first two cement Zones of Meyers and Lohmann (1985) were indeed precipitated from marine pore fluids. The isotopic composition of non-luminescent cement of King (1984) also lies within accepted range for ancient marine carbonate.

In the case of the New Mexico buildups, two reasons for a meteoric origin were proposed, based on trace element levels of manganese and magnesium found in cement Zones 1-3 (Meyers 1974; Meyers & Lohmann 1985). Meyers (1974) suggested that the difference between the manganese content of his brightly luminescing cements

(1000 ppm) and the calculated level of manganese in calcite precipitated out of normal seawater (10-50 ppm), was evidence of a meteoric source. Later, (Meyers 1978; Meyers & Lohmann 1985) the relatively low level of magnesium in Zone 1-3 cements was also cited as evidence of meteoric waters.

However, Meyers (1974, 1978) totally neglected the processes which can affect the solubility and transport of manganese within a sediment where cementation was occurring, and concentrated instead on the processes occurring in the water column. Although the concentration of dissolved manganese in seawater is very low, it is commonly elevated in pore waters by suboxic diagenesis and the dissolution of surficial Mn oxyhydroxides. Levels as high as 1% Mn (in oxide form) are commonplace in modern sediments where an oxic upper layer exists (N.B. Price pers. comm.). Such levels of Mn oxyhydroxides are particularly common on Great Barrier Reef cavity walls (T.P. Scoffin pers. comm.). On burial of these Mn oxyhydroxides and the onset of reducing conditions in the shallow subsurface, sufficient Mn^{2+} could be released to be incorporated into precipitating carbonate at the levels necessary to satisfy the luminescence and trace element requirements of the cements reported by Meyers.

The case for low magnesium levels reflecting meteoric pore fluids tends to ignore the succeptability of HMC to lose Mg^{2+} during diagenesis. Furthermore, if these inclusion-poor cements were shallow burial phases as proposed herein, LMC may have been the stable carbonate phase (cf. Frykman 1986).

Freeman (1971) suggested vadose diagenesis for similar cements showing black-bright-dull CL sequences, on the strength of "pendant" development of calcite overgrowths. His examples contained no other characteristic features of vadose fabrics such as meniscus cements. Although the overgrowths in his rocks were preferentially developed in one direction, the crystals grew to fill the entire porespace, which suggests that the pores were entirely fluid-filled, i.e. in phreatic conditions.

The only example of cements with a black-bright-dull CL sequence which show significantly different features to those of this study,

and could therefore be related to meteoric diagenesis, is that given by Walkden & Berry (1984b). In upper Dinantian platform limestones of Derbyshire, several thin bright CL zones occurred within non-luminescent cements. The bright zones rest on irregular surfaces which suggest dissolution episodes. These dissolution episodes were related to cyclic emergence of the limestone units which underwent repeated karstification (see also Berry 1984). Walkden and Berry concluded that meteoric fluids entered the sequence during the emergent episodes. Unfortunately, they gave no isotopic data for the zoned, non-luminescent calcites and therefore the origin of the diagenetic fluids cannot be confirmed. It is possible that bacterial activity in freshwater environments could also produce similar black-bright-dull CL sequences to those formed in marine diagenesis, but there are distinct problems. Primarily, the very low levels of dissolved SO_4^{2-} in meteoric waters mean that sulphate reduction is obviously limited (hence the occurrence of siderite in fresh water sediments). Furthermore, the presence of pyrite in association with such cements must be indicative of sulphate reduction and therefore more probably marine pore fluids.

7.12 RELATIVE TIMING OF CFC AND STAGE B-D CEMENTS

Having established the diachronous nature of the Stage B-D cements, it remains to be established whether the CFC cements were also diachronous or whether they represent a period when cementation was only taking place in the bank facies.

The thickness of CFC layers in some void-fills of the bank facies is often several millimetres and may reach up to 1cm. Even with the presumed relatively rapid crystal growth rates of the fibrous cements, these thick layers still represent significant periods of time.

Is it likely then, that the toe and off-bank time-equivalents of the buildups remained totally uncemented during this time, and also (because the "black-bright-dull" sequence is complete in all facies) remained entirely within the oxic zone?

Certainly, sediment accumulation rates in the peri-Waulsortian facies were much slower than on the banks, but because of the

relatively poor primary permeability in the organic-rich wackestones of the off-bank, the boundary between oxic and suboxic zones probably lay only a few centimetres or tens of centimetres below the surface, and before reaching that boundary, slow-growing Stage B cements had developed. Furthermore, CFC and Stage B are geochemically very similar, and no disconformity occurs between the two stages in the bank facies i.e both could precipitate from pore fluids of the same composition.

It would appear that pore restriction by CFC cements reduced fluid circulation through the void network in the banks, and this led to the change to scalenohedral habit, possibly during a period of continuous cementation. It seems likely, therefore, that in sediments such as the peri-Waulsortian facies, where such extensive interconnected porespace did not exist, scalenohedral crystals could have begun to develop while CFC was precipitating at the same time in the bank facies.

The diachronous nature of the processes which effected cementation in the shallow subsurface of the Waulsortian buildups and peri-Waulsortian facies indicates therefore that the CFC, Stage A cements of the bank facies were also partial time equivalents of the Stage B-D cements in other facies and perhaps even within different parts of the banks themselves.

CONCLUSIONS

Several lines of evidence suggest that the non-ferroan scalenohedral calcites of this study were precipitated during progressive shallow burial of the Waulsortian buildups in the marine phreatic environment:-

1. The cements developed conformably upon marine CFC cements in the Waulsortian bank facies, while in the off-bank facies they are the first recogniseable cements in the sequence, pre-dating early stylolites.

2. The CL, staining, geochemical and isotopic characteristics of the earliest non-ferroan prismatic cements are not significantly different to those of the CFC marine cements, therefore suggesting a common fluid source for both stages, i.e. marine. Restriction of the pore system excluded the micritising organisms which affected earlier Stage A marine cements.

3. The cements are commonly the first void-filling phases in mouldic porosity following the dissolution of metastable bioclasts, a process known to take place during early diagenetic, shallow burial environments in Recent sediments.

4. A characteristic 3-fold sequence of cement stages is identified on the basis of CL observations and trace element composition which can be related to the documented zones of changing redox potential associated with the biodegradation of organic matter in modern pelagic and hemipelagic sediments:

CEMENT	CL.	Fe^{2+}	Mn^{2+}	Diagenetic Zone
Stage B	Non-luminescent	0%	0%	Oxic
Stage C	Bright orange CL	0%	<2%	Suboxic
Stage D	Dull-luminescent	0.1%	0.2%	Sulphate reduction

5. The association of pyrite framboids with the Stage B-C boundary confirms the proposed relation between those cements and the change from oxic to reducing conditions in the marine environment. Furthermore, the existence of pyrite within both Stage C and Stage D infers the existence of micro-environments associated with variations in bacterial activity and the distribution of organic matter within the sediments.

6. The stable isotopic composition of the cements indicates a depletion of $\delta^{13}C$ in Stage C which was probably associated with the onset of reducing conditions. Oxygen isotope data reveals a gradual depletion through Stage B to C, relative to the unequivocally marine CFC cements and non-luminescent bioclasts which are believed to have

retained the original composition of the Carboniferous seawater. This depletion in $\delta^{18}O$ reflects increasing pore fluid temperature with burial.

7. The non-ferroan scalenohedral cements are the first facies-independent cements in the sequence. Their development in several hundreds of metres of sediment compared to the potential few tens of metres for the extent of the geochemical zones which controlled the cement composition, indicates that the cements were diachronous. Furthermore, the consistency of the cement sequence indicates the persistence of stable diagenetic and tectonic environments during the course of their development.

8. No evidence of a regionally extensive meteoric lens as postulated by Meyers (1974) for the Waulsortian of the Sacramento Mts, has been found in this study. Perhaps with the exception of the bright zones associated with dissolution surfaces and emergence episodes in shelf carbonates of Walkden and Berry (1984b), the compositions and fabrics developed in similar cements from the literature suggest that they may also have developed as a result of diachronous, progressive bacterial reduction during shallow burial in the marine phreatic diagenetic environment.

9. Crumbly fractures associated with sediment dewatering commonly contain Stage D and Stage C cements, and rarely Stage B. This suggests that the cements and fractures were early diagenetic and diachronous.

10. Local variation on both cavity and buildup scales occurs within the earliest stages of the cements in the form of small scale repetition of bright and non-luminescent zones whose compositions are comparable with those of Stages C and B respectively. These zoned cements reflect a cyclicity in the trace element chemistry of pore waters during cement precipitation, possibly related to variation in biogenic activity and the supply of organic matter to the sediment. The variation in zones within and between buildups supports the diachronous origin of these cements. Precipitation from a regionally extensive meteoric zone, as suggested by previous workers for similar cements, is therefore unlikely.

CHAPTER 8
FISSURES AND NEPTUNIAN DYKES

Sediment-filled fractures are common features in the Waulsortian buildups of the Craven Basin, as they are elsewhere. Often they are several metres or tens of metres in length and up to 0.5m across, usually occurring at high angles to bedding, but with irregular trends so that they may become sub-horizontal or bifurcate. Similar features can also be identified at the hand specimen and thin-section level, and some of these contain early diagenetic cements which are useful in dating fracture episodes.

A full investigation of the Waulsortian sediment-filled fractures has not been attempted herein. However, the framework of the cement stratigraphy has been used to place constraints on the timing and development of some fractures sampled in this study.

The case histories described below indicate that these features developed on a small scale in very early diagenesis and continued to expand intermittently during shallow burial of the buildups.

The large scale structures can be divided into two groups:

a) Fissures: where sediment infiltrated into the fractures from above by gravity.
b) Neptunian dykes: where sediment was actively injected along the fractures as they opened, often from below.

Neptunian dykes occur in most Waulsortian buildups in the study area, while fissures are rarely encountered. The description of fissures given below is based entirely upon the example described by Miller & Grayson (1972), and Miller (1973), which was covered over before their work was published, and from unpublished notes made available by both authors during the course of my study. The only other known fissure example in the area occurs in a quarry at Twiston (R.F. Grayson, pers. comm.), but unfortunately, permission to visit this exposure was not granted by the present landowner.

8.1 FISSURES

Fissures opened towards the Waulsortian bank surface and were filled by bioclastic sediment from above.

Miller and Grayson (1972) described a fissure which was filled, primarily with crinoid debris but also contained a rich fauna, including two new species of trilobite (Miller 1973), which may have lived on the sea floor near the open fissure. The predominantly crinoidal packstone was later infiltrated by micrite which subsequently settled into the fissure, filling the intergranular voids and leaving only small shelter voids. Virtually no overgrowth cements developed on the echinoderm grains (J. Miller pers.comm.).

The fissure, 3m deep and opening up to 0.75m at the buildup surface, occured directly below a boulder bed. It apparently formed by dilational opening, probably as a result of cambering of large blocks on the steeply-dipping buildup flank. This allowed post-buildup crinoidal sediment from the overlying sea floor to fall or be washed into the downwards-tapering fracture (J. Miller, pers. comm.). The fissures at Twiston also occur near a steep erosional palaeoslope (R.F. Grayson, pers. comm.) and may also have formed by cambering. One of these fissures contains concentrations of orthoconic and coiled nautiloid shells. In both cases, the buildup surface onto which the fissures opened was formed by erosion, and the covering sediments and boulder beds belong to the Cap Beds (Fig 1.3).

Although these erosion surfaces were initially thought to be products of littoral wave-zone exposure (Miller & Grayson op. cit.), recent developments in studies of Waulsortian palaeoenvironmental settings (Lees et al. 1985; Lees & Miller 1985) suggest that submarine erosive processes were a more likely cause. Furthermore, the presence of a fill dominated by marine bioclasts, and the lack of any evidence of vadose silts, calcrete clasts or other fabrics characteristic of emergence, supports the present view that the fissures formed, and were filled, entirely in the submarine environment (J. Miller, pers. comm.).

Similar features filled with crinoidal packstones have been recorded from Waulsortian buildups elsewhere (Cotter 1966; Pray 1982).

The relative timing of these fissures is difficult to determine as no samples of their margins are avilable to identify which cement stages and fabrics they cut. However, their tendancy to be associated with erosional surfaces suggests that they may be relatively late features, post-dating buildup completion, compared to the neptunian dykes described below. Such fissures are important in preserving relicts of sediments which draped some buildups after they ceased to grow and were eroded, and thus record some post-accretional depositional environments which were otherwise not preserved.

8.2 NEPTUNIAN DYKES

Sediment-filled neptunian dykes occur in most Waulsortian buildups in the Craven Basin. The most obvious of them may be tens of metres in length and attain maximum widths of 0.5m, but the commonest are only about 15cm across, extending for several metres. As noted above, vertical or sub-vertical fractures are the rule but they may follow sinuous trends deviating significantly towards the horizontal, where they may also bifurcate and anastomose. Dykes may taper upwards or terminate in irregular cavernous voids over 1m in length and tens of centimetres in depth, which contain several generations of laminated geopetal sediment. The sediment fills of most of the dykes are characteristically finely-laminated, parallel to the fracture margins, although some contain areas with a mixture of wall-parallel and geopetal lamination.

The most common dyke-fill is creamy or light-grey porcellanous mudstone, which may locally contain clasts of the wall sediment, including CFC cements (Fig. 8.1A). Complex arrangements of sediments comprising several generations may occur in a single dyke. Less commonly, neptunian dykes may contain laminated peloidal or intraclastic sediments (Fig. 8.1 B&D) . These peloids vary in size up to 150μm, but are usually in the order of 50-60μm across, and their shape varies from ellipsoidal to quadrate.

Intraclasts vary in shape and size. Most have peloidal textures, but others contain skeletal grains, and many have cryptalgal micrite coatings.

The intergranular porosity of the peloidal dyke sediments is usually filled with inclusion-rich microsparitic calcite. It is difficult to distinguish cement from replacement in these coarse dyke-fills, and although most spar has the appearance of cement, often forming inclusion-rich rims around the peloids, some display highly irregular crystal boundaries, and undoubtedly formed by neomorphic replacement of a former interstitial micrite. On rare occasions, layers of CFC cements, (sometimes containing peloids) also developed, but these are usually discontinuous and are often truncated by subsequent generations of lime-mud.

8.2.1 Cavernous structures associated with Neptunian Dykes

In many of the Craven buildups there are large, cavernous structures which may, in some cases, be over a metre in length and tens of centimetres deep. These structures are filled by thick, often multi-generational, deposits of laminated and sometimes cross-laminated geopetal sediments, composed largely of a porcellanous mudstone comparable to that filling neptunian dykes (Fig. 8.1C). In some exposures, neptunian dykes, entering from below, terminate within these caverns, and clearly they were the source of the internal sediments.

The majority of these geopetal sediments either post-date or may be interbedded with CFC and Stage B-D non-ferroan scalenohedral calcites, but never cut any later cements. Any void space which remained above the geopetal sediments was filled by blocky calcite spar representing various deep burial cement stages.

Some of the best exposed caverns occur in Bellmanpark Quarry. Here, several sinuous neptunian dykes trending anywhere from vertical to almost horizontal are seen to terminate within large sediment-filled cavernous structures, containing laminated and sometimes cross-laminated or graded multi-generational sediments (Fig. 8.1D). The caverns have highly irregular embayed margins which are strongly suggestive of dissolution, while some of the geopetal sediments contain clasts of the bank facies material within them which are often angular and are indicative of erosive processes. In some of the cavities, a layer of crustiform iron sulphide cements developed

Figure 8.1 Neptunian dyke sediments

A Photomicrograph showing a lithic clast containing interlaminated micritic sediment and layers of CFC botryoidal mosaic (arrowed), contained within porcellaneous micrite filling a neptunian dyke. Dyke sediments are vertically laminated and parallel to the walls, indicating mud-injection. Stained thin section, Crow Hill buildup.

B Photomicrograph of peloidal sediments, laminated parallel to the walls of a high-angle neptunian dyke cutting M1 sediment. Dyke sediments comprise peloids with interstitial inclusion-rich microspar and micrite-rich laminae (arrow 1). Peloids are micritic, and vary in shape from ellipsoidal to quadrate, and occasionally tubular (arrow 2), and many may originate from breakdown of mud-filled calcified algal sheaths (cf. Conglio and James, 1985). Thin section, New Laund Hill buildup complex.

C Field photograph of laminated light-grey porcellaneous lime mudstone filling a large cavernous structure associated with neptunian dyke development. Internal sediments are multi-generational and occasionally cross-laminated (arrow). Sugar-loaf Quarry.

D Photomicrograph of graded, intraclastic, peloidal internal sediment filling a cavernous structure. Lithic intraclast (arrowed) has peloidal microfabric and also contains small fragments of bryozoan. The coarser intraclastic band was cemented by Stage A-D cements (S). Thin section, Bellmanpark Quarry.

Fig. 8.1

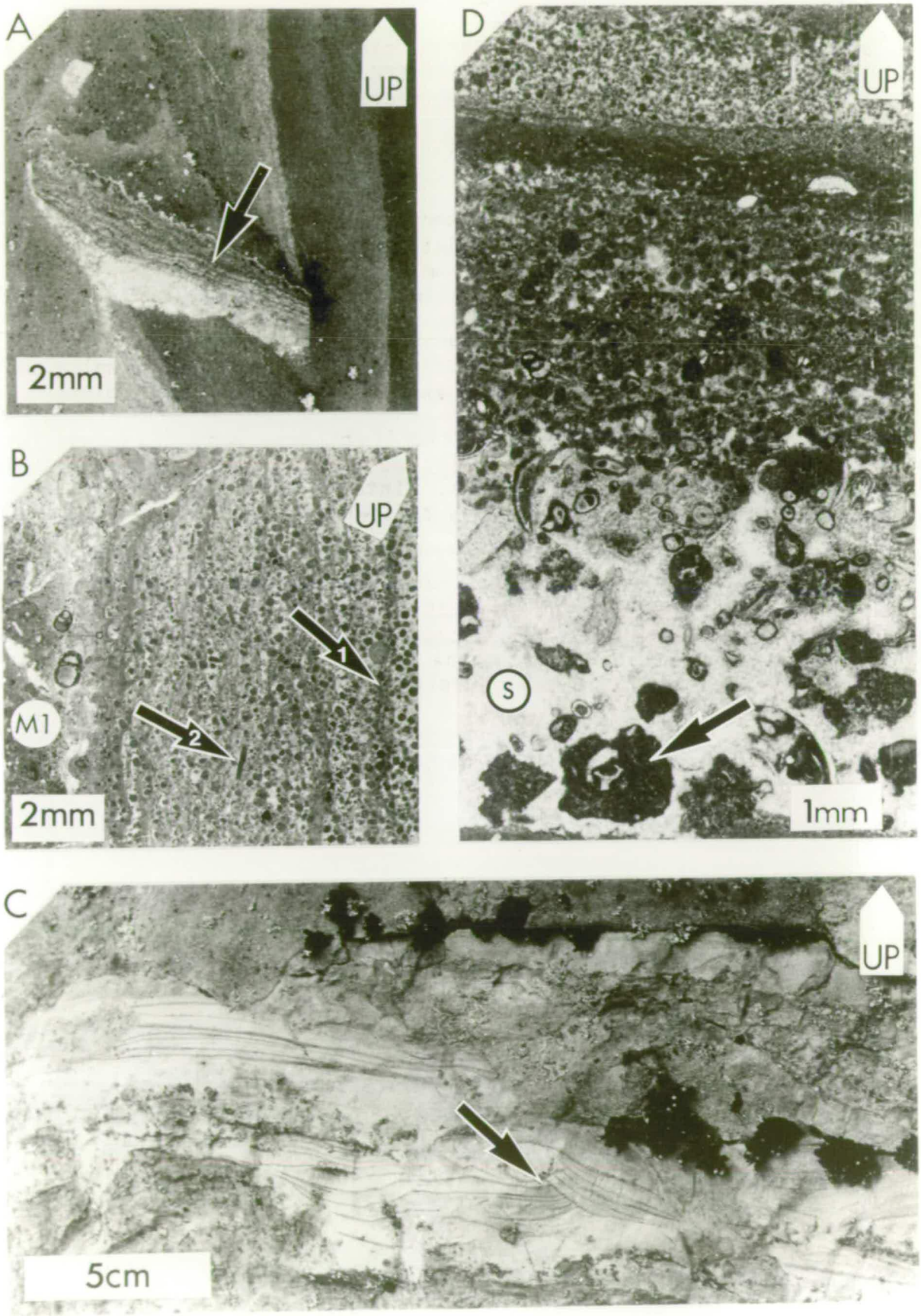

during a pause in sedimentation, before themselves being buried by a subsequent sediment influx (see Chapter 13), showing that cavern filling was accomplished by episodic pulses of sediment, separated by signficant periods of quiescence which allowed cements to precipitate. In thin section, these internal sediments are found to post-date Stage A-D cements, but are fractured by the first deep-burial cement stages (E & F) (see Chapter 13). Many parts of the primary network void system of the bank facies in the vicinity of these fissures contain similar geopetal sediments, which adopt the same position within the cement stratigraphy and thus were derived from the same source.

8.3 DISCUSSION

The lamination of neptunian dyke sediments parallel to the walls indicates the injection of a viscous fluidised sediment. Those which taper upwards, and those which terminate in large cavernous voids which were accessed from below, suggest that the dykes propagated upwards and were sourced at depth within the buildup. This being the case, significant volumes of unconsolidated lime mud must have persisted within the buildups throughout much of their shallow burial.

The pulsating nature of sediment influx as indicated by multiple generations of geopetal muds and the presence of intercalated cement layers both within geopetals and on fracture walls, indicates that the neptunian dykes opened incrementally, with intervening pauses without sediment influx between increments which were long enough to allow thin cements to develop.

8.3.1 Possible mechanism of dyke formation

The development of these neptunian dykes appears to have been related to an increase in hydrostatic pressure during burial within unconsolidated sediment which was undergoing collapse and dewatering, but which was confined within a rigid, partially lithified buildup. Eventually, the pressure head became great enough to cause dilatational fracture of the buildup, with the rapid injection of mobilis-

ed lime-mud as a viscous flow through the upwardly propagating structure. On encountering resistant, well-cemented regions in the buildup, the fractures were deviated and became bifurcated. In some regions, the primary void system adjacent to the fractures was sufficiently well-developed and interconnected that it was entered and exploited by the viscous flow, which locally produced erosion and enlargement of the original cavities to form cavernous structures.

Having been sourced at depth, the fluids in the dyke material were probably anoxic, and therefore would have been aggressive towards the wall-rock, so inducing dissolution and cavity enlargement. The anoxic nature of these fluids is indicated by the presence of crustform iron sulphide cements (see Chapter 13).

The laminated and geopetal nature of internal sediments in most cavernous structures suggests that the hydrostatic pressure-head of the injected slurry was largely dissipated within these voids, so that sediment was deposited under gravity from suspension. In some cases, however, sufficient fluid flows were created by the dyke injection itself, or induced by restricted pore throats, that cross-lamination was developed in more dilute suspensions.

Many cavities, even though not directly accessed by the neptunian dykes, also received lime mud internal sediments during and after shallow burial cementation. It is highly probable that a significant proportion of this material was freed into suspension in the pore fluids as a result of pressure changes induced by neptunian dyke development. Evidence from thin sections (below) indicates that similar processes were occurring even at a small scale during the shallow burial of the buildups.

8.3.2 Small-scale sediment-filled fractures

Thin section studies show that sediment re-mobilisation and microfracturing occurred on the microscopic as well as the macroscopic level.

Several sample sets provided an excellent opportunity for studying the development of complex, sediment- and spar-filled fractures in the bank facies.

Figure 8.2

The development of complex sediment and spar-filled micro-fracture systems during early diagenesis and into deep burial realms. All PPL photomicrographs are of the same stained thin section; Arbour Farm quarry.

A General view, showing areas of frames B-E in white outline. Also shows sequential fracture phases F1-4 (black arrows)

F1: Incipient crumbly-edged fracture network filled with dense bio-micrite.

F2: High angle fracture truncated F1 network and was partially cemented by CFC cement.

F3: Incremental fracture which breached F2 and stromatactoid cavity which developed in F1 micrite-fill. Filled by several layers of CFC and scalenohedral calcite, interlayered with internal sediments.

F4: Late, irregular micro-fractures associated with recrystallisation of earlier cements by deep burial fluids.

B Crumbly-edged F1 microfracture developed in primary bioclastic wackestone matrix (M1), and filled by very fine-grained M2 internal sediment. Delicate shells bridged the voids (arrow 1) indicating pull-apart. Others were broken (arrow 2) showing that sediment moved upward through the fracture.

C Stromatactoid cavity developed in M2 and was partially filled by interlayered CFC, possibly botryoidal mosaic (b), micrite and peloids (p). The cavity was later breached by an F3 fracture (arrowed) and was subsequently filled by another generation of CFC cement. Deep burial spar (S3) developed partially by recrystallisation of this CFC along an F4 microfracture.

D Showing incremental opening of F2 fracture. CFC cement S(S1) is truncated and followed by a thicker layer of CFC with dog-tooth terminations of scalenohedral calcite (S2). Further sediment and spar layers developed during subsequent dilation increments in the fracture.

E Sequence of cements in a stromatactoid cavity which developed by collapse of M2 muds. The sequence is directly comparable to the general cement stratigraphy of the Craven Waulsortian; A: Isopachous, inclusion-rich non-ferroan CFC cement; Stage A equivalent
B: Scalenohedral inclusion-poor non-ferroan calcite cement; Stage B-D equivalent
E: Blocky ferroan calcite; probably deep burial Stage E equivalent.

Fig. 8.2

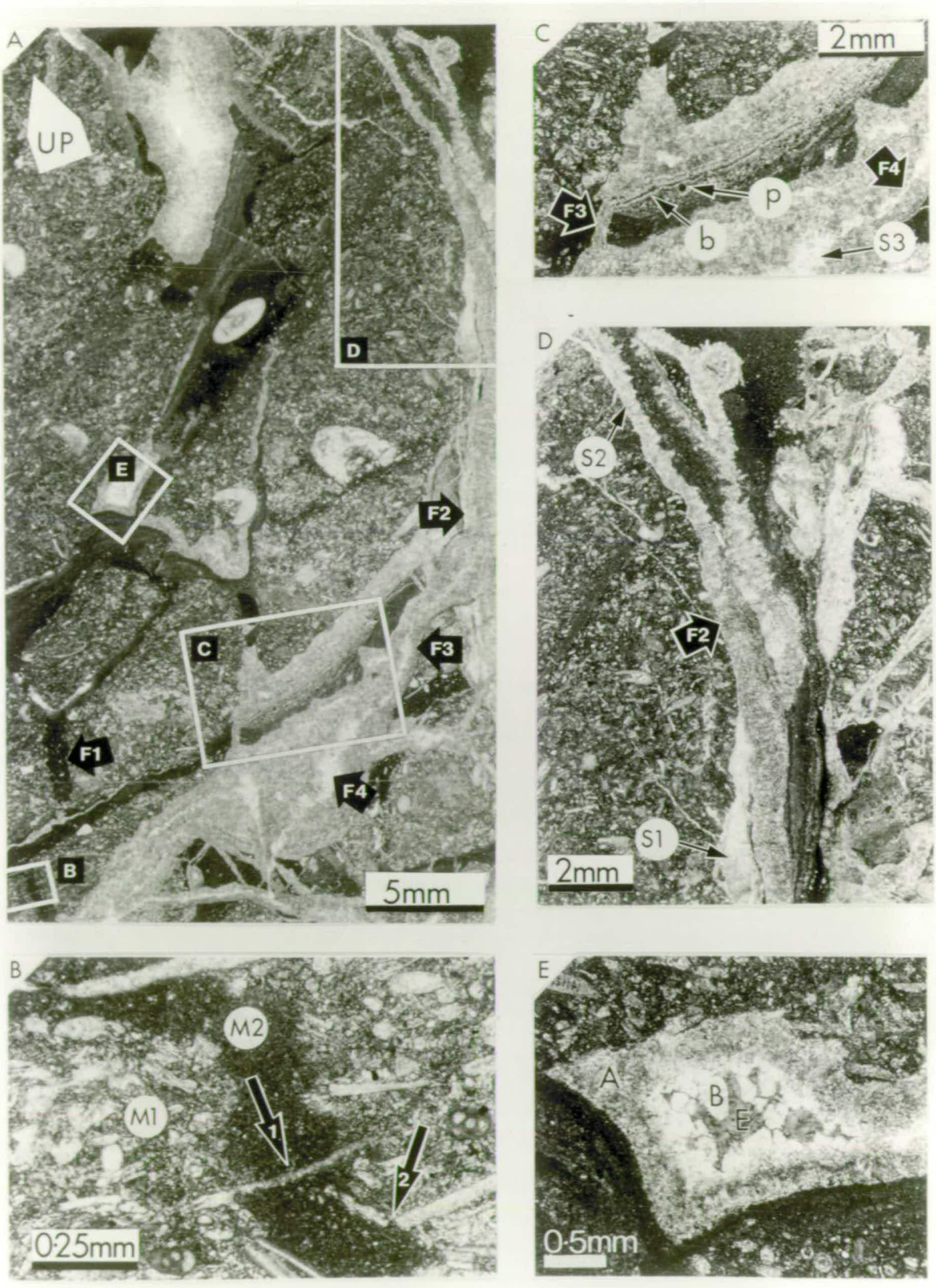
A
UP
D
E
F2
C
F3
F1
F4
B
5mm
C
2mm
F4
F3
P
b
S3
D
S2
F2
S1
2mm
B
M2
M1
1
2
0·25mm
E
A
B
E
0·5mm

Figure 8.3 Fracturing and dyke formation in early diagenesis.

A Thin section negative print. Sparry areas show black or dark grey. Dense micrites are lighter grey:
Movement on a microfracture (depicted by white half-arrows) displaced a stromatactoid cavity system which itself whose evidence of incipient, parallel 2-stage downstepping (black triangles, D). White dashed lines show different levels of the geopetal floors in each part of the stromatactoid system. A thin layer of scalenohedral calcite (s) developed preferentially on the upper wall of the microfracture which was subsequently filled by laminated micrite (m) which was initially injected through anastomosing networks (n) at the base of each of the two segments of the fracture. Bank facies, Porters Wood buildup.

B Photomicrograph showing exploitation of a neptunian dyke by later diagenetic veinlets. Sparry veinlet of Stage E and F (E) was cut by a later veinlet filled with Stage M kaolinite cement (k). Large arrow indicates an original stromatactoid cavity that was broken by the neptunian dyke fracture. Bank facies, Crow Hill buildup.

Fig. 8.3

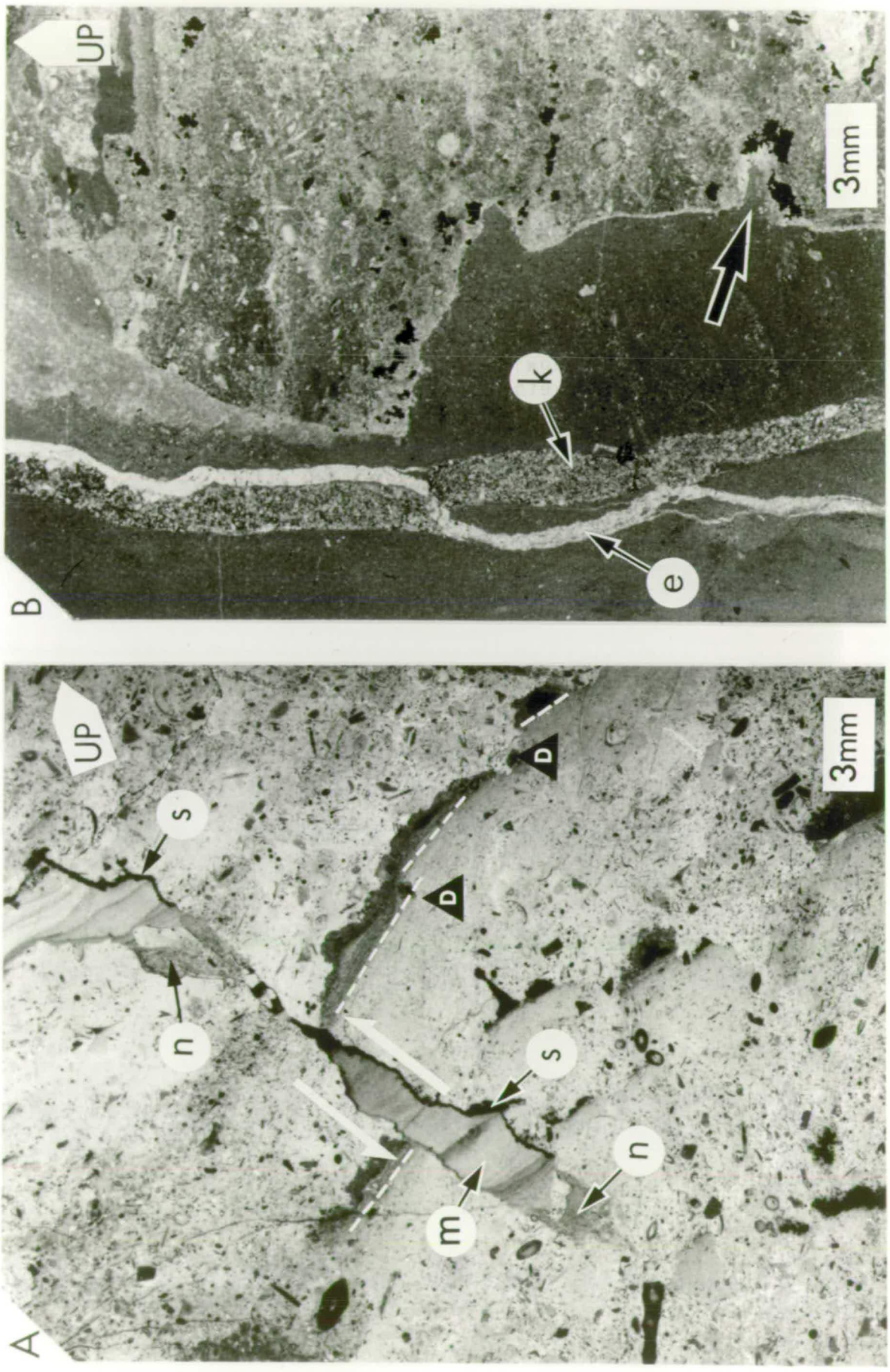

Case histories are given below to illustrate the variety of fabrics and textures which could develop.

A). From Arbour Farm quarry, where many neptunian dykes cut a Waulsortian buildup which is associated with extensive post-accretion boulder bed deposits. This illustrates sequential development of a complex fabric including incipient fracture, sediment remobilisation and cementation (Fig. 8.2).

Sequence of events:

1. A network of incipient crumbly-edged fractures (F1) first developed within the M1 bioclastic wackestone. These were filled with dense M2 lime-mudstone. Characteristically for crumbly-edged fractures the walls are refittable and often contain delicate shells which bridged the voids, showing that the matrix pulled apart around them rather than breaking in a brittle fashion. Some protruding shells were, however, broken at the facture margins, and in Fig. 8.2B, the direction in which a broken fragment was displaced indicates that the sediment in the fracture moved upwards.

2. A second phase of fracturing, F2, developed a straight-sided high-angle fracture which was partially cemented by a thin isopachous layer of CFC spar (S1). At about the same time, stromatactoid cavities developed by shrinkage and collapse within the F1 system, and became partially filled with peloidal geopetal sediments and thin layers of CFC (?botryoidal mosaic) cements. The source of the peloids is uncertain as the M1 sediment has no apparent peloidal component. They must therefore have been transported into the system along the F2 fractures or else developed <u>in situ</u>, either as micrite cement or organically precipitated material.

3. Successive incremental openings of F2 allowed the introduction of diagenetic fluids which precipitated a thicker layer of CFC cement and scalenohedral calcite (S2). The F2 fracture then was breached and an irregular cavity system (F3) developed truncating earlier structures and showing evidence of dissolution at its margins. The

F3 fractures also breached the stromatactoid cavities in the F1 system, and precipitated CFC and Stage B-D scalenohedral non-ferroan cements. Several increments of opening occurred at this stage resulting in alternating cement and sediment layers. Each of these incremental spar layers consists of CFC followed by non-ferroan scalenohedral calcites of Stage B, (this is further evidence to support the diachronous nature of these cements).

4. The final phase involved the development of a series of micro-fractures,which were modified by dissolution of the fracture margins, into which zoned ferroan calcite cements precipitated (S3). These cements also occluded any remaining pore-space in the stromatactoid cavities.

Significant recrystallisation of the earlier CFC cements by ferroan calcite was also associated with the influx of these fluids. The S3 cements are identified as deep burial stages.

B). From Porters Wood buildup, showing how microfaulting occurred in association with a sediment-filled fracture (Fig. 8.3A)

Sequence of events:

A stromatactoid cavity was displaced on either side of the initial fracture, which was then partially filled by a rim of scalenohedral calcite cement and laminated geopetal sediments.

The cement layer (s) is discontinuous and better developed on one wall of the fracture than the other. It is apparent that the geopetal sediment layers in the fracture were draped at an angle across the cavity margins, probably because the fracture was not vertical, and thus cement on one wall would have tended to be buried while the other remained uncovered, i.e allowing crystallisation of cement in open space. A suggestion of down-stepping occurs in the stromatactoid system which was cut by the fracture. Lees (1964) related such down-stepping to the development of stromatactoid cavities in beds with steep depositional slopes.

The fracture is divided into 2 segments, the lower portions of which are not sharply defined. Instead, they consist of anastomosing

networks (n) filled with lime mud which show no evidence of lamination. It would appear that these are regions where the lime mud was injected through the M1 sediment as a viscous flow until the larger fracture pulled apart, opening upwards and thus dissipating the hydrostatic pressure. This would also explain the discontinuity of the fracture-lining cements in these lower regions where there was never an open void into which cements could directly precipitate.

Both of these case histories indicate how neptunian dykes were formed incipiently during early burial. The same processes acted on a larger scale, with progressive burial developing greater hydrostatic heads within the buildups, from a combination of dewatering and overburden pressure, resulting in large neptunian dyke systems.

8.4 SUBSEQUENT DIAGENESIS

The formation of the neptunian dyke system provided numerous planes of structural weakness in the Waulsortian buildups. These were often re-activated during later periods of tectonism, so that deep burial vein phases often followed the course of the dyke structures. A dyke from Crow Hill (Fig. 8.3B) demonstrates this with two veinlet phases, the first containing Stage E and F cements and the latter containing Stage M kaolinite cement (see below Chapters 9 & 12), developing within the earlier dyke-fill sediments.

8.5 PREVIOUS WORK

Neptunian dykes have been reported from a range of Waulsortian and other carbonate buildups, (Philcox 1963; Pray 1965, 1982; Cotter 1966; Stone 1972; Logan & Semenuik 1976; Enos 1986, Kerans et al. 1986). Most accounts identify fissures cutting the host sediment at steep angles, but it has also been noted that they may persist laterally or vertically (Pray 1982; Philcox 1963, Fig. 2).

Most of those described are in the order of tens of centimetres across and up to several tens of metres in length (Philcox 1963; Pray 1982; Kerans et al. 1986), but the most striking examples from the Devonian reef complexes of the Canning Basin Western Australia are

6km long, 20m wide and 80m deep (Kerans et al. 1986).

As in the Craven Basin Waulsortian, dyke-filling sediments were reported to be largely composed of lime mud (Pray 1982), usually banded, often parallel to the fracture margins (Kerans et al. 1986) and sometimes also contained layers of a variety of larger particles such as small shells, intraclasts and peloids (Philcox 1963). Layers of cement, particularly radiaxial fibrous calcite, have also been reported from neptunian dyke-fills (Logan & Semenuik 1976; Kerans et al. 1986).

Although the features described are superficially similar, a variety of mechanisms have been proposed for neptunian dyke formation. In association with Waulsortian "mudstone fissures", Philcox (1963) identified a set of prominent sub-parallel planes along which movement of wedges and blocks of 'reef' had taken place. These were then filled by banded calcite mudstone, thought to have infiltrated from above.

Pray (1965, 1982) reported "tabular dikes and more irregular injection bodies" in the larger Mississippian bioherms (Waulsortian type) of southern New Mexico. The mechanism which he proposed was one of injection, largely of carbonate mudstone or crinoid-rich packstones, into dilational fractures which apparently formed prior to burial of the buildups. Cementation, consisting of fibrous and syntaxial rim cement within these buildups preceeded injection. Pray (1965) cited four factors which he believed to be important in the origin and localisation of injections:-

1) High differential sedimentary loads on the substrate
2) Low permeability of the (buildup) core facies
3) Loose-packing of "avalanche face" deposits
4) Little early cementation of the substrate.

In his 1982 paper on the New Mexico bioherms, Pray suggested that fracturing of the heavy, partially uncemented mass of a buildup might cause injection of sediment from below. Stone (1972) also believed that sediment had been injected along the neptunian dykes, while he and Enos (1986) showed that dyke formation was contemporaneous with early marine cementation.

Neptunian dykes (and sills) have also been identified in Devonian reef complexes of the Canning basin (Logan & Semenuik 1976; Kerans et al. 1986), and these are related to internal sediments which occlude significant volumes of pore space. Kerans et al. (1986) concluded that the neptunian dykes were early diagenetic and developed during an often complex, multi-generational series of fracturing, cementation and sediment-filling episodes. Cements associated with these dykes had similar isotopic composition to their host-rock counterparts, which was given as further evidence for an early diagenetic origin. In these examples, neptunian dykes were filled by a combination of sediment from above, growth of encrusting organisms down the walls, internal sedimentation, and precipitation of marine cement.

The association of cavernous sediment-filled voids with neptunian dyke development has also been recognised from the Canning Basin examples (Logan & Semeniuk; Kerans et al., op. cit.), and these voids contain laminated lime mud, peloidal and intraclastic sediments, while Pray (1982) reported that dyke sediments were occasionally injected into primary cavities in the New Mexico Waulsortian bioherms. However, in the case of the Waulsortian, until now, no detailed petrography of the fractures and their adjacent sediment had been undertaken to support the hypotheses for their origin.

8.6 CONCLUDING REMARKS

Surface-opening fissures appear, at least in the Craven cases so far known, to have been localised phenomena connected with erosion of buildups after they had ceased to accrete. They apparently had little significance in the diagenetic history of the buildups. However, the neptunian dyke systems provide evidence as to the consistency of buildup sediments and the origins of internal sediments, and had a substantial influence on diagenesis within the buildups over a long period of their burial history. The three main areas of influence are summarised below:-

1. Cement stratigraphy

a) Neptunian dykes developed throughout the early (shallow burial) diagenetic history of the Waulsortian buildups of the Craven Basin. Field and thin section observations show that dyke formation ceased before the development of the first deep burial cements in the sequence.

b) The development of shallow burial cements (Stage A-D) within incremental dyke-fills shows that the neptunian structures were early diagenetic. Furthermore, the repeated development of layers of Stage A-D cements within single dyke-fills shows that these early diagenetic cements were diachronous.

c) Neptunian dykes acted as planes of weakness during deep burial tectonic episodes, so that later veinlet phases exploited the dyke trends.

2. Porosity

On both macroscopic and microscopic scales, the development of neptunian dykes opened up significant volumes of secondary porosity, but the majority of this, including the large cavernous voids which formed in some instances, was filled by sediment during or shortly after dyke development. Furthermore, some of the original bank porosity was occluded by sediment fed by dyke injection at all stages of their development from the incipient microfractures to large-scale systems. This is not to say that all internal sediments that post-dated early diagenetic cements were sourced in fissures. Localised stoping of bank muds, either mechanically or dissolution induced, would also have been a source for such internal sediments (Logan & Semeniuk 1976). It must also be highly probable that many of the spar-filled fractures which contain early diagenetic cements (Chapter 7), were directly or indirectly associated with the intrusion of neptunian dykes or the development of similar small scale structures i.e. they influenced some early, secondary porosity increase in the banks.

3. Lithification of buildups

The development of neptunian dykes was an important aspect of the early burial diagenesis of the Waulsortian buildups. They show that although the buildups were sufficiently competant to respond to stress by fracturing, they could only have been partially lithified because they still contained significant volumes of unconsolidated material.

Initially, the partially-lithified sediment had a firm gel consistency which responded to extensional forces by developing crumbly-edged, refitable micro-fractures. Later, when lithification was more advanced, large-scale neptunian dyke systems developed which showed evidence of brittle fracture. However, there were still unlithified areas providing substantial volumes of sediment which filled the dykes and some of the existing void-network in adjacent regions of the bank facies. Complete lithification of the bank facies clearly did not occur until a later stage in the burial history of the Waulsortian buildups.

In general, the neptunian dykes appear to have been sourced at depth within the buildup after episodic surges of hydrostatic pressure caused by collapse and sediment dewatering. This obviously exerted substantial tensional stress upon the buildup which could have resulted in displacement of large blocks of sediment.

DIAGENESIS

PART TWO

DIAGENESIS PART TWO

DEEP BURIAL DIAGENESIS

Introduction

Cement stages which developed after Stage D are recognisable in all the Craven buildups. Each stage is associated with the development of brittle fractures which acted as conduits for the diagenetic fluids. This suggests that individual cement stages precipitated from these fluids were developed more or less synchronously, indicating the establishment of effectively homogenous formation waters across the entire Craven Basin. Combined with geochemical and isotopic data (see below), the post-Stage D cements are therefore interpreted as products of deep burial diagenesis.

A major part of the diagenetic history of the Waulsortian facies therefore took place in the deeper subsurface, an environment which is much less understood than the well-documented surface and near-surface diagenetic environments.

Following the emplacement of Stage D and earlier cements, the next sequence of diagenetic episodes involved the development of secondary porosity. Cements of different mineralogies including calcite, dolomite and kaolinite were emplaced; recrystallisation and replacement of existing fabrics and mineralogies occurred and mineralisation with quartz, fluorite, barytes, sphalerite and marcasite took place.

Much of the original porosity of the rocks had been occluded by earlier cements, and therefore the cross-cutting relationships of veinlet phases, stylolites and previous sparry calcite cements were used as the main constraints on the relative timing of each cement stage.

The basic carbonate cement sequence which developed during deep burial can be conveniently divided into three packages which represent two periods of calcite cementation (Chapter 9 and Chapter 12) separated by a phase or phases of dolomitisation and dolomite cementation (Chapter 11). This three-fold subdivision provides the

framework into which the timing of stylolitisation (Chapter 10) and mineralisation (Chapter 13) can be integrated.

Burial diagenesis in the literature: A brief review.

Most studies of carbonate diagenesis have concentrated on the effects of near-surface diagenetic environments because their modern analogues are more readily accessible. However, in recent years, detailed studies of the effects of deep burial diagenesis have received more attention. Scholle & Halley (1985) give a general review of progress, and more detailed studies include those of Wong & Oldershaw 1981; Moore 1985; Prezbindowski 1985; Woronick & Land 1985; and several papers in Schroeder & Purser 1986.

The important effect of deep burial diagenesis on porosity loss during compaction and cementation has received particular attention because of obvious consequences for hydrocarbon reservoir characteristics. Many carbonate sediments maintain high porosities through the shallow subsurface diagenetic environments (Halley & Harris 1979), the exceptions being those cemented at the seafloor or in marine phreatic environments, where almost total porosity loss may occur (Scholle & Halley 1985).

Compaction results from mechanical or chemical processes, often in combination. In deep burial situations, evidence of mechanical compaction in the form of grain breakage textures is uncommon in fine-grained carbonate sediments (Pray 1960; Zankl 1969; Bathurst 1970), including Waulsortian buildups (Meyers 1978, 1980). Processes effecting pressure dissolution and the production of stylolites have been associated with porosity loss either as a result of compaction or the remobilisation of carbonate into the pore fluids which subsequently precipitated as void-filling cement (Oldershaw & Scoffin 1967; Bathurst 1975; Wong & Oldershaw 1981).

Cementation in deep burial situations is often associated with pressure dissolution features (Buxton & Sibley 1981) and the development of sets of fractures (Nelson 1981).

A major influence on the study of deep burial cements has been the development of fluid inclusion and stable isotope studies which have assisted in the identification of deep burial cements and

their fluid source (Hudson 1977; Walls et al. 1979; Dickson & Coleman 1980; Moore & Druckman 1981; Buruss et al. 1985; Moore 1985). Unfortunately, most authors have tended to group all deep burial cements together, concentrating only on the fine detail of the shallow burial diagenesis (e.g. Meyers & Lohmann 1985, Fig. 4).

The two most commonly reported deep burial carbonate cement mineralogies are ferroan calcite (Meyers 1974; Walkden & Berry 1984b; Oldershaw & Scoffin 1967; Grover & Read 1983; Wong & Oldershaw 1981) and ferroan dolomite. The ferroan dolomite often exhibits a characteristic habit with curved crystal faces and sweeping extinction which has been called baroque dolomite (Folk & Asseretto 1974) or saddle dolomite (Radke & Mathis 1980). Many other examples of deep burial dolomite have been identified e.g. by Woronick & Land (1985), Choquette (1971), Taylor & Sibley (1985) and Schofield and Adams (1985).

Figure 9.1 Burial cements

A Photomicrograph of a stained peel showing burial calcite Stages B to I developed in a cavity supported by a productid brachiopod. Notice 'horse tail' veinlet feeding the strongly-ferroan (deep blue, centre) Stage I. Field of view = 2.5cm. Coplow bank facies.

B Cathodoluminescence macro-photograph showing a stromatactoid cavity containing marine, shallow burial and vein-fed deep burial cement Stages (A-I, and N). Notice two separate veinlet sets and cognate hairline microveinlets, illustrating the problems encountered in ensuring purity of material for geochemical analyses. Field of view = 4cm. Coplow bank facies.

Fig. 9.1

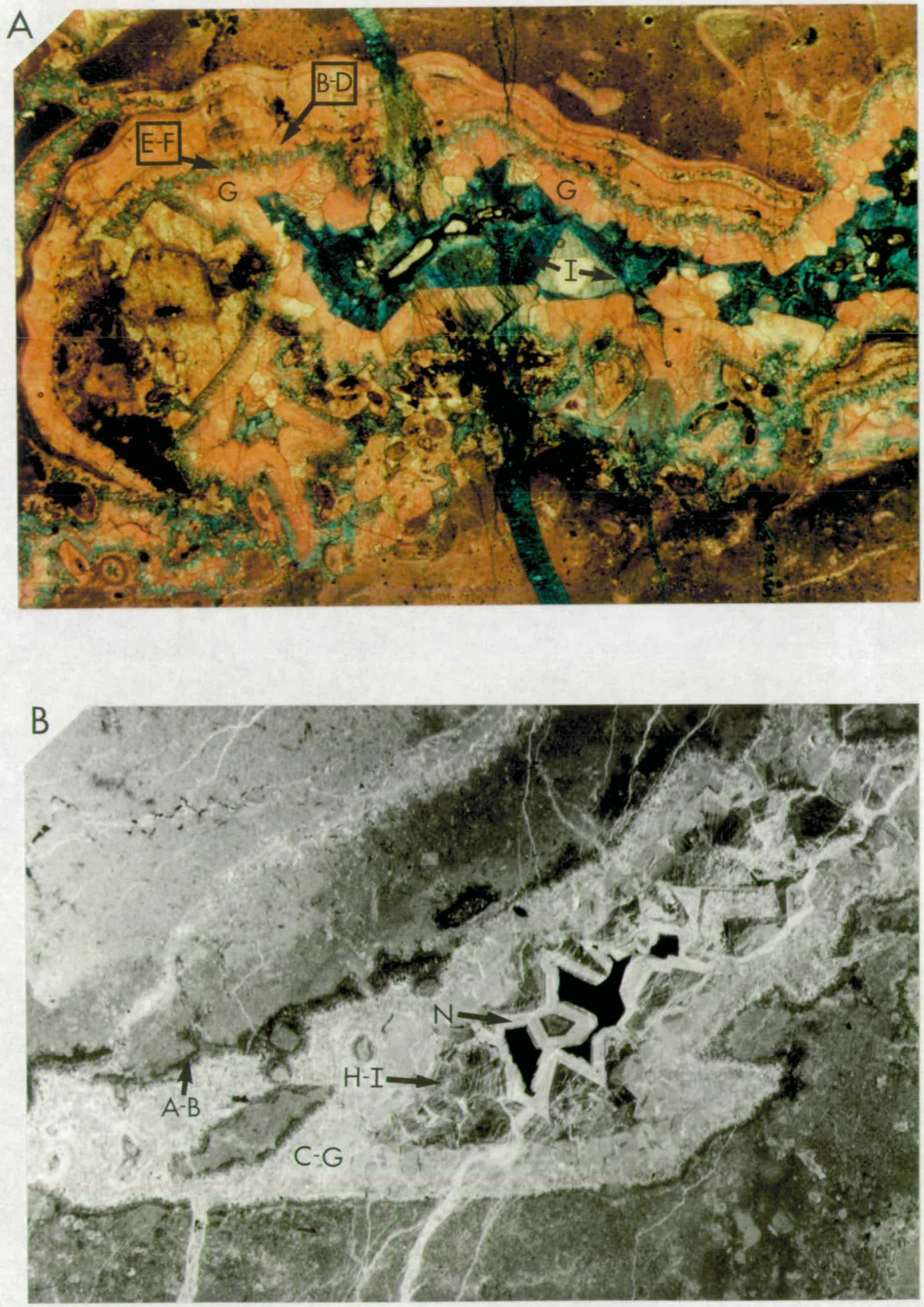

CHAPTER 9

CEMENT STAGES E-I: Fracture-fed blocky calcite spars

Five blocky calcite cement stages (E-I) formed that part of the void filling cement sequence between the non-ferroan scalenohedral calcites of Stage B to D, and the later dolomite cements (Fig. 9.1). Four of the five cement stages in this section are ferroan calcites. They fall into two groups (E-F,H-I), divided by a non-ferroan calcite spar (Stage G).

Under plane (PPL) and crossed polars (XPL), these cements exhibit the classic drusy textures of planar intercrystalline boundaries and increasing crystal size away from the substrate (Bathurst 1975). Staining and CL reveal a centripetal sequence of cement stages which cut intercrystalline compromise boundaries.

All these cements are vein-fed, and the fractures which acted as conduits for the carbonate-bearing fluids were the product of tensional strain. The morphology of the fractures and cement fabrics precipitating within them can be related to the nature of the strain acting upon the rocks (see Chapter 16).

The sequence of cements in this chapter was determined primarily from the ARS /PF staining characteristics (Table 9.1). The cathodoluminescence of adjacent cement stages in this group is often very similar, making it difficult to separate individual stages on the basis of their CL alone. Furthermore, compositional sector zonation is common in these cements, and this can cause further difficulties when attempting cement classification solely on the basis of CL characteristics. Staining also revealed sector zonation, but not as sensitively as CL, so the overall stain intensity of each stage was more consistent. Trace element analysis of cements identified as ferroan calcite from their staining response, on average contained at least 0.1 wt % FeO.

Although the sequence of cements outlined in Table 9.1 is consistent on a basinwide scale, local disconformities and unconformities within the cement sequence are common. The thickness (volume) of an individual cement stage may vary considerably in neighbouring cavities, and some stages may be completely absent.

This suggests that the bulk of the porespace remaining after the non-ferroan scalenohedral calcites was effectively sealed from migrating formation fluids, probably by a combination of this earlier occluding cementation and by compaction of the less permeable peri-Waulsortian facies, so that subsequent cements only precipitated when tectonic fracturing allowed ingress of fluids to the remaining pore-system in the banks (see Chapter 18).

Table 9.1 Staining and CL characteristics of pre-dolomite blocky calcite cements.

Stage	Stain (colour)	CL (intensity)	Mineralogy
I	Royal blue	Very dull	Ferroan calcite
H	Purple	Moderate to light	Ferroan calcite
G	Pink	Moderate to dull	Non-ferroan calcite
F	Purple	Moderate dull to light	Ferroan calcite
E	Light blue	Dull	Ferroan calcite

The first vein-fed cements in the sequence consist of two ferroan calcite stages (Stage E and F) which are associated with a single phase of fracturing. As result of this, they are always found in close association, and in many respects can be treated as a single unit in the cement sequence.

The two cement stages are separated on the basis of their staining characteristics and the common occurrence of a dissolution surface between them. The dissolution of the earlier Stage E by the later Stage F is often accompanied by recrystallisation and the development of complex crystal aggregates (see below 9.6). Fracturing developed a series of irregular sub-parallel-sided veinlets and microveinlets which often show evidence of grain breakage and displacement at their margins confirming brittle behaviour. Fractures feeding these stages are relatively uncommon, particularly outwith

the bank facies. It is possible, therefore, that they may have been related to a localised stress-field around the banks which developed due to their greater resistance to compaction relative to the peri-Waulsortian envelope during the earliest phase of deep burial. Cements within the Stage E veinlets are post-dilational, i.e. they grew under zero stress conditions after fracturing had ceased (see below Chapter 16). Equant blocky calcite crystals developed in the narrow veinlets, while in larger veins, centripetal void-filling sequences formed.

9.1 STAGE E Ferroan Calcite

These are the first ferroan calcite cements in the sequence. They stain light blue and exhibit dull orange luminescence. Multiple growth zonation on a micron to sub-micron scale is common.

9.1.1 Composition

1. Trace elements

Of the trace elements analysed (Table 9.2) only the concentration of iron is of major significance (av. 0.32 wt% FeO). This represents a marked increase in Fe relative to earlier cements, confirming the blue staining response of this stage (Fig. 9.2). Mn contents are also increased over Stage D, while Mg is relatively depleted. Despite the greater concentration of Mn activator, the duller CL of Stage E compared with Stage D represents CL quenching by Fe.

2. Stable Isotopes

The close association of Stage E and F made it impossible to obtain pure samples of each stage of the required weight for isotope analysis by the method employed in this study. Samples of aggregate mixtures of the two stages were therefore analysed (Table 9.2)

The isotopic analyses show depleted $\delta^{18}O$ and slightly enriched $\delta^{13}C$ relative to earlier cements (Fig. 9.3).

Table 9.2 Mean Composition of Stage E cements

Oxide	Mean wt%	S.D.	C.V.	n=30
CaO	54.47	2.44	0.05	
MgO	0.18	0.06	0.32	
FeO	0.32	0.10	0.33	
MnO	0.10	0.11	1.03	

30 analyses from 3 buildups

S.D. = Standard deviation at 95% confidence level
C.V. = Coefficient of variation

Table 9.3 Isotopic composition of Stage E and Stage F aggregates in per mil (°/₀₀) against PDB standard

Sample	$\delta^{13}C$	$\delta^{18}O$
C28	2.56	-5.28
GE1	3.63	-5.65
mean	3.10±0.54	-5.47±0.19

9.2 STAGE F Ferroan Calcite

Stage F cements are also ferroan calcite, but they exhibit a distinctive purple staining colouration which indicates lower Fe concentration than Stage E. Two substages are occasionally developed in Stage F, the first giving a stronger purple stain than the second. Under CL, the earlier substage F1 has moderate to dull intensity luminescence whereas Substage F2 has brighter luminescence which locally exhibits a gradational decrease in intensity towards distal regions of crystals. Dissolution and recrystallisation of Stage E

cements (by Stage F fluids) is common, resulting in the development of complex crystal aggregates (see Fig. 9.5).

9.2.1 Composition

The purple stain of Stage F indicates a weakly ferroan calcite.

1. Trace elements

The decrease in iron relative to Stage E as indicated by staining, is accompanied by depletion of other trace elements (Table 9.4 and Fig. 9.2).

Table 9.4 Mean Composition of Stage F cements

Oxide	Mean wt%	S.D.	C.V.	n=37
CaO	53.35	3.40	0.06	
MgO	0.12	0.05	0.45	
FeO	0.13	0.04	0.35	
MnO	0.06	0.04	0.72	

37 Samples from 3 buildups

S.D. = Standard deviation at 95% confidence level
C.V. = Coefficient of variation

9.2.2 Distribution of Stage E and F cements

1. Bank facies

Stage E and F cements were fed by infrequent veinlets and occur in primary intraskeletal porespace and stromatactoid cavities, usually in the form of crystal aggregates. Rarely, they developed syntaxially as crinoid overgrowths.

Development of these cements is extremely variable. In many spar sequences, they are represented by a thin sub-millimetre layer, and may even be confined to overgrowths on non-ferroan scalenohedral calcites which are only visible as spires in c-axis sections.

2. Toe facies

In the toe facies, Stage E and F cements developed mainly in secondary cavities which formed after early micrite dissolution, and also in primary intergranular and intraskeletal voids. Fractures containing these cements are slightly less common than in the bank facies.

3. Flank/interbank facies

Stage E and F cements are relatively common in the volumetrically limited inter- and intra-granular pores of the flank and, especially, the interbank facies (Chapter 18, Fig. 18.2).

9.2.3 Interpretation of Stages E and F.

Stages E and F are the first ferroan calcites in the sequence. Although related to fractures, their isotopic composition indicates that they were formed at moderate burial depths, perhaps in the order of a few tens to hundreds of metres. The transition from oxic through suboxic to sulphate reduction environments in the shallow subsurface, as indicated by the cements described in the previous chapters, was followed by the onset of bacterial fermentation of organic matter at moderate burial depths (cf.Irwin et al. 1977). It is in this environment that the first major development of iron-rich diagenetic carbonate phases is likely to occur (Curtis 1978).

It is suggested therefore, that the Stage E and F calcites precipitated from reducing fluids in the zone of fermentation. Curtis (1978) suggests that this zone is achieved within the first few to a few tens of metres of burial in pelagic sediments. In more oxygenated environments, such as those in which the Waulsortian buildups developed, it is possible that the zone of bacterial fermentation would be deeper in the sediment pile.

Fig. 9.2 Trace element geochemistry of Stage E–I cements.

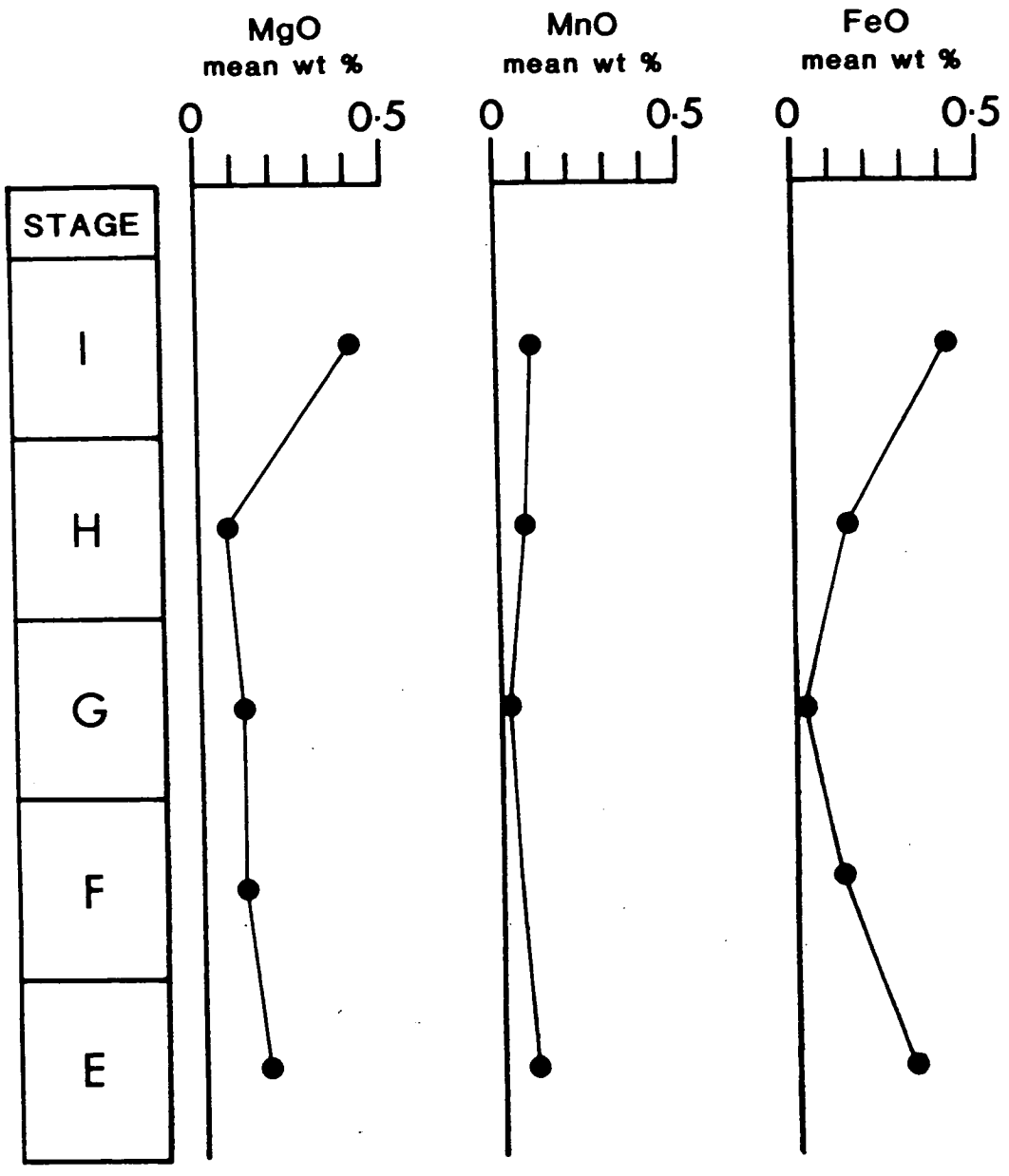

Fig. 9.3 Isotopic composition of deep burial calcite Stages E to I compared with earlier cements.

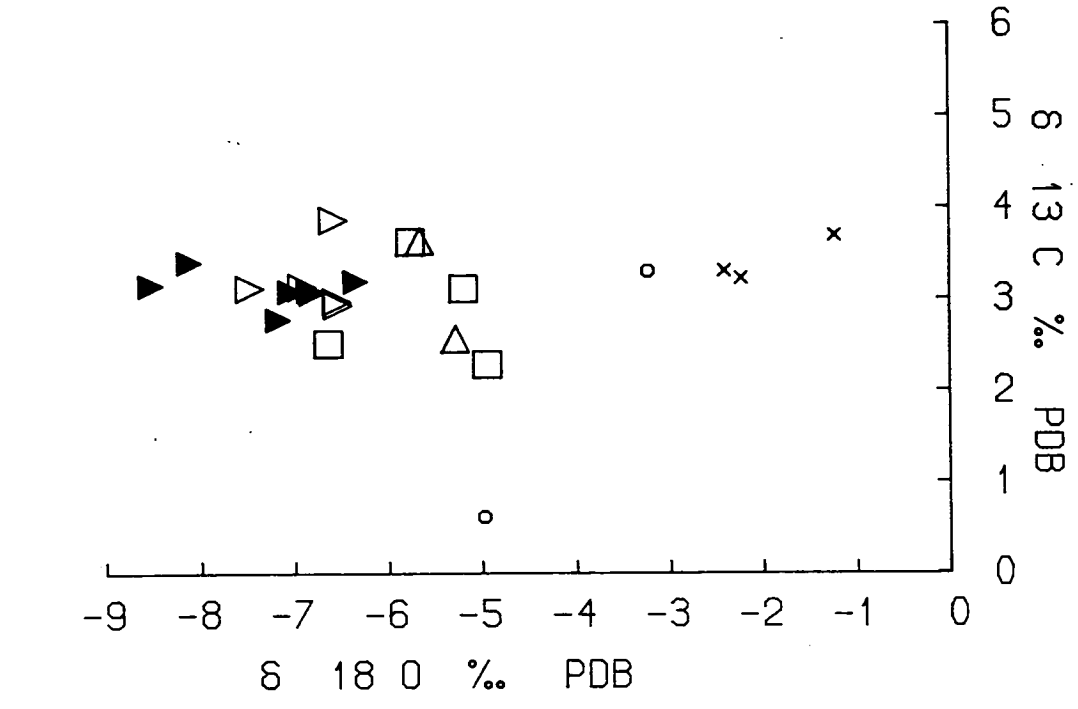

△ STAGE E&F Ferroan calcite
□ STAGE G Non-ferroan calcite
▽ STAGE H&I Ferroan calcite aggregates
▼ STAGE I Ferroan calcite
× Stage A
o Stage B&C

9.3 STAGE G Non-ferroan Calcite

Stage G cements are associated with the development of a series of irregular-sided fractures, which show evidence of dissolution at their margins. These veinlets are often discontinuous and may taper to a point. Cements within the veinlets are post-dilational and always exhibit classic drusy spar textures. Microbrecciation of earlier cements, particularly CFC is observed in some samples (Fig. 9.4).

9.3.1 Composition

Stage G cements give a pink staining response with ARS and PF, indicating non-ferroan calcite. Luminescence is usually dull or moderate orange, with some brighter orange substages and crystal sector zonation.

1. Trace elements

The depletion in iron relative to Stage F cements is accompanied by a slight enrichment of magnesium (Fig. 9.2), while the level of manganese is lower (Table 9.5).

2. Stable Isotopes

The $\delta^{13}C$ isotopic composition of Stage G (Table 9.6), shows little departure from that of earlier cements, whereas its $\delta^{18}O$ is slightly depleted (Fig. 9.3) relative to previous stages.

Table 9.5 Mean Composition of Stage G cements

Oxide	Mean wt%	S.D.	C.V.	n=52
CaO	55.10	2.00	0.04	
MgO	0.12	0.05	0.46	
FeO	0.03	0.03	1.05	
MnO	0.03	0.02	0.66	

S.D. = Standard deviation at 95% confidence level
C.V. = Coefficient of variation
52 Samples from 6 buildups

Table 9.6 Isotopic composition of Stage G cements
Values stated in per mil (°/₀₀) against PDB standard

Sample	$\delta^{13}C$	$\delta^{18}O$
GE1	2.51	-6.63
C43	3.11	-5.19
CA9	3.62	-5.75
C25	2.28	-4.94
Mean	2.88 ± 0.52	-5.63 ± 0.65

9.3.2 Distribution of Stage G cements

1. Bank facies

Stage G cements are mainly confined to stromatactoid cavities and fracture-fills, because most primary intraskeletal and intergranular pore space in the banks had been occluded by earlier cements. They are, however, better developed in the banks than in any other facies due to the availability of open space in the remaining void network.

2. Toe facies

Stage G cements are uncommon in the toe facies, accounting for only 3% of the total cement volume (see Chapter 18; Fig. 18.2).

3. Interbank facies

Only a trace of Stage G cement occurs in the interbank facies, most pore space having been occluded by earlier cements. Although fractures containing non-ferroan calcite are common in the interbank, it is often difficult to assign them to a particular cement stage in the absence of void-fills which can relate them to the cement stratigraphy (see Chapter 12).

9.3.3 Interpretation of Stage G

Oxygen isotopic analyses indicate that these cements reflect continued burial of the Waulsortian buildups, while the consistency of $\delta^{13}C$ values with earlier cements indicates no major change in carbon (fluid) source.

The most probable cause of a relative drop in Fe content would be a change in Eh of the formation waters, resulting in an oxic fluid in which iron existed only in the Fe^{3+} state and therefore could not substitute into the calcite lattice. The resultant oxic fluid may well have been sufficiently aggressive to cause the dissolution episode prior to the development of Stage G cements. The processes affecting the composition of formation waters in the deep burial realm are poorly understood and it is therefore impossible to identify the source of these aggressive fluids. The influx of such fluids could suggest a partially meteoric source, but if this was the case then the $\delta^{13}C$ of the fluids must have been completely buffered by carbonate dissolution from the rocks, as there is no departure from $\delta^{13}C$ values of earlier cements.

Figure 9.4

A PPL Photomicrograph showing micro-brecciation and dissolution of Stage A cements prior to the precipitation of blocky, non-ferroan calcite of Stage G. Thin section, Dunnow bank facies.

B Cathodoluminescence photomicrograph showing burial calcite stages in a cavity-fill cement sequence. Non-luminescent Stage B; moderate intensity orange-luminescent Stage G; and very dull-luminescent Stage I are identified (white circles). Stages C-F cannot be clearly delineated in CL. Stage I contains many fine zones (z) and is fed by a swarm of veinlets and micro-veinlets (v). Thin section, Coplow bank facies.

Fig. 9.4

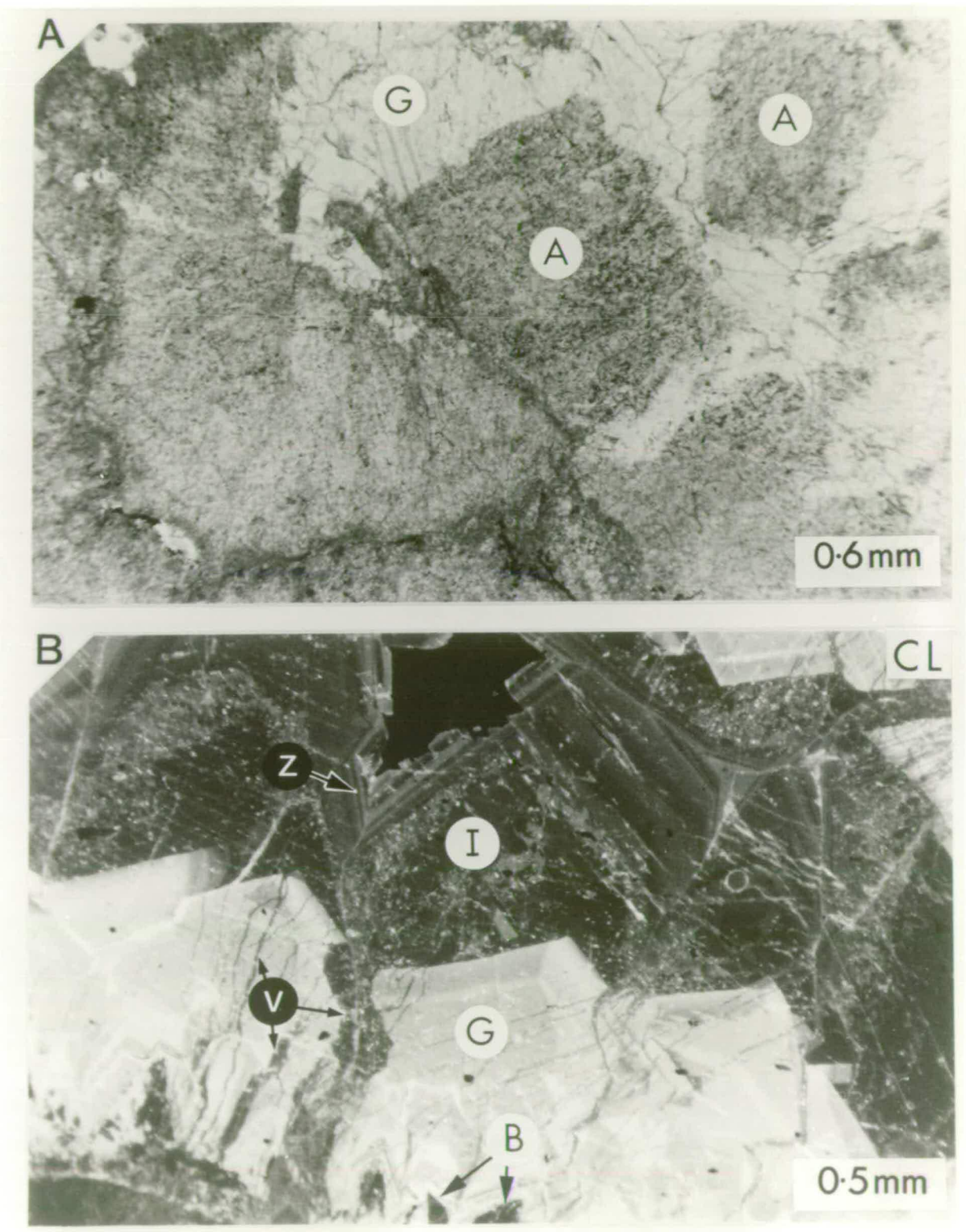

9.4 STAGE H Ferroan Calcite

These cements developed following a further phase of fracturing. Cement crystals filling veinlets are usually tabular but occasionally fibrous. They are elongated perpendicular to the fracture margins, suggesting that they developed under directional stress and are therefore syntectonic (Chapter 16). Fractures containing Stage H cements occur on all scales from microveinlets to centimetre-scale veins.

Stage H usually developed as crystal aggregates together with the following Stage I (see below) in veinlets and cavities. Only rarely, in volumetrically large spar sequences, are the two stages centripetally differentiated. Where they can be clearly separated, a dissolution surface commonly separates Stage H from Stage I (Fig. 9.5).

9.4.1 Composition

Stage H cements give a purple stain indicative of weakly ferroan calcite. Luminescence intensity is usually dull orange although in crystals which have sector zonation, some sectors may exhibit much brighter luminescence.

1. Trace elements

The increase in iron relative to Stage G as indicated by staining is confirmed by microprobe analyses (Table 9.7). A slight relative increase in manganese accompanies the increase in iron, while magnesium is slightly depleted.

2. Stable Isotopes

The paucity and thinness of undoubted Stage H cement meant that it was necessary to sample aggregates from veinlets and cavities which contained both Stage H and Stage I (Table 9.8).

Table 9.7 Mean Composition of Stage H cements

Oxide	Mean wt%	S.D.	C.V.	n=8
CaO	50.07	2.85	0.06	
MgO	0.08	0.05	0.56	
FeO	0.15	0.05	0.32	
MnO	0.08	0.04	0.52	

S.D. = Standard deviation at 95% confidence level
C.V. = Coefficient of variation
8 samples from 2 buildups

Table 9.8 Isotopic composition of Stage H-I aggregates
Values stated in per mil (°/₀₀) against PDB standard

Sample	$\delta^{13}C$°/₀₀	$\delta^{18}O$°/₀₀
C(1)	2.97	-6.54
C(2)	3.86	-6.57
C(3)	3.11	-7.47
WW10	2.93	-6.53
CH42	3.13	-6.91
.....		
Mean	3.20±0.34	-6.80±0.36

9.4.2 Interpretation of Stage H

The chemistry of Stage H calcites is extremely similar to that of Stages E and F. It is probable, therefore, that Stage H also precipitated from reducing fluids in the zone of bacterial fermentation of organic matter. The fracturing episode prior to Stage H would have allowed renewed influx of fluids, possibly displacing the oxic fluids of Stage G.

9.5 STAGE I Ferroan Calcites

A further set of fractures developed prior to the precipitation of Stage I cements. These fractures often followed the course of earlier veinlets and are commonly associated with replacement of the cements contained within them. This replacement is particularly noticeable with those veinlets which contained Stage H cements.

Two common styles of veinlet were developed and subsequently filled by Stage I cements. Both show evidence of brittle fracture at their margins. The first style is typified by straight margins which are parallel to sub-parallel. Cement crystals filling these fractures are usually tabular or fibrous and are characteristic of syntectonic vein-filling cements (Chapter 16).

The second style of veining produced irregular margins. The veinlets are often tapered like small tear fractures and commonly display dissolution textures at their margins. Crystals filling these fractures developed a blocky habit indicative of post-dilational vein-filling cements (Chapter 16).

Where veinlets cut existing sparry cement sequences, they often propagated along crystal boundaries as well as along cleavage and twin planes. The result is that the veinlets split into many fine micro-veinlets which have a 'horse-tail' appearance (Fig.16.1).

Widespread recrystallisation of sediments and earlier cements by Stage I is common, often resulting in the development of complex crystal aggregates. This is particularly apparent where Stage H cements were involved.

Euhedral void-filling crystals of Stage I are relatively uncommon, but where they are present, CL reveals several substages which are composed of many micron to sub-micron growth zones (Fig. 9.4).

9.5.1 Composition

Stage I cements are quite strongly ferroan. They give a royal blue stain and a very dull intensity, quenched luminescence which often has a brownish-red hue.

1. Trace elements

Stage I cements contain much higher levels of Fe than any previous stage (Fig. 9.2). The increase in iron is accompanied by a marked increase in Mg and a slight increase in Mn (Table 9.9).

2. Isotopes

The $\delta^{13}C$ value for Stage I of 3.0°/₀₀ is comparable with that of previous cements. The $\delta^{18}O$ value is further depleted relative to previous cements (Table 9.10 and Fig. 9.3).

Table 9.9 Mean composition of Stage I cements

Oxide	Mean wt%	S.D.	C.V.	n=21
CaO	55.52	2.16	0.04	
MgO	0.41	0.12	0.28	
FeO	0.42	0.14	0.35	
MnO	0.10	0.03	0.30	

S.D. = Standard deviation at 95% confidence level
C.V. = Coefficient of variation

21 Samples from 4 buildups

Table 9.10 Isotopic composition of Stage I cements
Analyses stated in per mil (°/₀₀) against PDB standard

Sample	$\delta^{13}C$°/₀₀	$\delta^{18}O$°/₀₀
Ash 3	3.15	-8.52
C27	3.08	-7.04
C26	3.09	-6.84
C25	3.19	-6.34
WW1	2.77	-7.17
Du	3.06	-6.81
CHQ1	3.40	-8.11
Mean	3.10 ±0.17	-7.26 ±0.72

9.5.2 Distribution of Stage H and I cements

Since they are usually closely associated in sparry crystal aggregates, Stages H and I may be considered as one unit as far as their distribution and volumetric abundance is concerned.

However, it is important to note that while Stage H cements are usually developed together with Stage I in crystal aggregates, it is common to find Stage I developed separately in larger cavities, or where Stage H was lost through dissolution, or did not precipitate. Such mono-phase cements however, are volumetrically insignificant compared to the combined H and I aggregates.

1. Bank facies

Aggregates of Stages H and I occluded one third of the post-CFC porespace in the bank facies (Fig. 18.2). They are most common in veinlets, stromatactoid cavities, and larger intraskeletal and shelter pores respectively.

2. Toe and interbank facies

Cements of Stage H and I are relatively uncommon in toe and interbank facies, accounting for approximately 5% of the total cement volume (Fig. 18.2). They occur in veinlets and some intraskeletal voids, and may also be associated with replacement textures in sediments and bioclasts.

9.5.4 Interpretation of Stage I

The marked increase in iron and magnesium in Stage I cements indicates a significant change in the formation water chemistry. Taken in the context of the variations in Fe content over the whole series of Stages E-I cements, the increase in iron alone would not be very significant, but when accompanied with an increase in magnesium and further depletion of $\delta^{18}O$, more substantial changes in ambient fluid chemistry are indicated.

Source of Iron and Magnesium

Reducing fluids are neccessary to maintain dissolved Fe^{2+} concentrations. In diagenesis, the most likely cause of reducing conditions is the bacterial degradation of organic matter (see Chapter 7). Below the sulphate reduction zone, the lack of sulphide ions brings a halt to the formation of authigenic pyrite and marks the beginning of the zone of bacterial fermentation of organic matter (Irwin et al. 1977). Iron-rich carbonates are likely to be precipitated in this zone (Curtis 1978). However, another potential source of iron is from the dewatering of shales and clay mineral transformations as a result of burial compaction (Oldershaw & Scoffin 1967). These effects also provide a source for increased Mg^{2+} in porewaters (Jodry 1969; Davies 1979). It is unlikely that dissolution of primary carbonate within the Waulsortian buildups or enclosing strata was a source for magnesium, as all original HMC would have inverted to LMC long before the precipitation of Stage I cements.

The Waulsortian facies limestones are particularly pure. Insoluble residue levels are less than 3% (Harrison 1982). It also seems unlikely that iron or magnesium could have been derived from clay mineral diagenesis occurring within the Waulsortian bank facies itself. I therefore propose that the marked increase in iron and magnesium in Stage I cements was the result of clay mineral diagenesis from shaley peri-Waulsortian facies, in the zone of bacterial fermentation of organic matter, at a time of increased compaction and pressure dissolution.

9.6 CRYSTAL AGGREGATES: Problems in cement stage identification

The problems of the would-be cement stratigrapher are well-illustrated by the development of complex crystal aggregates which often exhibit no clear cement stratigraphy.

Dickson (1983) eloquently described the intricate three-dimensional geometry of crystal fabrics which can develop in void-filling cement sequences, and the way in which these affect the pattern of crystal zonation which would be seen in thin section. The main factors controlling the complexity of such aggregates, as outlined by Dickson (op.cit.) are:-

1. Impingement of adjacent crystals resulting from competition for a restricted growth space;

   Crystals with their greatest linear crystallisation velocities, or greatest growth vector (g.g.v.), unfavourably oriented with respect to the growth space, are 'crowded out' by more favourably oriented crystals, the most favourable orientation being when the g.g.v. (in the case of calcite, the c-axis) is oriented normally to the substrate (Dickson 1983).

2. The distance from crystal nucleation points to the plane of the thin section;

3. The angle between the plane of the section and the crystallographic axes. This affects the pattern of crystal zonation seen in the section.

These controls are further complicated by the occurrence of dissolution surfaces between cement stages, and compositional sector zonation within cement stages.

In the present study, such crystal aggregates are particularly characteristic of ferroan calcite Stages E-F and H-I and their development is illustrated by means of case histories described below.

9.6.1 Types of Aggregate

Three types of crystal aggregate occur in cement filled voids of the Waulsortian bank facies, as revealed by CL and staining:-

1. Overgrowth aggregates

Particularly common as large syntaxial overgrowths on crinoid grains, these aggregates developed where the g.g.v. was oriented normally to the substrate (Fig. 9.8). The aggregates maintain the general form of a syntaxial overgrowth but tend to contain isolated irregular patches of early cement stages 'floating' in later cement.

The main control on aggregate formation in these cases appears to have been the occurrence of dissolution episodes at cement stage boundaries, healed by later cements. The sequence of events described from an actual example (Fig. 9.5) shows how three periods of dissolution, each followed by cementation (and probably associated with some recrystallisation), can produce such aggregates.

2. Impingement aggregates

This, the commonest form of aggregate consists of irregular areas of apparently randomly distributed sectors of two or more different cement stages, the overall texture being reminiscent of graphic intergrowths in igneous rocks (Fig. 9.6).

Individual sectors are usually angular to sub-angular. Frequently, however, the planar sector boundaries are embayed and apparently etched ('d' in Fig. 9.6). The processes involved in the development of such aggregates are complex:-

a). The apparently random distribution of sectors and their overall angular morphology indicates impingement of crystals whose g.g.v.s are unfavourably oriented with respect to the substrate (c.f. Dickson 1983, Fig. 12).

b). The etched and embayed surfaces reflect dissolution episodes between successive cement stages. Similar aggregates are described by Mazzullo (1986, Fig. 5).

3. Replacement aggregates

In some areas within these aggregates, where crystal g.g.v.s are favourably oriented to the substrate and the plane of section, fragments of zones or substages of cement appear to have been broken or dissolved. These regions were then infiltrated by later cements which replaced the core of the earlier cement, leaving the palimpsest solitary growth unit 'floating' in the later cement ('r' in Fig. 9.6). The fact that some of these earlier cement units are completely free from the substrate and suspended in apparent growth position suggests a replacement origin for this texture (Fig. 9.7).

Development of syntaxial crystal overgrowth aggregates.

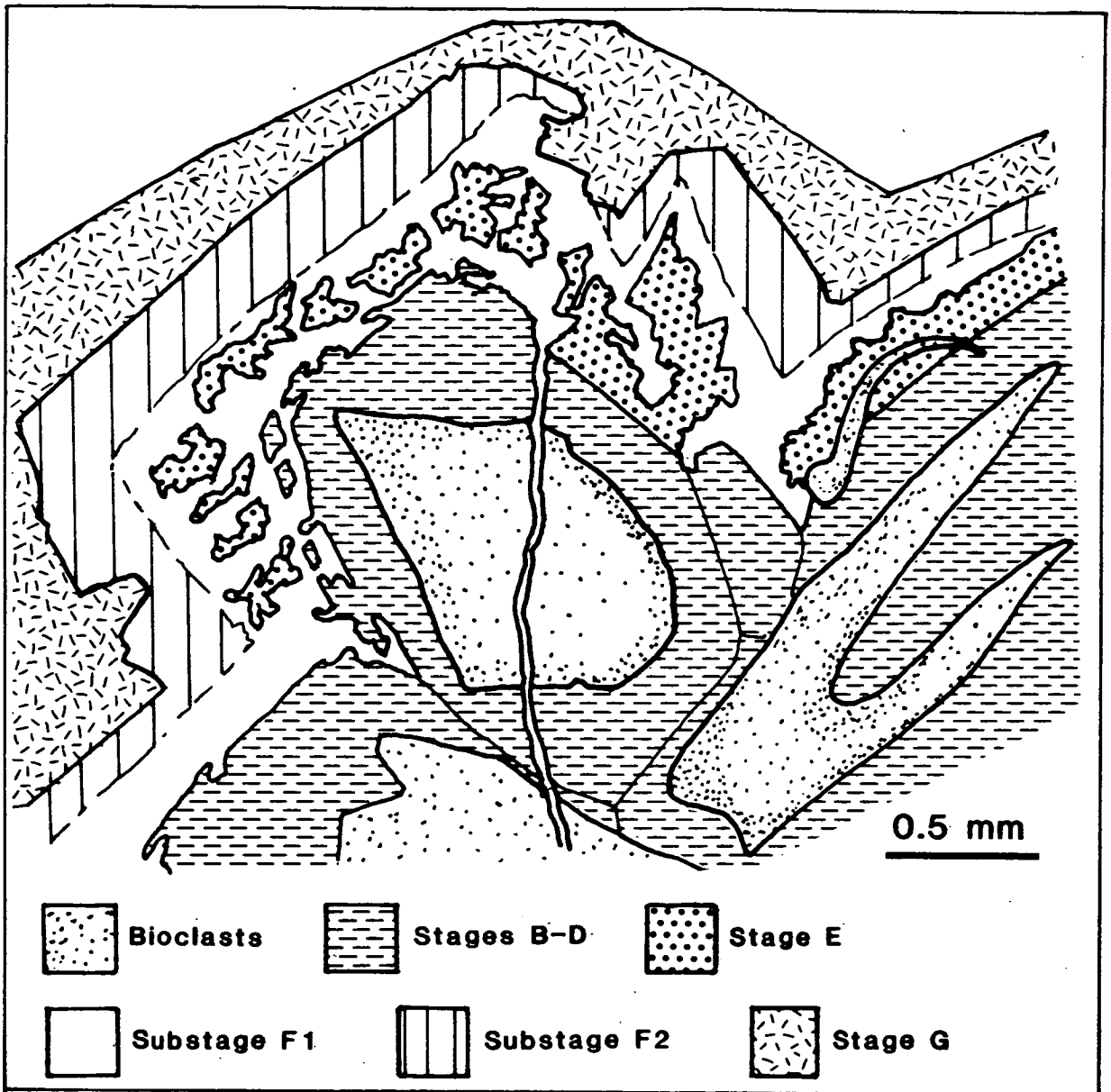

Figure 9.6 Impingement aggregates.

Tracing from a stained peel projection showing a deep burial cement crystal aggregate, formed largely by impingement of crystals during growth. Most of the aggregate sectors have angular faces controlled by impingement of crystals growing at irregular angles to each other, the earlier cement substrate, and the plane of the section. Some sectors have embayed and etched boundaries caused by dissolution (d), while other parts of the aggregate developed by partial replacement of earlier crystals (r; see also Fig. 9.7). Aggregate sectors bear little relationship to crystal boundaries (dashed lines). Salthill bank facies.

Fig. 9.6 Impingement aggregates.

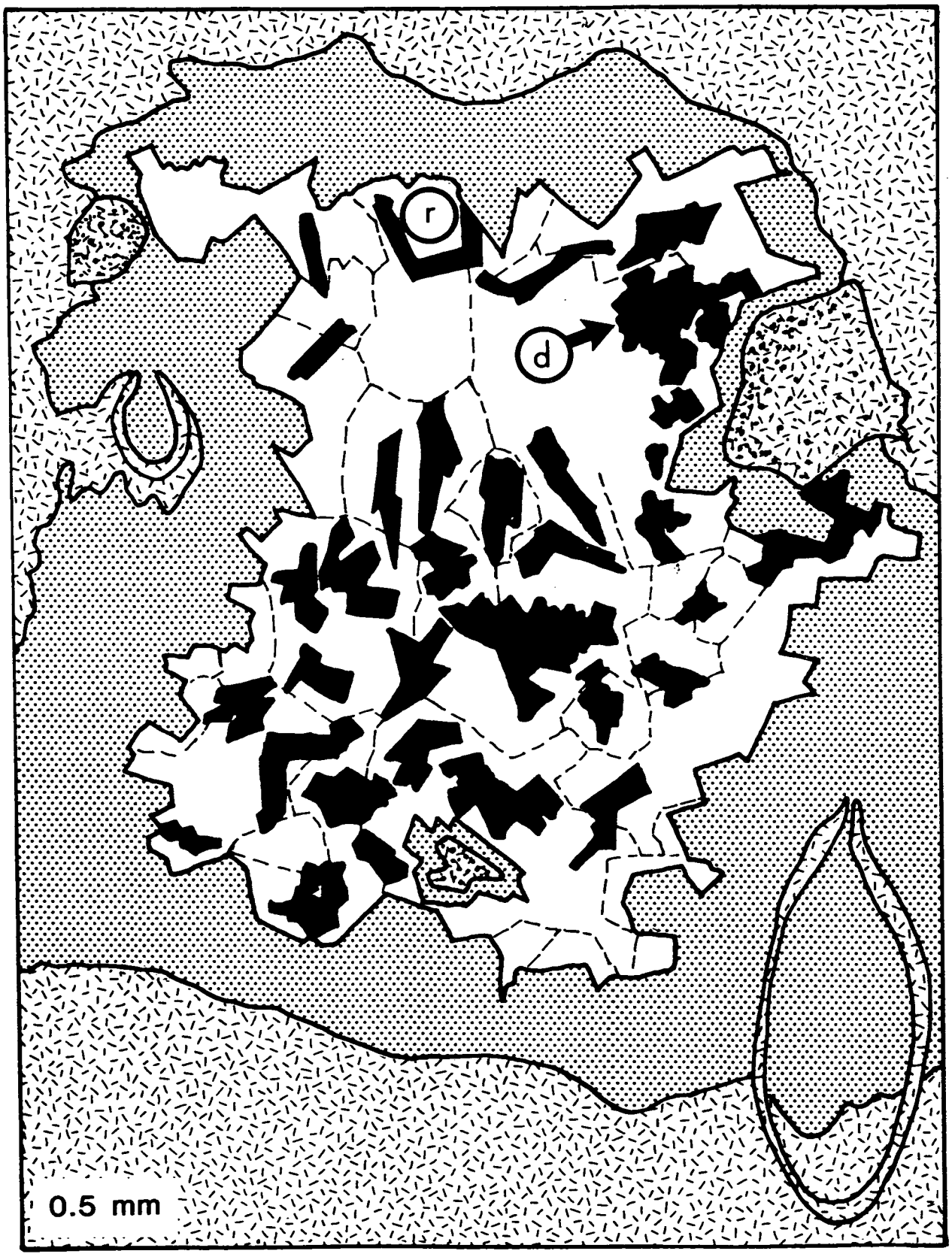

Fig. 9.7 Development of replacement aggregates.

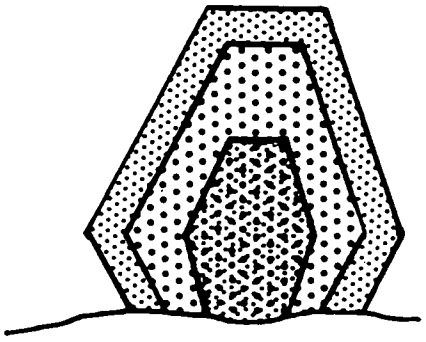

1. Zoned crystal

2. Influx of aggressive fluid

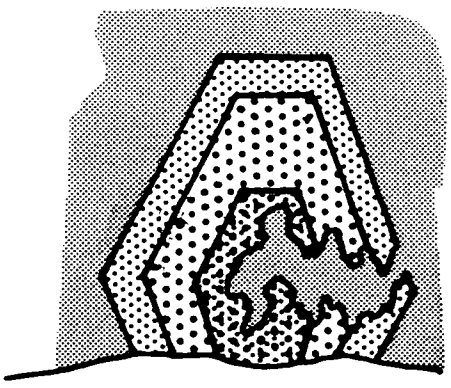

3. Solution–replacement of crystal core

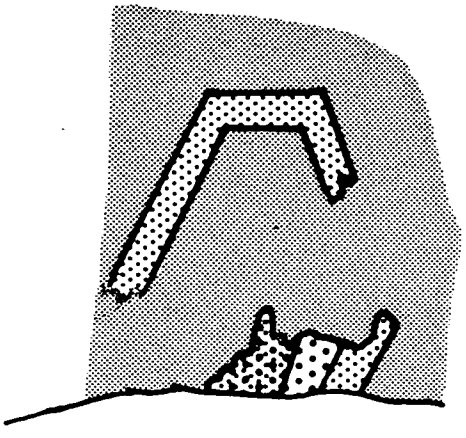

4. Replacement aggregate

The illustration in Fig. 9.7 is of a relatively simple case. Many more complex aggregates developed where fluids initiated the recrystallisation of cement crystals, particularly along planes of weakness such as crystal compromise boundaries, cleavage and twin planes. In some cases, the replacement is almost complete and it becomes very difficult to determine whether individual crystals represent cements or replacements of earlier void-filling spar. (See Chapter 17 Neomorphism).

Dickson (1983) discussed the formation of impingement aggregates by replacement, and used an example of dolomite replacing calcite, where idiomorphic dolomite crystals developed and grew until adjacent crystals impinged upon each other. Folk (1965) described aggregates with all the features of normal void-filling spar which were a product of recrystallisation i.e. pseudospar. He suggested that so long as recrystallisation started from a surface and progressed outwards, it could produce the same crystal fabric as precipitation.

CONCLUSIONS

1. Five cement stages, recognisable on a basin-wide scale, developed during the first phase of deep burial diagenesis. All stages are associated with episodes of brittle fracturing.

2. Trends of oxygen isotopic compositions for cement Stages E-I indicate continued burial through the sequence while $\delta^{13}C$ values suggest that either no major change in carbon source of the formation waters had taken place, or if meteoric waters were introduced, then they were completely buffered by carbonate dissolving out of the rock from pressure dissolution.

3. Stages E and F are the first ferroan calcite cements in the sequence. Their compositions and mineralogy indicate that the sediments had been buried as far as the zone of bacterial fermentation of organic matter (a few tens to hundreds of metres).

4. The early ferroan Stages E and F are followed by a non-ferroan calcite cement Stage G. The cause of iron depletion in Stage G fluidsis uncertain, although a change in Eh may have produced oxic conditions and concomitant disappearance of Fe^{2+} from solution. This would have prevented Fe substitution into the lattice of precipitating calcite. Oxic fluids could also have produced the dissolution surface which commonly pre-dates Stage G.

5. Stage H is ferroan, with very similar composition to Stages E and F. This similarity indicates a common origin. Iron-rich, anoxic pore fluids probably entered the system after renewed fracturing, displacing the low-Fe Stage G fluids.

6. Stage I marked a major change in the formation fluids, denoted by a significant increase in both Fe and Mg in this cement stage. The source of iron and magnesium in Stage I is likely to have been the diagenesis of clay minerals during compaction of shaley peri-Waulsortian facies.

7. Stages E and F and Stages H and I commonly form complex crystal aggregates as a result of growth impingement, dissolution between stages and recrystallisation. These aggregates pose great difficulties in the determination of the cement stratigraphy in many examples from the Craven Basin.

CHAPTER 10
STYLOLITISATION

Stylolites must be included in any diagenetic study for the following reasons:

1) They are linear features which tend to truncate earlier fabrics, or may in turn be truncated, thus allowing the placing of periods of stylolitisation within the framework of a cement stratigraphy.

2) Stylolites are the product of pressure dissolution of indurated limestones (and sandstones) which develop perpendicular to major stress fields (Dunnington 1954; Bathurst 1975; Logan & Semeniuk 1976; Wanless 1979) and therefore indicate the timing and direction of stress in the rocks.

3) They provided a significant potential source of dissolved ions which may in turn have been re-precipitated as cements.

4) Stylolites may have formed permeability barriers, or, after re-opening by subsequent tectonic processes, acted as fluid pathways.

5) Stylolites represent areas of material loss, the minimum being the distance between tips of saw-tooth projections on their surfaces (Bathurst 1975). They often record significant reduction in rock volume and porosity which may commonly be in the region of 35-70% of the original volume (cf. Park & Schot 1968; Coogan 1970; Meyers 1980).

Stylolites are manifested as irregular, often discontinuous surfaces which may have a zig-zag appearance resulting from differential dissolution rates along their length. Such differences in rate of pressure dissolution may have been brought about by the occurrence of certain grains within the sediment which were less susceptible than others to dissolution so the stylolite seams pass around or impinge upon them. The amplitude of the undulations produced along the stylolite surface as a result of differential solution may vary from a few microns to several centimetres.

The development of stylolites is controlled by the direction of the stress and the nature and degree of lithification of the stressed sediment.

Several classifications for stylolite description have been proposed. Wanless (1979) classified stylolites on the presence and degree of suturing, while Park and Schot (1968) devised a scheme based upon the two dimensional angular relationship between the stylolite and sedimentary bedding. Logan and Semeniuk (1976) suggested a purely morphological scheme with the recognition of five configurations of pressure solution surface which could be classified into one of three sets.

In an unpublished study, Berry (1984) identified six types of stylolite and expanded on the previous morphological classifications of stylolites.

It is not proposed to attempt a further classification of stylolite types and fabrics in this study. The decriptive terms used herein (Fig 10.1) are based on the established classifications.

Stylolites occur on all scales. The domains between them ("idens" sensu Logan & Semeniuk 1976) range from a few microns to over a metre in size. The majority of stylolites described herein were only studied in thin section.

10.1 STYLOLITES IN THE CRAVEN SAMPLES

The nature of the stylolites in the Craven sediments is highly dependent on facies and sediment texture. In particular, there are contrasting styles in Waulsortian bank and peri-Waulsortian facies.

Three main morphological configurations were identified (Fig. 10.1).

1. Irregular
2. Hummocky
3. Denticulate

It is common to find changes in configuration along a single pressure dissolution surface (cf. Logan and Semeniuk 1976, p.11).

Fig. 10.1 Stylolite morphology and fabrics.

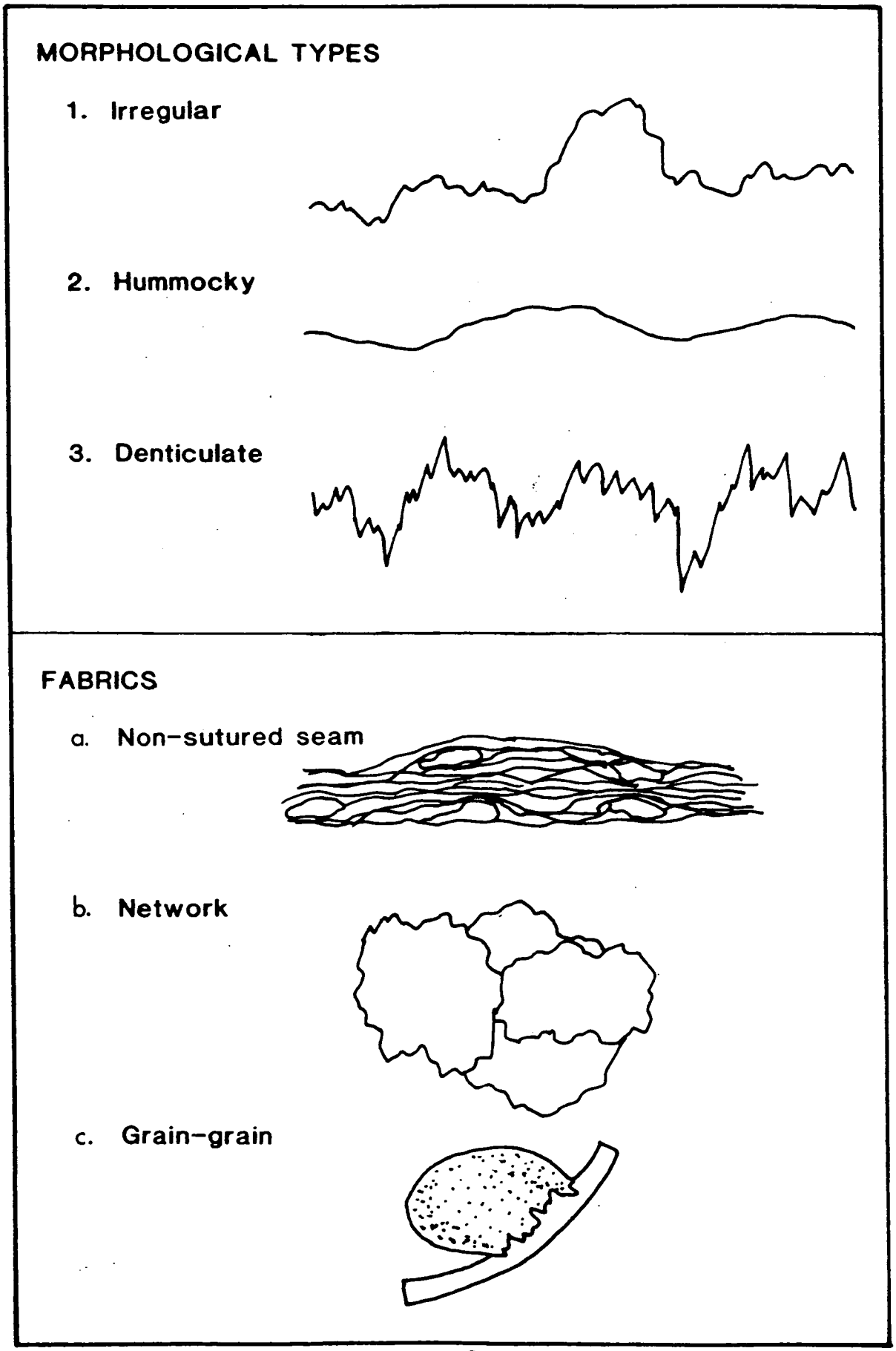

Figure 10.2 Stylolites.

A. Photomicrograph showing denticulate (arrow 1) and irregular (arrow 2) grain- grain stylolites in crinoidal flank facies. Stained peel, Coplow Quarry.

B. Photomicrograph showing stylolite networks in flank facies from Coplow Quarry including: non-sutured seams (Se) of dense insoluble residues comprising swarms of irregular and hummocky stylolites, and denticulate to irregular surfaces (arrowed) between larger idens which were more resistent to pressure dissolution. Stained peel.

C. Photomicrograph showing an irregular stylolite (St) exploited by dense organic matter and framboidal pyrite (p). Thin section, Coplow bank facies.

D. Photomicrograph showing a stylolite (arrowed) with associated pyrite and organic matter impinging upon a spar-filled cavity (S1) which was more resistant to pressure dissolution than the matrix sediment (M1). Coplow bank facies, stained thin section.

E. Cathodoluminescence (CL) photomicrograph showing ferroan dolomite (D) which exploited a stylolite surface. Later brightly luminescent calcite veinlets of Stage N (fine arrow) cut the dolomite, but are themselves displaced by a later set of high-angle stylolites (large arrow). Thin section, Coplow bank facies.

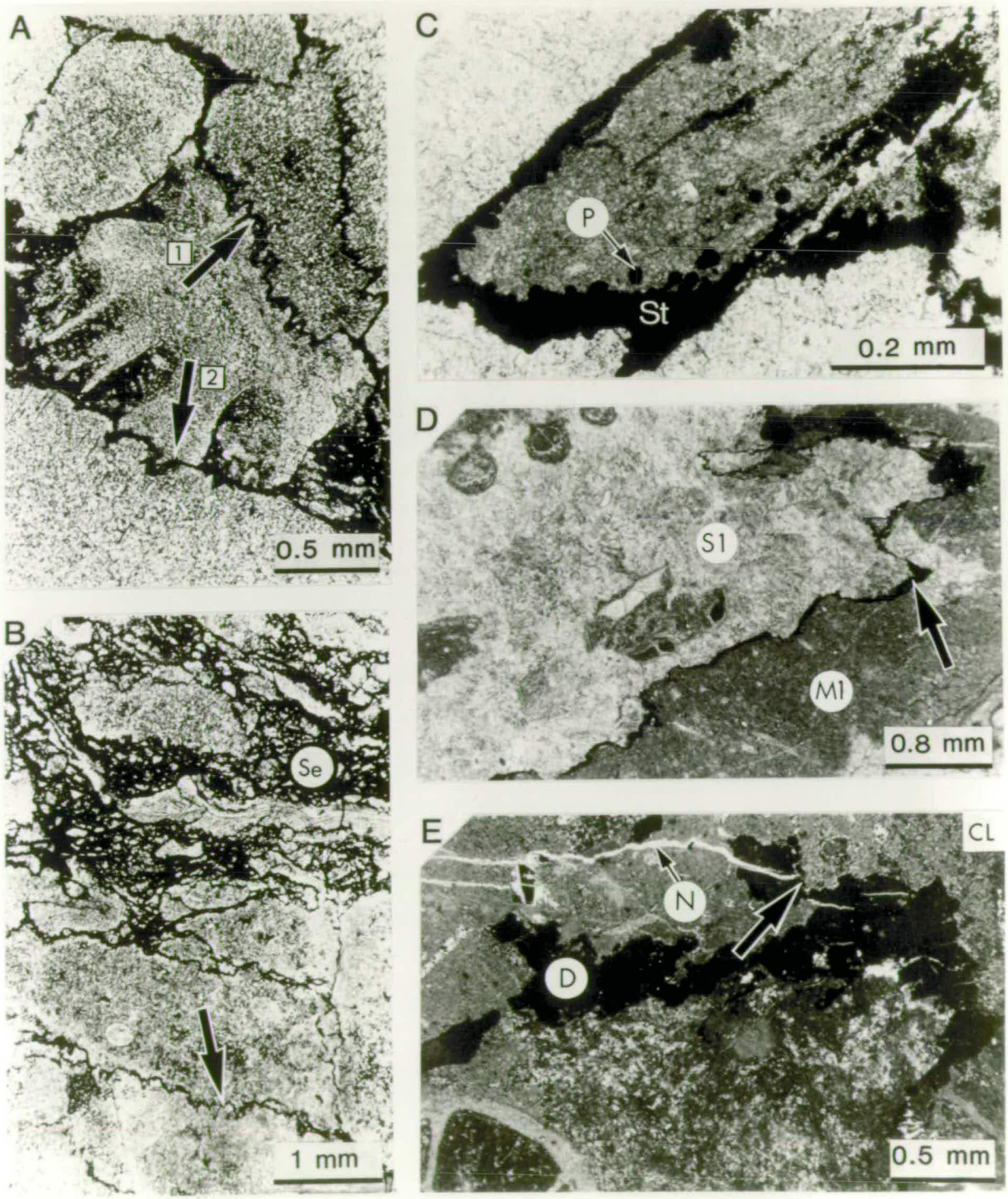
A
1
2
0.5 mm
B
Se
1 mm
C
P
St
0.2 mm
D
S1
M1
0.8 mm
E
CL
N
D
0.5 mm

10.1.1 Stylolites in peri-Waulsortian facies

Three common stylolite fabrics were encountered:-

a) Non-sutured seam solution (Wanless 1979)
b) Networks (Park & Schot 1968)
c) Grain-grain (Bathurst 1975).

a) Non-sutured seam dissolution

These are by far the most common pressure dissolution fabrics in the off-bank deposits. They consist of seams of dense insoluble residues (mainly clay minerals, organic matter and partially dissolved carbonate grains) which are usually composed of swarms of irregular or hummocky stylolites, and some denticulate surfaces (Fig. 10.2B). They range from a few tens of microns to a few centimetres in thickness and are usually sub-parallel to bedding, indicating that the main stress was from overburden rather than tectonism. An example from sub-bank facies at Hall Hill quarry illustrating the anastomosing nature of these seams, picked out by subsequent dolomitisation is shown below in (Fig.11.7). The high proportion of these solution seams in the off-bank/interbank facies would have had signficant effect on pore fluid migration during diagenesis by creating permeability barriers (Bathurst 1975).

b) Networks

These are particularly common in grainstones and packstones where there are a high proportion of grains which are not easily dissolved. Networks may also occur in some of the more massive mud-rich sediments. Stylolites pass around or impinge upon the edges of grains, e.g. crinoids or brachiopods, which were resistant to pressure dissolution, but do not cut them.

c) Grain-Grain

This fabric is exclusive to those sutured surfaces which mark the point of contact of adjacent grains, usually echinoderm bioclasts (Fig. 10.2A). The sutured surface is almost always denticulate. Where the adjacent grains are surrounded by carbonate mud (e.g. in wackestones) the stylolite often does not extend into the adjacent matrix, indicating that the mud matrix was able to disperse the stress. In grainstones and packstones, many grain-grain contacts occur and if these became overpacked, then stylolite networks would be produced. However, grain-supported lithologies are comparatively rare in Craven peri-Waulsortian facies.

The grain-grain dissolution fabric developed from the concentration of stress by overburden pressure at grain contacts with increased grain solubility resulting at those points (Bathurst 1975). In order for such a fabric to develop, the grains must have been able to move relative to one another, and therefore grain-grain stylolites pre-date significant cementation.

10.1.2 Stylolites in Waulsortian bank facies

Stylolites are much less common in the bank facies than in surrounding sediments, and therefore the inference may be drawn that the bank facies itself probably did not source much of the late diagenetic cement. Most commonly, bank facies stylolites are single, discontinuous, irregular to denticular surfaces, but they may also occur in networks surrounding idens of varying scales. Bedding is less regular and sometimes inclined in the buildups, and so stylolites developed at varying angles to the depositional horizontal, the main control on their distribution being the larger bioclasts and spar-filled areas which formed resistent idens.

The bank facies consists of a variety of microfacies ranging from bioclastic lime mudstones through to wackestones with rare packstones, all of which tended to respond differently to pressure dissolution. In mudstones the stylolites tend to have lower amplitudes (a few tens of microns) as a product of the homogeneous response of the matrix to pressure dissolution. Biomicrites with

higher proportions of larger grains developed higher amplitude stylolites as a result of differential grain response to stress.

However, these primary sedimentological textures were a less important influence on stylolitisation than the effects of cementation. Sparry cement masses apparently tended to be more resistant to pressure dissolution than the matrix, as stylolites tend either to pass around sparry areas, or to impinge upon their margins (Fig. 10.2D). In other cases, individual stylolites, or networks thereof, developed in apparently homogenous sediment. Close examination of such areas with CL and staining showed that the sediments had often undergone differential cementation or recrystallisation and so developed idens of different mechanical properties which responded differently to pressure dissolution.

The scale of the idens enclosed by such stylolite networks was often quite considerable. The base of Sugarloaf Quarry contains two displaced blocks of bank facies which reach 2m in diameter and were overgrown by the accreting bank. They show large angular displacements in the cavity system and geopetals between the adjacent blocks. The contact surfaces between blocks are sutured by irregular denticulate stylolites. In effect, the blocks are individual idens. Within the enveloping bank facies, idens tend to be a maximum of a few centimetres across.

Solution seams and grain-grain stylolites only occur occasionally in the toe facies, and very rarely in the true bank facies.

The style and development of pressure dissolution features are therefore significantly different in the bank facies compared with peri-Waulsortian facies. Cementation of the matrix was apparently the main control on stylolite development. The patchy nature of this cementation and any subsequent recrystallisation (Chapter 17) resulted in the formation of irregular stylolite networks. The amplitude of stylolites within the bank facies was, therefore, largely controlled by a combination of differential cementation and original lithology.

The lack of solution seams in bank facies limestones reflects their low levels of clay mineral impurities, while the absence of grain-grain stylolites is a product of two factors;

a) Fabrics in buildups are essentially mud-supported, and so fewer large grains came into contact with one another.

b) Grain-grain stylolites would only develop where freedom of movement existed in the sediment. The development of early diagenetic/incipient cements within the buildups would have reduced the likelihood of grains being pressed together (Bathurst 1975).

In general terms, stylolitisation was most effective in those sediments which were not significantly affected by pre-burial cementation, i.e. the offbank/interbank facies. This has also been indicated in other studies (see Purser & Schroeder 1986).

10.2 TIMING OF STYLOLITISATION

Dunnington's 1954 report was one of the first to investigate the relationships existing between stylolites and fractures. He noticed that some fractures cut across stylolites whereas others could be laterally displaced along pressure solution surfaces, and hence their temporal relationships could be determined. Dunnington (op. cit.) used these relationships as evidence that stylolites must have formed in indurated rocks, i.e. fractures could only develop after induration, and if they were displaced along pressure dissolution seams, then the stylolites must also have formed after lithification.

Buruss et al. (1985) also recognised the relationships between stylolites, hydrocarbon migration and fracturing, and Henrich and Zankl (1986) noted the relationship between fractures and stylolites and used the evidence to define a late diagenetic stratigraphy.

In the Waulsortian off-bank facies, pressure dissolution was a continual process which began soon after burial. Grain-grain stylolites in wackestones indicate some compression before significant cementation, while there are other examples where cement Stages B-D developed overgrowths on crinoids before stylolite development.

The cross-cutting relationships of cement-filled veinlets and stylolites in the off-bank facies are complex. In general, veinlets of cement stages up to Stage G are commonly truncated by stylolites, whereas those of Stage I onwards are more commonly seen to cut stylolites or exploit them as conduits. In the toe facies, Stage I

veinlets are the first to cut stylolites.

In the bank facies, however, all stylolites are late diagenetic, consistently truncating veinlets of all cement stages up to Stage I, while never showing evidence of themselves having been truncated by any of these stages. However, veinlets containing dolomite and later cement stages did consistently exploit stylolites, and so the major phase of pressure dissolution to affect the bank facies can be timed between Stage I and the dolomite stages (see below and Fig. 10.2E).

There is some evidence in the bank facies of a phase of stylolites which truncated cements up to and including Stage N. These stylolites are consistently at high angles to the depositional fabrics, indicating lateral (tectonic) stress rather than vertical (compaction) stress (Fig.10.2E).

10.3 ORGANIC MATTER ASSOCIATED WITH STYLOLITES

A large proportion of stylolites in all facies have concentrations of organic matter along their surfaces. This usually consists of dense black to brown amorphous material but may also be light brown and transparent. The organic matter is often associated with framboidal pyrite (Fig. 10.2C).

In the bank facies, evidence of migration of organic matter along stylolites is common. Often, the organic material propagated out from stylolites along crystal and grain boundaries in the matrix, particularly in dolomite mosaics, where dissolution of the dolomite was often associated with the organic matter. The Waulsortian bank facies themselves are very pure carbonate, and therefore it must be assumed that the organic compounds migrated into the buildups during maturation of the abundant organic matter in the enclosing bituminous limestones and shales.

Organic matter is extremely common along stylolites in the off-bank and interbank facies.

Many authors have reported a similar relationship between stylolites and bitumens. Buruss et al. (1985) were able to identify the timing of hydrocarbon migration from stylolite-fracture relationships and fluid inclusion studies.

CONCLUSIONS

1. Considerable differences in the degree and styles of stylolitisation occur between the Waulsortian and peri-Waulsortian facies.

2. Stylolites are much less common in the bank facies, reflecting greater resistance to pressure dissolution caused by early cementation.

3. In off-bank/interbank facies, stylolites are mainly anastomosing solution seams, containing high proportions of insoluble silicate residue and organic matter.

4. In the bank facies, most stylolites are irregular and denticulate. Areas of homogeneous micrite characteristically developed low amplitude stylolites, whereas higher amplitude forms characterise heterogeneous lithologies.

5. In peri-Waulsortian facies, primary sedimentary fabrics, especially bedding, were the main controls on stylolite development. In the bank facies, degree of cementation was the main control, and stylolites tended to be deflected around or impinged upon idens which were particularly well-cemented, especially sparry areas.

6. Grain-grain stylolites are common in peri-Waulsortian sediments. Their absence in the buildups indicates that early cementation in the bank facies prevented grains being compressed together.

7. Stylolitisation was an almost continual process in the off-bank and interbank facies. However, the consolidated bank facies resisted stylolitisation until a major episode of compression after cement Stage I. Dolomite was then the first mineral phase to exploit the stylolite system in the bank facies. Veinlets of later cement stages also commonly followed stylolites.

8. Hydrocarbons migrated along stylolites in the bank facies, mostly after dolomitisation.

9. A late phase of stylolitisation affected the bank facies after Stage N. Stylolites developed at high angles to the rock fabrics, indicating lateral tectonic stress, as opposed to vertical stress from overburden, and thus implying a phase of tectonism after Stage N.

10. The limited and late diagenetic development of stylolites in the bank facies means that dissolution within the buildups was a less likely source for carbonate cements than from the heavily stylolitised peri-Waulsortian facies. This in turn suggests there was only minor reduction in pore volume of the bank facies due to stylolitisation, but a major porosity reduction in the peri-Waulsortian facies.

CHAPTER 11
STAGE J-L: DOLOMITE

11.1 INTRODUCTION

A wide variety of cement and replacement textures and fabrics were developed in the Craven Waulsortian, reflecting the complexity of the dolomitisation process. Dolomitisation was generally selective and confined within the post-CFC volume of the bank facies, but its effects can also be traced in sediments enclosing the buildups. The development of dolomite in carbonate sequences has been assigned to a wide variety of diagenetic environments ranging from supratidal to deep subsurface. The dolomite cements in this study are related to fractures and are the first cements to post-date stylolites in the bank facies. They consistently occur after Stage I deep burial calcite cement in void-fill sequences and are therefore interpreted as products of deep burial diagenesis.

11.1.1 Previous Work

a). Textures and fabrics

A wide range of dolomite textures and fabrics have been described in the literature. The seminal paper by Friedman (1965) introduced the basic terminology for the description of rhombic dolomites. The terms idiotopic, hypidiotopic and xenotopic were proposed for equigranualar dolomite mosaics where the constituent crystals were mainly euhedral, subhedral and anhedral respectively. For inequigranular dolomite Friedman introduced the term 'porphyrotopic' to describe unusually large dolomite crystals analagous to the porphyritic texture of igneous rocks. These terms were later refined by Gregg and Sibley (1984) who added post-scripts to Friedman's idiotopic, xenotopic and porphyrotopic terms in order to indicate crystal morphology and, in one case, crystal origin. Hence 'idiotopic-p' refers to euhedral porphyrotopic crystals and 'xenotopic-c'

implies a xenotopic mosaic of cement origin in Gregg and Sibley's classification. Another important type of dolomite occurs as sparry masses of curved blade or 'scimitar'-shaped crystals. This was described as baroque (Folk & Asseretto 1974) or saddle dolomite (Radke & Mathis 1980).

One of the main problems in petrographic studies of dolomite is the similarity between cement and replacive dolomite textures. Friedman (1965) and Dickson (1983) have indicated how dolomite crystal aggregates which formed by replacement (neomorphism) could develop the same textures and fabrics as void-filling dolomite cements.

b). Origins.

Dolomite may form as void or fracture filling cement (Choquette 1971) or as a replacement of limestone sediments (Friedman 1965; Logan & Semeniuk 1976; Radke & Mathis 1980; Taylor & Sibley 1986). It may also form as a neomorphic replacement of earlier dolomite (Gregg & Sibley 1984).

The diagenetic environments and chemical constraints of dolomite formation were investigated and outlined in two related papers by Folk (1974) and Folk and Land (1975). Folk (1974) identified three chemical realms, meteoric, marine and subsurface/mixing zone, in which diagenetic carbonates precipitated. The companion paper by Folk and Land (1975) concluded that salinity and the Mg/Ca ratio of pore fluids controlled whether dolomite or other carbonate phases would precipitate in a particular chemical realm. Subsequently, factors effecting the stability of dolomite were investigated and summarised by Carpenter (1980). Also, the stoichiometry of dolomite was found to reflect the nature, source and migration path of dolomitising fluids (Lumsden & Chimahusky 1980).

Interest in the origin and processes of dolomitization initially arose out of the observation that many carbonate hydrocarbon reservoirs were dolomitised (Murray 1960). Early studies were biased towards the many easily accessible Recent examples of penecontemporaneous, particularly supratidal dolomites. Two theories of dolomitisation became dominant, namely the evaporitic/sabkha model

(Curtis et al, 1963; Pray & Murray 1965) and the dorag/schizohaline model (Hanshaw et al. 1971; Badiozamani 1973; Muir et al. 1980; Choquette & Steinen 1980). Over a period of years it has become apparent that the wide diversity of dolomite types which appear in nature are not related to a single process (see Beales & Hardy 1980 for review). There has been an increase in recent years of descriptions of dolomites which are ascribed to burial diagenetic processes (Choquette 1971; Dickson & Coleman 1980; Mattes & Mountjoy 1980; Fairchild 1980; Wong & Oldershaw 1981; Moore & Druckman 1981; Gregg & Sibley 1984; Taylor & Sibley 1985; Schofield & Adams 1986). Fundamental to many of these studies is the occurrence of saddle dolomite, which Radke and Mathis (1980) suggest forms at temperatures of 60-150°C.

Saddle dolomites occur in close association with epigenetic sulphide mineralisation (Beales & Hardy 1980; Mazzullo 1986), sulphate bearing carbonates (Folk & Asseretto 1974) and hydrocarbon accumulations (Choquette 1971; Davies 1979). The association of dolomite with stylolites has also been recorded (Logan & Semeniuk 1976; Wanless 1979; Mattes & Mountjoy 1980). It has, therefore, become apparent that the sequence of diagenetic episodes effecting dolomitisation may be polyphase, with examples of both early and late stage dolomitisation occuring in many studies (eg. Taylor & Sibley 1985). Polyphase burial dolomitisation has also been reported, most recently in an example from the edge of the Craven Basin (Schofield & Adams 1986).

Carbon and oxygen stable isotope analyses have been commonly employed in attempts to characterise dolomite types. (Mattes & Mountjoy 1980; Choquette & Steinen 1980; Taylor & Sibely 1985), while cathodoluminescence has also been used extensively to identify compositional zonation in dolomites (Katz 1971; Choquette & Steinen 1980; Frank 1981; Tucker 1983; Reeder & Prosky 1986) and also to map out dolomite cement history (Fairchild 1980).

Major and trace element analyses, usually conducted with electron microprobe techniques, have been employed by many workers (See Mattes & Mountjoy 1980) for a variety of reasons.

Major element calcium and magnesium analyses have been used in dolomite stoichiometry investigation (e.g. Lumsden & Chimahusky 1980). Trace element sodium and strontium contents may be used to define 'early' or 'late' dolomite (Weber 1964; Fritz & Katz 1972; Badiozamani 1973; Al-Hashimi 1976; Veizer et al. 1978; Mattes & Mountjoy 1980).

11.2 DOLOMITE TYPES IN THE WAULSORTIAN BUILDUPS OF THE CRAVEN BASIN.

It is apparent from the many articles describing cement versus replacement textures in dolomites (e.g. Radke and Mathis 1980; Fairchild 1980; Mattes & Mountjoy 1980; Gregg and Sibley 1984), that the interpretation of dolomite textures in terms of processes poses a complex problem. Identical dolomite textures may result from cementation and replacement. A detailed assessment of the relative timing and origin of the dolomites described herein was only possible because of the integration of data from the unusually large total area of thin sections and peels examined. Individual examples often presented equivocal or apparently contradictory evidence.

In the study area dolomite occurs in three crystal habits: rhombic and saddle (commonest) and anhedral (rare). All have a dusty appearance due to the presence of micron scale inclusions which impart a light sandy-brown colouration to the crystals. Inclusions are invariably rounded or elliptical and often have a brownish tinge under transmitted light, although some are a dense brown to black colour. All are interpreted as fluid inclusions. The distribution of these inclusions is often irregular, although they may parallel crystal growth surfaces in some dolomite types.

11.3 DOLOMITE CEMENTS

Dolomite cements occur as sparry masses in cavities or veinlets which were partially occluded by earlier cements. These dolomites formed at a consistent position within the cement stratigraphy, always post-dating Stage I cements where these are present. They often show a gradual increase in crystal size away from the subs-

trate, and some developed rhombohedral inclusion zonation in distal areas. Corrosion / dissolution surfaces on earlier cements are common.

All dolomite cements consisted of saddle dolomite crystals (Radke & Mathis 1980) (Fig.11.1). These coarse-grained sparry crystals range in size from hundreds of microns to several millimetres and are characterised by curvature of cleavage and crystal faces, and sweeping extinction (Fig. 11.1B). They contain variable amounts of inclusions which are often concentrated along curved crystal growth surfaces and cleavage planes, or may define internal curved rhombic zonation. Inclusion patterns, however, are often diffuse and discontinuous (Fig. 11.1C), and may exhibit pseudo-pleochroism.

In most cases, saddle dolomite forms a mosaic of curved blade-shaped subhedral to anhedral crystals. Some crystals have the form of large curved-faced rhombohedra with diffuse euhedral zones of varying inclusion density. When viewed with CL, particularly dense areas of inclusions often have a mottled, dusty appearance.

Despite the extensive sample set, only one example of dolomite cement (from Little Dunnow buildup) contained evidence of centripetal crystal growth zonation which is indicative of void-filling spar. Staining and CL revealed three dolomite cement stages; J, K and L (Fig 11.2A).

Stage J: Ferroan dolomite; turquoise-blue stain, very dull brownish-red to non-luminescent.

Stage K: Non-ferroan dolomite; no stain, brick-red to red-orange luminescence.

Stage L: Ferroan dolomite; identical staining and CL characteristics to Stage J.

11.4 REPLACIVE DOLOMITE (Dolomitisation).

The most common types of dolomite in this study are those which formed as a replacement of a precursor carbonate mineral. Replacement occurred in a range of styles, crystal habits and mosaics, which developed primarily along the complex cavity systems in the

Waulsortian bank facies (Fig.11.2B). Although rarely affecting CFC cements and younger sediments, replacive dolomites are not entirely absent from such areas, and commonly cross-cut the entire rock fabric, including cement-filled veinlets and cavities.

Three main crystal habits developed within replacive dolomite mosaics, the most common being rhombic dolomite, with lesser amounts of saddle dolomite and rare anhedral dolomite also occurring. Occasionally, both rhombic and saddle morphologies are found within the same mosaic.

i) Rhombic dolomite mosaics consist of crystals ranging from tens to a few hundreds of microns in size, which usually have straight to slightly curved faces and may contain broad concentric inclusion zones. Crystals are euhedral to subhedral (idiotopic and hypidiotopic textures of Friedman, 1965). Hypidiotopic texture is commonly developed in rhombic dolomite mosaics. However, when these are viewed under CL, euhedral luminescence zonation is commonly observed, suggesting that the hypidiotopic texture developed as a result of the impingement of euhedral crystals (cf. Dickson 1983 p468). In some examples where dolomite replaced geopetal sediment (see below), the impingement of dolomite crystals against more resistent (or larger) allochems caused restriction of crystal growth in certain directions, leading to the development of subhedral crystals.

ii) Replacive saddle dolomite is identified by the presence of inclusions of precursor phases and the truncation of earlier textural boundaries in cements and sediments. It is otherwise texturally and compositionally indistinguishable from saddle dolomite cements in the majority of examples.
A second, less common type of saddle dolomite consists of euhedral porphyrotopic crystals (cf. Friedman 1965; Gregg & Sibley 1984) which contain curved rhombohedral inclusion zones. These saddle dolomites occur as isolated crystals or small groups of crystals within veinlets, which are otherwise filled with later calcite cements and often extend into the sediment at the fracture margins (Fig.11.4).

iii) Anhedral dolomites are rare. Some are microcrystalline sucrosic dolomites while others are less regular and larger (up to hundreds of microns) and exhibit xenotopic textures of the type described by Friedman (1974).

11.4.1 Replacement Textures

Most dolomitisation involved the neomorphic replacement of calcite, including sediments, spars and some bioclasts, while some recrystallisation of pre-existing dolomite also occurred (neomorphic dolomite). Although most dolomitisation affected the post-CFC cavity-fill sequences in the bank facies, dolomite also developed in the primary M1 sediment and in association with stylolites.

11.4.1.1 Replacement after Calcite

A: Dolomitisation of Sediments.

The dolomitisation of calcite sediments almost always resulted in the development of rhombic dolomite crystals and mosaics. The process was largely fabric selective and confined to the post-CFC internal sediments, but some dolomitisation of the primary M1 sediment also occurred.

i) Dolomitisation of M1 sediment

Occasionally, rhombic dolomite mosaics developed as a non-selective replacement which truncated all pre-existing sediment and spar textures. In these cases, the M1 sediment and CFC cements were dolomitised along with the post-CFC material. More commonly, however, dolomitisation of the M1 sediment occurred in the form of scattered, isolated small dolomite rhombs up to tens of microns in size. In the majority of cases these scattered rhombs were subsequently calcitised and generally contain large amounts of goethite inclusions, which make them optically dense and indicate a ferroan dolomite precursor (Chapter 15) (Fig. 11.3A). This type of dolomitisation usually occurs in association with other dolomites and is often

concentrated along the margins of dolomitised void-fill material or dolomite cements.

ii) Dolomitisation of internal sediments

Selective dolomitisation of internal sediments in the complex cavity-fill sequences of the bank facies is a common feature of the Waulsortian buildups in the Craven basin. Rhombic mosaics again dominate, although rare anhedral mosaics were also identified. Both these dolomite types commonly mimic the geopetal texture of the internal sediments to form "geopetal" mosaics (Fig.11.3B).

Rhombic dolomite mosaics commonly occur at the base of cavity sequences, usually overlying CFC cements. The upper surface is flat and geopetal in nature and is overlain by calcite spar which fills the remaining porespace. The inter-crystal spaces of these mosaics commonly contain fine grained sediment, and it is also common to find similar sediment marking the upper boundary between the mosaic and the overlying spar. This suggests that these mosaics developed by the selective replacement of post-CFC geopetal sediment and are not examples of dolomite crystals deposited directly themselves as a geopetal filling.

Xenotopic dolomite textures consisting of mosaics where the constituent crystals are anhedral (Friedman 1975) were occasionally developed in the rocks of this study (Fig. 11.3C). These mosaics of equigranular, microcrystalline xenotopic dolomite (sucrosic dolomite; term of Murray 1960), formed as a partial or total replacement of micritic geopetal sediments in the bank facies and some interstitial muds in crinoidal wackestones of the toe facies. Crystal size is between 15 and 30 μm.

B: Dolomitisation of spar. (Fig.11.4)

Several different types of dolomite mosaic developed as a replacement of pre-existing calcite spar. They were generally fabric selective, consisting mainly of rhomb-shaped crystals, while others included saddle dolomite and rare irregular xenotopic crystals.

i) Rhombic "spar" mosaics

These dolomite mosaics commonly adopt the texture of a void-filling spar, overlying geopetal sediments and filling the rest of the "void" space (Fig. 11.4A). However, as with the "geopetal" mosaics, it is common to find remnants of a precursor material, in this case earlier calcite spar, in the mosaic interstices. This suggests that these mosaics also developed by selective replacement, but in this case it was pre-existing spar that was dolomitised. An example from Dunnow buildup shows that these mosaics probably developed initially along intercrystalline boundaries of the calcite spar, possibly following a phase of microfracturing, and then gradually replaced the entire sparry fabric (Fig. 11.4B).

ii) Saddle dolomite "spar" mosaics (Fig.11.4).

Saddle dolomites, either as mosaics or single crystals, occasionally developed preferentially and unidirectionally from one side of calcite spar-filled cavity sequences. The crystals often show evidence of rhombohedral zonation in the form of inclusions, staining or CL patterns. Adjacent calcite cement crystal boundaries are commonly truncated and the dolomites may extend across the entire void-fill, and even into the sediment beyond (Fig.11.4C). Another feature of this example concerns a framboidal pyrite aggregate of the kind described in Chapter 7, which is partly included within the saddle dolomite while being nucleated at the cavity wall where it is surrounded by earlier calcite cements. Other framboidal aggregates are completely enclosed by the dolomite crystals. Also of interest is the occurrence of small euhedral dolomite rhombs in the matrix sediment adjacent to the saddle dolomite.

In this case it is apparent that saddle dolomite crystals formed as a fabric selective replacement of calcite spar, whereas rhombic dolomite replaced the adjacent sediment. Such examples of saddle dolomite associated with rhombic mosaics are not uncommon. The rhombic material often adopts a geopetal fabric after internal sediment, whereas the remainder of the 'void' space contains saddle dolomite. In all cases, the replacive origin of the rhombic mosaic

is well displayed: however, it is usually difficult to assess whether the saddle dolomite originated as a cement or a replacement.

Porphyrotopic saddle dolomite (cf. Friedman 1965; Gregg & Sibley 1984) some may occur in association with calcite-filled veinlets. Crystals may extend across a veinlet and into the sediment at either side, where anhedral crystal shape developed and irregular inclusions of host sediment are enclosed by the dolomite crystal (Fig. 11.4 D&E). They are therefore not fabric selective. Within the veinlet, dolomite crystal faces may be euhedral to anhedral, and curved-faced rhombohedral zonation is observed. In most cases the porphyrotopic crystals were subsequently calcitised and it is difficult to assess whether the dolomite developed prior to, or after the calcite which occluded the remainder of the veinlet, i.e. whether it was a cement or replacement. Some examples of calcitised porphyrotopic dolomite exhibit a relict sweeping extinction pattern which was inherited from the dolomite precursor.

The anhedral faces of dolomite crystals which developed beyond veinlet margins undoubtedly formed by replacement of the adjacent sediment.

iii) Irregular xenotopic "spar" mosaic (Fig. 11.3C).

These rare mosaics consist of inequigranular xenotopic dolomite with crystal dimensions ranging from tens to hundreds of microns. They developed as a fabric selective replacement of botryoidal CFC cements in association with the development of sucrosic dolomite after internal sediments.

C: Dolomitisation of bioclasts.

Selective dolomitisation of bioclasts is rare. In examples where it does occur, there is no evidence which can definitely confirm whether dolomite formed after the development of bio-mouldic porosity, or as a result of selective replacement of the bioclast.

11.4.1.2 Replacement after dolomite (neomorphic dolomite)

This refers to dolomite which resulted from the recrystallisation of a pre-existing dolomite (cf. Gregg & Sibley 1984).

Examples of neomorphic saddle dolomite are particularly well developed at Sugarloaf Quarry. At this locality, a complex rhombic dolomite fabric occurs. The rhombic mosaics developed by replacement of geopetal sediments and calcite cements (see above). CL and staining reveal a stratigraphy within these replacive dolomites which is directly comparable with the stages in the dolomite cements. Rhombs within the mosaics contain a poorly-developed and often corroded equivalent of ferroan Stage J dolomite, followed by a well-developed non-ferroan, red luminescent equivalent of Stage K.

In the Sugarloaf Quarry faces, the rhombic dolomites are a sandy-brown colour due to subsequent calcitisation (Chapter15), but in some areas, patches of strong orange-brown weathered saddle dolomite occur within the rhombic mosaics. These may be irregular, randomly distributed areas or linear regions giving the impression of a veinlet texture. Outwith the areas of rhombic mosaic, the saddle dolomite often gives way to a white calcite-filled veinlet which may or may not be the same width as the dolomite 'veinlet'. This gives the impression that the calcite veinlet changes colour as it passes through dolomite. Close study of the saddle dolomite region of the veinlet reveals a lack of displacement of the rhombic dolomite fabric of the kind that would be expected after fracturing. This indicates that this particular saddle dolomite is a neomorphic replacement of earlier rhombic dolomite. The strong orange-brown colour of these weathered saddle dolomites is indicative of their high iron content, and in many cases, the intense colouration can be seen to extend into the rhombic dolomite mosaic as rims around the lighter coloured crystals (cf. also Fig.11.4E).

Staining confirms the high iron content of the saddle dolomites, and also confirms the observation that these later dolomites formed concentric rims around the rhombic Stage J and K equivalents. They are interpreted, therefore, as equivalents of the later ferroan Stage L dolomites. In some cases, the calcite in the associated veinlets cuts through the saddle dolomite. Dissolution and calcitisation of

the dolomite is common, and it thus appears, that both initial dolomitising and later calcitising fluids followed a common fracture system in the rock.

The sequence of events deduced for the development of this fabric is outlined below and in Fig.11.5.

A. Calcite spar and sediment was dolomitised by Stage J and K fluids, forming a rhombic mosaic.

B. Microfractures developed in the rock. Dolomitising fluids of Stage L entered along the microfractures, selectively neomorphosing rhombic dolomite and parts of the calcite spar not already dolomitised by Stage K equivalents.

C. A further period of veinlet extension followed. Dissolution and calcitisation of dolomite was followed by the precipitation of vein-filling calcite cement.

11.4.1.3 Dolomite associated with stylolites

Rhombic and saddle-shaped to anhedral dolomite crystals occur in association with stylolites in the Waulsortian bank facies. Examples of similar textures are described by Wanless (1979); Logan & Semeniuk (1976); Koch & Schorr (1986).

Rhombic dolomites may occur as ribbons or mosaics of hypidiotopic texture which follow stylolites. The rhombs commonly show signs of dissolution in the vicinity of the stylolite but some also appear to truncate stylolites.

Saddle dolomite may also be observed following stylolites. Crystals are usually anhedral and only rarely developed the characteristic curved-blade morphology (Fig. 11.6A). Many examples show evidence of stylolite displacement by the dolomite, which often appears to have been related to a degree of re-opening of the stylolite suture prior to dolomite crystal growth. The stylolites in these cases acted as fluid pathways for the dolomitising fluids and this suggests that these dolomites may have originated partly as cements. Excellent examples of such dolomitisation occur in the sub-bank facies at Hall Hill Quarry (Fig. 11.6B).

Some dolomite crystals themselves have sutured margins suggesting that they were subsequently modified by pressure dissolution.

Figure 11.1 Dolomite cements.

A. Photomicrograph of a thin section showing saddle dolomite cement (d) in a spar-filled cavity from Hall Hill buildup. The darker areas at the edge of the dolomite spar (arrowed) are caused by goethite inclusions formed during subsequent calcitisation.

B. XPL photomicrograph of vein-filling saddle dolomite cement. Dolomite crystals show characteristic sweeping extinction and curved faces (arrows 1 and 2 respectively). Crystal size increases towards the vein centre (top of picture), where crystals adopt the classic curved-blade habit (white box). These larger crystals also contain zones of inclusions which are sub-parallel to crystal faces. Thin section, Coplow Quarry.

C. PPL photomicrograph in plane polarised light corresponding to the white box area of 'B', showing a large single, saddle dolomite crystal with curved-blade habit. Zones of inclusions, while generally parallel to crystal faces, are noteably diffuse and discontinuous (arrow). The dolomite mosaic was cut by a later calcite-filled veinlet (v).

Fig. 11.1

DOLOMITE CEMENTS

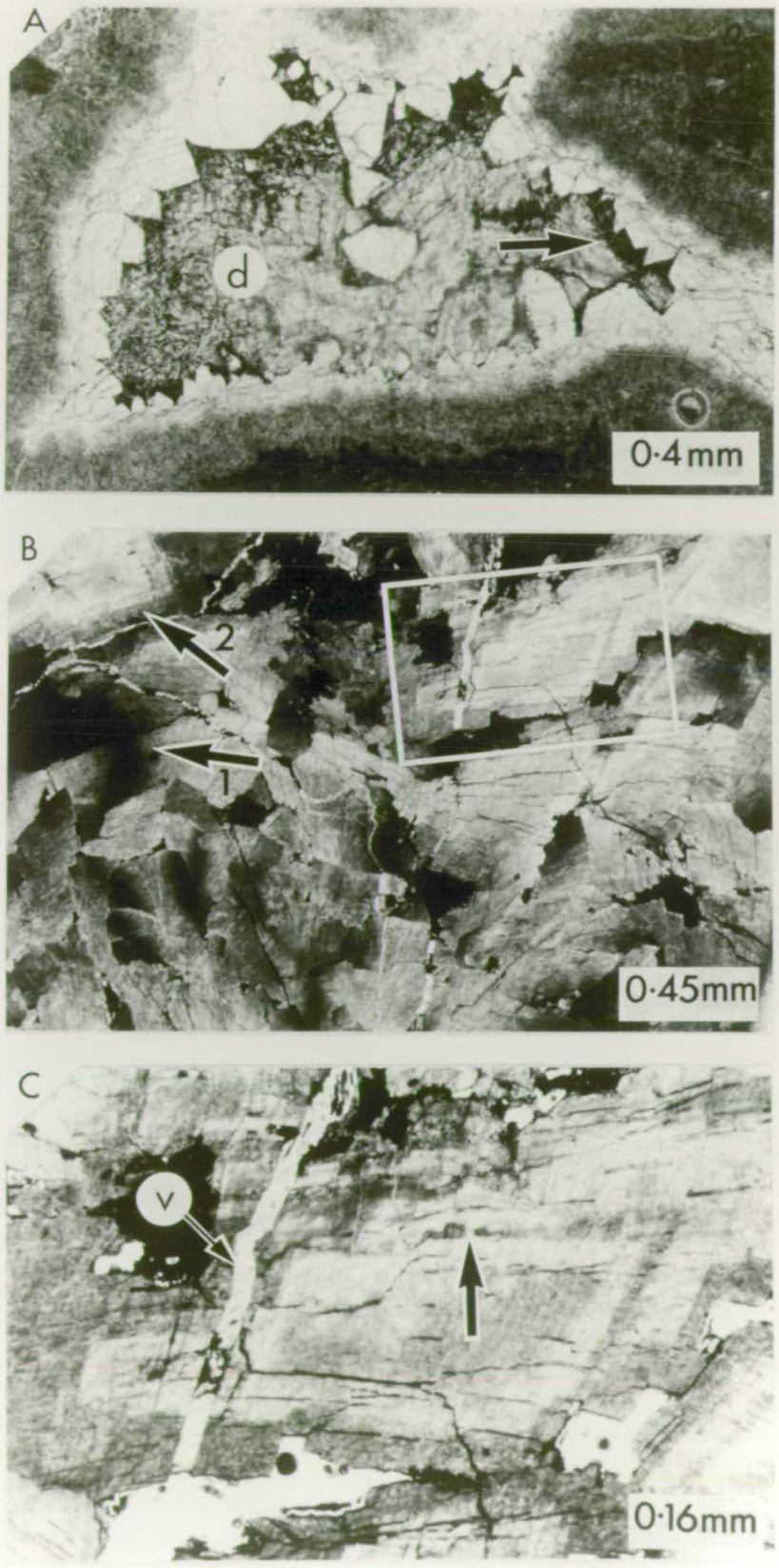

Figure 11.2 Dolomite stages and fabrics.

A. Cathodoluminescence photomicrograph showing centripetal development of dolomite stages in void-filling saddle dolomite. Very dull-luminescent, ferroan dolomite Stages J and L are separated by brick-red luminescent, non-ferroan Stage K. Bright orange luminescent calcite (arrowed) formed in one case by selective calcitisation of a dolomite crystal core. Field of view = 3mm. Little Dunnow bank facies.

B. Field photograph showing rusty-orange, replacive rhombic dolomite mosaic confined to the post-CFC area of sheet spars. Coin for scale; 2p, diameter = 2.5cm. Sugarloaf Quarry, bank facies.

Fig. 11.2

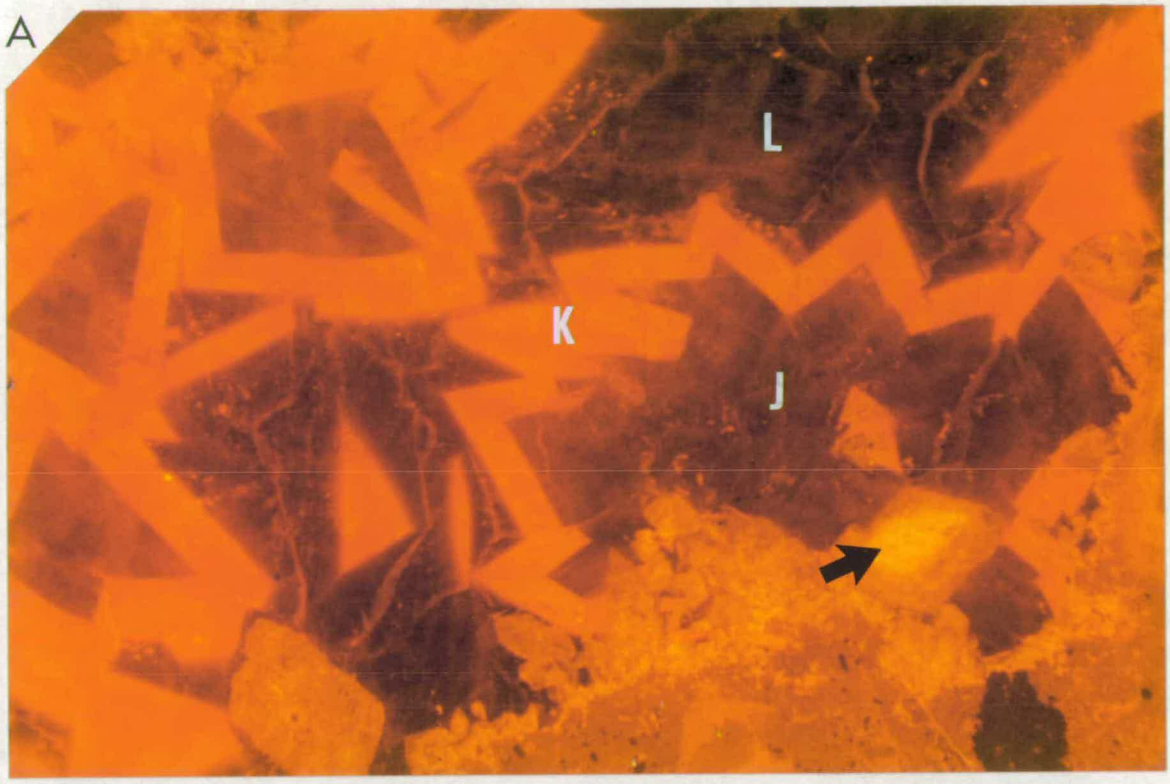

Figure 11.3 Dolomitisation of sediments.

A. Photomicrograph showing scattered dolomite rhombs (D) developed in M1 sediment. Subsequent calcitisation selectively replaced the rhomb-cores and produced dark areas, rich in goethite inclusions. Stained thin section, Gerna bank facies.

B. Photomicrograph showing geopetal mosaic formed by selective dolomitisation (D) of geopetal sediment in a spar-filled stromatactoid cavity. Remnants of the original fine-grained geopetal sediment are still visible at the spar/dolomite boundary (arrowed). Thin section, Spire Farm bank facies.

C. Photomicrograph showing a pervasively dolomitised sequence of laminated geopetal sediment (M) and CFC spar (S) consisting of anhedral dolomite. Thin section, Old Calamine Mines. (Shown in detail in D).

D. Photomicrograph of the same laminated cavity-fill as shown in C. This higher magnification picture shows the anhedral nature of the dolomite crystals which replaced both sediment (M) and spar (S).

Fig. 11.3

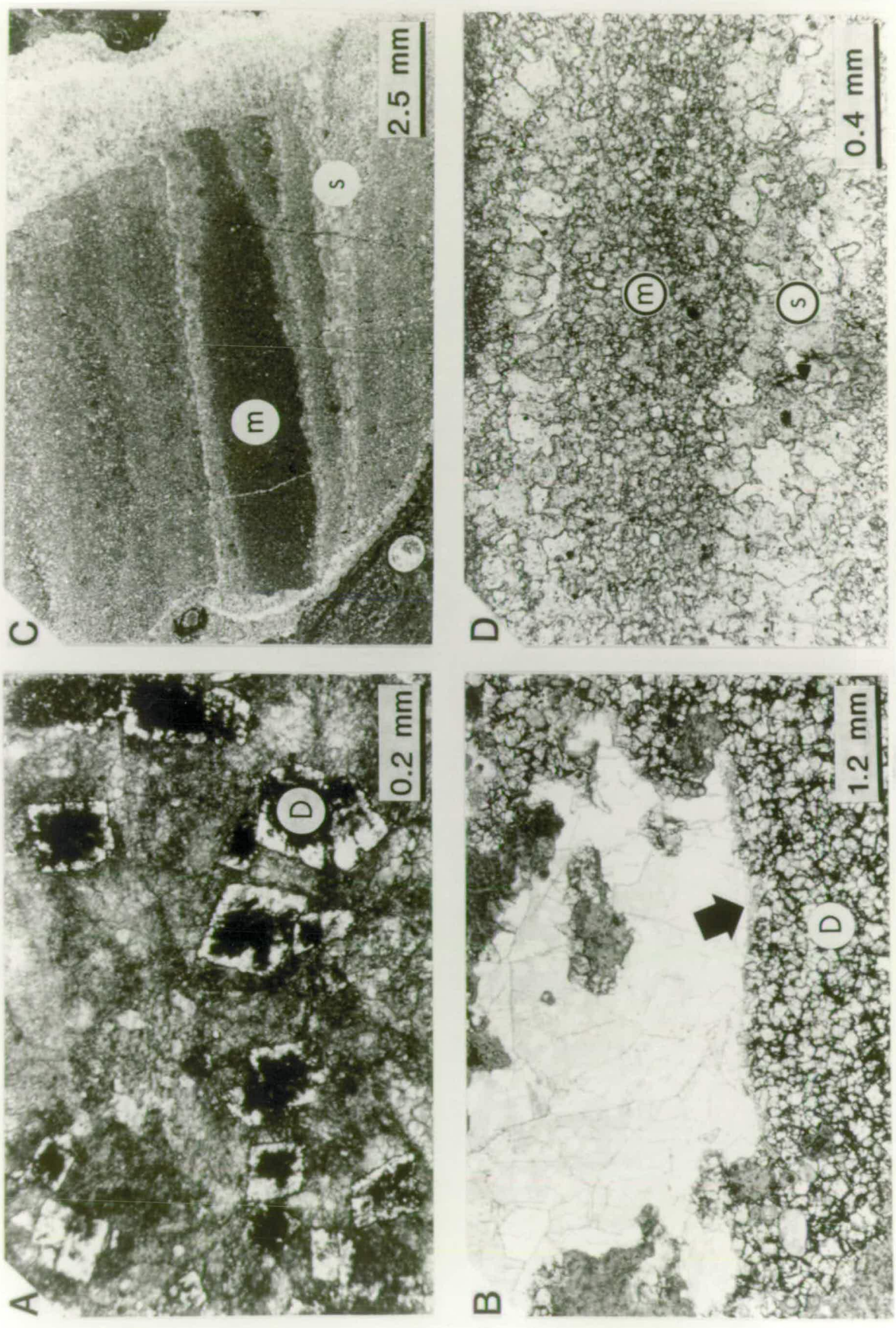

Figure 11.4 Dolomitisation of calcite spar, and neomorphic dolomite.

A. Macro-photograph of a stained rock surface showing a large stromatactoid cavity cutting across the primary M1 sediment, containing laminated geopetal sediment (M2) and rhombic dolomite 'spar' mosaic (D) formed by selective replacement of calcite cements. A later fracturing episode led to the development of ferroan calcite veinlets (v, arrowed). Sugarloaf bank facies.

B. Photomicrograph showing the selective replacement of calcite cement crystals by rhombic dolomite which developed preferentially along the calcite intercrystal boundaries. Thin section, Dunnow bank facies.

C. Cathodoluminescence photomicrograph showing non-luminescent porphyrotopic saddle dolomite (D) which replaced calcite cement in a veinlet (v) and also replaced the adjacent primary sediment (M1). Inclusions of M1 are contained in the dolomite crystal (arrowed). The porphyrotopic crystal faces are anhedral where adjacent to M1, but tend towards euhedral in the veinlet. Thin section, Newsholme bank facies.

D. Photomicrograph showing saddle dolomite "spar" mosaic (D) which selectively replaced calcite cement (S) in a cavity. A framboidal pyrite aggregate (p, arrowed) which developed on the micritised cavity wall (m, arrowed) was partially included in the saddle dolomite crystal, confirming the replacive origin of the dolomite. Dense areas within the dolomite are goethite inclusions formed during subsequent calcitisation of the dolomite. Such calcitisation was particularly concentrated along the dolomite-sediment boundary in this case (c, arrowed).

E. Quarry-face at Sugarloaf buildup showing dark regions of strongly ferroan neomorphic dolomite (Stage L equivalent) developed within rhombic dolomite mosaics (R). Arrow 1 shows a "veinlet" of neomorphic saddle dolomite which passes into white calcite outwith the rhombic dolomite mosaics. The "veinlet" does not appear to have caused any displacement of the rhombic dolomite fabric. Arrow 2; shows a diffuse, dark region where strongly-ferroan dolomite from the same fluids formed concentric rims on earlier dolomite rhombs (see also Fig. 11.5).

Fig. 11.4

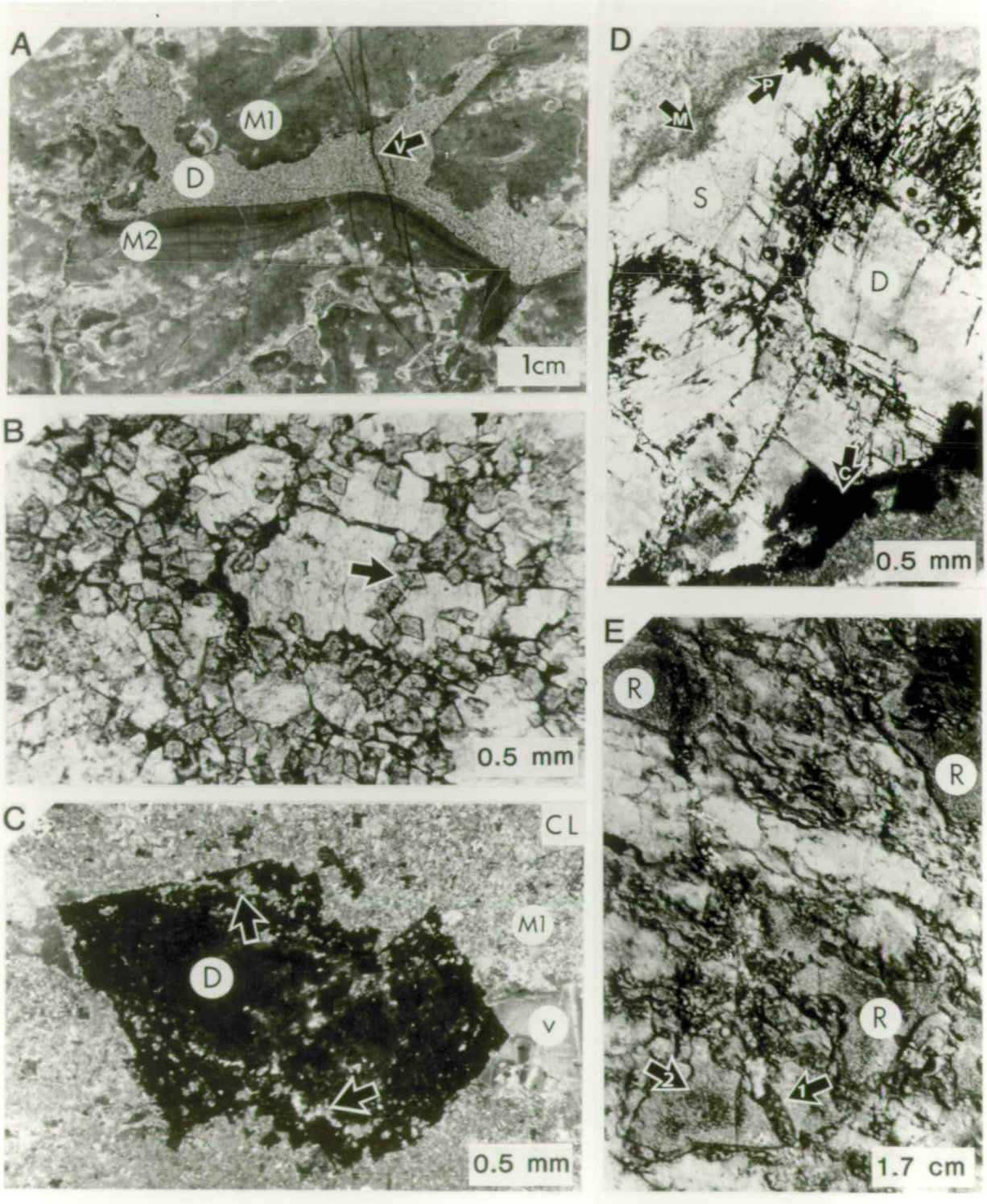

Fig. 11.5. Development of neomorphic dolomite.

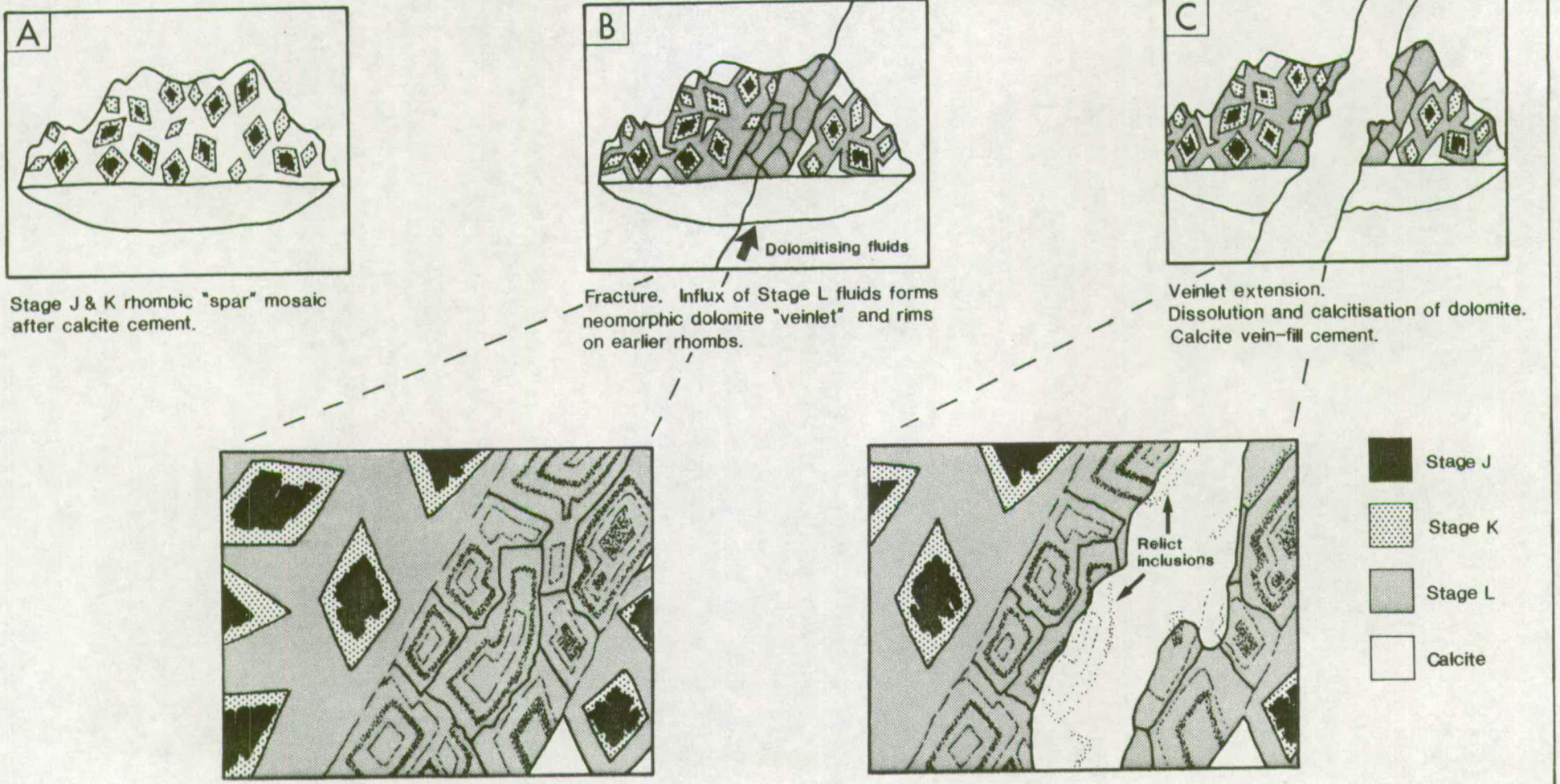

Stage J & K rhombic "spar" mosaic after calcite cement.

Fracture. Influx of Stage L fluids forms neomorphic dolomite "veinlet" and rims on earlier rhombs.

Veinlet extension.
Dissolution and calcitisation of dolomite.
Calcite vein-fill cement.

Figure 11.6 Dolomite associated with stylolites.

A. Photomicrograph of a stained thin section showing turquoise-stained ferroan dolomite (D) exploiting a stylolite. Field of view = 3mm, Coplow bank facies.

B. Field photograph showing ferroan dolomite (now calcitised giving rusty orange-brown colouration), exploiting sylolite seams in sub-Waulsortian facies at Hall Hill quarry. The characteristic anastomosing fabric of the stylolite seams are highlighted by the calcitised dolomite (arrow). Coin for scale, 2p, diameter = 2.5cm.

Fig. 11.6

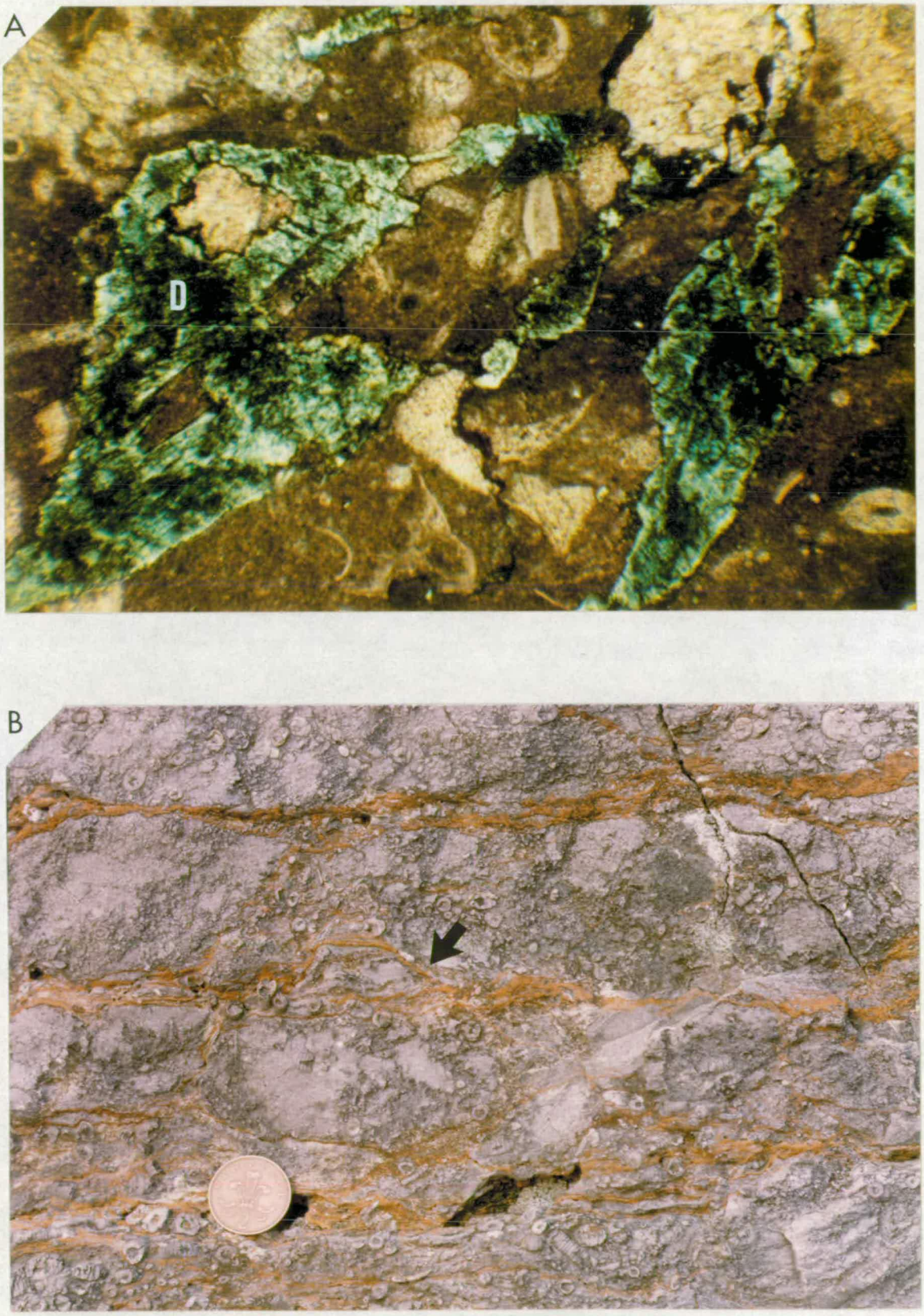

11.5 DOLOMITE COMPOSITION

11.5.1 Geochemistry

This study concentrated mainly on the major elements Ca, Mg and Fe, with trace element Mn. Analysis of strontium and sodium proved to be futile, as concentrations of either element rarely registered above the background level of the microprobe.

When dealing with percentage variations in composition, rather than ppm, it is necessary to re-calculate analyses to molar proportions, i.e. mole% carbonate. This was calculated from wt% oxide in microprobe analyses.

Very few samples contain all three dolomite stages, and in the absence of the intervening non-ferroan Stage K it is impossible to distinguish between the two ferroan dolomite stages petrographically. However, where all three stages are present, as in samples from the Dunnow-Little Dunnow buildup (Table 11.1, Fig.11.7A), microprobe analyses show that the earlier ferroan dolomite, Stage J, has lower Fe concentrations than the later ferroan Stage L. Manganese concentrations in all three stages are comparable at approximately 0.2 mole %.

Analyses from other buildups of ferroan dolomites which could not be assigned to a particular stage by petrographic means, consistently showed iron concentrations which were comparable to analyses of Stage L (Tables 11.1 & 11.2). Owing to this, and the restricted development of Stage J apparent in most thin sections, the majority of ferroan dolomites in the sequence are therefore considered to belong to Stage L.

The mean compositions of all dolomites analysed in this study are given in Table 11.2.

Iron concentration in ferroan dolomites ranges from a minimum of 1.56 mole % $FeCO_3$ in a Stage J dolomite, to a maximum of 16.37 mole % $FeCO_3$ in a Stage L dolomite. The mean $FeCO_3$ concentration for Stage J is 2.18 $\pm$0.48 mole %, whereas Stage L averages significantly higher at 7.92 $\pm$2.58 mole % $FeCO_3$.

Magnesium varies antipathetically to iron in the ferroan dolomites with concentrations ranging from 26.46 to 43.35 mole% $MgCO_3$ (Fig.11.8). The magnesium concentration in non-ferroan dolomites ranges from 34.98-44.99 mole% $MgCO_3$.

11.5.2 Stable Isotopes (Fig 11.9).

Sampling took account of the fact that diagenetic alteration of all dolomites was very common. The degree of alteration ranges from fine hairline veinlets of later cement stages, to complete calcitisation. Samples were therefore selected where diagenetic alteration was judged minimal, as indicated by homogeneous CL characteristics; however, some contamination of all samples was probably inevitable.

Samples of both saddle and rhombic dolomites were analysed (Table11.3; Fig.11.9) Saddle dolomites were essentially pure, whereas rhombic dolomite samples consist of a mixture of dolomite stages and interstitial calcites, along with other impurities including alteration products such as iron oxides, clay and silica, and in some cases, organic matter.

The purity of rhombic dolomite samples was checked by XRD analysis. The empirical dolomite proportion was calculated from XRD peak height ratios using the formula;

$$\frac{\text{Peak height Dolomite}}{\text{Peak height Dolomite + Peak height Calcite}} \times 100 = \text{Dolomite proportion}$$

This figure was then compared to a calibration curve constructed from mixtures of known calcite/dolomite proportions, from which the dolomite percentage in the unknown samples was derived.

Samples CA and SF are from the Cow Ark-Spire Farm Waulsortian complex (SF is from outcrop while CA is borehole material). Rhombic and saddle dolomite were collected from both samples. In the case of the SF sample, rhombic dolomite occurred as a replacement of geopetal sediment while the saddle dolomite filled the overlying space in the same cavity. Both SF and CA rhombic dolomite samples were only slightly contaminated with calcite and only consisted of a single ferroan dolomite stage.

11.5.3 Compositional variation in dolomite crystals

Compositional variation within individual dolomite crystals was investigated with CL, staining, back scattered electron imagery (BEI) and microprobe analysis. The compositional variation exhibited by dolomites in this study was generally independent of their origin, confirming the suggestion of Friedman (1965) and Dickson (1983) that the same crystal growth fabrics could develop in cements and replacements.

CL does not reveal compositional variation in either of the ferroan dolomite stages due to the luminescence quenching effect of the Fe^{2+} in the dolomite lattice. In the non-ferroan Stage K dolomite, variation in CL intensity is uncommon, although occasionally early dull-red and later bright-red substages could be identified in rhombic dolomites.

Staining and BEI do not reveal any compositional variation in Stage J ferroan dolomites. Stage L saddle and rhombic dolomites however, commonly exhibit compositional banding of two kinds:-

a) Subtle banding: parallel to curved crystal growth faces of saddle dolomites. Individual units are a few μm in size. The difference in stain or BEI intensity between zones is subtle, indicating low levels of iron variation.
b) Distinct concentric banding: in ferroan saddle dolomites which have a curved rhombohedral habit. Individual bands (which are essentially substages and often have fine-scale zones) may be up to hundreds of microns across and show significant variation in BEI or stain intensity between adjacent zones, indicating greater variations in iron content than those in type (a). A quantitative microprobe scan across such banding is shown in Fig.11.10.

Compositional sector zonation was not identified in any of the samples (cf Reeder & Prosky 1986), and no compositional difference was detected between inclusion-rich and less turbid areas of the dolomite crystals.

Table 11.1 Mean composition of dolomite stages from Dunnow - Little Dunnow buildup

Analyses given as mole % carbonate

Stage	$CaCO_3$	$MgCO_3$	$FeCO_3$	$MnCO_3$	n*
J	56.99 ±1.94	40.68 ±2.42	2.16 ±0.47	0.17 ±0.05	5
K	59.45 ±2.51	40.09 ±2.67	0.29 ±0.35	0.18 ±0.04	8
L	57.12 ±2.12	35.69 ±2.49	6.99 ±2.40	0.20 ±0.07	8

Table 11.2 Mean composition of all dolomites

Analyses given as mole% carbonate

Stage	$CaCO_3$	$MgCO_3$	$FeCO_3$	$MnCO_3$	n
J	57.31 ±2.40	40.89 ±2.30	2.18 ±0.48	0.17 ±0.05	5
K	58.87 ±2.99	40.52 ±2.93	0.45 ±0.41	0.16 ±0.04	14
L	57.41 ±2.82	34.56 ±3.06	7.83 ±2.56	0.20 ±0.13	57

n = number of analyses

Table 11.3 Isotopic composition of dolomites in per mil (°/₀₀) against PDB standard

SADDLE DOLOMITES

Stage	Sample	$\delta^{13}C$ °/₀₀	$\delta^{18}O$ °/₀₀
K	LDu6	4.60	-3.49
Stage			
L	LDu6	3.61	-5.96
L	C	4.48	-4.97
L	CX7	4.05	-5.80
L	WW	2.67	-5.90
L	SF	1.31	-5.06
L	CA	1.97	-5.57
L	CHQ	5.27	-5.21
	mean	3.34 $\pm$1.3	-5.50 $\pm$0.4

RHOMBIC DOLOMITES

Stage	Sample	% dolomite (XRD)	$\delta^{13}C$ °/₀₀	$\delta^{18}O$ °/₀₀
Ferroan	CA	89	2.12	-8.03
Ferroan	SF	97	2.41	-6.59
Ferroan	CALW	88	3.65	-7.29
K,L	Su17	73	4.80	-5.66
K,L	Su11	78	4.11	-4.87
Ferroan	BP	65	4.35	-5.04
K,L	Du30	12	2.37	-4.98

Locality codes

LDu = Little Dunnow
Du = Dunnow
C&CX = Coplow
WW = Hall Hill (Whitewell)
SF&CA = Spire Farm - Cow Ark
CALW = Calamine mines
Su = Sugarloaf
BP = Bellmanpark
CHQ = Chatburn Quarry

Fig. 11.7 Major element geochemistry of Craven dolomites.

a). Dunnow buildup

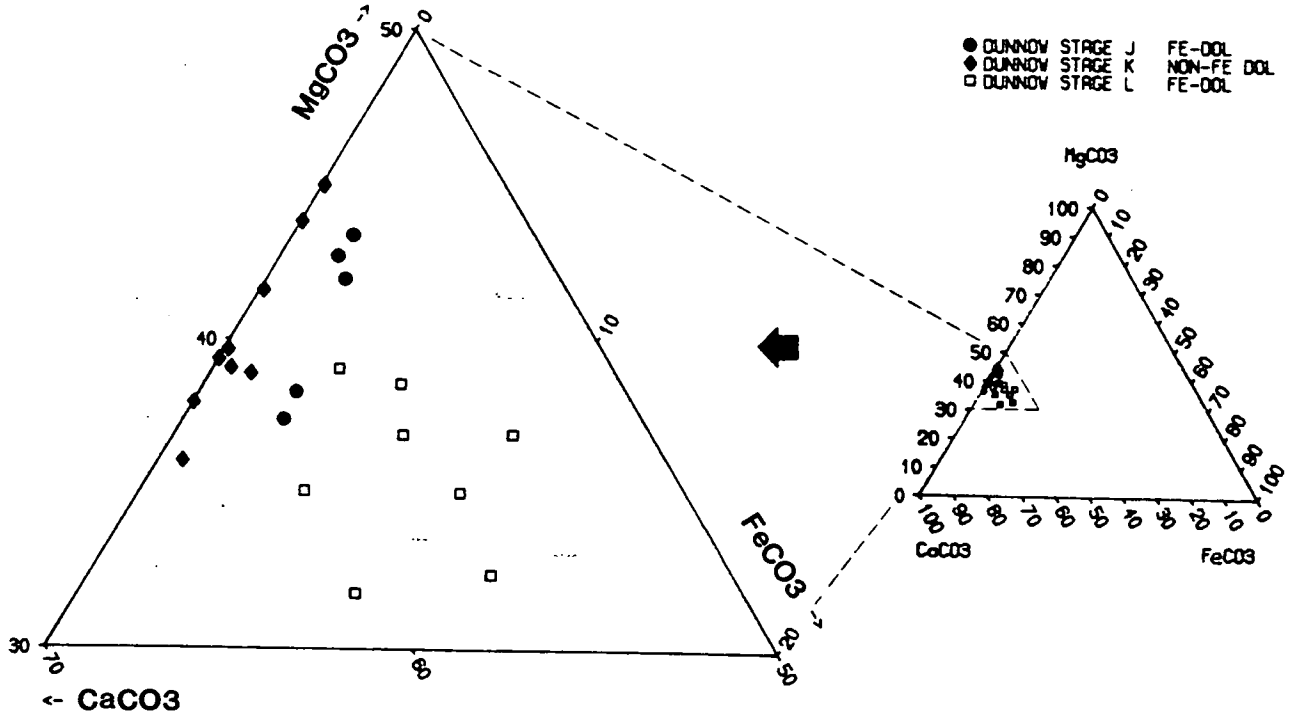

b). All buildups

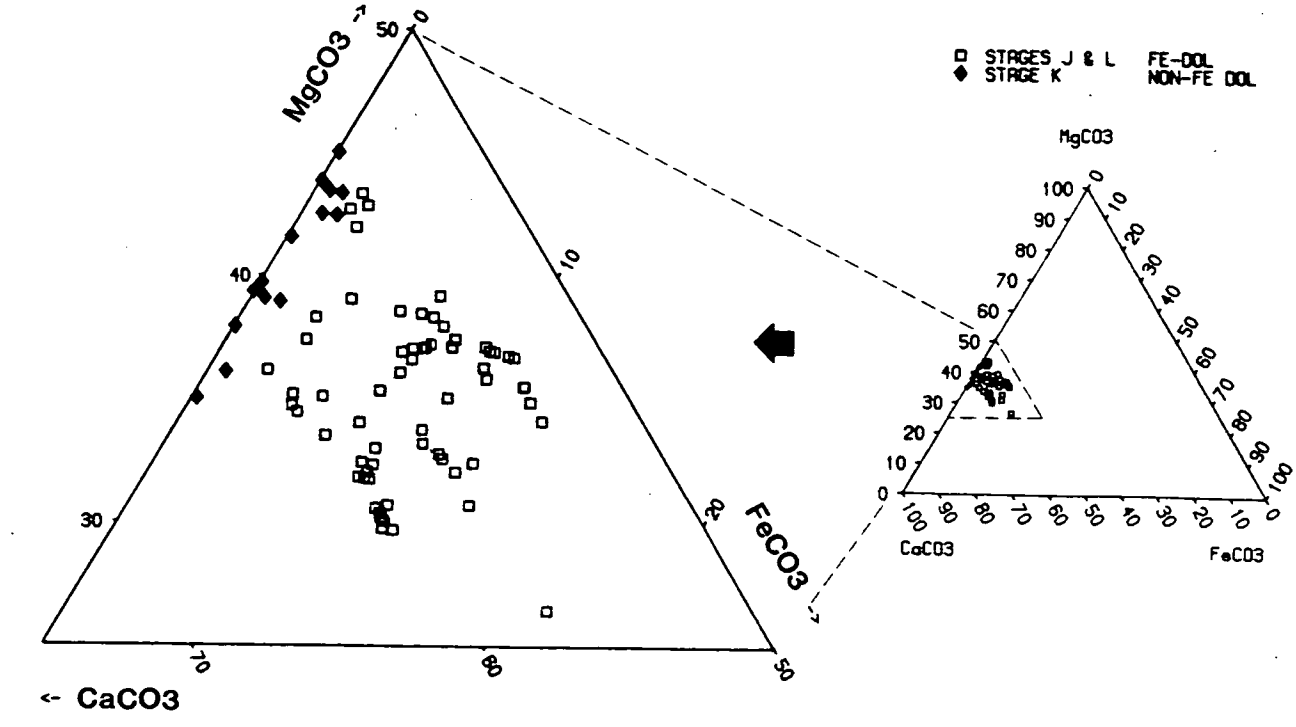

FIG 11.8 : MAJOR ELEMENT COMPOSITION of FERROAN DOLOMITES
(Reduced major axis linear regression)

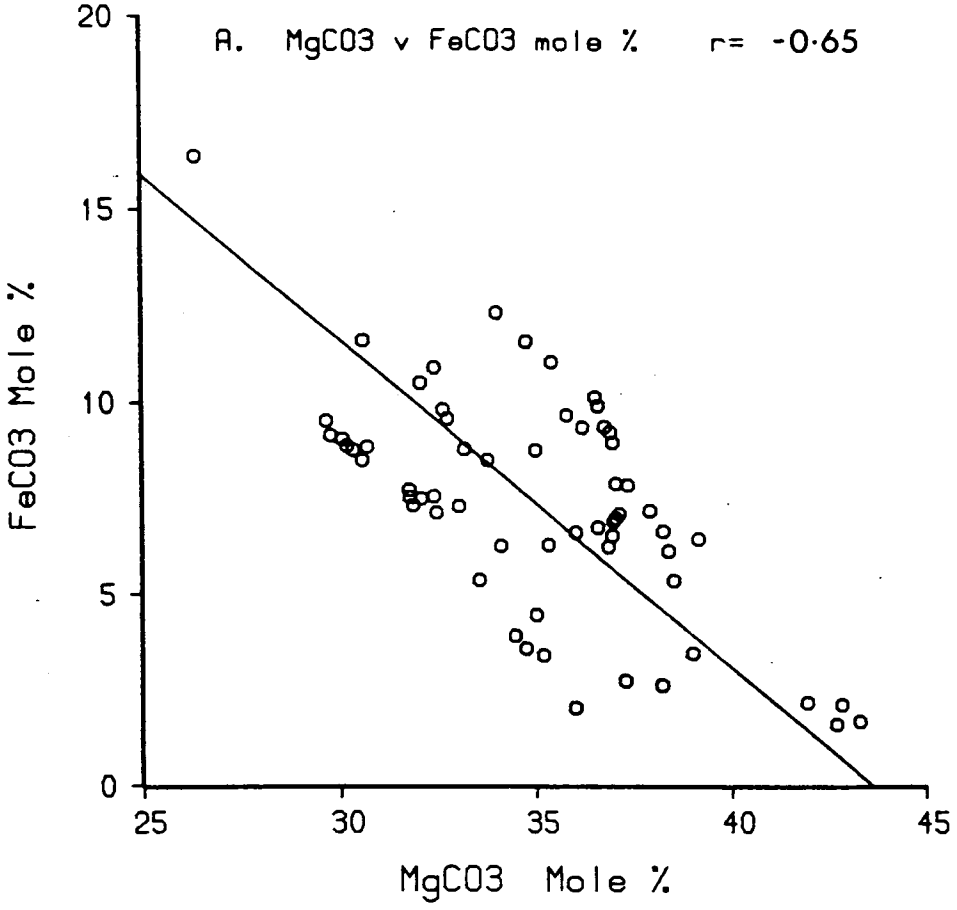

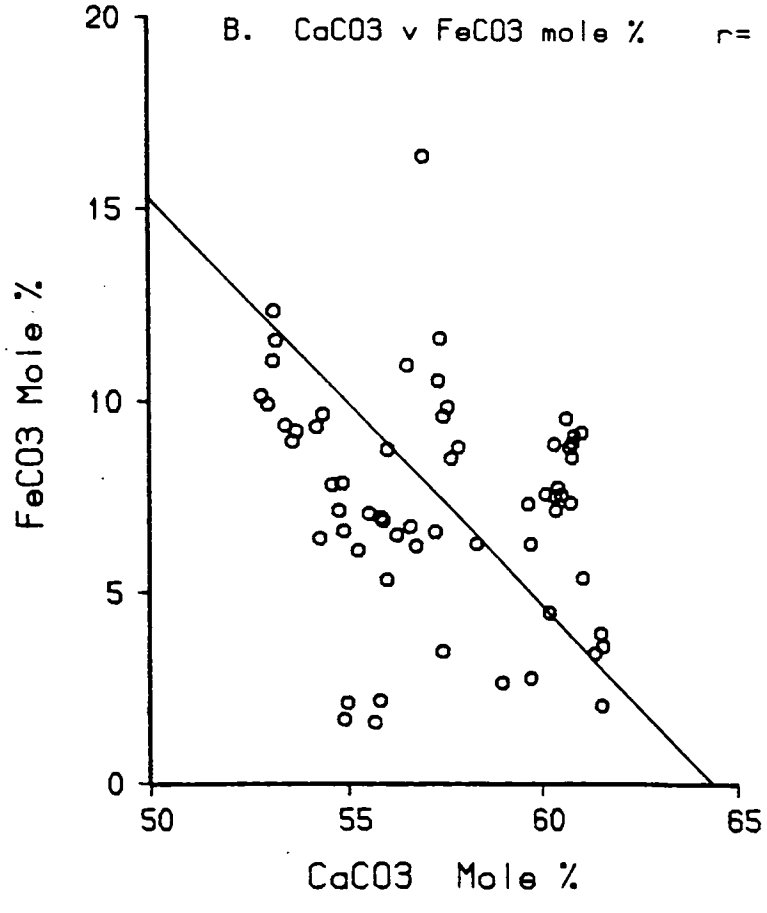

Fig. 11.9 Isotopic composition of Craven dolomites.

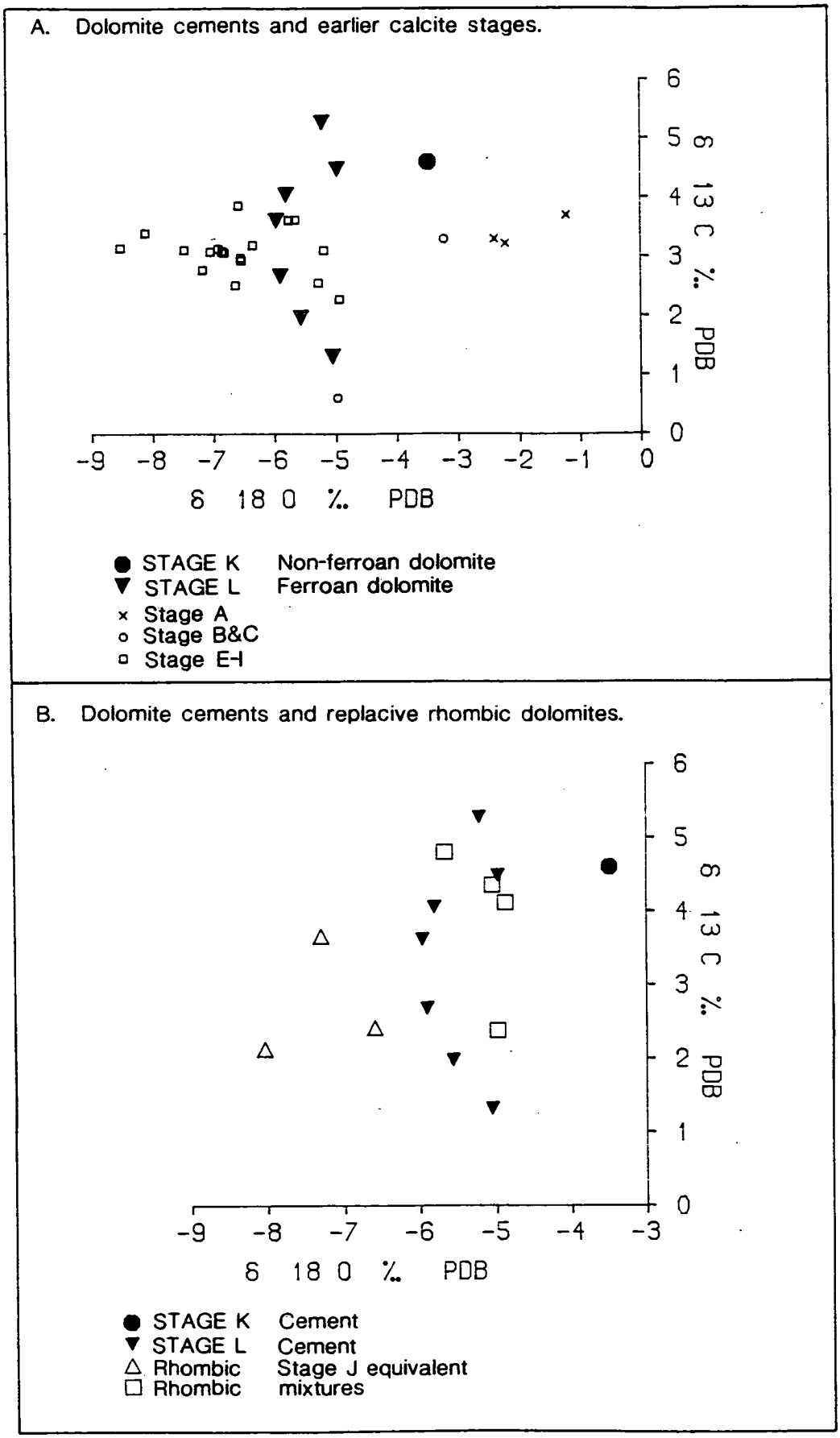

Figure 11.10 Compositional variation in ferroan dolomite.

The BEI photograph shows the row of black probe beam-damage pits produced during a 16-point quantitative analysis scan across compositionally zoned ferroan dolomite from the Old Calamine mines bank facies. The variation in BEI intensity corresponds chiefly to the Fe content of the dolomite, shown in the plot below the photograph. Bright areas in the BEI image contain higher Fe.

Fig. 11.10 Compositional variation in ferroan dolomite.

BEI.

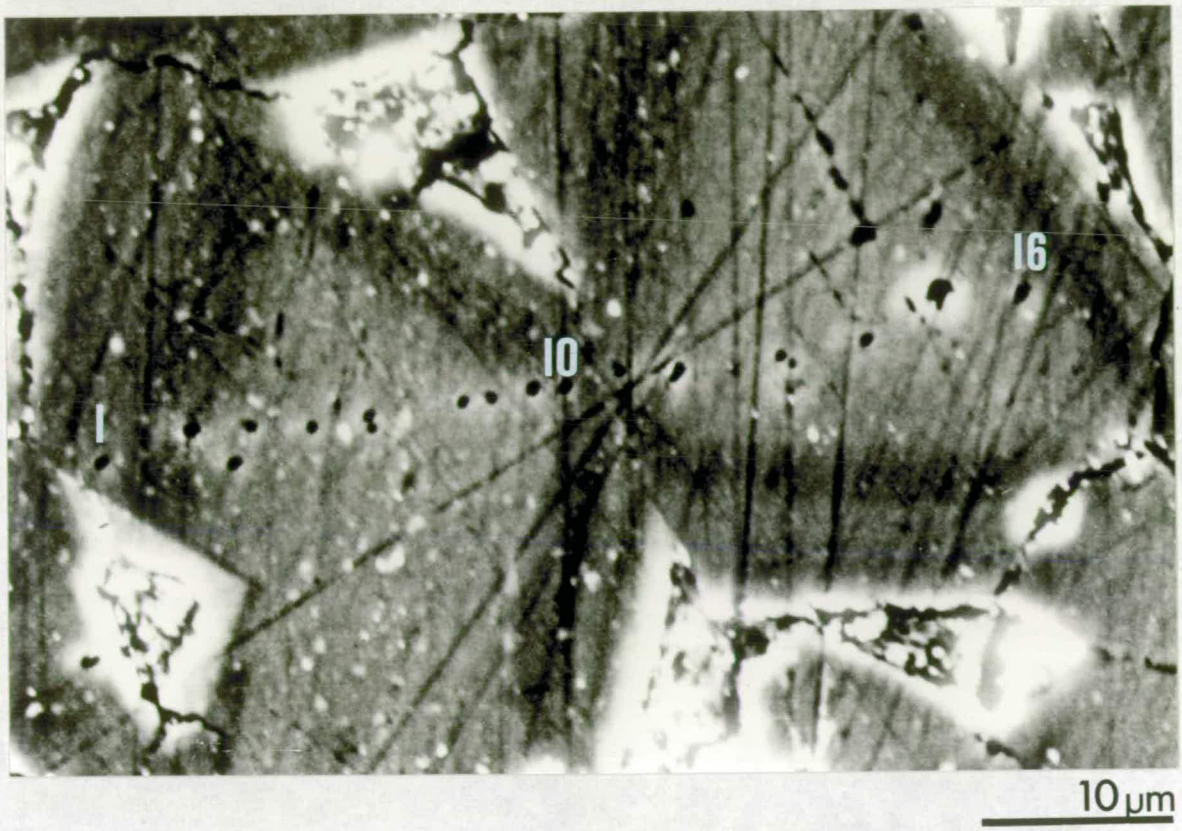

Quantitative microprobe scan.

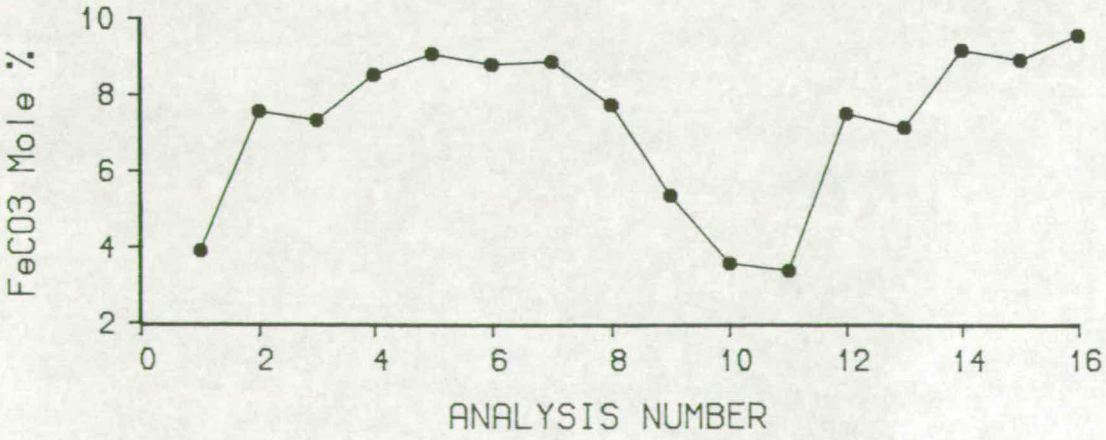

11.5.4 Dolomite stoichiometry

Dolomite rarely achieves its stoichiometric composition in nature ($Ca_{0.50}Mg_{0.50}CO_3$). The departure of major element composition from this formula, or nonstoichiometry, is expressed as a ratio in mole% carbonate. In non-ferroan dolomite, nonstoichiometry can be expressed purely in terms of mole% $CaCO_3$ (Lumsden & Chimahusky 1980).

As would be expected, a strong antipathetic relationship occurs ($r = -0.65$) between iron and magnesium in the Waulsortian ferroan dolomites (Fig. .8A), indicating substitution of iron for magnesium on close to a mole for mole basis. On the other hand, a plot of Fe against Ca shows a poor correlation ($r = -0.26$, Fig. 11.8B). Given, therefore, that Fe substitutes almost exclusively into Mg sites in the dolomite lattice, one can assume that the molar proportions of calcium were not affected by the iron content i.e. the dolomitising ratio can be considered to be (Fe + Mg)/Ca (Irwin 1980). Thus, for convenience, it is acceptable to express the nonstoichiometry in both ferroan and non-ferroan dolomites in terms of (mole) percent $CaCO_3$ (cf. Lumsden & Chimahusky 1980).

All of the dolomites in this study are calcian (Fig. 11.7B). Ferroan dolomites range from 53.1-61.5% $CaCO_3$ with a mean of 57.8 $\pm$ 3.9%, while non-ferroan dolomite stoichiometry varies from 54.95-64.83% $CaCO_3$ with a mean of 58.40$\pm$3.20%. Interestingly, the 14 non-ferroan dolomite analyses show greater stoichiometric variation than the 62 ferroan dolomite analyses. Lumsden and Chimahusky (1980) suggested that such variation can be related to the relative timing of different dolomitisation episodes (see below).

11.6 TIMING AND DISTRIBUTION OF DOLOMITE TYPES

11.6.1 Relationships Between Dolomite Types

The same three-fold stratigraphy, identified by CL and staining in the dolomite cements, can also be recognised in replacive dolomite mosaics. Identical styles of compositional banding occur in both cements and replacements. Major and trace element compositions of

the cement stages are indistinguishable from their replacive counterparts and therefore I conclude that they are equivalents that shared common source-fluids. This is demonstrated in an example from Little Dunnow buildup, which contains dolomite cement filling a void, associated with rhombic dolomite mosaic which replaced peloidal internal sediment (Fig. 11.11). The cement contains all three dolomite stages and exhibits void-filling centripetal growth zonation, while the rhombic dolomite mosaic also contains the same sequence of growth bands, this time developed concentrically. The distinctly red-luminescent Stage K in the cement is commonly connected to the equivalent growth band in the rhombic mosaic, indicating that they both originated from the same fluid.

Anhedral dolomites are never found in association with other dolomite types. It seems that these represent an unusual style of dolomitisation which developed due to the extremely fine grain size of the precursor mineral. If nucleation of dolomite crystals was closely spaced then impingement of crystals would occur before large euhedral forms had the chance to develop.

11.6.2 Development of dolomite stages with crystal type

The volumetric importance of the different dolomite stages varies with crystal type.

Saddle dolomites only rarely contain Stage J and K, the vast majority being composed of the late ferroan Stage L. Where Stage J and K do occur, they develop either as centripetal growth stages or as rhomb-shaped regions with curved margins within larger saddle dolomite crystals. Stage K only rarely occurs in veinlets, whereas Stage L is common. Stage J is volumetrically insignificant in most dolomites.

In rhombic dolomites, the red-luminescent Stage K is often the most volumetrically important. Stage J is poorly developed and shows evidence of substantial dissolution by, Stage K fluids. Stage L commonly occurs as a thin concentric coating on rhombic dolomite crystals (Fig. 11.12).

The rare anhedral dolomite types are always ferroan. However, in the absence of Stage K, the similarity in luminescence and

Figure 11.11 Relationship between dolomite types.

PPL and Cl photomicrograph pair (A and B respectively) from Little Dunnow bank facies. Field of view = 3mm.

A. Showing a cavity-fill comprising saddle dolomite cement (S) and peloidal internal sediment (M).

B. In CL, the characteristic sequence of Stage J, K and L occurs in the saddle dolomite spar. The peloidal sediment contains rhombic dolomite (arrows) which exhibits the same CL sequence. The youngest stages in the rhombs are generally adjacent to the orange-luminescent calcite sediment, indicating that they grew outwards by replacement of the sediment rather than inwards into void-space.

Fig. 11.11

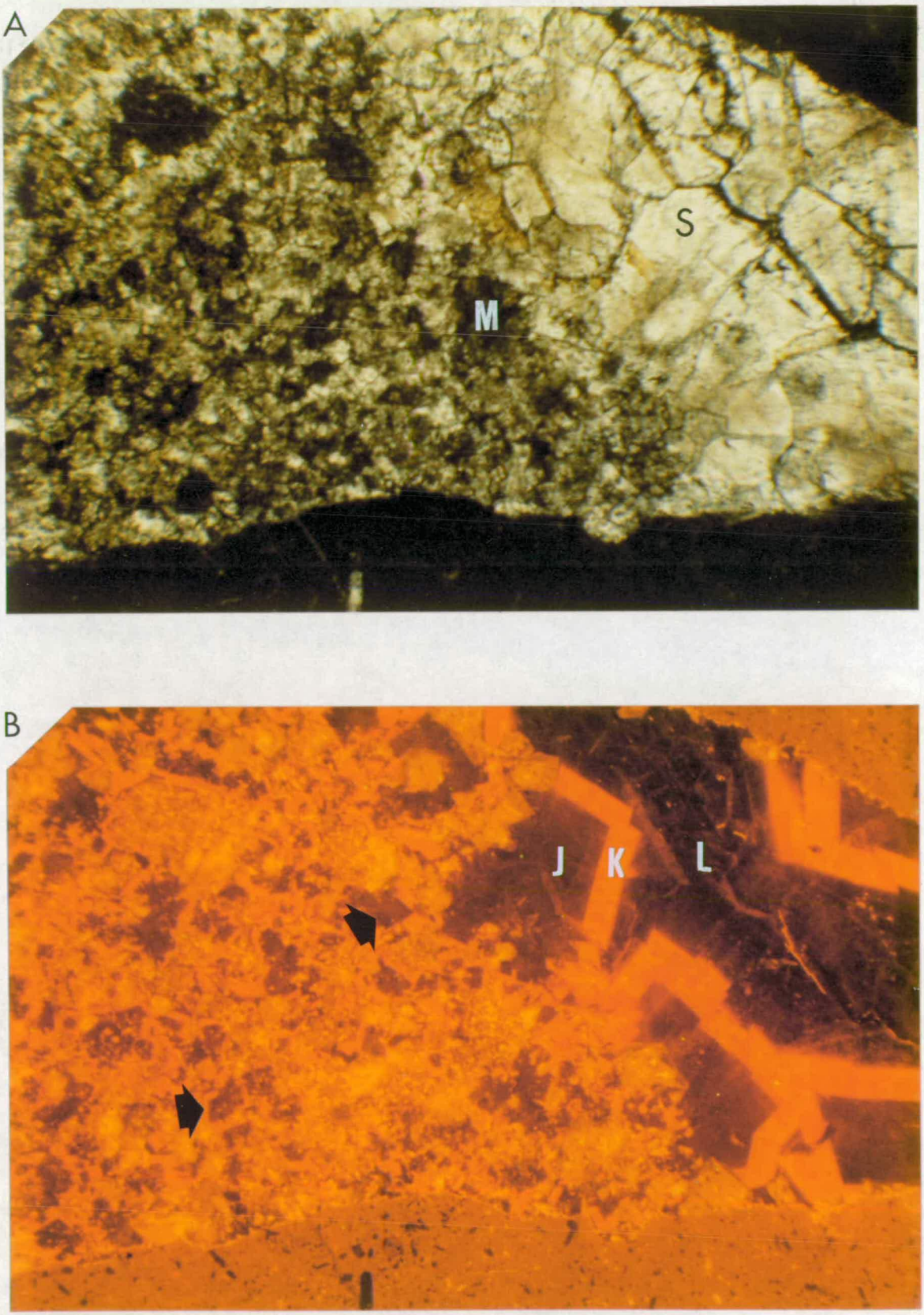

Figure 11.12 Rhombic dolomite stages.

PPL and CL photomicrograph pair. Sugarloaf Quarry bank facies. Field of view = 3mm.

A. PPL: showing rhombic dolomite with dense inclusion-rich rims (caused by partial alteration to goethite, see Chapter 15), replacing calcite spar. Marine CFC cement was not dolomitised. Golden-brown areas in dolomite mosaic are araldite mounting medium which has been burnt by the electron beam.

B. CL: Red luminescent Stage K is volumetrically most important in the rhombs. The earlier, very dull luminescent Stage J cores show irregular dissolution surfaces prior to Stage K (arrow 1). Stage L forms very dull luminescent euhedral outer layers to the rhombs. The CFC has been recrystallised by orange luminescent calcite. Bright-orange luminescent calcite has selectively replaced centripetal growth banding (arrow 2) in the CFC (see also Chapter 17).

Fig. 11.12

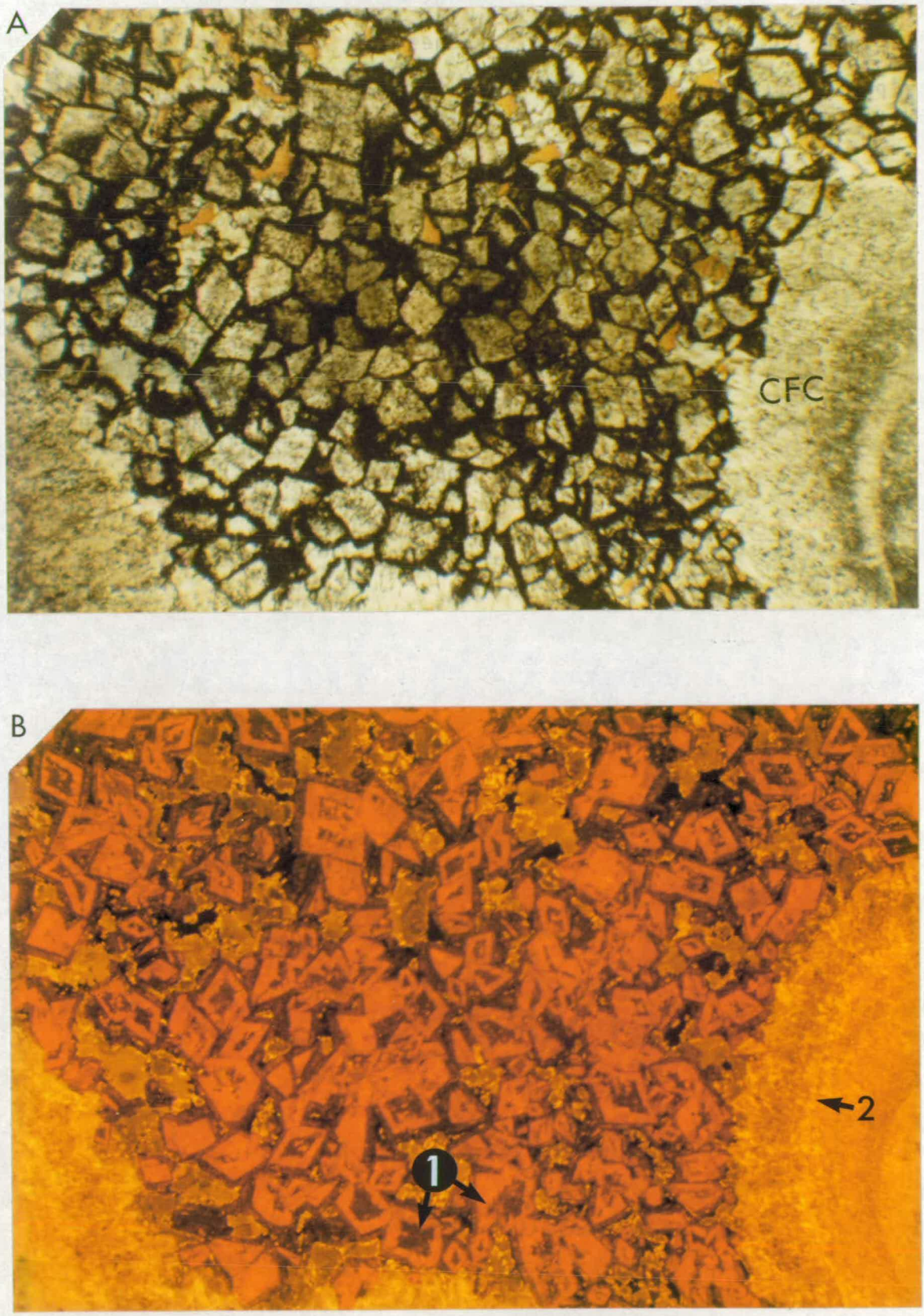

staining characteristics of Stage J and Stage L ferroan dolomites means that it is not possible to assign the anhedral material to a particular stage.

11.6.3 Distribution of dolomite type with facies.

All of the dolomite types described thus far occur in the Waulsortian bank facies. The fabric selectivity of the dolomites means that their distribution in the bank facies is heterogeneous. They are mainly confined to the complex cavity systems, with minor amounts occurring along stylolites and in veinlets. The volumetric abundance of dolomite differs widely between buildups, ranging from scattered replacement of spar or internal sediment fabrics (e.g. Knoll Wood buildup) to almost total occupation of the post-CFC area of the cavity system (e.g. Sugarloaf buildup). A noticeable increase in the degree of dolomitisation occurs near a fault which cuts the bank facies at the Old Calamine Mines near Dinkling Green, indicating that fracturing was another control on dolomite distribution in the bank facies.

From peri-Waulsortian facies, dolomites were found in bituminous limestone interbank equivalents of the Sugarloaf buildup, the Chatburn Limestone Formation in the vicinity of the Horrocksford Hall Thrust, and the Peach Quarry Limestone. Rhombic dolomite mosaics occasionally developed as a replacement of the fine grained intergranular matrix of bioclastic wackestones of the toe and flank facies. Non-ferroan dolomites were not identified outside of the bank facies, where all dolomites are ferroan and are primarily confined to veinlets.

Comparative material was collected from vein-fills in late Chadian/ Arundian carbonates from the northeast limit of the study area at Scarnber, shelf-slope/turbiditic facies of Arundian age in the Trough of Bowland (see Gawthorpe & Clemmey 1985), the Worston Shales immediately overlying the Worsaw Hill buildup, and the Bollandoceras hodderense Beds at Mitton-le-Main. These dolomites are similar in every respect to those in the Waulsortian buildups. The

samples from Worsaw Hill contain cements of identical staining and CL characteristics to Stage H and I aggregates which developed immediately prior to the dolomite, and the example from the B. hodderense beds has ferroan calcite prior to ferroan dolomite, and non-ferroan, bright luminescent calcite (comparable to the subsequent Stage N) after dolomite.

11.7 DISCUSSION

11.7.1 Nature of dolomitising fluids

Petrographic observations and geochemical analyses (see above) indicate that the three dolomite stages were not related to a single influx of diagenetic fluids.

The highly irregular dissolution surface which commonly separates Stage J and Stage K equivalents in rhombic dolomite mosaics (Fig 11.12), is strong evidence of a major change in pore-fluid chemistry, while the development of neomorphic dolomite associated with fracturing is further evidence that dolomitisation was not a continuous process. A considerable period of time may have elapsed between the development of each successive dolomite stage.

The most significant aspect is the development of the non-ferroan, Stage K between the two ferroan dolomite stages, J and L.

11.7.1.1 Fluid Sources

Although the existence of three dolomite stages suggests that fluid conditions, and therefore possibly fluid sources, underwent significant change, some general remarks can be made which may apply to all three dolomitising episodes.

Source of magnesium

A probable source for magnesium ions in the deep subsurface is transformation of clay minerals resulting from compaction and shale dewatering. (Jodry 1969; Davies 1979; Mattes & Mountjoy 1980). In

clay-rich carbonates the source of such Mg-rich fluids would not be a problem, but in the Waulsortian buildups themselves, the limestones are particularly pure with insoluble residues of less than 3% (Harrison 1982). As a result of the common and intimate association of dolomite with stylolites, the process of stylolitisation is often considered to release Mg. However, in the Waulsortian bank facies, petrographic evidence shows that dolomite usually post-dates stylolites. Furthermore, stylolites are often poorly-developed and undolomitised in the bank facies. These points strongly argue against an internal source of Mg for dolomitisation within the buildups. The peri-Waulsortian (and Chatburn Limestone and Worston Shales formations), however, are more shaley, and much compacted and stylolitised, offering a more plausible source for Mg.

Source of calcium

There was always sufficient calcium for dolomite formation, the most important source being the pressure-dissolution of primary carbonate related to burial compaction. It is obvious that the production of dissolved calcium would have been greater in the well-compacted off bank/interbank facies than in the bank facies, although evidence of stylolitisation in the banks indicates that the primary Waulsortian sediment also supplied some calcium.

Source of carbonate

Again, there is little problem in finding a potential carbonate source for the dolomites. As long as the carbonate alkalinity was high enough, dissolved carbonate would be supplied from the sediment column either from dissolution / pressure-dissolution of primary carbonate, or reactions involving organic matter (Irwin 1980) (see below).

Source of iron

Iron oxides and hydroxides which may be adsorbed onto clay particles can be reduced to ferrous iron during the sulphate reduction process or through direct or bacterial oxidation of organic matter. The ferrous iron released into pore fluids during sulphate reduction would be rapidly fixed as iron sulphide and therefore the

activity of iron would remain low (see Chapter 3). The onset of bacterial fermentation is marked by the disappearance of SO_4^{2-} ions from the pore fluids, and therefore the end of pyrite formation. Thus Fe^{2+} could build up in pore fluids and become incorporated in carbonate cement phases (Curtis 1978). The increase in Fe^{2+} ions may be sufficient to participate in dolomite formation by effectively maintaining the dolomitising ratio (Mg + Fe)/Ca (cf. Irwin 1980). Generally, the occurrence of ferroan dolomite in organic-rich sediments supports the involvement both of clay minerals and organic matter in iron reduction and dolomite genesis (Irwin op.cit.).

The lack of significant clay mineral or organic content in the Waulsortian facies indicates that iron, like magnesium, was derived externally to the buildups.

11.7.1.2 Compositional variation in dolomite stages

a) Major Elements

The relative lack of iron in Stage K indicates a major change in fluid source after Stage J. The two most likely reasons for the shift in dissolved Fe^{2+} concentration are;

i) Oxic fluids replaced the reducing fluids of Stage J, thus inhibiting the production of Fe^{2+} and forming Fe^{3+} which does not incorporate into the dolomite lattice.

ii) The Stage K fluids were originally low in Fe^{2+} or became depleted in iron due to diagenetic processes such as intensive sulphate reduction and pyrite formation (cf. Pisciotto 1981), external to the Waulsortian buildups.

It has been observed that early (shallow burial) diagenetic dolomites are usually less stoichiometric than older, deeper burial dolomites (Irwin 1980; Lumsden & Chimahusky 1980). Although the difference in mean stoichiometric values between ferroan and non-ferroan dolomites in this study is small, ferroan dolomites show less variation and are nearer to stoichiometric composition than the non-ferroan dolomites, despite the substantial bias in numbers of ferroan dolomite analyses. Taking this with the $\delta^{18}O$ data (see below) I conclude that the non-ferroan dolomites in the Waulsortian

buildups developed at shallower burial depths than the ferroan dolomites. It is therefore possible that different source fluids and processes were responsible for Stage K, or that a mixing of deep burial fluids and those from shallower burial environments occurred.

The stoichiometry of the subsequent Stage L ferroan dolomite is less calcian and less variable than Stage K, and thus appears to indicate a return to a deeper burial diagenetic environment of similar nature to that of Stage J (cf. Irwin 1980).

Iron concentrations in Stage L are extremely variable with the maximum level of 16.37 mole% $FeCO_3$ being essentially an ankeritic composition (cf. Hey 1962). This indicates significant variation in the degree of bacterial fermentation, and/or compaction during this time.

b) Stable Isotopes

The relatively poor understanding of low temperature dolomite kinetics leaves considerable uncertainty in assessing the genetic significance of isotopic data. Furthermore, unless the degree of openness of the system and composition of the ambient fluid is known, the likelihood of rock/water interactions causing isotopic buffering (Mattes & Mountjoy 1980) means that isotopic signatures cannot be directly related either to the temperature of dolomite formation or source fluid composition (Czerniakowski et al. 1984). Interpretations of isotopic compositions of dolomites in Stages J, K and L are discussed below with these provisos in mind.

i) Carbon isotopes.

Carbon isotopes of the ferroan and non-ferroan dolomites are widely variable, butgenerally heavier than in earlier cements (Table 11.3; Fig. 11.9). Of the possible sources for carbon in ground waters, neither meteoric nor marine fluids would be likely to produce such enrichment in $\delta^{13}C$ (see Mattes & Mountjoy 1980, Fig. 25).

Positive carbon values similar to those in this study, however, have been reported elsewhere (Murata et al. 1967; Mattes & Mountjoy 1980; Pisciotto 1981), and in these cases, most authors tend to

favour bacterial fermentation of organic matter as a source of heavy carbon (e.g. Curtis 1978, Table 1, p.111). Irwin (1980) also cites bacterial fermentation as the main cause for extremely heavy carbon isotope values. Significantly, the heaviest $\delta^{13}C$ isotope value in this study comes form a sample of the bitumenous Chatburn Limestone Formation at Clitheroe (sample CHL1). The $\delta^{13}C$ values for dolomite in this study are not as heavy as that predicted for bacterial fermentation (+15°/₀₀, Irwin 1980) and therefore probably indicate buffering by dissolution of marine carbonate from the sediments. The range of $\delta^{13}C$ in the ferroan dolomites in this study suggests that the degree of buffering was variable.

Stage L dolomite $\delta^{13}C$ varies from 1.31 to 5.27°/₀₀ while $\delta^{18}O$ values are more consistent at -5.50 $\pm$0.4°/₀₀. A similar example of widely variable carbon isotopic signatures with relatively consistent oxygen isotopic values was identified in dolomites from the Monterey Formation (Miocene) of California (Pisciotto 1981). The conclusion in this case was that the $\delta^{13}C$ values were indices of stages of organic matter decay. Pisciotto (1981) also reported heavy carbon, low iron dolomites and suggested that iron was removed from the pore waters in a highly active sulphate reduction zone prior to dolomite precipitation. A similar mechanism could be invoked for the heavy carbon, non-ferroan Stage K dolomites.

The variation in $\delta^{13}C$ in the ferroan dolomites could also be related to the often random distribution of fluid inclusions. It is possible that the inclusions contain fluid which is not in isotopic equilibrium with the host dolomite. Beales and Hardy (1980) report saline fluid inclusions in dolomites and sulphides associated with Mississippi valley-type mineralisation. Other studies have identified hydrocarbon inclusions in dolomite (Burrus et al. 1985). No detailed studies of inclusions have been made in the present study.

Another possible reason for the variability in $\delta^{13}C$ in the dolomites could be related to the replacive origin of many of them. Various authors have indicated that replacive dolomite could assume part or all of the isotopic compositon of the precursor carbonate depending on whether replacement was in an open or closed system (Land 1980; Mattes & Mountjoy 1980).

ii) Oxygen isotopes

As with $\delta^{13}C$ values, interpretation of $\delta^{18}O$ signatures depends on the isotopic composition of the ambient fluids and the openness of the system, evidence for which cannot be determined directly. Furthermore, there are differences in treatment when comparing calcite and dolomite isotopic signatures. Some authors have indicated that a fractionation factor should be applied to dolomite isotopic values in order to make them comparable with calcite. Northrupp and Clayton (1966) calculated that this fractionation factor should be -3‰. Other workers do not apply any correction to dolomite isotopic compositions (e.g. Mattes & Mountjoy 1980; see also Land 1980 for discussion). In the absence of any concensus of opinion, corrections were not applied to the dolomite isotopic compositions in this study, and my figures are thus comparable to other examples of burial dolomite from the literature (Choquette 1971, Zenger & Dunham 1980; Mattes & Mountjoy 1980; Cercone & Lohmann 1986).

No direct evidence of the isotopic composition of Stage J cement was obtained. However, samples of different crystal forms, (in what ostensibly appeared to be dolomite deposited from the same parent fluid), from the Spire Farm-Cow Ark buildup (samples SF and CA Table 8.3), showed significant variation in $\delta^{18}O$ composition.

The difference in isotopic composition between saddle and rhombic dolomite pairs taken from individual samples, and in one case the same cavity, is rather striking. Saddle dolomites are enriched in $\delta^{18}O$ (and depleted in $\delta^{13}C$) relative to the rhombic dolomites (Table 11.3). It could be argued that this difference was due to contamination from interstitial calcite within the rhombic crystal mosaics, but impurity levels indicated by XRD analysis are very low, and may be considered negligible in the case of the SF sample. Furthermore, no internal compositional variation was detected in either crystal form.

There are three possible processes which may have caused the observed isotopic discrepancy:-

a). A single fluid entered a void that was partially filled with geopetal sediment, replaced the sediment to form rhombic dolomite and precipitated saddle dolomite cement in the void space.

The variation in isotopic composition between the two types would be caused by buffering of the replacive phase by the geopetal sediment precursor.

b). Dolomitisation by a single dolomitising fluid of a geopetal sediment and overlying calcite spar in a filled cavity, which resulted in two separate forms of replacement. Buffering by the precursor material produced the variation in isotopic composition of the two dolomite types.

c). The two dolomite types were formed by separate fluids of different isotopic composition. The rhombic dolomite was undoubtedly a replacement of geopetal sediment while the saddle dolomite could be either cement or replacement of pre-existing spar.

If "a"or "b" were applicable, then we must consider the potential isotopic composition of any precursor minerals.

The precursor geopetal sediment would probably have had an isotopic composition close to marine values, while any precursor calcite cement that may have precipitated in the void above the sediment would have had a deeper burial signature, i.e. depleted in $\delta^{18}O$ relative to the geopetal sediment. Therefore, any dolomite replacement of the calcite spar would be expected to have depleted $\delta^{18}O$ relative to the replacement of the geopetal sediment. In assuming a single dolomitising fluid, then buffering must have taken place in order to produce the observed variation in dolomite isotopic composition. The same reasoning applies if the void was only partly filled by geopetal sediment and the rest was void space. If a single fluid were involved then the saddle dolomite cement would still be expected to be depleted in $\delta^{18}O$ relative to the "geopetal" dolomite mosaic, which must have been buffered by the precursor sediment in order to produce the isotopic variation between the two dolomite types.

In both cases, the expected $\delta^{18}O$ difference between rhombic and saddle dolomites in these examples is opposite to that determined from analysis, and therefore it must be assumed that two separate dolomitising fluids were involved. Saddle dolomites in these examples have similar $\delta^{18}O$ composition to Stage L (Table 11.3), while the geopetal sediments were dolomitised by a Stage J equivalent fluid to form the rhombic mosaics.

Other rhombic dolomite isotopic analyses (see Fig. 11.9B) support this conclusion. Those samples containing Stage K and L equivalents are isotopically dissimilar to the Cow Ark-Spire Farm samples, and are more comparable with Stage L. Of the two other mono-phase ferroan rhombic dolomites, one (CALW) is similar to the Cow Ark samples while the other (BP15) is of Stage L-type composition. Admittedly, the contribution of the calcite impurities in some of the rhombic dolomites is likely to have had a significant affect on the final isotopic value; however,it seems reasonable to suggest that the isotopic composition of the 'SF' rhombic dolomite sample is the closest representation of Stage J composition.

A significant enrichment of $\delta^{18}O$ occurs in Stage K dolomites. If the assumptions made above about the isotopic composition of Stage J are correct, then the recorded shift is in the region of +3 -+4°/₀₀ $\delta^{18}O$. Even discounting the Stage J result, the non-ferroan dolomite $\delta^{18}O$ composition is +2°/₀₀ heavier than ferroan dolomite values.

This suggests that the pore fluid temperature for Stage K was lower than for the ferroan dolomites, which in turn could suggest that the Stage K dolomites developed at shallower burial depths. Exactly how much shallower is impossible to say, without knowing the isotopic composition of the pore fluid, the degree of openness of the system (See Land 1980) and the geothermal gradient.

However, Pisciotto (1981) suggested that the lack of systematic variation of oxygen isotopes with carbon values in his study indicated that temperature may have been less of an influence than rates and stages of organic matter decay in determining the isotopic compositions of some dolomites.

The oxygen isotopic composition of Stage L is depleted by 2°/₀₀ $\delta^{18}O$ relative to Stage K, indicating a return to deeper burial conditions, but perhaps not as deep as Stage J.

11.8 A MODEL FOR DOLOMITISATION OF THE WAULSORTIAN BUILDUPS

Dolomitisation in the Waulsortian buildups of this study was a three-stage process.

1. The earliest dolomites (Stage J) are ferroan and reflect a major increase in the availability of Mg^{2+} and Fe^{2+} to the pore fluids, which is first indicated in the preceeding ferroan calcite Stage I (Chapter 9).

The oxygen isotopic composition of Stage J (from its replacive correlative) suggests a deep burial origin equivalent to that deduced for the depth of the preceeding calcite cements (estimated maximum = 3.5km, see Chapter 18, Fig. 18.1). The $\delta^{13}C$ values of Stage J dolomites, however, were enriched by the release of heavy carbon, as a result of reactions involving organic matter at depth. The heavy carbon was buffered during its passage through the rock to varying degrees by carbonate released from pressure dissolution.

Divalent iron and magnesium are assumed to have been sourced from the bacterial fermentation of this deep source organic matter, together with clay-mineral transitions caused by compaction.

Migration of pore fluids within the facies mosaic of the Clitheroe Limestone Formation may have been restricted by permeability barriers such as shaley interbank facies and stylolitised horizons. The compacted and shaley peri-Waulsortian lithologies probably formed an effective seal around the Waulsortian buildups. However, with the development of fracture systems in the competent, lithified pure carbonate masses of the buildups, dolomitising fluids could have gained access to the bank facies. Stylolites which had experienced pressure release or extension during previous tectonic episodes formed other pathways for dolomitising fluids.

The Waulsortian buildups would have been more permeable than the surrounding sediments, due to their resistance to compaction and the remnants of the complex, interconnected pore system. This would have made them a region of relatively low hydrostatic pressure towards which fluids would have migrated after fracturing.

Within the bank facies, fluids migrated initially along veinlets and microfractures, and through any remaining space in the existing interconnected void network. They also invaded and selectively dolomitised the rock fabric, particularly the spars and internal sediments which formed after CFC marine cements. This strong fabric selectivity suggests that the marine phreatic lithification process had resulted in a 'tighter' fabric which was less susceptible to dolomitisation.

2. The early ferroan dolomite was followed by the influx of fluids bearing the non-ferroan Stage K. They were aggressive and often resulted in the dissolution and/or replacement of Stage J. This was the main phase of replacive dolomitisation, with geopetal sediments and earlier calcite spars often being totally replaced, usually by rhombic dolomite mosaics.

Stage K formed from cooler pore fluids at shallower burial depths than Stage J, probably after a period of uplift or erosion (see Chapter 18, Fig. 18.1). This is indicated by an enriched $\delta^{18}O$ signature and a greater degree of nonstoichiometry. The low concentration of Fe^{2+} in Stage K dolomites indicates either an oxic source or the depletion of iron in a highly efficient sulphate reduction zone at a higher level in the sediment body compared with Stage J. The aggressive nature of these fluids would tend to support an oxic source, possibly of meteoric origin.

3. Following Stage K, burial was resumed. At moderate burial depths, a phase of fracturing and reactivation of earlier fractures occurred which can be detected in rocks up to the level of the Bollandoceras hodderense Beds, thus suggesting that it affected the bulk of the Dinantian succession in the Craven Basin. This fracturing allowed the migration of Stage L fluids into the Waulsortian buildups, resulting in the precipitation of ferroan dolomite.

Saddle dolomites were the dominant forms, occurring both as replacements of calcite spars, and as void-filling cements. Some neomorphism of earlier, rhombic replacive dolomites took place. Burial compaction and organic matter degradation again were probably the main source of Mg^{2+}, Fe^{2+}, Ca^{2+} and CO_3^{2-} ions.

The main episode of hydrocarbon migration post-dated Stage L, occurring preferentially along stylolites and spar crystal boundaries, and causing some dissolution of the ferroan dolomites. The association of hydrocarbons and saddle dolomites indicates that the ferroan dolomites developed within the "oil-window" at temperatures of 60-150°C (Radke & Mathis 1980).

CONCLUSIONS

1. Dolomitisation of the Waulsortian buildups occurred during moderate to deep burial in post-Chadian times.

2. A consistent sequence of three chemically distinct dolomite phases were identified by CL and staining comprising;

   Stage J Very dull to non-luminescent ferroan dolomite
   Stage K Red luminescent non-ferroan dolomite
   Stage L Very dull to non-luminescent ferroan dolomite

   These three phases developed both as cements and as replacements of earlier sediments and spars.

3. Three main dolomite habits developed of which two, rhombic and saddle dolomite, are the most abundant. The third type of dolomite is very rare and consists of anhedral crystals which sometimes developed sucrosic texture.

4. Dolomite cements developed in veinlets and within the void network of the Waulsortian bank facies where they consistently post-date the preceeding Stage I calcite cements. All cements developed saddle dolomite habit.

5. Replacive dolomites showed strong substrate selectivity. They largely affected pre-existing spars and internal sediments in the post-CFC areas of the void network, although some dolomitisation of the M1 primary sediment also occured. It is often difficult to establish the replacement origin of these dolomites. Replacive saddle dolomites are identified by the presence of relict inclusions of precursor material while rhombic

dolomite mosaics often contain remnants of the precursor in their interstices. Rhombic dolomite mosaics were the commonest form of replacement texture of both sediment and spar, while saddle dolomites tended to replace pre-existing spars, and the rare anhedral dolomites developed as a replacement of internal sediment or CFC cement. Dolomitisation of the M1 sediment usually occurred as scattered dolomite rhombs. Occasionally, neomorphic saddle dolomite developed after earlier rhombic dolomite.

6. Dolomite was the first diagenetic phase to post-date stylolitisation in the bank facies. Fluids migrated into the Waulsortian facies along fractures and some reactivated stylolites. After fracturing, the relatively permeable void network which remained in the Waulsortian buildups acted as lower pressure "sinks" for the migrating fluids, whose movement would have been restricted by shaley and stylolitised horizons in peri-Waulsortian facies.

7. The magnesium required for dolomitisation in the buildups had an external source. For ferroan dolomites this was probably in fluids expelled by compaction of impure limestones and shales surrounding the Waulsortian facies. While this may also have been the Mg-source for the non-ferroan dolomite, the difference in its composition compared to Stage J and L, accompanied by the strong dissolution surface which commonly preceeds Stage K, suggests that the non-ferroan dolomite pore fluids may have had an entirely separate origin, or perhaps evolved from a mixing of deep and shallower burial formation fluids. Iron was also externally derived, from clay mineral transitions, shale dewatering and/or reduction of iron as a result of bacteriogenic degradation of organic matter.

8. The low level of Fe^{2+} in Stage K suggests an oxic source, possibly meteoric, or that Fe^{2+} was removed by extensive sulphate reduction of the fluid on its downward passage through the sediment body.

9. Dolomite stoichiometry and $\delta^{18}O$ composition indicates that the non-ferroan Stage K dolomite probably precipitated from cooler fluids than that producing the ferroan dolomites. These Stage K fluids may have entered the system after or during a period of uplift or erosion. It is therefore possible that the non-ferroan dolomites had a completely different fluid source, with magnesium being derived from shallower diagenetic environments

10. Dolomites have heavy $\delta^{13}C$, which indicates mixing of fluids derived from bacterial fermentation and those from dissolution of primary carbonate.

11. Stoichiometry, geochemistry and isotopic compositions of the two ferroan dolomite stages are very similar, suggesting that both developed in deep burial conditions.

12. The association of hydrocarbons, particularly with ferroan saddle dolomites, indicates that these carbonates formed within the "oil-window" at temperatures of 60-150°C.

CHAPTER 12
POST-DOLOMITE DIAGENETIC STRATIGRAPHY

Introduction

In the study of cement sequences, there is a point beyond which it becomes very difficult to place even regionally extensive cement stages in their correct position in the cement stratigraphy. This limit is usually attained when the bulk of pore space in a rock has been occluded. After this time it may be difficult or impossible to identify cements with sufficient confidence for them to be mappable. The reduced volume of pore space also means that larger thin section areas are needed for each sample in order to increase the chances of their including the necessary evidence for the precise identification of the diagenetic sequence. Eventually the sampling area becomes prohibitive in terms of the finer resolution of deep burial diagenetic processes.

To add to the complexity, late diagenetic fluids are only likely to have had access to any remaining porosity if the effective permeability seal of earlier cements was broken. Commonly, this was achieved through fracture and veinlet development, but even then it is unlikely that all remaining pore space would have been accessed by any single veinlet phase.

The latter stages of diagenesis in the Craven Basin Waulsortian buildups are thus characterised by the development of an extensive series of cement-filled veinlets, which cannot be accurately assigned to a precise position within the cement stratigraphy.

The sequence of post-dolomite cements is highly complex. Different veinlet phases accessed different voids and therefore large scale disconformities occur between late cement stages. However, despite some uncertainties as to their precise relative timing, the late fractures and their associated vein cements offer much intrinsic information about deep burial diagenetic environments. Furthermore, it is often possible to use the sequence of vein formation to establish limits for the timing of faulting or folding on a basin-wide scale, thus enhancing our knowledge of the basin's

tectonic history (see Chapter 18). The timing of hydrocarbon migration can also be integrated into this sequence.

Apart from cementation, there are other processes that may leave some diagenetic imprint even after most of the pore space has been occluded. One important example is the development of secondary porosity. Dissolution episodes, often related to influx of aggressive fluids along fractures, are known to produce secondary porosity, and fracturing is often associated with hydrocarbon migration (Moore & Druckman 1981). The related processes of recrystallisation and neomorphism can also continue to affect a rock body after pore occlusion, indeed up to and including present day exposure and weathering.

In the present case, it was not always possible to define the later diagenetic sequence following dolomitisation with the precision of pre-dolomite cement stratigraphy, but certain episodes could be distinguished and placed into an approximate time sequence with reasonable confidence. Two of these episodes were evidently of basin-wide significance, whereas three other fracture-related episodes were of only local importance.

For the purpose of continuity, it is proposed to extend the alphabetic sequence of stage identification into this section. However, it is no longer suggested that consecutive stages followed on immediately after one another. It is most probably the "rule" rather than the "exception" that other diagenetic episodes and their products occurred between the recognisable stages.

12.1 HYDROCARBON MIGRATION.

Amorphous light-brown to dense brown-black opaque to translucent material often occurs along dolomite crystal boundaries in mosaics and along stylolite seams which have associated dolomite (Fig. 12.1). It is commonly accompanied by framboidal pyrite.

Sometimes, the amorphous material occurs as irregular inclusions in saddle dolomites and may also be associated with dissolution surfaces along intercrystalline boundaries. The degree of dissolution in this study was not sufficient to cause large scale secondary porosity development (cf. Prezbindowski 1985).

This material is unstable under the electron beam of the microprobe instruments and commonly outgasses and liquifies. It is therefore interpreted as organic matter.

In most cases, organic matter which is associated with dolomite mosaics occurs along dissolution surfaces, suggesting that hydrocarbon migration post-dated dolomite formation.

The hydrocarbons are volumetrically insignificant in the bank facies. However, their close association with dolomite may suggest that they formed under similar conditions. Radke & Mathis (1980) invoked similar evidence to suggest that saddle dolomite formed at temperatures which are equivalent to the oil-window (60-150°C).

Considerable thicknesses of bituminous limestones and shales occur in the Dinantian sequence of the Craven Basin. The limited amounts of organic matter which occur in the Waulsortian buildups could easily have been sourced in these sediments. The fact that organic matter in the bank facies is largely confined to stylolites and dolomite mosaics, which are often closely associated with stylolites, indicates that the source was external to the buildups, and that the stylolites formed the main migration pathways.

12.2 STAGE M: KAOLINITE

Authigenic kaolinite occurs occasionally as cement along veinlets but most commonly as a replacement, particularly of rhombic dolomite. It can be easily identified with CL as it luminesces a

characteristic royal blue colour (Fig. 12.2). Identification of the kaolinite was confirmed with SEM and XRD. Kaolinite always pre-dates other post-dolomite cement phases.

The high purity of the Waulsortian limestones indicates that the kaolinite source was external to the buildups, possibly resulting from the diagenetic alteration of other clay minerals. Kaolinite may also be a low-temperature hydrothermal product, typically precipitated from acid waters (Keller 1978; Longman & Mench 1978 p261).

12.3 STAGE N: LATE CALCITE CEMENT

The last distinguishable basin-wide cement consists primarily of non-ferroan, brightly luminescent calcite. Stage N is associated with a dissolution episode which resulted in the development of a limited amount of secondary porosity. These largely non-ferroan calcites are related to a set of veinlets which acted as conduits for the aggressive fluids, as shown by dissolution at some veinlet margins. The post-dolomite age of these cements is confirmed by the presence of veinlets of Stage N cutting dolomite (Fig. 12.2). In the example shown, taken from a stained thin section, the pink, non-ferroan calcite (N) cuts the turquoise-stained ferroan dolomite (D). and white kaolinite (K). In CL the kaolinite has blue (most commonly, royal blue) luminescence, and is also cut by the bright-orange luminescent Stage N veinlet. The dolomite has dull reddish brown luminescence.

Stage N commonly rests disconformably or unconformably on previous cements. The immediately preceding saddle dolomites (Stages J-L) tended to completely fill any cavities in which they formed, and thus excluded Stage N. Therefore, although it is common to find Stage N after pre-dolomite cements, it is rarely found in contact with dolomite in a void-filling sequence.

Stage N is compositionally somewhat variable, with some ferroan substages. Cathodoluminescence complements the staining observations such that ferroan substages show dull luminescence while the non-ferroan substages are characterised by bright yellow-orange luminescence and commonly exhibit zonation.

Figure 12.1 Hydrocarbons.

A. Photomicrograph showing organic matter (OM) which migrated along a re-activated stylolite (arrow 1) following the precipitation of zoned ferroan dolomite (D). The dolomite shows evidence of dissolution by the organic matter (arrow 2). Stained thin section, Spire Farm bank facies.

B. Photomicrograph showing hydrocarbons with associated pyrite which migrated along a stylolite (arrowed) and infiltrated the intercrystalline boundaries of a rhombic dolomite mosaic (D). Thin section, Spire Farm bank facies.

Fig. 12.1

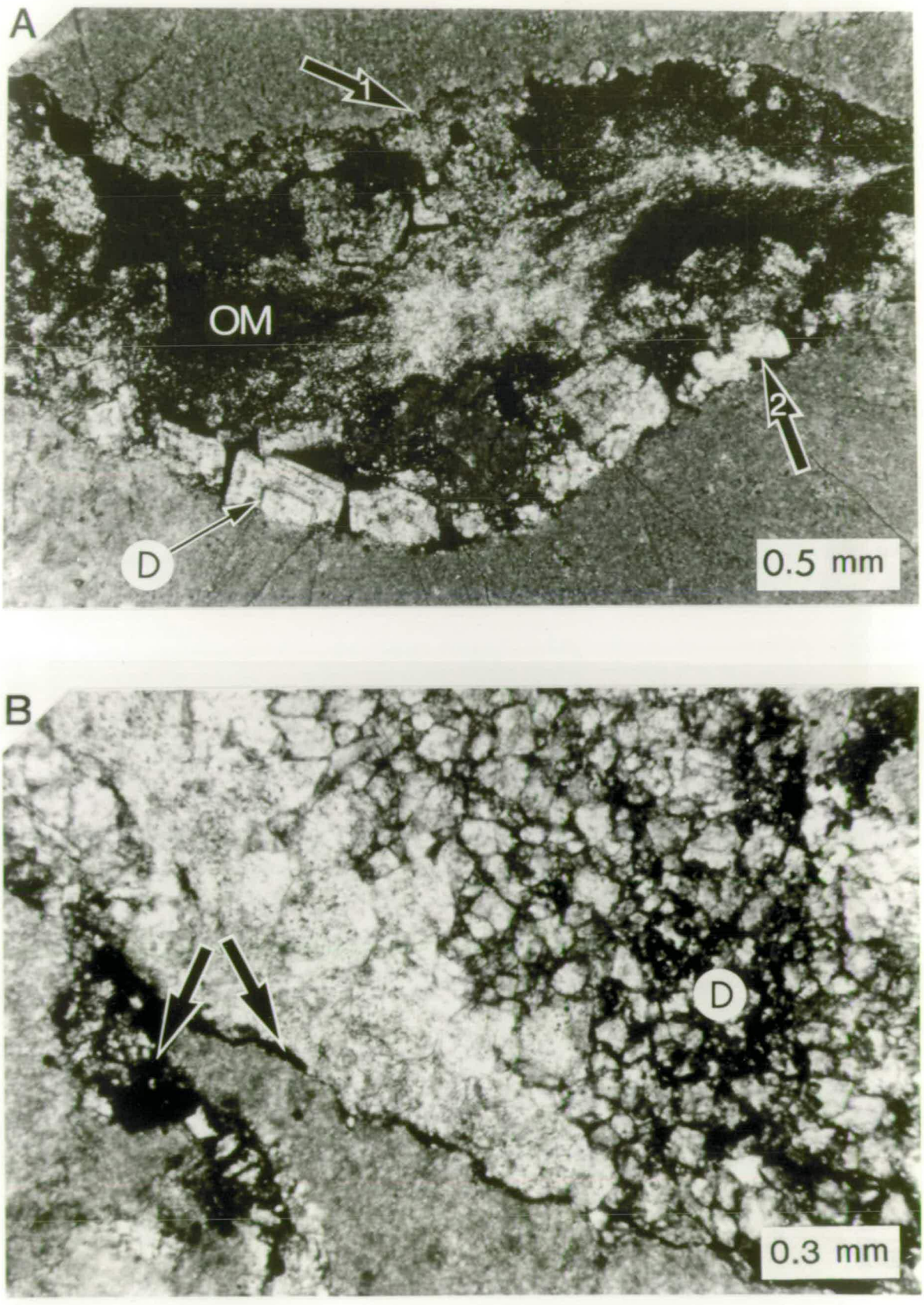

Figure 12.2 Post-dolomite cements.

Photomicrograph pair. Stained thin section in PPL and CL from Coplow bank facies. Field of view = 3mm.

A. Stained thin section showing turquoise-stained ferroan dolomite (D) which exploited stylolites, followed by kaolinite (K) of Stage M. These are cut by a veinlet containing non-ferroan calcite (N) of Stage N.

B. In CL, the denticulate stylolite surface becomes more apparent (arrow). The ferroan dolomite (D) shows characteristic dull brown luminescence while Stage M kaolinite (K) shows blue, and Stage N is bright orange-yellow in CL.

Fig. 12.2

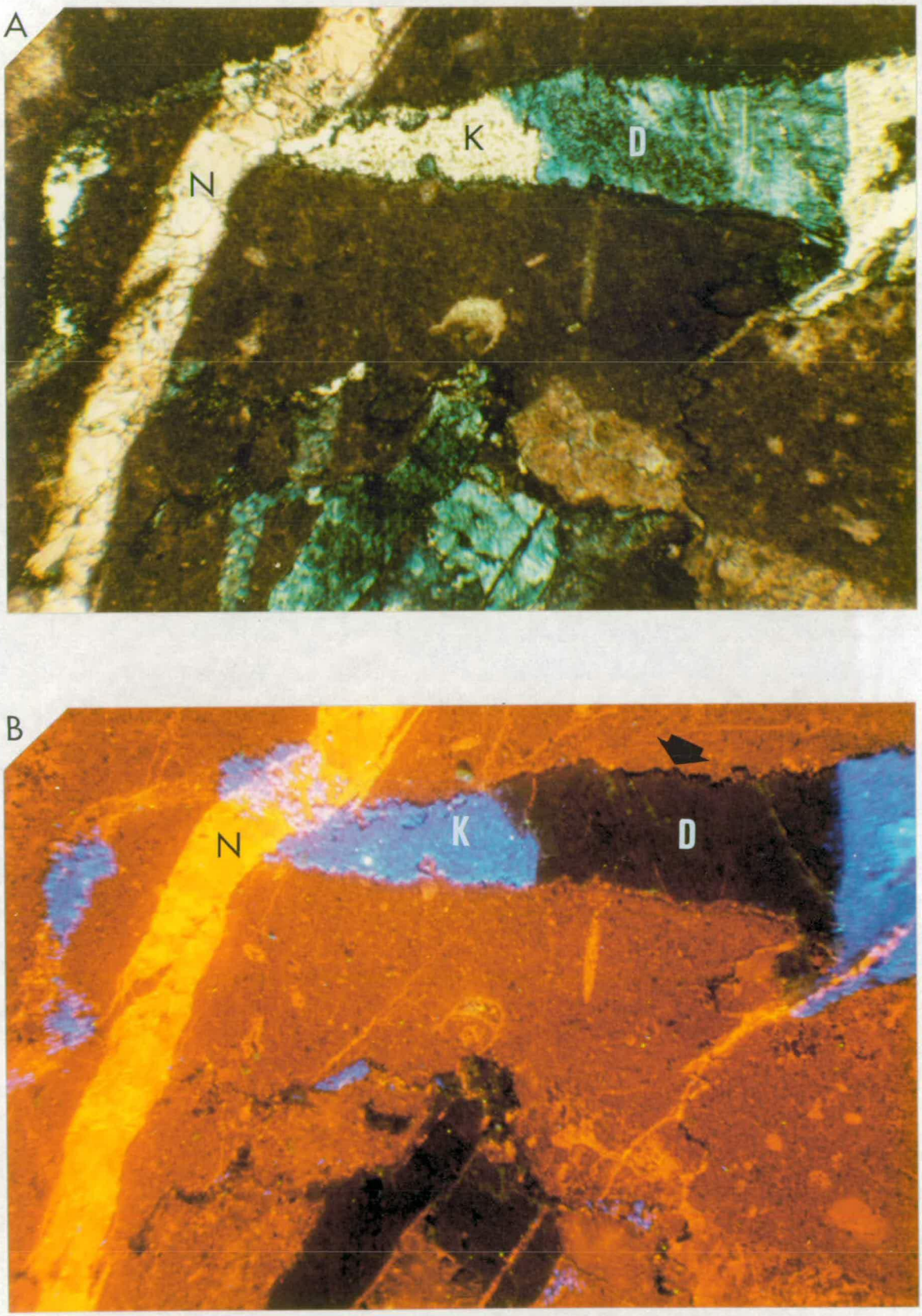

12.3.1 Geochemistry

12.3.1.1 Trace elements

Microprobe analysis of one sample of non-ferroan, bright luminescent calcite (Table 12.1) showed very low levels of Fe (below detection limits of the microprobe) and appreciable levels of Mn, thus explaining the bright luminescence.

12.3.1.2 Stable Isotopes (Fig. 12.3; Table 12.2)

Of the three samples analysed, those from Coplow buildup (C) contained ferroan calcite substages whereas the Ashnott sample (ASH 3) was without ferroan substages. In all cases non-ferroan calcite was the dominant material.

Table 12.1. Composition of Stage N (non-ferroan substages) Sample TNIB (Twiston Buildup) in wt% oxide

Oxide	Wt%	S.D.	C.V.	n=9
CaO	55.11	0.90	0.02	
MgO	0.10	0.03	0.24	
FeO	0.01	0.01	1.45	
MnO	0.07	0.02	0.28	

S.D. = Standard deviation @ 95% confidence level
C.V. = Coefficient of variation
n = Number of analyses

Table 12.2. Isotopic composition of Stage N, non-ferroan calcite

Sample	$\delta^{13}C°/_{oo}$	$\delta^{18}O°/_{oo}$
ASH 3	+2.05	-7.75
C	+2.38	-7.88
C	+2.14	-7.71
Mean	+2.19±0.14	-7.78±0.07

Analyses given in per mil vs PDB standard

Fig. 12.3 Isotopic composition of Stage N calcite

A. Comparison with earlier cements.

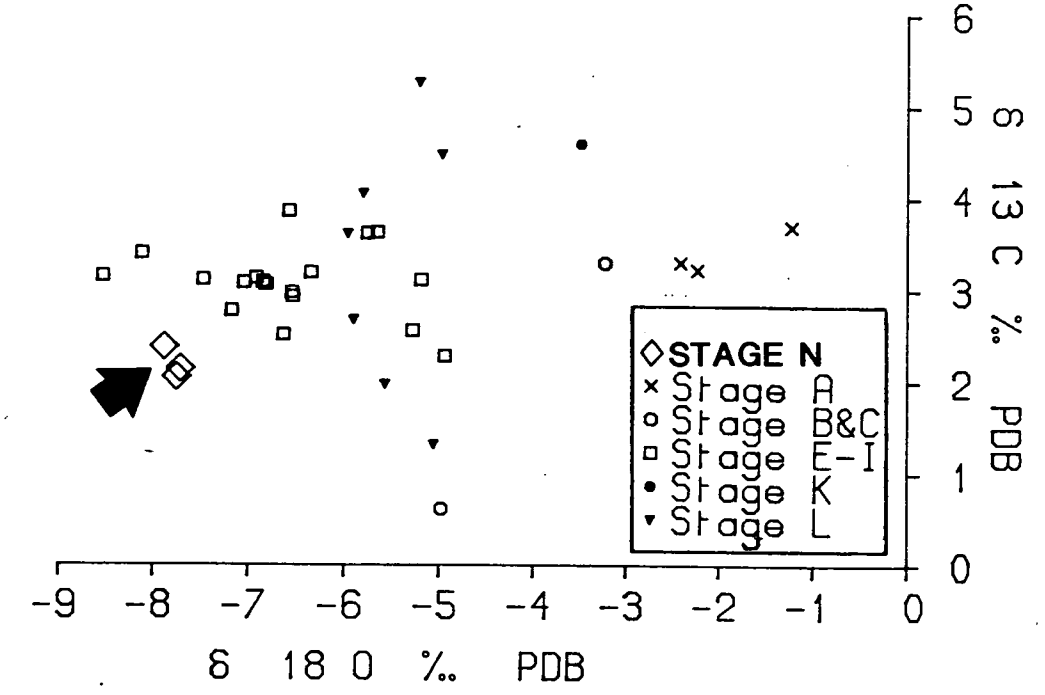

B. Comparison with other post-dolomite vein cements.

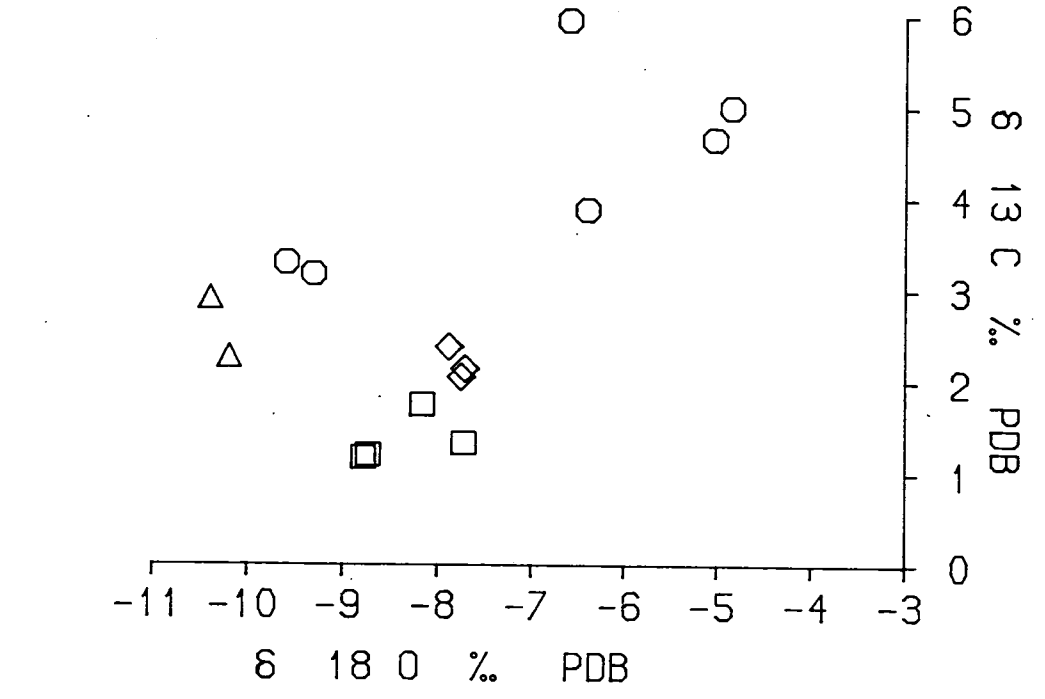

◇ STAGE N
□ Ferroan calcite veins, Calamine Mines
△ Ferroan calcite veins, Sugarloaf & Long Knots
○ Non-ferroan calcite veins

12.3.2 Distribution of Stage N

The distribution of Stage N cement was primarily controlled by the fractures which allowed the fluids into the rocks. Post-fracturing dissolution tended to selectively enlarge what little pore-space was left in the rocks, but also locally developed centimetre scale secondary vuggy porosity. The porosity increase resulting from this dissolution episode was less than 1% and most was subsequently occluded by the Stage N cements. A significant proportion of the residual present-day porosity in the banks was apparently developed by the pre-Stage N dissolution.

No examples of Stage N occurring in cavity filling sequences were observed outwith the bank facies.

12.3.3 Interpretation of Stage N

The processes effecting carbonate precipitation at such late stages in burial diagenesis are poorly understood.

The change to dominantly non-ferroan calcite with only moderate levels of manganese suggests that the pore fluids from which Stage N precipitated were less reducing than those of preceeding ferroan calcite stages, or were otherwise heavily depleted in iron as a result of other diagenetic processes.

The fluctuations which caused the iron-rich substages in Stage N suggest that complex interactions between fluids and diagenetic processes were taking place, probably controlled primarily by redox conditions. Isotopically, the Stage N cements are more depleted in $\delta^{18}O$ than any previous cements. It would appear that these cements represent the deepest burial phases in the sequence thus far (Fig.12.3A).

The general depletion in $\delta^{13}C$ values relative to Stage J-L dolomites and earlier cements suggests either that input from heavy carbon in maturing hydrocarbons had decreased, or the degree of buffering by dissolution of primary carbonate had increased.

12.4 OTHER POST-DOLOMITE CEMENTS

The fracture related, and thus localised distribution of post-dolomite cements inevitably poses a sampling problem, first at the hand-specimen level, and then more acutely at the thin section level. Where indications of Stage N cements occur, they are sporadic and often difficult to place in the cement stratigraphy for reasons discussed above. To further complicate matters, apparently petrographically indistinguishable cements were found to differ widely in composition when analysed for trace elements or stable isotope composition.

Three examples are considered below:

1. Late non-ferroan calcite in veinlets.

Several examples of non-ferroan calcite from late diagenetic veinlets were collected for isotopic analysis in the belief that they all represented Stage N cements. However, the isotopic signatures of these samples showed extreme variation compared with Stage N, which could not be explained by sample variation or analytical errors (Fig. 12.3B).

These anomalous results highlight the difficulties of determining cement stratigraphical relationships when no void-filling sequences occur. The wide range in isotopic compositions of these samples indicates the possibility that several late non-ferroan calcite veinlet phases developed. As a result of this discovery, only those samples taken from cavities where the cement stratigraphy could be proven were cited in Table 12.2 as being representative of Stage N, while isolated veinlet samples were discarded.

This example illustrates the dangers of indiscriminate sampling of superficially similar materials during cement stratigraphy studies. Although large numbers of isotopic analyses from such samples might facilitate distinction between petrographically similar materials, this would not be of use in mapping cement stratigraphies. This example, however, does show the advantage of using stable isotope analysis to discriminate between cements which are petrographically indistinguishable.

2. Late diagenetic veinlets from Cow Ark buildup.

The only borehole material available for study during the course of this research was the B.G.S. Cow Ark No.9 borehole (see Harrison 1982). Throughout this core, fractures containing slightly ferroan calcite (as indicated by purple stain) consistently cut through saddle dolomite veinlets.

Isotopic analysis of the slightly ferroan material reveals depletion in $\delta^{18}O$ and $\delta^{13}C$ relative to dolomite stages and the non-ferroan, post-dolomite Stage N (Table 12.3, Fig.12.3B). Continuation of the $\delta^{18}O$ depletion trend indicates that burial and fracturing continued after Stage N.

3. Late diagenetic ferroan calcite from Sugarloaf and Long Knots buildups

Swarms of very fine, strongly ferroan calcite veinlets occur in many of the buildups. Their maximum age, based on cross-cutting relationships, is Stage I. However, in Sugarloaf and Long Knots samples, a set of strongly ferroan veinlets cut all diagenetic fabrics including rhombic dolomite mosaic, and at Long Knots, veinlets showing similar cross-cutting relationships can be connected to late ferroan calcite spar in void-filling sequences.

Isotopic analyses of the Sugarloaf veinlets and spar from Long Knots show some of the most depleted $\delta^{18}O$ values encountered in this study (Table 12.4, Fig. 12.3B). It thus appears, from the burial trend, (Chapter 18), that these cements represent some of the deepest burial phases in the diagenetic history of the Waulsortian buildups of the Craven Basin.

The difference in $\delta^{18}O$ between these and Stage A CFC marine cements is approximately -8°/₀₀. In order to accurately relate $\delta^{18}O$ signatures to burial depth it is neccessary to know the isotopic composition of the pore fluids and the geothermal gradient for the time of each cement stage. This data is not available for the cements in this study and therefore it is impossible to relate these $\delta^{18}O$ signatures reliably to a precise burial depth. However, a calculation can be made which gives a useful indication:-

$$T°C = 16.9 - 4.38 (\delta_C - \delta_W) + 0.10 (\delta_C - \delta_W)^2$$

Where

δ_C: Isotopic composition of CO_2 produced from the carbonate at 25°C

δ_W: Isotopic composition of CO_2 in equilibrium with formation water.

The original equation for calculating palaeotemperature from oxygen isotope values (Epstein et al., 1953) was modified by Shackleton and Kennet (1975) and it is the latter version which is used here.

Substituting a value of $\delta_W = -1.2$ for the sea water composition prior to the establishment of polar ice caps (Shackleton & Kennett, 1975) would give a palaeotemperature of approximately 20°C for CFC marine calcites. It is impossible to estimate δ_W for the late burial cements as the fluid composition is unknown. However, in the absence of any indication of meteoric diagenesis in the cement sequence thus far, a rough estimate using the Stage A value for the starting composition and assuming that only marine fluids were involved, gives values of approximately 130-160°C for the deepest burial cements.

The present-day goethermal gradient in a borehole at Clitheroe (B.G.S. borehole index No. SD 66, drilled to 341m, GR:3686,4463) is 27.9°C/km (Burnley et al., 1984). Applying this to the approximate temperature difference between marine (effectively at the surface) and deepest burial calcites gives a maximum burial depth of somewhere in the order of 5km.

It must be stressed that this is purely a 'working estimate' and serves only as a guideline i.e. it appears that the deepest burial cements are likely to have formed at depths of kilometres rather than hundreds of metres.

Table 12.3. Isotopic analyses of post-dolomite vein-filling cements from Cow Ark buildup

Sample	$\delta^{13}C°/_{oo}$	$\delta^{18}O°/_{oo}$
1	+1.20	-8.73
2	+1.75	-8.16
3	+1.17	-8.78
4	+1.33	-7.72
Mean	+1.36 $\pm$0.23	-8.34 $\pm$0.45

Table 12.4. Isotopic composition of deepest burial ferroan calcites from Sugarloaf and Long Knots buildups.

Sample	$\delta^{13}C°/_{oo}$	$\delta^{18}O°/_{oo}$
Su17	+2.19	-10.39
LK4	+2.27	-10.19
Mean	+2.59	-10.29

CONCLUSIONS

1. Hydrocarbon migration immediately post-dated dolomite cements, and entered the bank facies primarily along stylolites.

2. The restricted pore space available after dolomite cement Stages J-L limited the development of subsequent cements to fracture-fills and small volumes of remnant pore space. This causes increasing difficulty in accurately defining the temporal relationships of the later diagenetic cements.

3. Two basin-wide diagenetic episodes can be identified following Stage L Dolomite cementation and replacement:
   Stage M: Authigenic kaolinite and the kaolinitisation of dolomite.
   Stage N: Late non-ferroan calcite cement.

4. The kaolinite was identified from SEM, XRD and its characteristic royal blue luminescence. It sometimes occurs in veinlets but is predominantly associated with the kaolinitisation of rhombic dolomite mosaics. All other post-dolomite cement stages are younger than kaolinite.

5. Following dolomitisation and kaolinitisation, a basin-wide dissolution episode associated with fracturing was followed by the precipitation of Stage N non-ferroan, brightly luminescent calcite cement in this secondary porosity and any other remnant pore space. Isotopic composition of Stage N cement indicates continued burial of the Waulsortian buildups. Fluctuations in pore-fluid composition during Stage N precipitation are indicated by the presence of ferroan calcite substages in some instances.

6. Apart from the Stage N cements, the subsequent sequence of diagenetic processes is uncertain. Two examples of late ferroan calcite vein cements indicate that burial probably continued after Stage N to a maximum depletion of $\delta^{18}O$ which indicates ultimate burial depths of several kilometres.

7. Once the pore space of the Waulsortian rocks was completely occluded, evidence of further cementation episodes during their deep burial diagenesis comes mainly from cements deposited in fractures. Several of these cements cannot be distinguished using petrographic characters, including CL, but they do have distinctive stable isotope signatures. This illustrates the value of combining petrographic, geochemical and stable isotope analyses in a study of diagenetic stratigraphy.

CHAPTER 13
MINERALISATION

Introduction

Detailed study of the mineralisation in the Craven Basin was not a primary concern of this research. However, a limited number of samples were collected in an attempt to confine the mineralisation within the framework of the carbonate cement stratigraphy.

Two main episodes of mineralisation were identified. The first consists of an early diagenetic iron sulphide mineralisation which occurred during the shallow burial phase, prior to dolomite development. The majority of Waulsortian buildups were affected by silicification and quartz cements which were locally associated with a late diagenetic mineralisation episode. This restricted, intensified hydrothermal mineralisation led to the emplacement of fluorite, barite, sphalerite and galena assemblages in addition to silicification.

In addition to the two main episodes of mineralisation, other authigenic phases developed in the Waulsortian and associated facies whose relative timing is uncertain.

13.1 EARLY DIAGENETIC MINERALISATION

The first mineralisation episode involved the development of crustiform iron sulphides at cavity margins in the bank facies, particularly those voids containing fissure-fed internal sediments. The crusts formed directly on cavity walls or on Stage B-D non-ferroan scalenohedral calcite cements. Cubic crystals of sulphides also developed within geopetal sediments. (Fig. 13.1A).

The centripetal sulphide crusts average 100-200 μm in thickness, and the individual cubic crystals which developed within internal sediments may also reach hundreds of microns across.

With reflected light microscopy, the crusts were found to consist primarily of anisotropic marcasite, which shows greenish

grey-yellow polarisation colours. Commonly contained within the crusts are framboidal aggregates of pyrite. The marcasite evidently post-dated this pyrite and often developed radiating bladed crystals nucleated on the framboids (Fig. 13.1B).

The crustiform sulphides are uncommon in the Craven Waulsortian. Their formation, as centripetal layers which are often covered by geopetal sediments, is evidence that they were largely cements, although some show evidence of truncation of former fabrics and may be partially replacive (Fig. 13.1C).

13.1.1 Petrography

Some of the best examples of crustiform sulphides which demonstrate critical evidence of their place in the diagenetic history occur in the bank facies of Bellmanpark quarry.

The crustiform sulphides are found in large dissolution and erosion cavities related to the influx of fissure-fed internal sediments. They commonly coat the scalenohedral Stage B-D cements but never any later cements.

In one particular example (Fig. 13.1D&E), a sulphide crust developed within a sequence of internal sediments. This crust can be traced around the walls of the cavity above the level of sediment, suggesting that it developed during a pause in sediment influx. The crust was then partially reworked by a subsequent pulse of sedimentation, emphasising the early diagenetic origin of the sulphides. During later diagenesis, the sulphide crust in Fig. 13.1 D&E acted as a barrier to dolomitising fluids so that the post-sulphide internal sediments were dolomitised but the pre-sulphide ones were not.

Fig. 13.1A shows that sulphide crusts were brecciated and spalled-away from cavity margins prior to the precipitation of Stage E and F aggregate cements, thus pre-dating these stages.

13.1.2 Sulphur Isotopes

Sulphur has two naturally occurring isotopes, ^{32}S and ^{34}S. The ratio of these two isotopes is defined as $\delta^{34}S$ and is measured relative to the Canyon Diablo Troilite (CDT) standard.

Studies of sulphur isotopes in sedimentary deposits are generally concerned in determining $\Delta\delta^{34}S$, the difference between the $\delta^{34}S$ of the contemporaneous seawater and the $\delta^{34}S$ of the sulphide phase. The $\delta^{34}S$ of seawater SO_4^{2-} is taken as +20°/₀₀ (see Kaplan 1983 p.2-53).

In early sediment diagenesis the most common sulphide phase is pyrite. The main control on its sulphur isotope composition is the degree of bacterial sulphate reduction in the sediments.

In general, as sulphate reduction increases during burial, the precipitating sulphide phase becomes isotopically heavier so that the $\Delta\delta^{34}S$ decreases, the limiting factors being;

1) The $\delta^{34}S$ of contemporaneous seawater sulphate

2) The amount of pyrite present (less pyrite means less $\delta^{32}S$ enrichment).

3) Whether there is an open or closed system with respect to ocean water. (See Kaplan 1983 p.2-56).

Three samples of early sulphide were analysed, two of crustiform pyrite/marcasite associations and one sample of cubic pyrite from a pre-CFC geopetal mud (Table 13.1).

Table 13.1. Sulphur isotopic composition of early sulphides

Sample	Description/Mineralogy	$\delta^{34}S$‰CDT
LH2	cubic pyrite pre-CFC geopetal	+22.9
BP	pyrite/marcasite	+20.1
BP15	pyrite/marcasite	+18.3

Analyses given in per mil (°/₀₀) against Canyon Diablo Troilite standard (CDT)

The predicted value for Lower Carboniferous seawater sulphate is approximately 20°/₀₀ (Barnes 1979). If we are to consider, from their association with early diagenetic cements, that the sulphur

Figure 13.1 Early iron sulphide mineralisation.

A. PPL photomicrograph of thin sectionshowing pyrite/marcasite crusts (1) developed after scalenohedral calcite in a large sediment-and spar- filled cavity. Aggregates of cubic pyrite (2) also developed within the homogeneous internal sediment. The pyrite crusts were spalled-off from cavity margins and brecciated (3 and 4) prior to Stage E and F spar (s). Way-up is indicated by geopetal sediment in a bioclast (dashed line). Bellmanpark bank facies near neptunian dykes.

B. XPL, reflected light photomicrograph showing radially developed anisotropic marcasite nucleated on pyrite framboids (f) in crustiform iron sulphide. Bellmanpark bank facies.

C. SEM photograph of the same crustiform iron sulphide (p). The crust truncates a fenestellid bryozoan fragment (f) in the M1 sediment, and later spar (s).

D. Field photograph of loose material in Bellmanpark Quarry floor, showing a large, early diagenetic dissolution cavity developed in the M1 primary sediment, in association with neptunian dykes. The cavity is partly filled with layered internal sediment (M2) and later calcite spar. A pyrite/marcasite crust (arrowed) developed around the cavity margin during a pause in sediment influx. The crust acted as a permeability barrier to later diagenetic fluids which dolomitised later sediment layers (D) but did not affect those prior to the sulphide. Coin for scale is one shilling (5 pence, 2.3 cm).

E. Negative print from a thin section of the sample shown in the previous photograph. The M1 sediment surface is irregular due to dissolution prior to spar development.(Spars are black in negative). The pyrite/marcasite crust (white in negative) followed scalenohedral calcite (1), and can be traced around the cavity margins and within the geopetal sediments in the cavity floor (2). The crustiform sulphide was partially re-worked (3) into later sediment which was subsequently dolomitised (D).

Fig. 13.1

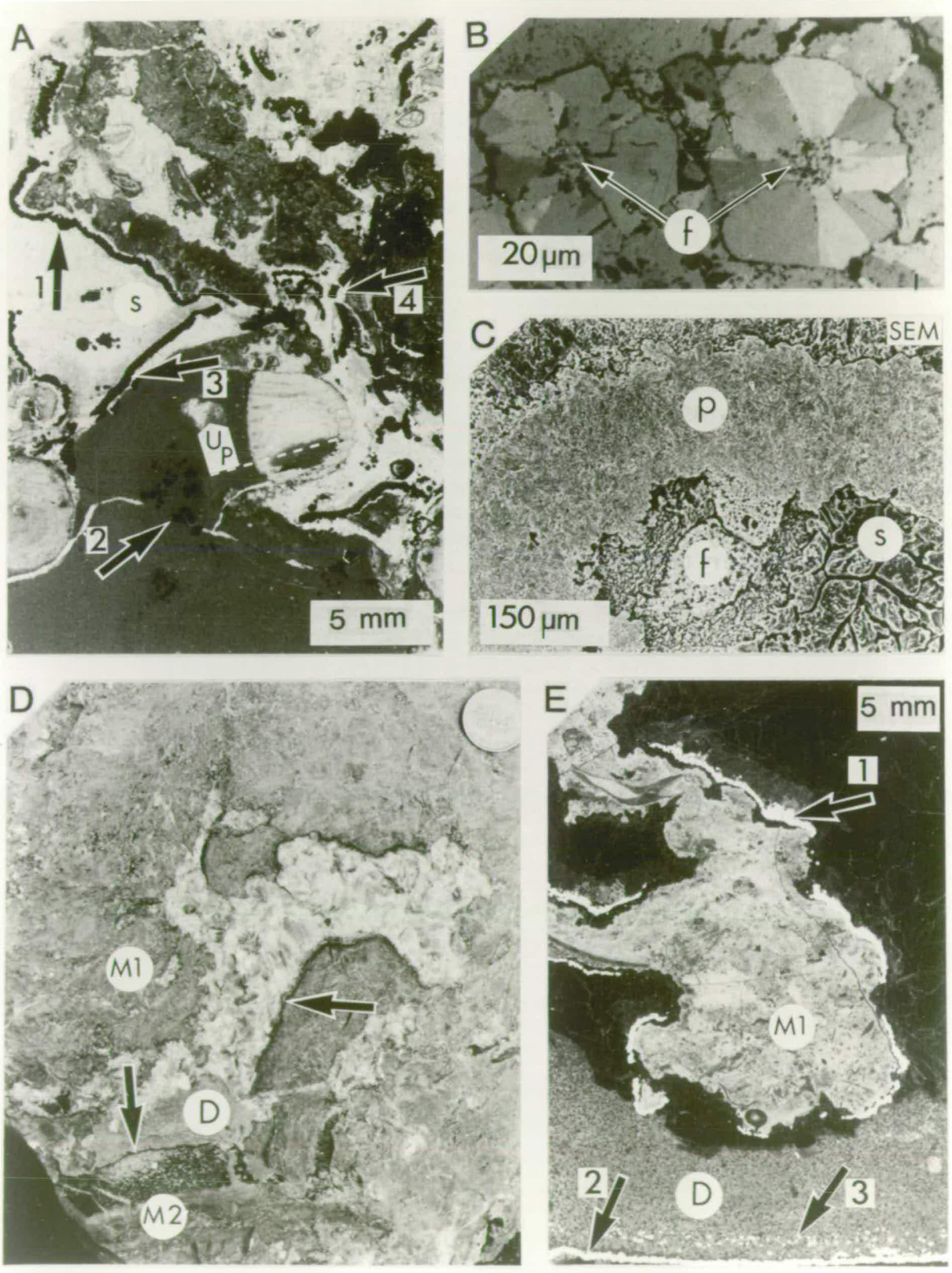

source of the crustiform sulphides was derived from the bacteriogenic fractionation of seawater sulphate, then their $\delta^{34}S$ values suggest that the bacteria were operating in a system which was closed with respect to that source. Furthermore, the heaviest values (Table 13.1) are very close to the predicted value for Lower Carboniferous seawater sulphate, implying that there was almost total reduction of the sulphate reservoir. This isotopic evidence thus confirms the petrological evidence that the sulphide mineralisation occurred after Stage D, but prior to Stage E, during a period when the pore fluids were cut off from their seawater source so that reduction of the sulphate reservoir went towards completion.

Summary

Crustiform iron sulphides occur directly on void walls or on Stage B-D cements but never later, and therefore could have formed at any time during shallow burial. They formed within the sulphate reduction zone but are not neccessarily all synchronous.

13.2 LATE DIAGENETIC HYDROTHERMAL MINERALISATION

13.2.1 Silica

Silica is the most abundant non-carbonate phase in the Waulsortian buildups. Over 90% of the silica is replacive, the remainder being cement. Four different styles of silicification can be identified in the Waulsortian and peri-Waulsortian facies.

a). Replacive microcrystalline silica (Fig. 13.2)

This is the commonest silica phase. It occurs largely as a replacement of earlier carbonate cements and allochems. In thin section, the microcrystalline silica ranges from very turbid to almost clear. Inclusions are very common, mainly consisting of relics of precursor minerals. The colour of the replacive silica varies from almost colourless through straw yellow to light brown. Under crossed polars, polycrystalline and fibrous mosaics are common,

and while the gross morphology of precursor materials is commonly preserved, fine-scale structures are usually destroyed. In many cases, subhedral quartz crystal terminations are developed within the siliceous material. These are most clearly seen in SEM samples which have been etched to remove the surrounding carbonate (Fig. 13.2A). It is also possible in such preparations to identify etched pits which represent the former position of inclusions of precursor carbonate.

Very commonly, microcrystalline silica developed as a selective replacement of CFC marine cements in the bank facies, and formed irregular patches or rinds which mimic the gross morphology of the earlier cement, but which rarely effected total replacement. In weathered outcrops, for example those at Sugarloaf and Dunnow quarries, the replacive silica stands proud on the rock face, depicting the original CFC cement fabric. The reasons for this selective silicification are probably the same as the controls on the recrystallisation of CFC by other calcites, i.e., the presence of relict fibrous terxtures in the CFC which are easily exploited by diagenetic fluids.

Microcrystalline silica may also occur as a replacement of post-CFC blocky calcite cements. Usually, this type of silicification occurs as thin stringers along intercrystalline boundaries within the calcite cements (Fig. 13.2B), although patches of more extensive replacement may occur.

In addition to the silicification of carbonate cements, bioclasts were also replaced by microcrystalline silica. The most commonly affected bioclasts are crinoid ossicles, where silicification is never complete and usually develops as irregular rims close to the outer edge and inner canals of the crinoid material (Fig. 13.3A). In other bioclasts however, silicification was often complete. Another typical example of bioclast replacement (Fig. 13.3B) shows a relic of a bryozoan bioclast contained within a mass of microcrystalline silica which also affected some neighbouring CFC cements, while a neighbouring bryozoan bioclast was unaffected by the silicification. This irregular, non-pervasive development of the silica, confirms its replacive origin, together with some textural and mineralogical selectivity.

b). Authigenic quartz crystals (Fig. 13.2c)

Subhedral to euhedral authigenic quartz crystals occur as a replacement of some fine grained carbonate sediments in a number of the Waulsortian buildups, and are, in some cases, associated with veinlets (see below). Crystals range from a few tens to hundreds of microns in length and are characterised by the occurrence of fine grained carbonate inclusions in their cores. Apart from the inclusion rich cores, the crystals are generally quite limpid.

Silica is detected in M1 sediment by microprobe analysis (and in insoluble residues). These sediments tend to be more optically dense than secondary muds, and are slightly more resistant to the acid etch which is used in the staining technique. SEM imagery reveals microscopic quartz euhedra and indicates an authigenic phase. In the absence of any evidence of early silicification in the bank facies it is probable that this silica is related to late selective silicification of the primary M1 micrite. King (1984) reported similar properties in the Irish Waulsortian, and came to a similar conclusion.

c). Coarsely crystalline quartz cement (Fig. 13.2 F&G)

Blocky quartz cement occurs in many bank and off-bank deposits, but is volumetrically insignificant. It occurs either as a mosaic of interlocking quartz crystals with compromise boundaries and enfacial junctions, or as large euhedral crystals (<0.5 cm), partially filling cavity space or veinlets.

d). Fibrous/spherulitic chalcedony cement (Fig. 13.2F)

This is a relatively uncommon form of silica in the Craven buildups. Most often, it consists of centripetal layers within a cavity which are in the order of a few tens to hundreds of microns in thickness. The layers commonly exhibit a mammilated texture and usually contain finely-spaced centripetal and substrate-normal inclusions patterns which give them a fibrous appearance. Sweeping extinction patterns indicative of fibrous habit are also observed.

The chalcedony ranges from colourless to dark brown depending on inclusion density. Occasionally, isolated spherulitic fibrous forms developed. These spherulites are usually hemispherical and may exhibit extinction crosses under crossed polars.

The fabrics developed by the chalcedonic silica are indicative of an origin by cementation rather than replacement. The lack of any evidence of relict textures within this material confirms its primary origin.

13.2.1.1 Relationships between silica phases (Fig.13.2)

In most cases it is impossible to identify any direct relationships between the different silica phases. Of the four main types of silica developed in the rocks of this study, two originated as void-filling cements while the others had a replacive origin. In the rare example of Fig. 13.2F, quartz cement occurs after chalcedonic silica in the same cavity. These two types are, therefore, closely related, and may have originated from the same fluid.

It is also possible to show the relationship between quartz cement and replacive silica (Fig. 13.2G). In this example, coarsely crystalline quartz cement was precipitated after non-ferroan scalenohedral calcite of Stage B-D while earlier CFC cements were partially silicified by an irregular microcrystalline silica mosaic. Close examination of this example reveals thin stringers of silica occurring along intercrystalline boundaries in the prismatic calcite cements which connect the pore-filling quartz cement with the replacive silica. This suggests that both forms of silica precipitated from a common fluid. The silica phases in this example were then cut by a fracture containing deep burial ferroan calcite.

A further example (Fig. 13.2F) shows a calcite-filled veinlet cutting CFC cements in a sample of Waulsortian bank facies from Long Knots. In one area of the veinlet margin, euhedral quartz crystals occur before the calcite cements, showing that the quartz grew into the fracture porosity prior to calcite cementation. Beyond the veinlet margins, silicification then extended into the surrounding carbonate, where a microcrystalline silica replacement of CFC cement developed. This not only suggests that the quartz cements and

microcrystalline silica precipitated from a common fluid, but also indicates that the silica-bearing fluids entered the system after a phase of fracturing. A final example (Fig. 13.3B) shows a similar situation where euhedral authigenic quartz crystals developed as a replacement of fine-grained carbonate sediment at a veinlet margin. In this case, the silica pre-dates sphalerite mineralisation which occurs within the veinlet. The veinlet was finally cemented by deep burial ferroan calcite.

Similar styles of silicification, where the degree of silicification decreases away from the veinlet margins, have been identified in mineralised Dinantian limestones from Derbyshire (Kanaris-Sotiriou et al. 1986).

We can therefore conclude, that a range of late diagenetic silica fabrics resulted from different processes (i.e. cementation and replacement) while sharing a common source fluid.

13.2.2 Sphalerite-Galena-Fluorite-Barite mineralisation

Locallised lead-zinc mineralisation, associated with barite and fluorite occurs throughout the Craven Basin.

While never of any great economic significance, base metal mining was carried out for many hundreds of years in the Craven basin. The industry declined severely by the turn of the century, but recently there has been a resurgence of interest and exploration in the area.

Examples of mineralised Waulsortian facies occur at Withgill, Ashnott, Spire Farm - Cow Ark, Hammerton Hall and Fogger (Fig. 1.1). Mineralisation also occurred in off-bank sediments associated with the Ings Beck buildup and in the Chadian-Arundian limestones at Raygill Quarry near Lothersdale (GR SD:940,454). There are several examples of mineralised faults in post-Dinantian sediments (e.g. at the Nick of Pendle in the Pendle Grit).

In most of the cases listed above, significant mineralisation is associated with veins, and these are probably related to faulting. Other buildups such as Bellmanpark, Hall Hill, Porters Wood and Sugarloaf contain only traces of a late mineralisation which are also usually associated with veins or fault zones. Calamine ($ZnCO_3$), a

weathering product after sphalerite, was also worked at the Old Calamine Mines at Dinkling Green (SD:642,447). The calamine was associated with a fault zone which cuts the Long Knots area. The surface of the fault plane at the Calamine Mine is in Waulsortian facies and is associated with dolomitisation.

Although a detailed paragenesis of these base metal deposits was not considered during this study, the limited suite of mineralised samples exhibited some interesting textures which may give some indication of the timing and nature of their genesis.

A suite of samples from Withgill buildup contain the most extensively mineralised material collected during the course of this study. The dominant mineral is fluorite which developed as coarsely crystalline material in veins and cavities, and also as a replacement of the host sediment and bioclasts. In many cases, it appears as though fluorite precipitated into mouldic voids after the dissolution of allochems, whereas in others, direct replacement is indicated by the presence of relict textures. Under CL, the fluorite gives a light blue luminescence, and often reveals faint zonation. Prolonged exposure to the electron beam results in permanent "electron staining" of the fluorite (cf. Dickson 1980) which, in transmitted light, shows strong zonation in different shades of purple. The textures exhibited by the stained fluorite are identical to those observed in carbonate cements. Stages, substages and growth zones can be identified along with irregular corrosion surfaces at stage boundaries, compositional sector zonation and crystal aggregates (Fig. 13.3B).

The fluorite in the Withgill samples post-dates replacive euhedral quartz but pre-dates barite and sphalerite.

The barite only occurs as a void-filling phase and is developed as mosaics of either tabular or fan-shaped crystals. Corrosion of fluorite prior to barite emplacement is common (Fig. 13.3C). The sphalerite is largely oxidised, but occasional remnants of honey-coloured crystals do occur. Other honey-coloured sphalerite occurs as a replacement along fluorite crystal boundaries, often being associated with small-scale corrosion features.

Other minor examples of sphalerite mineralisation were encountered in the general petrographic work. At Porters Wood, euhedral

authigenic quartz crystals (which developed as a replacement of fine grained carbonate sediment) are found as inclusions within poikilotopic sphalerite crystals. The sphalerite crystals are subhedral to anhedral and may be up to several hundreds of microns in size. The poikilotopic texture is clearly revealed using reflected light microscopy, and indicates that sphalerite formed after silica. A similar occurence is shown in Fig. 13.3A, from the Hall Hill buildup, where sphalerite occurs within a calcite-filled veinlet after the silicification of the fracture margins and adjacent sediment by authigenic quartz.

All sphalerites encountered in the Craven material tend to be honey-coloured, indicating low levels of iron. This was confirmed by electron dispersive system (EDS) analysis on the Microscan-5 microprobe. Some sphalerite crystals contain occasional darker brown zones which probably represent higher iron content (Fig. 13.3 A&B).

Although galena is known to have occurred in association with the late mineralisation in many deposits across the Craven Basin, it was found in only two of my samples and these were only isolated patches. However, one of these samples, from the B.G.S. Cow Ark No 9 borehole was useful in constraining the timing of mineralisation (see below).

13.2.3 Timing of the mineralisation

Despite the limited suite of samples, petrographic observations are consistent in suggesting that the silica, sphalerite, fluorite, barite and galena were all related to a common phase of hydrothermal mineralisation of which the most widely distributed component was an early silica phase. Most of these late minerals occur in veins or veinlets which are related to the major NE-SW tending faults which dissect the Craven Basin. At the eastern end of Bellmanpark quarry for example, fluorite occurs in slickenside material on a NNE-trending fault plane. This fluorite post-dates some ferroan calcite cements, but was fractured during subsequent movements on the fault plane: these fractures in turn were cemented by later ferroan and non-ferroan calcite phases, including Stage N.

At Hall Hill quarry, a parallel set of mineralised veins developed, which trend towards 030°N, i.e. in accordance with the major Hercynian faults in the Craven Basin. The veins cut cavities in the bank facies which were filled with blocky calcite and dolomite spars, whereas in the sub-bank facies which occurs in the quarry, silicified veinlets cut stylolites which themselves have been dolomitised. Therefore, the mineralisation occurred some time after the Stage J-L dolomite episode in the cement sequence. This relationship is also reflected in samples from Sugarloaf Quarry, where replacive silica occasionally transects and partially replaces rhombic dolomite mosaics. Galena was found in the Cow Ark No 9 borehole, where it followed coarsely crystalline saddle dolomite.

Having established the earliest time in the sequence at which the hydrothermal episode occurred, it now remains to place the episode within the somewhat disconnected late, deep burial history.

At Withgill, fluorite is post-dated by veinlets containing late ferroan calcite cements, and in one critical example, a sequence of ferroan calcites followed by zoned Stage N cements precipitated after fluorite in a cavity. In a sample from Sugarloaf Quarry, the same sequence of calcite cements was found in a veinlet which cut saddle and mosaic dolomite of Stages J-L. Within the post-dolomite cements were rare, small crystals of fluorite and quartz.

At Hall Hill quarry, mineralised veinlets are occluded by the same post-dolomite ferroan calcites (Fig. 13.3 A&B). From this combined evidence it is possible to constrain the late mineralisation episode to that part of the burial history after the development of dolomite Stages J-L, but before Stage N cement.

As the majority of mineralised examples are associated with veins which roughly parallel the major fault trends in the Craven Basin, the mineralisation was probably a product of hydrothermal fluids which migrated along the fractures during a period of high heat flow after the Permo-Trias (cf. Earp et al. 1961).

The evidence from Hall Hill indicates that a set of fractures, sub-parallel to the regional trend, developed immediately prior to the mineralisation episode. However, it is also apparent from the example of slickenside material in Bellmanpark quarry that movement on the major faults occurred at various stages both before and after

Figure 13.2 Authigenic silica.

A. SEM photograph of replacive microcrystalline silica standing proud after acid etch of a polished surface had removed surrounding carbonate. The originally flat sample surface is preserved in the silica (1) and shows the kind of irregular 2-D surface which is seen in many thin sections (cf. 13.2H). In 3-D, however, the silica is seen as a mosaic of subhedral crystals (2) containing etched pits representing the former position of carbonate which was included in the silica during replacement. Knoll Wood buildup.

B. PPL Photomicrograph showing extensive selective silicification of CFC cement coating fenestellid bryozoans (f). The turbid replacive silica (r) adopts the general morphology of the CFC, but forms in irregular patches and does not preserve fine-scale CFC textures. Thin section, bank facies, Sugarloaf buildup.

C. Negative print from a stained thin section of crinoidal flank facies. Silicification has formed irregular rims (black in negative) close to the outer surface and inner canals of some crinoid ossicles (1), while others were unaffected (2). Flank facies, Hammerton hall buildup.

D. PPL Photomicrograph showing replacive microcrystalline silica containing relict inclusions of a bryozoan (r), while a neighbouring bryozoan bioclast (b) was unaffected. Silicification also affected some of the CFC cements which coat the fossil grains. Thin section, bank facies, Sugarloaf buildup.

E. Subhedral to euhedral authigenic quartz crystals containing fine grained carbonate inclusions in their cores (arrowed). PPL photomicrograph of a thin section from Hall Hill buildup.

F PPL photomicrograph in PPL showing inclusion-rich banded chalcedonic silica cement (ch) and limpid, coarsely crystalline quartz cement (q) in a crinoidal flank deposit from Hammerton Hall. The fibrous chalcedonic cement layer is mammilated, with strong substrate-parallel inclusion banding.

G. Photomicrograph showing coarsely crystalline quartz cement (q) after scalenohedral calcite cement (c) of Stages B-D. Silicification of CFC cement formed an irregular, discontinuous rim of microcrystalline silica around the cavity (r), which is linked to the quartz cement by thin stringers along scalenohedral calcite crystal boundaries (large arrow) indicating that both cement and replacive silica share a common fluid origin. Later ferroan calcite veinlets (v) cut the silica. Stained acetate peel, Spire Farm buildup.

H. PPL photomicrograph showing how the development of a veinlet allowed silicifying fluids into a cavity-fill sequence, resulting in silicification of CFC cement at the veinlet walls (r) while euhedral quartz cement (q) developed in the open fracture. The veinlet was subsequently filled by ferroan calcite cement (fc). Stained thin section, Long Knots buildup.

Fig. 13.2

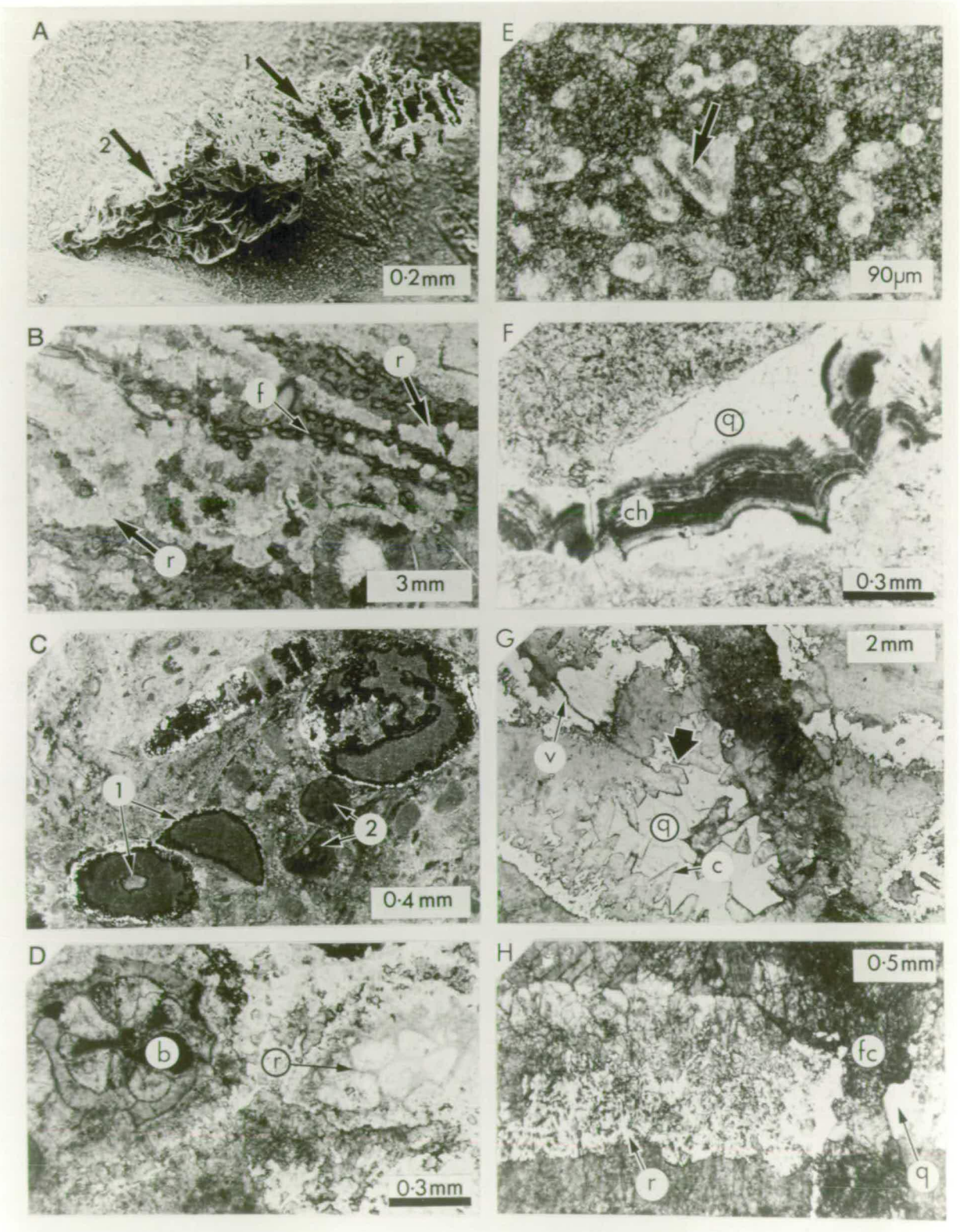
A
1
2
0·2mm
E
90μm
B
r
f
r
3mm
F
q
ch
0·3mm
C
1
2
0·4mm
G
2mm
v
q
c
D
b
r
0·3mm
H
0·5mm
fc
r
q

Figure 13.3 Late diagenetic mineralisation.

A. Photomicrograph of a stained thin section showing euhedral authigenic quartz (Q) developed at a veinlet margin prior to honey-brown sphalerite (Sp) and blue-stained ferroan calcite. Field of view = 3.8mm. Hall Hill bank facies.

B. Lower magnification photomicrograph of same thin section as 'A'. The veinlet bifurcates. Authigenic quartz (Q) forms a layer prior to coarsely crystalline sphalerite (Sp) and blue-stained ferroan calcite. Field of view = 6.5mm.

C. Photomicrograph in PPL of fluorite (F) which has been electron-stained during CL investigation, giving a purple colouration to previously colourless crystals, and showing fine-scale zonation and corrosion surfaces which were otherwise invisible. Corrosion of the fluorite also occurred prior to barite (B). Golden-brown areas are araldite which has been burnt by the CL electron beam. Withgill buildup. Field of view = 4.3mm.

Fig. 13.3

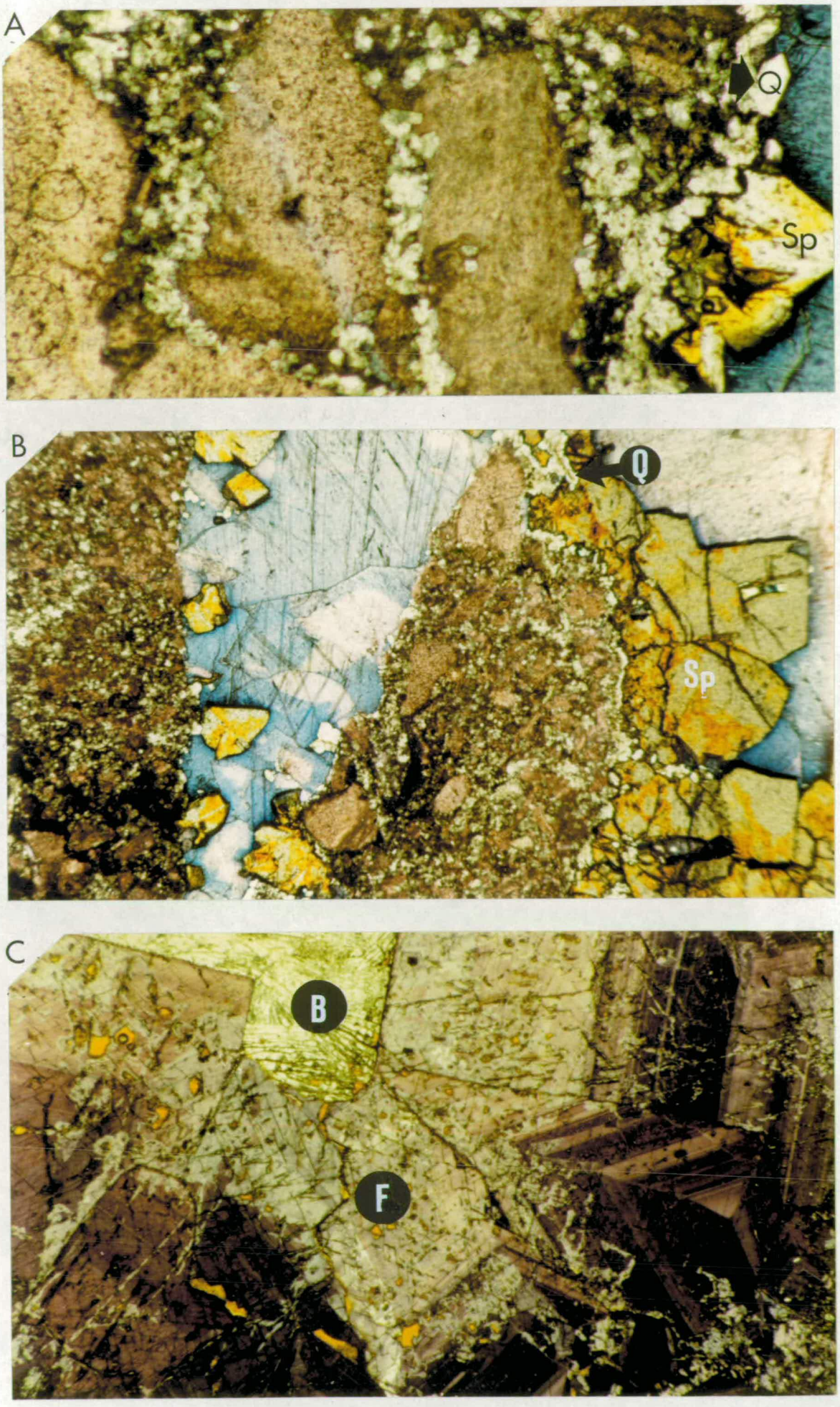

the mineralisation, i.e. many of the regional fractures developed considerably earlier than the mineralisation, and continued to be active, providing pathways for the hydrothermal fluids.

13.3 OTHER AUTHIGENIC MINERALS

A variety of other authigenic phases were observed which could not be directly related to the mineralisation episodes described above.

13.3.1 Albite (Fig. 13.4)

Isolated euhedral to subhedral crystals of albite were identified in fine grained carbonate muds of the Waulsortian bank facies from petrography and microprobe analysis (Table 13.2). Crystals range up to a maximum of 120 μm in length and 50 μm in width. Tabular and basal sections were observed. Many crystals exhibit multiple twinning in crossed polarised light and may also contain irregular zones of inclusions composed of carbonate (Fig. 13.4), while in CL the crystals are completely non-luminescent, characteristic of authigenic feldspars as reported by Kastner (1971). Other examples were identified in SEM samples.

The generally good crystal form and presence of inclusions of the surrounding carbonate sediment within these crystals indicates an authigenic rather than detrital origin.

Turner et al. (1982) reported authigenic albites in the Pendleside Formation (upper Dinantian) of the Craven Basin. They showed evidence that the albite crystals formed around detrital volcanogenic K-feldspar. This is not the case with the authigenic albites in this study. The only sample which showed compositional variation had a core of calcite.

13.3.2 Silica and Clays

In the shaley interbank facies, authigenic quartz crystals of tens to hundreds of microns in length are also common. SEM shows that these quartz crystals are often associated with authigenic clay

Table 13.2 Authigenic Albite analyses from Coplow Quarry

Sample Wt%	C24	C25(E:3)	C25(E:4)	C25(E:9)	Mean
K_2O	0.05	0.06	0.09	0.05	0.06
Na_2O	11.39	8.63	11.70	11.55	10.82
CaO	1.09	0.36	0.66	0.38	0.62
MgO	0.03	0.01	0.03	0.03	0.03
Al_2O_3	18.76	19.79	19.37	18.80	19.18
FeO	0.02	0.03	0.02	0.05	0.03
SiO_2	68.08	68.08	68.52	69.06	68.65
BaO	0.00	0.00	0.00	0.05	0.01
Total	99.42	97.83	100.39	99.92	99.42

Figure 13.4 Other non-carbonate authigenic phases.

A. Photomicrograph under crossed polars showing a euhedral authigenic albite crystal with a zone of carbonate inclusions (arrowed). Bank facies, Coplow buildup.

B. SEM photograph showing a clay mineral (c), probably smectite, after corrosion of authigenic quartz (q). Interbank facies, Ings Beck.

C. SEM photograph showing an authigenic quartz crystal (q) partially coated with small platy kaolinite crystals (k). Interbank facies, Ings Beck.

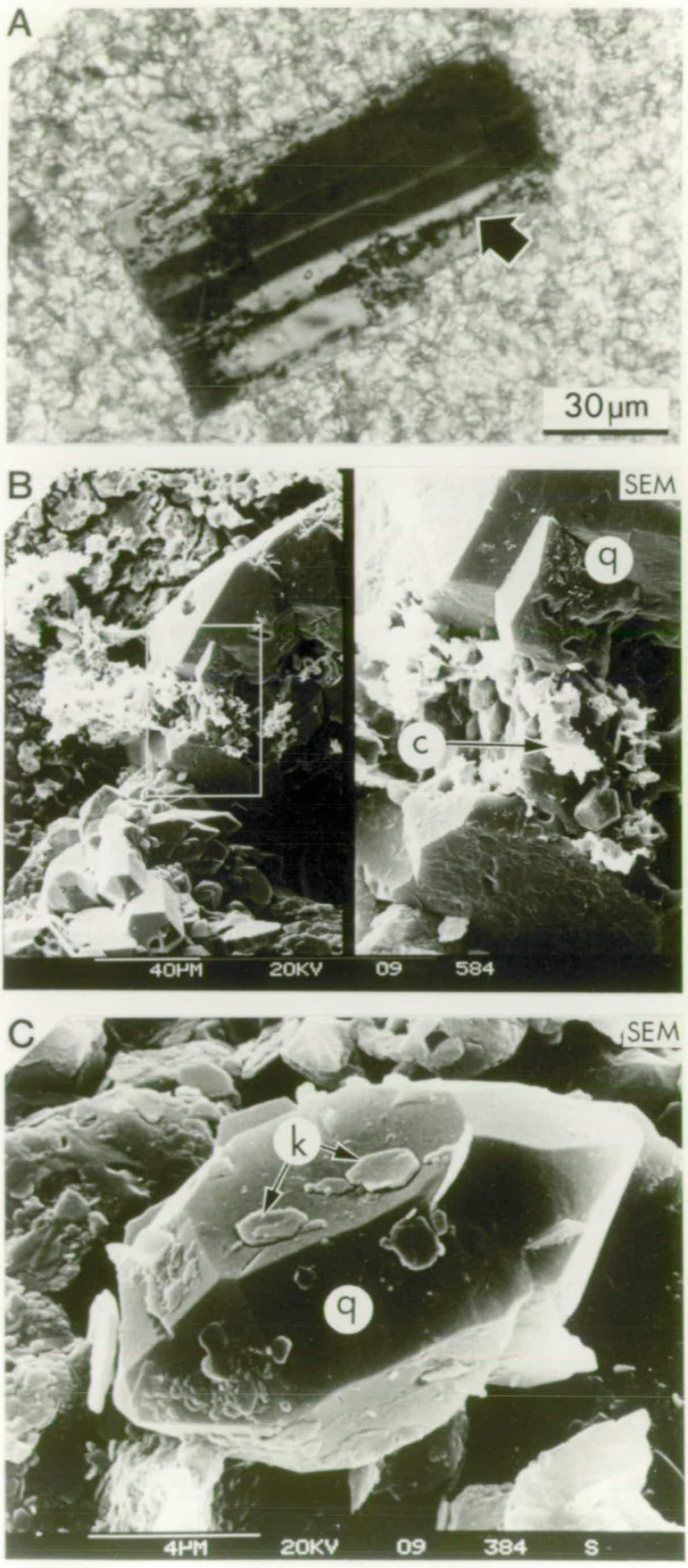
A
30µm
B
SEM
q
c
40µM 20KV 09 584
C
SEM
k
q
4µM 20KV 09 384 S

minerals. In one example (Fig.13.4B), euhedral quartz was corroded prior to the development of authigenic clay (probably smectite), while in the second example (Fig. 13.4C), small platy kaolinite crystals coat an authigenic quartz crystal. This suggests that silica diagenesis occurred prior to clay mineral diagenesis in these examples. The association of quartz and kaolinite points to a late stage in the diagenetic history.

In off-bank and interbank facies, nodular chert is very common and often quite extensive in its development. Nodules are usually elongate and may be tens of centimetres in length. They are usually developed parallel or sub-parallel to bedding in the interbank facies.

In thin section, chert nodules reveal a polycrystalline, often fibrous texture under crossed polars. With plane polarised light, relics of bioclasts, particularly hyalosteliid sponge spicules are common. The internal structure of the spicules is commonly preserved in the silica nodules, whereas most spicules outwith the nodules are either replaced by calcite or exist in the form of calcite-filled moulds. In some cases, spicules which have been replaced by calcite are contained within chert nodules, indicating that silicification was not early.

Although many of the chert nodules are conformable with bedding features in the off-bank facies, none showed evidence of bedding being compacted around them as is apparent in some cases of early diagenetic nodule formation elsewhere. In the interbank facies near the Ings Beck buildup, silicification cuts compaction seams which are draped over a coarse-grained crinoidal lens in the sediment, indicating that, in this case, silicification occured after compaction and sediment lithification.

CONCLUSIONS

1. Two periods of mineralisation can be recognised in the Waulsortian and associated facies in the Craven Basin;

a). Early iron sulphide crusts formed in voids during early diagenesis after Stage B but prior to Stage E.

b). Late hydrothermal silica, fluorite, barite, sphalerite and galena formed after dolomite (Stages J-L) but before non-ferroan Stage N calcites.

2. Early iron sulphide crusts consist mainly of marcasite which is often nucleated on framboidal pyrite aggregates. Sulphur isotopes indicate a highly reduced seawater sulphate source for these minerals, which are commonly found in cavities where they are overlain by internal sediments fed by neptunian dykes.

3. Late hydrothermal mineralisation is closely associated with fractures which follow the major Hercynian structural trends in the Craven Basin.

4. The most common late hydrothermal phase is replacive, microcrystalline silica which selectively replaced CFC cements and some bioclasts in the Waulsortian bank facies. This can be related to coarsely crystalline quartz cements which were the earliest hydrothermal mineral phase, and were followed by sphalerite, fluorite and barite in that order. The exact timing of galena mineralisation within this part of the sequence is uncertain, although it at least post-dates dolomite.

DIAGENESIS

PART THREE

DIAGENESIS PART THREE

METEORIC DIAGENESIS

Introduction

Two late diagenetic carbonate phases in the Waulsortian buildups have significantly different isotopic signatures compared to the rest of the sequence. Primarily these record major depletion in $\delta^{13}C$ accompanied by enrichment in $\delta^{18}O$, which are interpreted as indicative of a relatively near-surface to moderate burial environment with fluids derived, at least in part, from a meteoric source.

One of these carbonate phases is a late vein-filling cement, while the other is an alteration product after calcitisation of dolomite. They are discussed in the following brief chapters.

CHAPTER 14
LATE FRACTURE-FILLING CEMENTS

A late non-ferroan calcite stage was identified in a veinlet-filling sequence in samples from two buildups. The veinlets are at least post-dolomite in age, and contain a characteristic sequence of ferroan calcite followed by bright-luminescent non-ferroan calcite (Fig. 14.1).

It was not possible to isolate the earlier ferroan cement for isotopic analysis, but a sample containing a mixture of ferroan and non-ferroan calcites gave $\delta^{13}C$ = +2.70°/₀₀; $\delta^{18}O$ = -5.95°/₀₀. This analysis says little about the actual isotopic composition of the individual cements without knowing the proportions of each in the mixture. However, non-ferroan calcite from both samples was isolated and analysed (Table 14.1).

These analyses show significant enrichment in $\delta^{18}O$ and the most depleted $\delta^{13}C$ value of all prior cements.

The indications are that these cements represent a return to shallow burial conditions as a result of erosion/uplift during the late burial history of the deposits in this study. The depletion in $\delta^{13}C$ is similar to that of the bright luminescent, non-ferroan Stage C cements, and it is possible that the later cements also formed in a suboxic shallow burial environment. However, the relative depletion in $\delta^{13}C$ could also be related to a different source fluid containing light carbon. If the assumption that these cements formed after uplift / erosion during late diagenesis is correct, then a very probable source fluid would be meteoric water. This would represent the first reasonable evidence for a meteoric recharge of formation waters in the diagenetic history of the Waulsortian buildups.

Table 14.1 Isotopic composition of late non-ferroan calcite cements

Sample	$\delta^{13}C$°/₀₀	$\delta^{18}O$°/₀₀
Su	+1.00	-3.19
SF3	+0.03	-3.73

Analyses in per mil (°/₀₀) versus PDB standard

Figure 14.1 Meteoric cement.

Photomicrographs (A & B) showing a late diagenetic vein-filling cement sequence in PPL and CL respectively. In CL, the sequence consists of a very dull- luminescent, ferroan calcite stage containing three substages (1,2 and 3), followed by brightly luminescent, non-ferroan, meteoric calcite cement (M). Thin section, Spire Farm bank facies.

Fig. 14.1

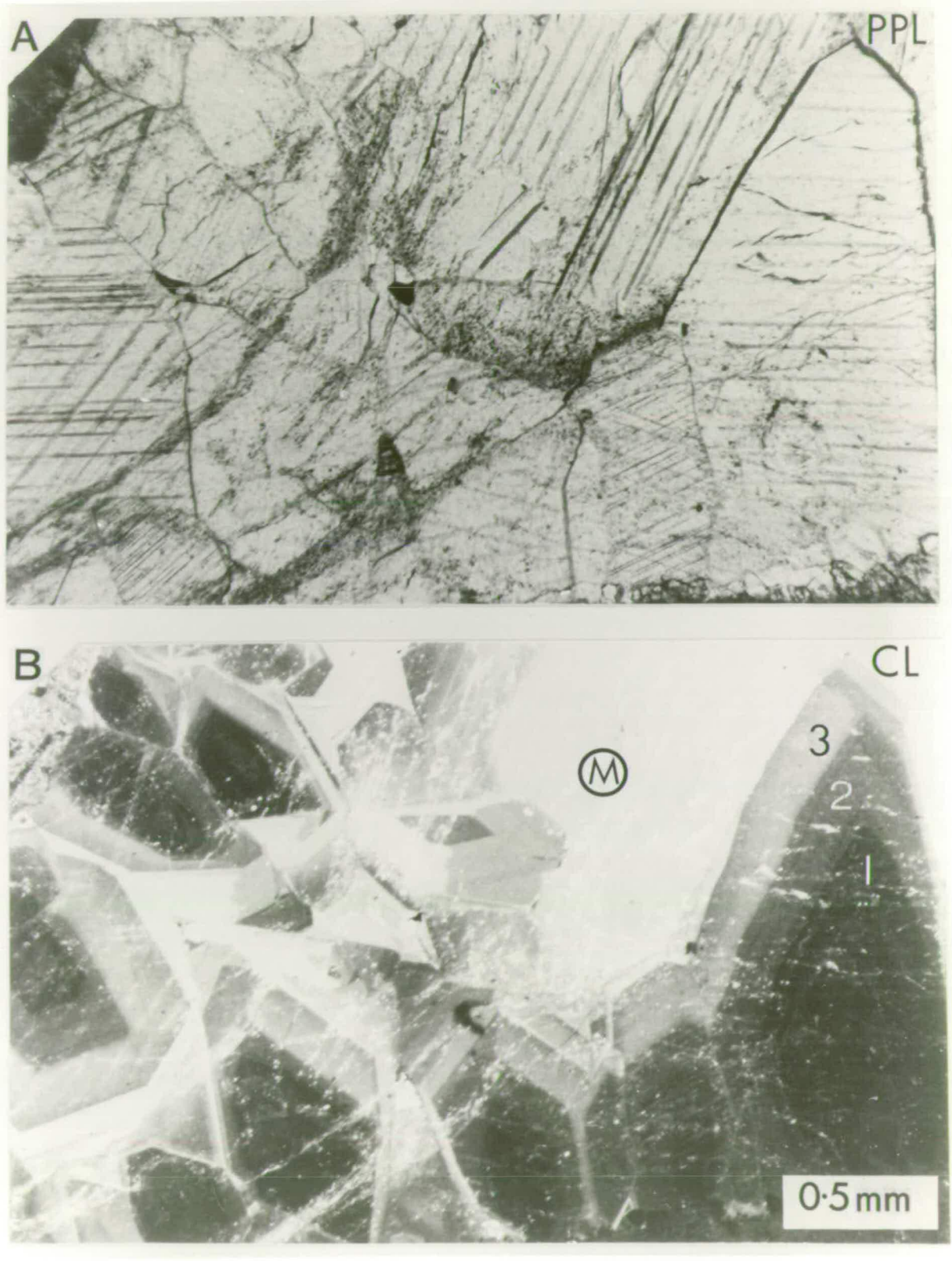

Fig.14.2 Isotopic composition of meteoric cements and calcitised dolomite compared with earlier cements.

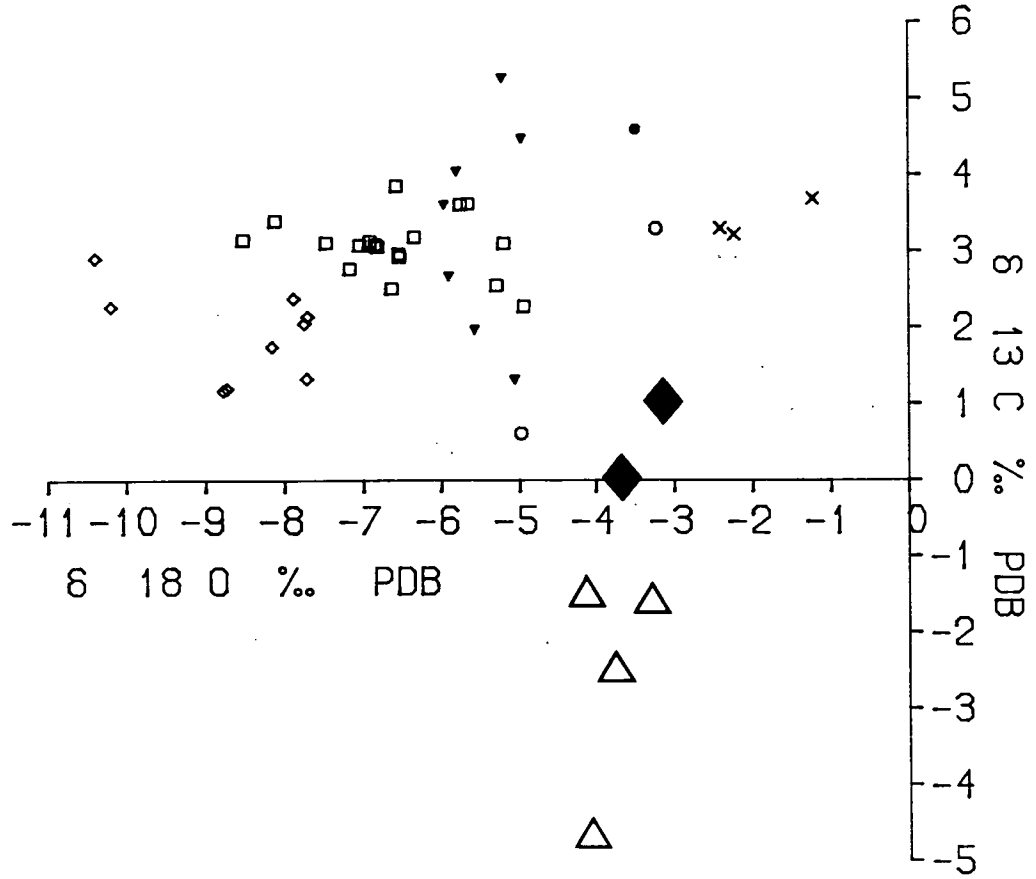

◆METEORIC NON-FE CALCITE
△METEORIC CALCITISED DOLOMITE

× Stage A
○ Stage B&C
□ Stage E-I
• Stage K
▾ Stage L
◇ Stage N (et al.)

CHAPTER 15
CALCITISATION OF DOLOMITE

Dolomites occurring at outcrop in the Waulsortian and peri-Waulsortian facies of the Craven Basin are invariably a strong rusty-orange colour, and often extremely friable. Locally, the material has been transformed to an orange clay. In samples broken from outcrop, dolomites also commonly have a calcitised outer edge which grades into fresher crystals away from the exposed surface. Although in many cases this calcitisation has extended throughout the entire dolomite fabric of some buildups, no calcitised dolomite was identified in material from the BGS Cow Ark No.9 borehole. It is apparent, therefore, that calcitisation is a near-surface phenomenon.

15.1 PETROGRAPHY

Calcitised dolomite exhibits all the fabrics which are characteristic of their parent dolomites (Chapter 11), including scattered rhombs, zoned rhombic and saddle mosaics. The mineralogy, however,is calcite, with finely disseminated inclusions of a dense brown mineral which imparts the rusty colouration. These inclusions depict relict fabrics and pseudomorphs after dolomite which underwent calcitisation (dedolomitisation). Irregular patches of unaltered dolomite often occur.

In CL, calcitised dolomite has a characteristic bright yellow-orange luminescence, which is often blotchy but is generally unaffected by the distribution of the opaque inclusions. This shows that, even in examples which are optically very dense so as to appear to be totally composed of the brown mineral, the opaque material is actually disseminated within the calcite.

Staining shows the calcite itself to be non-ferroan. In order to identify the brown inclusions, samples were examined with SEM having first removed the calcite by etching with EDTA. (Fig. 15.1B). The inclusions comprised radiating bundles of a rod-shaped mineral whose identity as goethite, FeO.(OH), was confirmed by XRD analysis.

15.1.1 Styles of calcitisation

Three styles of dolomite calcitisation were identified in this study:

1. Calcitisation along crystallographic and intercrystalline planes of weakness.
2. Calcitisation of compositionally distinct regions within crystals.
3. Pervasive calcitisation.

1. Calcitisation along planes of weakness

Crystallographic planes (eg. cleavage planes) within dolomite mosaics and intercrystalline boundaries were often exploited by calcitising fluids (Fig. 15.2). Evidence of dissolution along the planar surfaces is common in these examples. Calcitisation was often most extensive at the margins of dolomite mosaics, where fluids infiltrated the surfaces between the mosaics and surrounding material. Rarely, sinuous micro-veinlets fed calcitising fluids along intercrystalline boundaries in sediment which surrounded dolomite mosaics. No larger-scale fractures were found to be associated with calcitisation of dolomite. This represents a different kind of fracture to those identified in association with deep burial cement stages. Cognate sets of veins and veinlets do not occur and it would appear that these structures are most probably the result of small-scale, local fracturing events, or the calcitising fluids exploiting pre-existing micro-fractures, rather than any significant phase of tectonism.

2. Calcitisation of compositionally distinct crystal regions.

In many cases, calcitisation occurred selectively along compositionally distinct growth bands within dolomite crystals. These bands follow euhedral zonation patterns within the crystals and are usually marked by an increase in density of goethite inclusions. In rhombic mosaics it was commonly the rims of crystals and, on rare occasions, their rims and cores which were selectively calcitised.

In CL it was noticeable that the non-ferroan dolomites were commonly unaltered while ferroan dolomites were selectively replaced. The example in Fig. 15.1C shows selective calcitisation of Stage L equivalent which formed the crystal rims in a rhombic dolomite mosaic.

In ferroan dolomites, calcitisation often depicts a euhedral banding which is not identifiable in unaltered samples either by changes in inclusion density, by CL or by staining. However, with BEI it is often possible to detect euhedral compositional zonation of iron in these mosaics. When BEI is combined with microprobe analysis, it can be demonstrated that calcitisation was most active along the zones of highest iron content (Fig.15.2D&E). This confims the observation that iron-rich dolomites were more susceptible to the calcitising fluids than iron-poor dolomites.

3. Pervasive calcitisation

In many examples, calcitisation of dolomites was complete (see Fig.15.1A). Relict textures such as the rhombic mosaics, and the characteristic curved faces of saddle dolomites, are usually the only indications of precursor mineralogy, although replacive calcite in saddle dolomite mosaics often inherited weak sweeping extinction patterns.

15.2 GEOCHEMISTRY

15.2.1. Trace elements

Samples of calcitised dolomite were identified for analysis from their CL characteristics. Their mean composition is given in Table 15.1.

The relatively high concentration of FeO compared with MnO appears to be at odds with the non-ferroan staining response and bright luminescence of this material. However, contamination by the finely disseminated goethite will have significantly affected the FeO concentrations in these analyses. The magnesium concentration may well be a true reflection of the calcitising pore fluid composition,

but the replacement origin of the calcite makes this no more than a possibility. The relatively high concentration of SiO_2 is probably related to the development of clay minerals after calcitisation.

15.2.2. Stable Isotopes

Four samples of completely calcitised dolomite were analysed for isotopic composition (Table 15.2; Fig.15.4). The purity of the samples were checked by XRD analysis as described above (Chapter 8).

The $\delta^{18}O$ values may have been inherited, at least in part, from the dolomite precursor as indicated by the range of variation. They are generally heavier than the values for Stages J and L and comparable to those of Stage K. The $\delta^{13}C$ values, however, are strikingly different from any other carbonate phase in this study. Such negative values almost certainly indicate that the calcitisation was the product of meteoric fluids entering the rocks.

Table 15.1 Mean Composition of Calcitised Dolomite

Oxide	Mean wt%	S.D.	C.V.	n=11
CaO	54.53	2.53	0.05	
MgO	0.68	0.88	1.29	
FeO	0.98	1.51	1.55	
MnO	0.10	0.04	0.42	
SiO_2	0.56	0.71	1.28	

11 analyses from 2 buildups
S.D. = Standard deviation at 95% confidence level
C.V. = Coefficient of variation

Table 15.2 Stable Isotopic Composition of Calcitised Dolomite, in per mil (°/₀₀) vs PDB standard

Sample	% Dolomite (XRD)	$\delta^{13}C$ °/₀₀	$\delta^{18}O$ °/₀₀
IB	0	-4.60	-4.08
PQL	0	-2.43	-3.77
WW	0	-1.51	-3.30
Du26	1	-1.41	-4.14

Locality codes:
IB = Ings Beck
WW = Hall Hill (Whitewell)
PQL = Peach Quarry Limestone
Du = Dunnow

Figure 15.1 Calcitisation of dolomite.

A. PPL photomicrograph of pervasively calcitised saddle dolomite mosaic. Cleavage planes and the characteristic curved crystal faces and growth zones (arrowed) are marked by concentrations of goethite inclusions (FeO-OH), a hydrated oxidation product, which give the dense appearance to the mosaic. The dolomite has otherwise been completely altered to non-ferroan calcite. Thin section, Leagram buildup.

B. SEM photograph of partially calcitised dolomite. Calcite was removed by EDTA etch, revealing inclusions of goethite (G) in the partially altered dolomite (D). The goethite consists of radiating bundles of rod-shaped crystals (arrowed). Bellmanpark buildup.

C. PPL photomicrograph showing selective calcitisation of iron-rich outer rims of crystals in a rhombic dolomite mosaic (arrowed) producing non-ferroan calcite and dense goethite inclusions. The rhomb cores are unaltered dolomite (D).

Fig. 15.1

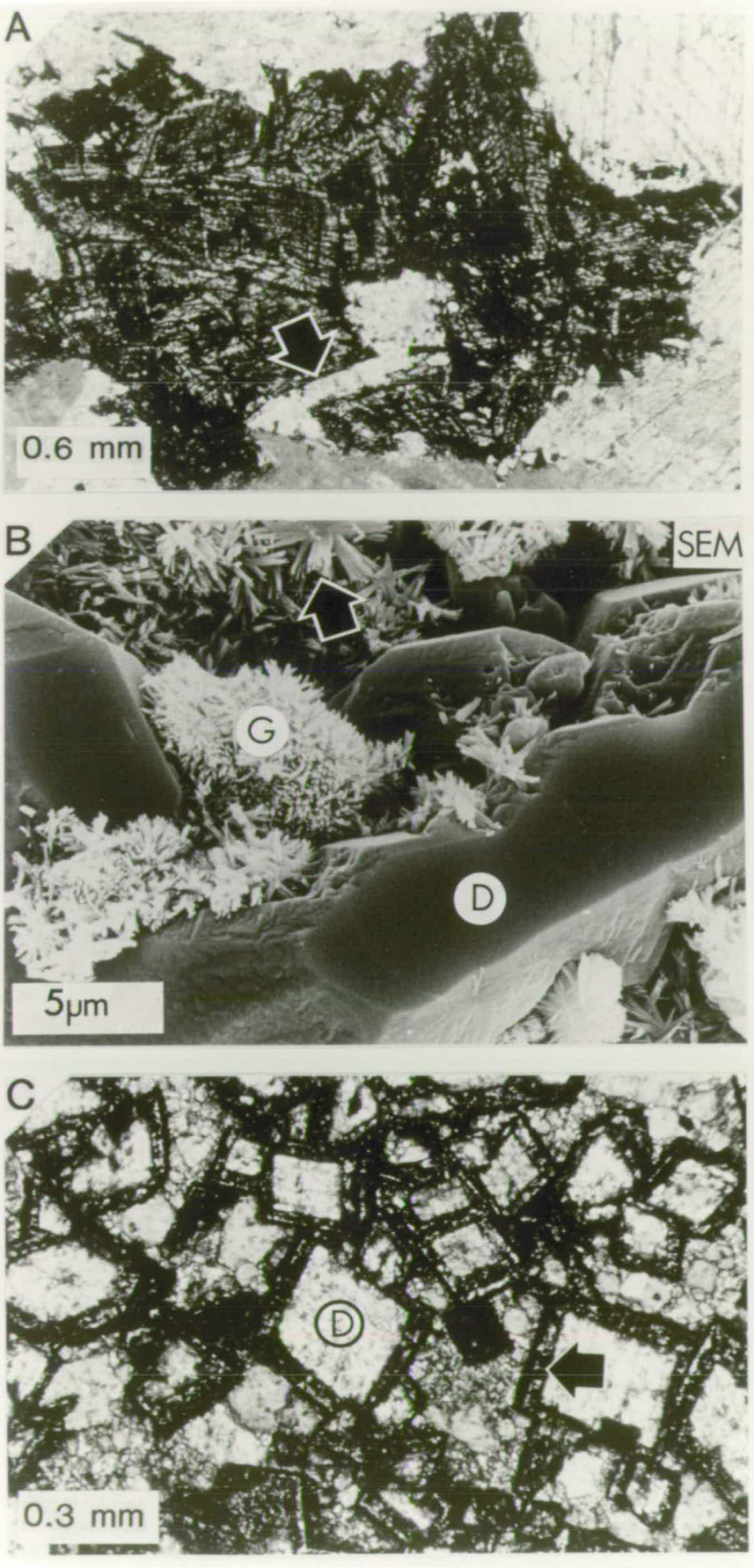

Figure 15.2 Calcitisation of dolomite.

Photomicrograph pair from Dunnow bank facies. Field of view = 3mm.

A. PPL: Showing a dolomite mosaic comprising rhombic (R) and saddle (S) crystal morphologies after calcite cement (C). Dense goethite (G) has formed after selective calcitisation of the outer layers of the rhombs and also occurs within the saddle dolomite.

B. CL: Showing characteristic bright orange-yellow luminescent calcite which has selectively replaced the ferroan dolomite (Stage L) along rims within the rhombic mosaic and along euhedral compositional zonation (Z) and cleavage planes (Cp) within the saddle dolomite. Non-ferroan dolomite Stage K is relatively unaffected by calcitisation. One of the rhombs (arrowed) shows a complex dissolution surface between Stage K and earlier, very dull-luminescent Stage J.

Fig. 15.2

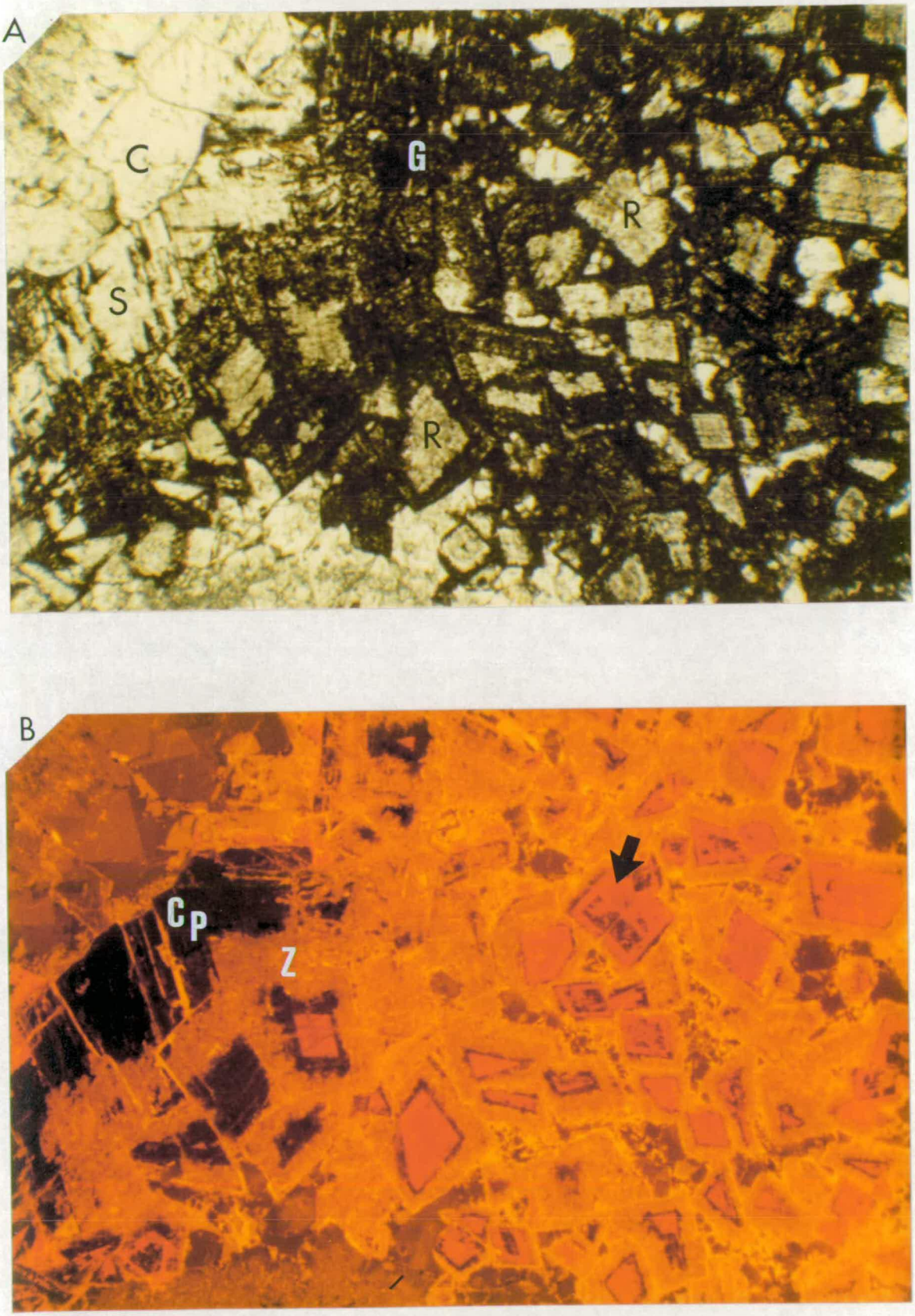

Figure 15.3 Back-scattered electron images showing Fe zonation and calcitisation in ferroan dolomite.

A. Showing euhedral bands of varying Fe content. The brighter bands have higher Fe content (confirmed by quantitative microprobe analysis). The bright glare occurring in some regions is a product of surface charging which corresponds with friable, calcitised parts of the dolomite mosaic. Calcitisation was selective along the zone of highest Fe content (arrowed). Striations are surface polishing defects. Old Calamine Mines.

B. The bright charged area is composed of friable calcitised dolomite (c), confirmed by microprobe spot analysis. Again, the calcitisation selectively followed the zone of highest Fe-content in the dolomite mosaic ($FeCO_3$=16.37 mole%; bright band arrowed). Polished thin section, Old Calamine mines.

Fig. 15.3

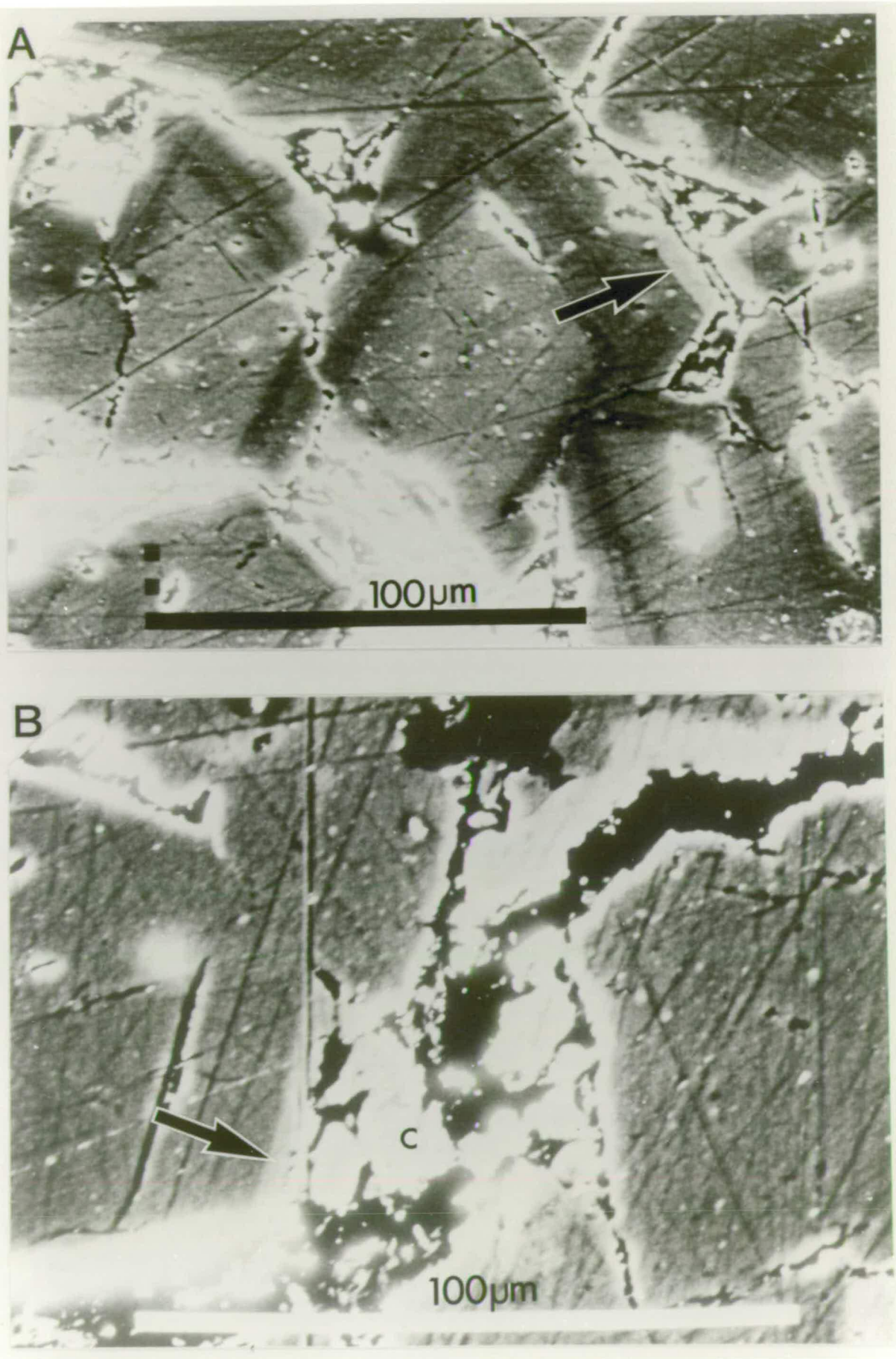

15.3 DISCUSSION

Two possible process have been mooted for dolomite calcitisation in natural examples (see Frank 1981);

1. The reaction of dolomite with $CaSO_4$ in solution
2. Alteration of ferroan dolomite by oxygenated meteoric water.

The development of calcitised dolomite near the present day surface in the Craven Basin and the lack of any potential source for significant quantities of dissolved $CaSO_4$ accompanied by the present day climatic conditions, strongly suggest that meteoric oxygenated fluids were responsible for the calcitisation. The $\delta^{13}C$ signatures from calcitised dolomites support such an hypothesis (c.f. M'Rabet et al. 1986).

The association of dolomite calcitisation with near-surface oxidation processes has been observed by many authors, all of whom report a strong brown colouration of affected dolomite (Evamy 1963; Al-Hashimi & Hemmingway 1973; Frank 1981; Henrich & Zankl 1986; Koch & Schorr 1986; M'Rabet et al. 1986). The brown colouration is, in all cases, due to the presence of ferric oxides and hydroxides (principally hematite and goethite). These minerals are by-products of the calcitisation process (Al-Hashimi & Hemmingway 1973) resulting from the inability of the replacive calcite to hold as much Fe^{2+} as the precursor dolomite (Evamy 1963).

De Groot (1967) showed experimentally that near-surface conditions with a high rate of water flow, low pCO_2 and temperatures less than 50°C were required for calcitisation of dolomite.

Frank (1981) identified non-ferroan composition and bright orange-yellow luminescence as a characteristic of calcitised dolomite in his study. The homogeneity of the luminescence, despite the often high concentration of goethite inclusions, reflects Evamy's (1963) suggestions that the hydrated iron oxides precipitated colloidally.

There is strong evidence from the rocks of this study that high $FeCO_3$ content in the dolomites makes them more prone to calcitisation. Other workers have reached similar conclusions. Both Katz (1971) and Frank (1981) identified calcitisation in well-defined

zones which corresponded to regions of high $FeCO_3$ in unaltered samples of the precursor dolomite. Frank (1981) and Koch and Schorr (1986) also identified preferential calcitisation along planes of weakness in dolomite mosaics and the presence of pervasive calcitisation in some samples.

CONCLUSIONS

1. Calcitisation of dolomite in the Waulsortian buildups of the Craven Basin was effected by oxygenated meteoric waters at or near the present day surface. This is supported by the presence of calcitised surface layers in hand specimens and the lack of calcitisation in borehole material, together with stable isotopic analyses which indicate meteoric fluids.

2. Bright orange-yellow luminescent non-ferroan calcite and disseminated inclusions of goethite (FeO.OH) were the products of calcitisation. The goethite formed from excess iron which could not be incorporated into the calcite lattice after alteration of ferroan dolomite.

3. Calcitisation was often pervasive, but could also be selective;
   a) along cleavage and intercrystalline boundaries or other planes of weakness.
   b) along chemically distinct regions of originally high Fe^{2+} concentration. Non-ferroan dolomites were least susceptible to calcitisation.

4. The occurrence of a dolomite precursor is indicated by the presence of relict textures such as:-

   a) The occurrence of relict patches of precursor dolomite in calcitised material.
   b) The presence of dolomite pseudomorphs composed of calcite.
   c) The existence of relict dolomite fabrics within the new replacive generation of calcite.

DIAGENESIS

PART FOUR

CHAPTER 16
FRACTURES AND VEINS

The development of fractures had a major effect on the diagenesis of the Waulsortian rocks, because they allowed the influx of diagenetic fluids into an otherwise largely cement-filled or otherwise isolated pore system. Several phases of fractures developed, which could be related to the cement stratigraphy by their intersections with void-filling spar sequences, and cross-cutting relationships with other veins, stylolites and earlier cements. To date, little mention has been made of the importance of fractures in the development of burial cement sequences, notable exceptions being the studies of Mattes and Mountjoy (1980) and Schroeder (1986).

Fractures are extremely common in the Waulsortian buildups, and they occur on a range of scales which can be conveniently divided into three groups:

1. Veins (centimetre scale)
2. Veinlets (millimetre scale)
3. Microveinlets (micron scale)

Veins and veinlets are usually identifiable in hand specimen, while micro-veinlets are only apparent in thin section and then often only with CL or staining.

Vein phases in this study are usually accompanied by a cognate set of veinlets and micro-veinlets, and can often be related to particular cement stages in the void-filling cement sequence. Most fractures are cement-filled, but there are sediment-filled neptunian dykes and fissures which had a very important influence on the early diagenesis of the buildups (see Chapter 8). A variety of different styles of fracture were observed. The morphology of the fractures, and the nature and textures of the materials which fill them, reflects the style of fracturing and the stresses involved.

Although a number of separate fracture-phases developed, they can be broadly divided into two groups, namely:

a) those associated with early diagenesis which include neptunian dykes and spar filled cavities.
b) those associated with later diagenetic tectonic processes.

16.1 EARLY DIAGENETIC FRACTURES

Both sediment- and spar-filled fractures developed during the early diagenesis of the Craven Waulsortian.

16.1.1 Sediment-filled fractures (Neptunian dykes)

Neptunian dykes formed early in the diagenetic sequence and are described in detail in Chapter 8.

16.1.2 Spar-filled fractures

These fractures are often crumbly-edged (sensu Miller 1986) consisting of pull-apart structures with refittable walls. They are laterally discontinuous and often appear as small tears in the sediment. They invariably truncate Stage A CFC cements and are commonly filled by early diagenetic cement Stages C and D, while Stage B is only rarely developed. Cement crystals developed as open void-fills, often with centripetal stages showing progressive growth away from the fracture margins. No evidence was observed of cement crystal strain, indicating that crystals did not grow under directional stress (see below).

The margins of these fractures commonly show evidence of modification by dissolution prior to cementation. These fractures are interpreted as early diagenetic for the following reasons:

a) they are filled with early diagenetic cements
b) their morphology indicates development in a partially lithified sediment which must have been of firm gel-consistency (Miller 1986).

Other fractures, usually veinlets, which are filled with early diagenetic calcite spars, have less of a crumbly-edged appearance but

appear more like brittle fractures with sub-parallel margins (although still tending to be laterally discontinuous and showing some tearing). Evidence of dissolution at the walls of these veinlets is common.

The variation in styles of these early diagenetic fractures reflects the partially lithified nature of the sediment at the time of their development. Crumbly-edged fractures developed in poorly lithified sediment, while in areas of more extensive lithification, brittle fractures developed. The intrusion of neptunian dykes was probably partly responsible for the development of these fractures. Such dykes were being developed throughout early diagenesis in the buildups, and must have induced large-scale tensional stress upon the partially lithified sediment.

16.2 LATE DIAGENETIC (TECTONIC) FRACTURES

All cement stages occurring after the prismatic non-ferroan calcites of Stage D are consistently associated with phases of fracturing. Most of the observations reported below are from thin section petrography, at which scale the most common fracture forms are veinlets. It should be assumed that all veinlets described in this section are accompanied by cognate sets of veins and microveinlets.

All late diagenetic veinlets show evidence of brittle fracture in the form of breakage and separation of originally entire bioclasts to their opposite walls, or the exploitation and extension of planes of weakness in the host matrix. Fractures may be further modified by dissolution and recrystallisation after or during their development.

The cement fabrics which developed within veinlets reflect the nature of the stress which affected veinlet development. Two groups were recognised;

1) Post-dilational cements

2) Syntectonic cements.

16.2.1. Post-dilational cements filling veinlets

These have all of the characteristics of void-filling cements including increase in grain size away from the substrate, and euhedral or centripetal compositional banding. Crystals may develop prismatic or blocky habits. They do not exhibit any effects of crystal strain during growth. Veinlets containing these cements have walls which range from irregular and non-parallel to regular and parallel.

The development of void-filling cements within these veinlets indicates that the crystals grew in a zero-stress environment by precipitation from a pore fluid after the veinlet opened, i.e. they are post-dilational.

More than one cement stage may occur in a single veinlet (Fig. 16.1).

16.2.2 Syntectonic crystals in veinlets

Many veinlets contain elongate crystals. The crystals show little or no sign of having grown centripetally or otherwise into open void space and are therefore interpreted as having grown syntectonically (Durney & Ramsay 1973).

Veinlets containing these crystals exhibit a variety of forms, but are usually parallel to sub-parallel sided and may pinch out, or develop en echelon.

The direction of elongation of the crystals is parallel to the direction of veinlet dilation, and therefore to the maximum tensile strain direction (Durney & Ramsay 1973; Phillips 1974). Therefore, the crystal fabric was dependent upon the degree and direction of strain.

With increasing strain, crystal habits range from slightly stretched prismatic forms through tabular to fibrous types (Fig. 16.1B).

The degree of strain is reflected in the extinction patterns of the different forms. Stretched prisms exhibit largely uniform extinction, becoming slightly undulose in more elongate crystals which show evidence of greater stretching. Tabular crystals all show

sweeping extinction, which is generally stronger than in prismatic forms, although still relatively uniform when compared to crystals with fibrous habits which exhibit strong undulose extinction. Stretched prismatic and tabular crystals tend to be straight, whereas fibrous crystals may be either straight or curved.

With only rare exceptions, crystals are optically continuous along their length; in many cases, particularly in tabular forms, this continuity extends across the entire width of the veinlet. There is no evidence of median sutures within veinlets, about which optic orientation changes, as reported by Durney and Ramsay (1973) in their description of syntaxial and antiaxial veinlets. All of the syntectonic veinlets in this study represent Durney and Ramsay's "Type 4; stretched crystals", where crystals are "optically continuous across the entire vein and there is no central surface separating fibres of different optic orientation".

Durney and Ramsay showed that stretched crystals developed as a result of incremental dilation of the veinlet so that repeated microfracturing, as the crystals were stretched, was followed by their progressive healing by overgrowth. Straight crystals represent a constant stress direction during dilation whereas curved crystals indicate changes in stress direction during veinlet opening.

Phillips (1986) suggested that the fibrous fabric was produced by hydraulic dilatation and tensile strain crystallisation so that "If the fluid pressure were just sufficient to form hydraulic fracture, new crystals might nucleate along an incipient fracture. If this fluid pressure were maintained ....crystals bridging the fracture would suffer tensile strain without breaking".

A noticeable change in fabric occurs where syntectonically cemented veinlets intersected resistant areas of the substrate such as large crinoid ossicles or cement-filled cavities. These more resistant areas reacted inhomogeneously to the tensile strain applied to them, and instead of propagating a single fracture, numerous microfractures developed (Fig. 16.1C). In the case of veinlets intersecting calcite spar, the microfracturing tended to propagate along planes of weakness in the spar mosaic, such as cleavage, twin planes and intercrystalline boundaries, resulting in the development of a "horse-tail" fabric. If there was any void space left in the

cavity before fracturing, then the microfracturing allowed fluids from the veinlet to enter this pore space and precipitate cement (Fig. 16.1D). Such void space would have been an area of zero-stress and therefore centripetal void-filling cements developed without any crystal strain fabrics. Horsetail veinlets were commonly developed and cemented during deep burial stages (i.e. Stages G to N), and are rarely seen in association with shallow to moderately deep burial stages.

Where syntectonic veinlets encountered large bioclasts such as crinoid ossicles, swarms of anastomosing microveinlets developed sub-perpendicular to the stress field or along any primary skeletal structure which may have been present. In some cases, horsetail microveinlets were large enough to allow identification of the cement crystal fabric which filled them. These examples show less evidence of strain than in the 'feeder' veinlet. This is best understood by first considering the process of stretched crystal development.

Stretched crystals form as a result of crystals initially being stretched and then fractured, leaving a microscopic open void which is healed by overgrowth. Further increments of repeated strain, fracture and cementation propagate the elongation of the crystal and the strain in the lattice. The "horsetail" microveinlets represent single increment fractures, which were subsequently healed but did not undergo repeated incremental dilation, and therefore they exhibit simple void-filling cement characteristics.

16.2.3 Multi-stage fractures

Once a fracture is developed it marks a plane of weakness within the rock body which, even if it is totally cemented or filled with sediment, is likely to be exploited by subsequent phases of fracturing.

Examples of fractures containing more than one cement stage are very common in the rocks of this study, and the neptunian dykes (Chapter 8) were also generally affected by subsequent fracturing and cementation.

Multi-generation fractures that were filled after dilation may reflect one of two different histories, so that:

a) The fracture was partially filled by an initial stage of centripetal cement, leaving some porosity to be filled by a later cement stage (Fig. 16.1A).

b) The fracture was completely filled by cement and then re-opened by a second period of extension leaving a void to be filled by a subsequent cement (Fig. 16.1E).

In (a), the cements filling the veinlets exhibit all of the characteristics of void-filling spars, with subsequent cement stages occurring nearer to the centre of the fracture. Where large monocrystalline grains such as crinoid ossicles occurred as part of the veinlet wall, syntaxial overgrowths often developed in the void space. In some cases, however, where the veinlet margins were irregular, subsequent cementation sometimes resulted in restriction of the void space, forming narrow pore throats and even isolating some of the void space within the veinlet. In such cases, the remaining void space would only become cemented if subsequent fracturing allowed later diagenetic fluids to gain access to the void. This is not an uncommon occurrence in Waulsortian and peri-Waulsortian facies, where the later fluid often caused dissolution or recrystallisation of earlier cements.

In case (b) the existing cement stage in the veinlet may be fractured and displaced to either side of the later cement, (but not necessarily exactly in the median zone), or the second phase fracture may have developed at or near one of the margins of the early veinlet. Commonly, as is the case in Fig. 16.1E, the second phase of fracturing does not merely develop a single break, but tends to develop with a main veinlet and cognate microveinlet set; these are often anastomosing and may break across the earlier veinlet into the host sediment.

The later fracture phase may also cause breakage of the first cement, whose crystals may then be annealed by a subsequent cement stage. In syntectonically cemented veinlets, changes in pore fluids during the incemental opening of the fracture can result in a fabric containing more than one cement stage (e.g. Fig. 16.1B).

Secondary microbrecciation and dissolution of fracture-filling material are common effects of multi-stage fracturing. The most

Figure 16.1 Fractures.

A. Photomicrograph of a stained peel showing the two-stage post-dilational cementation of an irregular-sided early diagenetic fracture. Early non-ferroan calcites (nf) of stages B-D formed an irregular cement layer on the fracture walls. Large syntaxial overgrowths developed on a crinoid ossicle (c) which formed part of the wall. Ferroan calcites (fe) of Stages E and F filled the rest of the open fracture during a subsequent period of cementation. Coplow bank facies.

B. Photomicrograph of a stained thin section showing syntectonic crystal growth in a brittle fracture under low stress conditions. Although cement crystals filling the vein increase in size away from the walls and have euhedral compositional zonation (arrow), they are slightly stretched in the direction of vein opening. Bellmanpark bank facies.

C. Photomicrograph showing a syntectonically cemented veinlet with tabular cement crystals, which intersected a resistant crinoid grain (c). Rather than propagating a single fracture, the crinoid was dissected by numerous micro-veinlets (mv), now seen as diffuse stringers cutting the inclusion-rich relict crinoid in the body of the veinlet. Thin section, Gerna bank facies.

D. Photomicrograph of a stained peel showing "horse-tailing" texture in a ferroan calcite veinlet (v) cutting heterogeneous sediment and spars. Where the fracture encountered blocky non-ferroan calcite (G) of Stage G, micro-veinlets propagated along the cleavage planes in the cement crystals (arrowed). The veinlet allowed fluids to enter void space that was enclosed by Stage G, resulting in the development of Stage I ferroan calcite cements. Coplow bank facies.

E. Photomicrograph of a stained thin section showing a two-stage syntectonically cemented fracture. The first veinlet phase (v1) was cemented by ferroan calcite. This was followed by a second period of extension and the development of a second veinlet (v2), which was cemented by non-ferroan calcite. Both v1 and v2 comprise a series of anastomosing micro-veinlets (mv). Post-Waulsortian mudstones, Raven Scar Plantation.

F. Photomicrograph showing the relative timing of veinlet (v) and stylolite (st) formation. The fibrous, syntectonically cemented veinlet cuts the stylolite (large arrow) at several points, and is therefore younger.

Fig.16.1

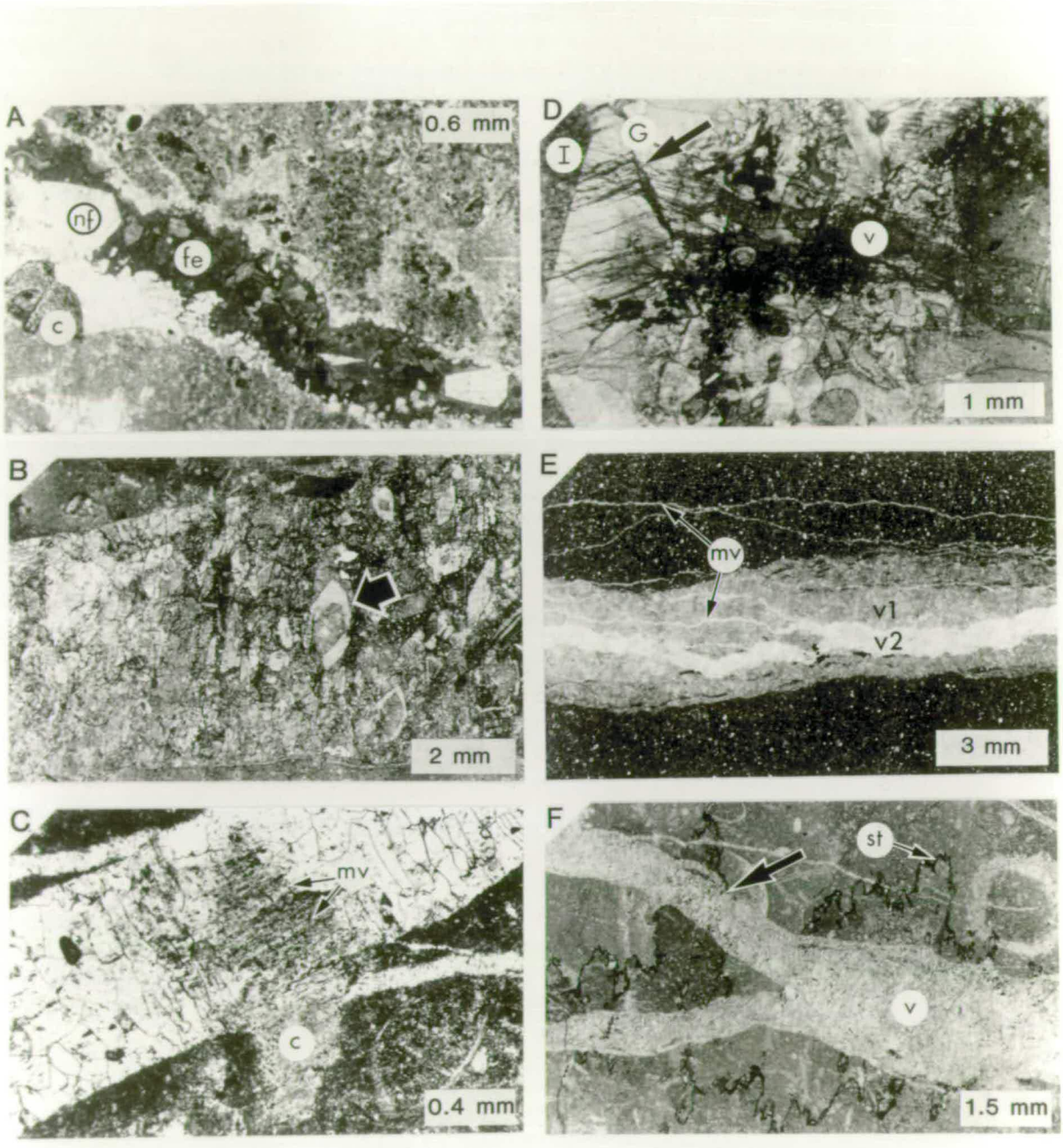

complex examples are those in slickensides which occur along fault planes, and may contain several cement stages from fluids which exploited the fracture during repeated opening over a long period.

16.3 FIELD RELATIONSHIPS OF VEINS (Waulsortian and associated facies)

The trends of vein sets in the Craven Waulsortian are generally associated with major structural trends in the basin.

At the east end of Bellmanpark quarry, measurements on a fault slickenside showed a major dextral trend towards 320°N and a minor sinistral trend towards 220°N. Veinlets increased in frequency in the area of this fault and tended to run sub-parallel to one or other of these trends. The slickenside material contained fluorite, with prior and post-mineralisation calcite cements. At Hall Hill, a strong set of sub-parallel veins cut the Waulsortian facies in a trend of 030-210°N, which is close to the minor sinistral trend measured at Bellmanpark. These veins are also partially mineralised.

Large-scale veining can be seen in the north face of the Chatburn Limestone quarry at Clitheroe, in the vicinity of the Horrocksford Hall thrust. These veins contain saddle dolomite and Stage N non-ferroan calcite as well as pre-dolomite ferroan calcites, probably of Stage H and I. Veins are also associated with low amplitude folds which occur in sub-bank sediments in Coplow Quarry. Two phases of folding were developed. The first consists of low amplitude folds with wavelengths in the order of 5-7m and axial trend towards 032°N. The second phase folds are superimposed upon the earlier folds and have wavelengths of about 1m, trending towards 100°N. Veinlets in these folds run parallel to the axial directions of both fold sets. Samples from the veins contain ferroan calcite cements of Stage H and I along with later ferroan saddle dolomite.

16.4 ASSOCIATION OF FRACTURES WITH STYLOLITES

Fractures and stylolites are both linear features and therefore commonly intersect one another, or are found in close association. This relationship is of value to the cement stratigrapher, as it can give useful evidence about the relative timing of cement stages and

their association with periods of tension and compression in the rocks.

The three common fabrics developed are:-

1. Stylolite truncates and displaces veinlet (e.g. Fig. 10.2E)
2. Veinlet cuts stylolite (Fig. 16.1F).
3. Veinlet exploits stylolite after tensional dilation along the solution seam. (e.g. Fig. 10.2E).

16.5 SIGNIFICANCE OF FRACTURES IN THE WAULSORTIAN BUILDUPS

Fractures had a critical influence on the progress of burial diagenesis in the Waulsortian buildups, after the large volumes of CFC cement, which precipitated early in the diagenetic history, had considerably restricted the available pore space in the buildups. Together with early compaction in the clay-rich peri-Waulsortian facies, this shallow burial cementation would have effectively sealed the buildups from migrating pore fluids. The occlusion of any remaining pore space was therefore totally dependent upon the development of fractures allowing cementing fluids into the system.

Considering any economic potential of the Craven Waulsortian, the late diagenetic fluorite-barite-lead-zinc mineralisation also developed along fractures, while the large volume of vein-fed cements which formed prior to hydrocarbon migration reduced the reservoir potential of the buildups.

The nature of the fabrics developed in cement-filled veinlets gives some idea of the degree of strain applied to the rock during vein formation. Cements in fractures which were occluded by burial calcites up to Stage G were usually post-dilational, whereas syntectonic veinlets were only filled by deep burial cement stages. Those veinlets which fed late diagenetic but shallow burial calcites (see Chapter 14) were also filled after vein dilation.

Fibre veins are geologically significant because they record the extensional strain directions during progressive deformation (Phillips 1986). They afford potential for further detailed work on stress fields in the Craven Basin by measuring the strain direction of the crystals.

In summary: study of the cross-cutting relationships of veinlets and stylolites and their association with void-filling cements is of critical importance when erecting a cement stratigraphy, and the application of that stratigraphy to determining relative timing of tectonic episodes.

CHAPTER 17
NEOMORPHISM

Introduction

The effects of the complex diagenetic history of the Waulsortian buildups of the Craven Basin were not solely confined to the development of cements in open voids. The ambient pore fluids imposed changes upon the entire rock body including sediments, bioclasts and existing cements.

The comprehensive term "neomorphism" was introduced as a definition for all processes which involve "transformations between one mineral and itself or a polymorph ... whether the new crystals are larger or smaller or simply differ in shape from the previous ones" (Folk 1965, p.21). Neomorphism is a broad term which encompasses two specific processes:

a) Inversion: a transformation from one polymorph of a mineral to another (e.g. aragonite to calcite).

b) Recrystallisation: a change in morphology or orientation while mineralogy remains unchanged (e.g. calcite to calcite, and including HMC-LMC transformations. See Folk 1965).

In the vast majority of cases, the diagenetic replacement of previously existing $CaCO_3$ phases (excluding dolomitisation) in the Waulsortian buildups involved the process of recrystallisation. There is no evidence that aragonite-calcite inversion was important. None of the cement phases in the buildups were originally aragonite, and most skeletal fragments which may have originally been aragonite were dissolved and the mouldic voids were subsequently filled by cement with little evidence for replacement of aragonitic bioclasts by neomorphic calcite. It is uncertain as to what proportion, if any, of the primary buildup mud was aragonite, either as detrital grains from the degradation of molluscan shells or early cement. Since mollusc fragments form only a small proportion of bioclasts, and

since the Dinantian was not an "aragonite period" in terms of early cementation (Sandberg 1983), inversion was probably of only minor importance in Waulsortian diagenesis.

The criteria for the recognition of neomorphic textures were based as much upon the absence of "characteristic" cement textures as the presence of distinctive neomorphic features (Bathurst 1959, 1975, 1983; Folk 1965). They were said to include:

a) the development of interlocking crystal mosaics with irregular intercrystalline boundaries, as opposed to the planar boundaries, including 180° enfacial junctions, held to be indicative of cements (sensu Bathurst 1975). Crystal mosaics were developed by a process of grain enlargement, or aggrading neomorphism to produce microspar (grain size 5-30 μm; Folk 1965).
b) presence of relict cement or grain structures as seen in CL, or in the form of inclusion patterns, which cut intercrystalline boundaries of crystal mosaics.
c) "patchy" extinction of crystals (Bathurst 1975, 1983).
d) Variability of grain size in a crystal mosaic with little tendency for increased grain size away from substrates as would be expected in cement mosaics.

It is apparent, however, that some of the textures which were suggested by Bathurst (1975) as being exclusive to void-filling cements, namely planar intercrystalline boundaries and uniform extinction, can also be developed by recrystallisation. Folk (1965) described "pseudospar", which is a recrystallisation product but has all of the characteristics of void-filling spar, while Dickson (1983) suggests that the total removal of precursor material during recrystallisation could produce a crystal aggregate where it was not possible to distinguish whether cementation or recrystallisation had been the effective process. Dickson (op. cit.) went on to show by crystal modelling that none of the proposed criteria for distinguishing cements were definitive, and that great caution should be used in distinguishing neomorphism and cementation in sparry fabrics.

17.1 RECRYSTALLISATION IN THE WAULSORTIAN BUILDUPS

Cements and sediments were both affected by recrystallisation during diagenesis. Although the "critical" textures described in the classic papers mentioned above were often observed, the main evidence is based upon observations using CL and staining techniques. Cathodoluminescence in particular is extremely effective in identifying relict structures which would not otherwise be visible.

17.1.1 Cement recrystallisation

A variety of textures were observed which evidently reflect the changes brought about by the effects of recrystallisation of pre-existing cements. The style of recrystallisation apparently depended upon the nature of the precursor cement, for example CFC cements exhibit recrystallisation textures which differ from those of scalenohedral and blocky calcite cements.

17.1.1.1 CFC cements

a) Origin of CFC

Many of the fabrics exhibited by CFC cements have been invoked as evidence for recrystallisation of a fibrous cement precursor (see Chapter 3 for a full discussion). The most important are the existence of palimpsest fibrous textures in isopachous layers of bladed crystal mosaics, including:

i. Inclusion trails which mimic textures in Recent fibrous cements and cut intercrystalline boundaries of the mosaic;
ii. Sweeping extinction but with a tendency towards more uniform extinction with decreasing inclusion density, loss of relict fibrous texture and the development of radiaxial fibrous calcite along a single CFC layer;
iii. Consistent palimpsest texture of isopachous fibrous cement in CL irrespective of all other textures.

One of the characteristic textures of CFC mosaics is the existence of irregular intercrystalline boundaries, defined by Bathurst (1975) as one of the classic neomorphic fabrics. However, it has subsequently been suggested that these irregular boundaries reflect primary, irregular impingement surfaces between growing composite crystals (Kendall 1985) or bundles of precursor fibres (Kendall & Tucker 1973; and this study, Chapter 6), and therefore irregular crystal boundaries need not be purely of neomorphic origin.

The overall conclusion from the majority of examples of CFC (RFC of Kendall & Tucker 1973) cited in the literature, and that which is confirmed by my own work herein, is that these cements were originally fibrous HMC. They were subsequently replaced by LMC and are therefore, in the strict sense of Folk (1965), a product of recrystallisation.

Stable isotope composition of the non-luminescent CFC is typical of Lower Carboniferous marine water values (see Chapter 6) and therefore it must be assumed that the HMC-LMC transition took place while the voids into which the cement precipitated were still filled with seawater.

b) Secondary recrystallisation of CFC

Diagenesis continued to affect CFC cements after the original HMC-LMC recrystallisation. The resultant fabrics follow the inclusion patterns in the CFC and are only identifiable in CL or occasionally by staining, as they do not affect the overall morphology of the crystals. They are the result of trace element substitutions within the calcite lattice brought about by the influx of subsequent diagenetic fluids. These fabrics represent an added dimension to the original definition of recrystallisation. Folk (1965) suggested that recrystallisation "... should be restricted to the case wherein the mineral species, in the petrographic microscope sense, remains identical through the change ... ignoring subtle changes in trace-elements or isotope proportions." The process involved in the development of the fabrics described below is a result of such subtle trace-element changes while still maintaining the gross mineral composition and is therefore still a form of recrystallisation in the

strict sense of Folk. The CFC cements have in fact, undergone a secondary recrystallisation.

CFC cements rarely exhibit homogeneous non-luminescence. Most commonly, they have a blotchy CL appearance which consists of irregular sub-micron-sized patches of brighter luminescence. Some of these small areas have a brick red luminescence and have been interpreted as microdolomite, itself a product of the original HMC-LMC transition (Lohman & Meyers 1977). The degree of blotchiness of these cements ranges from cases where the CFC cements have a dusty appearance in CL, to those where the brighter luminescent material occupies most of the crystal mosaic, leaving only small relics of the original non-luminescent material.

In other cases, bands of brighter luminescent material selectively follow the centripetal inclusion banding within the CFC mosaics. These centripetal bands, or fringes, often correspond to micrite crusts within the CFC cements, where there is often uncertainty if the brighter luminescence reflects a primary mineralogical difference between the micrite and the cement, or whether it reflects selective recrystallisation of the micrite. However, SEM investigation of micrite crusts revealed an irregular interlocking mosaic of anhedral microspar, indicative of neomorphism. In other cases, micrite is absent and the luminescent bands developed as conformable centripetal layers within the CFC cements, often extending completely around the cavity in which they formed. Such centripetal fringes appear, at first sight, to be conformable primary substages occurring within the CFC mosaic (Fig. 17.1 A&B). However, close examination shows that the majority of the fringes have diffuse margins, are laterally discontinuous in detail and may transgress the centripetal inclusion banding which does represent the primary growth fabric of the CFC cements.

These features indicate that the bright fringes are secondary fabrics which developed by recrystallisation along the centripetal growth fabric of the CFC cements. In the example shown (Fig. 17.1 A&B), the recrystallisation has highlighted the original growth fabric of a CFC mosaic composed of irregular layers of botryoidal mosaic which coalesced to form a thicker isopachous layer of bladed mosaic. This example also illustrates the diffuse nature of the margins of these brighter luminescent bands.

The commonest type of fringe developed along the conformable boundary between Stage A and Stage B calcites (Fig. 17.1 C&D). The primary growth fabrics of the cements, which would otherwise have remained undetected, were therefore revealed.

c). Mechanism of replacement and origin of diagenetic fluids

By what mechanism could this secondary recrystallisation of CFC take place? There is ample evidence in the Craven Waulsortian. Many of the luminescent fringes are associated with swarms of sub-micron hairline micro-veinlets. These micro-veinlets can often be traced through the CFC cements, along intercrystalline boundaries of the non-luminescent Stage B scalenohedral calcite cements and into cavity-filling spar sequences where they most commonly terminate within the bright luminescent Stage C or later Stage D cements, but rarely truncate them (Fig. 17.1 B&D). Invariably, the frequency of micro-veinlets decreases peripherally from the centre of the cavity. Micro-veinlets appear to have exploited the scalenohedral calcite intercrystalline boundaries, but on encountering the already once-recrystallised CFC cements, tended to propagate laterally, especially along the Stage A - Stage B interface.

This relationship is generally the rule in the rocks of this study, and indicates that the recrystallising fluids extended from the open void space towards the void walls along intercrystalline boundaries of existing cements, before selectively recrystallising CFC along some inherent physical / crystallographic or geochemical fabric. Probably for the same reasons, late diagenetic silica, associated with mineralisation in parts of the buildups, also selectively replaced CFC (see Chapter 13).

Spectacular examples of similar bright luminescent calcite fringes "soaking" into non-luminescent CFC cements were observed in samples of Waulsortian facies from Eire (Fig. 17.2). The fringes are fed by micro-veinlets which terminate in a thin bright luminescent cement stage, which itself post-dates non-ferroan non-luminescent scalenohedral calcite in a cement sequence very similar to that of the Craven Basin. The CL intensity of the diffuse region gradually passes into duller and finally non-luminescent CFC cement, indicating

that the recrystallisation had propagated by soaking out from the void centre. A microprobe trace-element traverse across this fringe showed a steady decrease in Mn in the CFC away from the centre of the original void. This Mn decrease was accompanied by a more erratic, but generally increasing trend in Mg towards the non-luminescent (i.e. least recrystallised) CFC, while Fe showed no systematic variation. The combined CL and trace element analysis from the Irish Waulsortian confirms the observations on the Craven Basin Waulsortian, and indicates that recrystallisation fringes developed by outward migration of diagenetic fluids from open voids within the bank facies. However, the precise means by which the recrystallising fluids penetrated the earlier cements is uncertain. Two examples of recrystallised CFC cements from the Craven Basin, showed a major isotopic shift in composition from those of non-luminescent CFC Stage A (Table 17.1), emphasising the need to select cement samples for isotopic analysis with great caution.

Table 17.1. Comparison of mean isotopic composition of Stage A with recrystallised CFC, in per mil (°/₀₀) vs PDB standard.

Sample	Calcite type	CL intensity	$\delta^{13}C$	$\delta^{18}O$
ASH3	Fe and Non Fe	Dull blotchy	+2.07	-5.41
HN	Fe and Non Fe	Moderate blotchy	+2.81	-4.17
Stage A	mean value for comparison		+3.40±0.2	-1.96±0.5

Use of the term "micro-veinlet" in describing the hairline features associated with recrystallisation fringes requires some qualification, arising from the genetic implications of fracture and open void space that the term implies. The brightly-luminescent hairline features extend along intercrystalline boundaries in the prismatic cements but tend to terminate at the CFC-Stage B boundary

or sometimes within the CFC. Were they a product of fracturing, some degree of penetration into the surrounding sediment forming the walls of the void would be expected, yet this is uncommon. It appears, therefore, that these particular micro-veinlets exploited inherent planes of weakness in the crystal aggregates of the affected cements, particularly intercrystalline boundaries (primary or relict inclusion trails) and the Stage A- Stage B boundary which is itself commonly marked by a dense layer of inclusions.

The development of the hairline micro-veinlets did not involve noticeable fracturing, but at the same time, dissolution is evident along their margins (Fig. 17.2), and the blotchy patches of recrystallised material into which they are infiltrated also give the impression of a dissolution fabric. It would appear, therefore, that diagenetic fluids gained access to the earlier cements by fine-scale dissolution - precipitation fronts which were concentrated along crystallographic planes of weakness, perhaps as a solution-film process (cf. Bathurst 1975, pp.497 & 501).

Further complexities arise when considering the tendency of many diffuse fringes of bright CL to form as a selective replacement of centripetal bands within the CFC cements, where the bands themselves do not appear to represent any physically discrete fabric. Such selectivity was not consistent. In many CFC layers, the fringes developed along centripetal zones of inclusions, but in others the recrystallisation was concentrated along less turbid horizons.

The lack of consistency indicates that there were factors other than the inherent or relict physical properties of the CFC cements which controlled the development of the diffuse fringes.

Chemical variation within the CFC (either resulting from the HMC-LMC transition or, more probably, from a relict chemical zonation of the fibrous precursor cement), may have been exploited by the secondary recrystallisation. Returning to the data from the Irish Waulsortian (Fig.17.2) which shows Mg decreasing with increasing Mn (and CL) across the CFC layer, it was noticed that the Mg decrease was eratic, compared to the smooth Mn increase. It is possible, therefore, that the nature of the Mg trend in this example not only reflects Mg^{2+} loss from the cement during recrystallisation, but also a degree of primary variation in the Mg content of its precursor cement.

A similar (if tentative) explanation of comparable textures in oolites from Jurassic hardgrounds was proposed by Marshall and Ashton (1980) which may be applicable to the examples in this study. Their explanation proposed that:

1. Chemical and mineralogical variation is common in recent submarine cements.
2. Zones of variable Mg content could have been developed in the fibrous precursor cement, perhaps caused by temperature fluctuations during growth (cf. Fuchtbauer & Hardie 1976).
3. The stability of HMC is inversely related to its Mg content (Richter & Fuchtbauer 1978) and therefore high Mg zones within the precursor cement (occurring as a relict chemical zonation) would be particularly susceptible to replacement (in their case by ferroan calcite which was only apparent after staining).

17.1.1.2 Recrystallisation in post-CFC cements

The main effect of recrystallisation in the coarse blocky calcite spars which post-dated CFC was the development of crystal aggregates (see Chapter 9). The recrystallisation fabrics are only visible in CL or by staining. The aggregates formed in centripetally cemented voids and consist of irregular, often angular patches of calcite which occur within crystals of different trace element composition as indicated by CL or staining. Close examination of these aggregates shows that the crystal faces of the angular regions are parallel to the cleavage planes of the host crystal (Fig. 17.1E) while the cleavage planes extend across the entire crystal fabric. The patches with angular faces are optically continuous with the rest of the aggregate. Some of the angular patches reach the margins of the host cement, and are commonly connected to a later void-filling cement stage, so it is obvious, from their common CL and staining characteristics, that both cement and replacive calcite were precipitated from the same fluid. As with the CFC replacements, the aggregates appear to have developed outwards from the open void space in the cavity centres which were themselves subsequently filled by cements. Near the cavity centres, small relict fragments of the unaltered original cement 'float' in the later material, indicating

that the neomorphic process was one of recrystallisation and not dissolution, which would have produced a void stage leading to collapse of the early crystal fabric. However, evidence of small-scale dissolution also commonly accompanies the development of these aggregates. Some of the aggregate sub-crystals exhibit irregular dissolution surfaces, and it would appear that the process of fine-scale dissolution-precipitation or solution film recrystallisation was responsible for the development of the aggregates. Impingement aggregates also show evidence of recrystallisation (Chapter 9).

In some cases, the recrystallisation of the existing cement went almost to completion, and here again the problems of distinguishing cement from replacement become acute.

17.1.2 Recrystallisation of sediments.

The primary (M1) sediments occurring in the Waulsortian facies consist of a complex mixture of different mud generations which underwent patchy and partial cementation and dewatering during early diagenesis. Internal reworking of this primary sediment was accomplished by dissolution, collapse, neptunian dyke development and possibly a degree of micro-organic activity. This resulted in the development of a variety of secondary internal sediments within the complex void system in the banks.

There are three main components of the sediments in the Waulsortian facies of the Craven area:

1. Micrite-Microspar
2. Peloids
3. Bioclasts

The problems of distinguishing cement, neomorphism and original grains in such very-fine grained sediments are acute, and almost impossible to resolve.

1. Micrite-microspar

The Waulsortian facies is characterised by the high proportion of fine-grained sediment over other constituents. This consists primarily of dense micrite (< 4 μm) and varying amounts of microspar (5-30 μm sensu Folk 1965).

Some of the thin-sections used in this study were wedged, leaving ultra-thin regions (less than 5 μm) at the edges. This was fortuitous, as the ultra-thin areas clearly revealed the micrite fabric in single-crystal thickness (Fig 17.1F). The fabric comprised an inequigranular mosaic of irregular shaped micrite and microspar crystals which contained relics of former sedimentary fabrics, i.e. the classic neomorphic spar of Bathurst (1975, p.485), presumably formed by aggrading neomorphism (Folk 1965). As the wedged sections grade towards increasing thickness, the apparent neomorphic texture passes into the dense micritic appearance which is normally characteristic of these sediments in sections of standard thickness. Within the 30 μm thickness of the standard thin sections, numerous grain boundaries may overlap, thus disguising the neomorphic fabric of the micrite. Earp et al. (1961, p.41) reported similar observations on Craven bank facies. (It is probably because she did not look at ultra-thin sections, that Cowan (1980) concluded that aggrading neomorphism was absent in Waulsortian bioherm muds from New Mexico). SEM examination of Craven bank facies micrites also showed inequigranular, interlocking crystal mosaics with no evidence of grain fabrics.

Staining shows that most Waulsortian micrite and microspar is non-ferroan calcite, while in CL the micrite varies from dull to bright orange and defines complex regions of differing luminescence which usually have diffuse boundaries and are often not visible in PPL (Fig. 17.1 G&H). From the evidence of pre-CFC dissolution episodes (Chapter 5), it is apparent that some precursor intergranular cement must also have been present. Close examination often reveals scattered euhedral crystals (<50 μm) which have non-luminescent cores and bright to dull rims which are equivalent to the Stage B-D sequence, indicating neomorphism during shallow burial diagenesis. These euhedral crystals frequently developed on larger skeletal grains, and grew at the expense of the surrounding micrite. They are similar to the solution corona overgrowths described by Walkden & Berry (1984b) in that they have euhedral compositional zonation and yet are single crystals entirely surrounded by micrite. They differ from solution corona overgrowths in that they have euhedral margins whereas the solution corona overgrowths have characteristically

irregular margins. Furthermore, examples of this type of crystal occur in geopetal sediments which have no bioclastic component and seem to have grown purely at the expense of the micrite sediment by recrystallisation. These crystals may well represent the true pseudospar of Folk (1965).

CL often reveals relics of fossil grains in the recrystallised sediments which are not visible by other means. Geopetal micrite is also often clearly defined in CL as it tends to have different luminescence characteristics to the surrounding material. It is not uncommon to find diffuse gradation in luminescence across a geopetal sediment with intensity decreasing away from the cavity centre to form identical "soaking outwards" fabrics to those developed in CFC. The difference in luminescence of the geopetal micrites from that of the M1 sediments indicates that they recrystallised at different times to the M1. The relative timing is uncertain, as there is no consistency in the CL characteristics of either primary or secondary micrites. In any case, the diachronous nature of shallow burial cements indicates that neomorphic processes, which were induced by the same ambient pore fluids, would also be diachronous.

These neomorphosed geopetal muds are only common in post-CFC geopetal fills or those in cavities where CFC cements are only thin or absent. In these cases, the fluids residing in void centres were able to penetrate the cement seal and access the sediment beyond.

2. Peloids

Peloids make up a significant proportion of both primary and geopetal sediments and commonly exhibit blotchy luminescence similar to the micrite sediments. Interstices of peloidal sediments may be micrite or spar-filled.

Intergranular spar in peloidal sediments is usually inclusion-rich microspar and it is uncertain if it was originally cement or if it resulted from selective neomorphism of precursor cement or interstitial micrite. In some examples, however, thin CFC cement fringes coat peloids, confirming that some at least were cemented. Pelsparite fabrics are varied and often complex. In many cases the peloids are well defined, showing simple ellipsoidal or quadrate

shapes, and tending to 'float' in the sparry matrix which itself often exhibits cement textures. In other cases however, especially in the M1 sediments, the peloids are diffuse and highly irregular in shape and often impart a mottled appearance in PPL (Fig. 17.1G) that has been referred to as "structure grumeleuse" (Cayeux 1935), and is interpreted as a replacive fabric (see Bathurst 1975, p.511 for discussion). Intergranular cement in peloidal sediments is usually a duller luminescence than the peloids and indeed is often non-luminescent.

Those peloids which occur in a micritic matrix may show CL identical to their parent matrix, but more commonly the two components have different CL. Variation in luminescence between peloids in the same sediment was also occasionally observed. Usually, those peloids which have a more dense appearance in PPL (i.e. smaller grain size) tend to have brighter CL characteristics. This indicates that grain size of the original peloid did have some control on the neomorphic process. The brighter luminescence of the finer-grained components is similar to that of Stage C while the duller luminescent coarser components are similar in CL to Stage D. It is possible, therefore that fine-grained material was slightly more susceptible to recrystallisation by early diagenetic fluids.

3. Bioclasts

In the bank facies, those fossils thought to have been originally composed of aragonite (mainly molluscs), and siliceous hyalostelid sponge spicules are only preserved as cement-filled moulds. Non-mouldic bioclasts often luminesce characteristically. Bryozoans and most ostracods, originally HMC, usually luminesce moderate to bright orange, while other originally HMC bioclasts, such as echinoderm grains, range from non-luminescent to bright orange-yellow. Pleurilocular foraminiferan walls and the calcified sheaths of Girvanella were composed of micrite which commonly luminesces brightly. Brachiopods are the only common fossils in the Waulsortian facies which were originally LMC, and this is reflected in the fact that they are consistently non-luminescent and have well-preserved microstructure. The vast majority of fossil grains also give a non-ferroan calcite staining response.

Figure 17.1 Neomorphism of calcite cements and sediment

A&B PPL and CL photomicrograph pair showing recrystallisation of a CFC cement layer. In PPL, the inclusion-rich CFC is seen to contain zooecia of a fenestellid bryozoan frond (F), but is otherwise structureless. In CL, a complex sequence of irregular, sub-isopachous, brightly-luminescent fringes are identified, revealing the relict textures of the CFC layer which nucleated on the fenestellid. While giving the impression of a conformable primary cement sequence, the fringes (arrowed) are diffuse in detail and are inter-connected by hairline, substrate normal micro-veinlets, indicating that recrystallisation had occurred along relict structures of both the CFC precursor fibrous crystal boundaries, and the centripetal growth banding. Sugarloaf buildup.

C&D PPL and CL photomicrograph pair. In PPL a cavity supported by a bryozoan grain is filled by a sequence comprising: A; inclusion-rich CFC of Stage A followed by B; less turbid scalenohedral calcite followed by M; geopetal mud and finally S; clear blocky spar; all cut by micro-veinlets (V). In CL, a difuse and discontinuous brightly luminescent recrystallisation fringe (f) is revealed marking the boundary between stage A and non-luminescent scalenohedral crystals of Stage B. Microveinlets (mv) connect the fringe to brightly luminescent calcite spar in the cavity. In one area (tr) the fringe transgresses from the cavity spars, across Stage B to the Stage A-B boundary. Notice also that the geopetal mud shares the same luminescent characteristics as the fringe, and was therefore probably recrystallised at the same time. The micro-veinlets (V) seen in PPL contain a later duller luminescent calcite cement (probably Stage E or F). Coplow buildup.

E Photomicrograph of a stained thin section, showing the development of a crystal aggregate by the recrystallisation of a deep burial ferroan calcite cements (fe) by later non-ferroan calcite (nf). The recrystallised areas have irregular but angular boundaries (arrow 1), which parallel the major cleavage planes in the ferroan calcite crystals (depicted by white dashed lines). Arrow 2: shows where the boundary of the ferroan calcite was breached by the fluids which sourced the recrystallisation. Bellmanpark buildup.

F PPL photomicrograph of an ultra-thin area (approx. 5 microns thick) of a thin section showing auhedral neomorphic microspar and relict skeletal grains (arrowed) crystal boundaries in a bank facies sediment from Bellmanpark Quarry. In areas of the same sample which are standard 30 micron thickness, the overlapping of several auhedral grain boundaries masks the overall neomorphic texture, and the sediment takes on the appearance of a fine grained biomicrite.

G&H PPL and CL photomicrograph pair of a mottled peloidal sediment from Sugarloaf buildup. In CL, a patch of blotchy to non-luminescent sediment (nl) is separated from an area of brighter luminescence (bl) by a spar-filled cavity (s) containing cement Stages B-D. The brighter luminescent (bl) region contains many euhedral crystals (arrowed), largely consisting of non-luminescent Stage B but occasionally with rims of bright Stage C, and, rarely, dull Stage D. These crystals largely developed as overgrowths on bioclasts, including crinoid grains (c), but must have grown by recrystallisation of the peloidal sediment.

Fig. 17.1

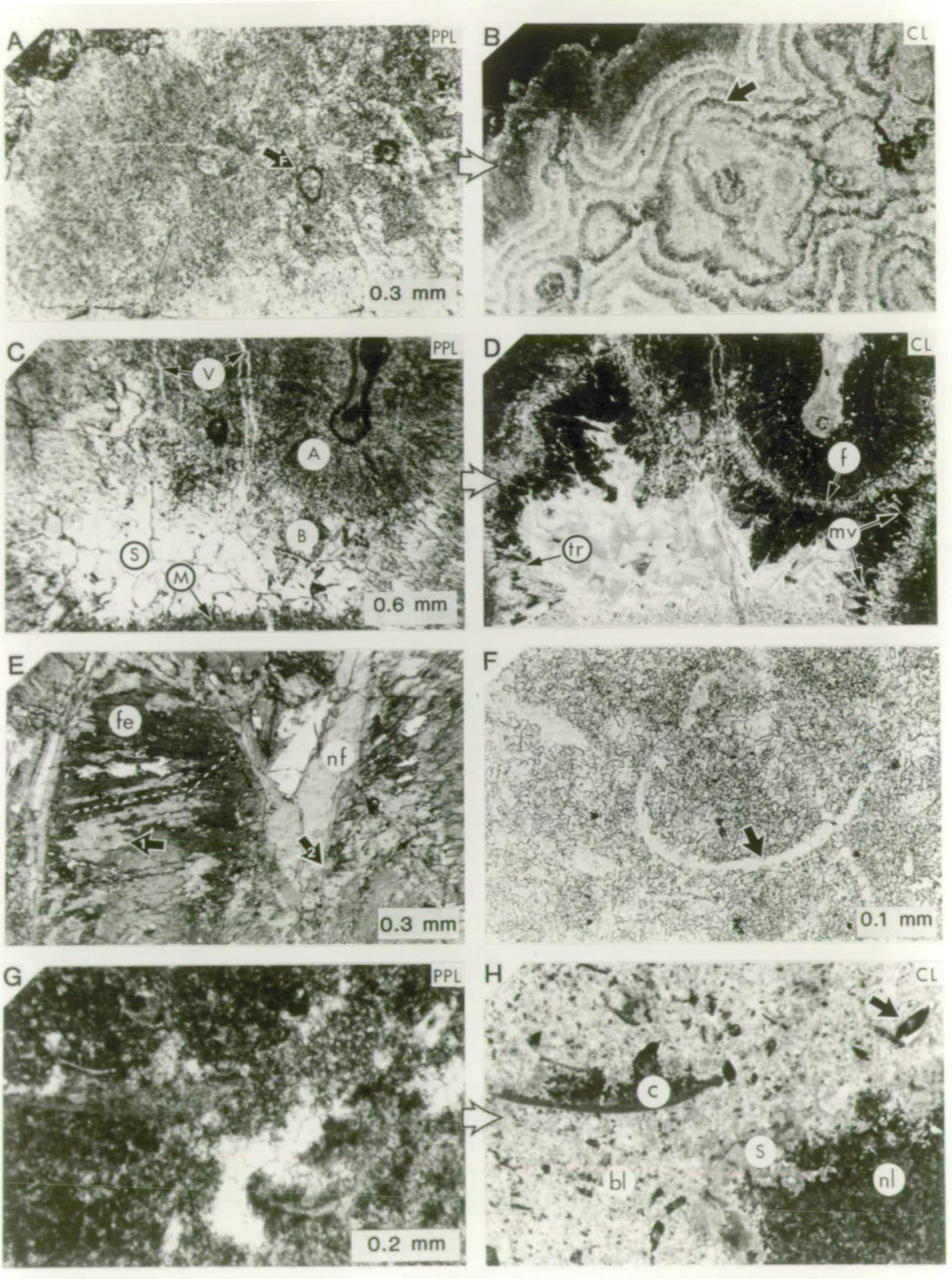
A
PPL
0.3 mm
B
CL
C
PPL
V
A
B
S
M
0.6 mm
D
CL
f
mv
tr
E
fe
nf
0.3 mm
F
0.1 mm
G
PPL
0.2 mm
H
CL
c
S
bl
nl

Figure 17.2 Compositional variation in recrystallised CFC.

A Cathodoluminescence photomicrograph showing a recrystallisation fringe in CFC cement. The brightly luminescent area was caused by replacive fluids "soaking-out" from the cavity centre (right hand side of picture) via micro-veinlets along intercrystalline boundaries in non-luminescent scalenohedral calcite (arrowed). The micro-veinlets, which can be traced to a brightly luminescent cement in the void-fill, have irregular margins indicating dissolution of the non-luminescent cement stage. Luminescence intensity of the fringe decreases away from the cavity centre (towards '1'). Location of a microprobe traverse (1-8) across the fringe from unaltered, non-luminescent CFC (1) to highly recrystallised cement near the CFC-scalenohedral calcite boundary (8) is marked by a dashed arrow. Trace element analyses are given in B. Example from Waulsortian bank facies, Silvermines, Central Irish Basin. Field of view = 1.5mm.

B. Plot showing MnO, MgO and FeO variation in eight spot analyses along the microprobe traverse shown in 'A'. MnO increases while MgO decreases towards the more recrystallised area (brighter CL). FeO is effectively absent.

Fig. 17.2 MnO, MgO and FeO VARIATION ACROSS RECRYSTALLISED CFC

A

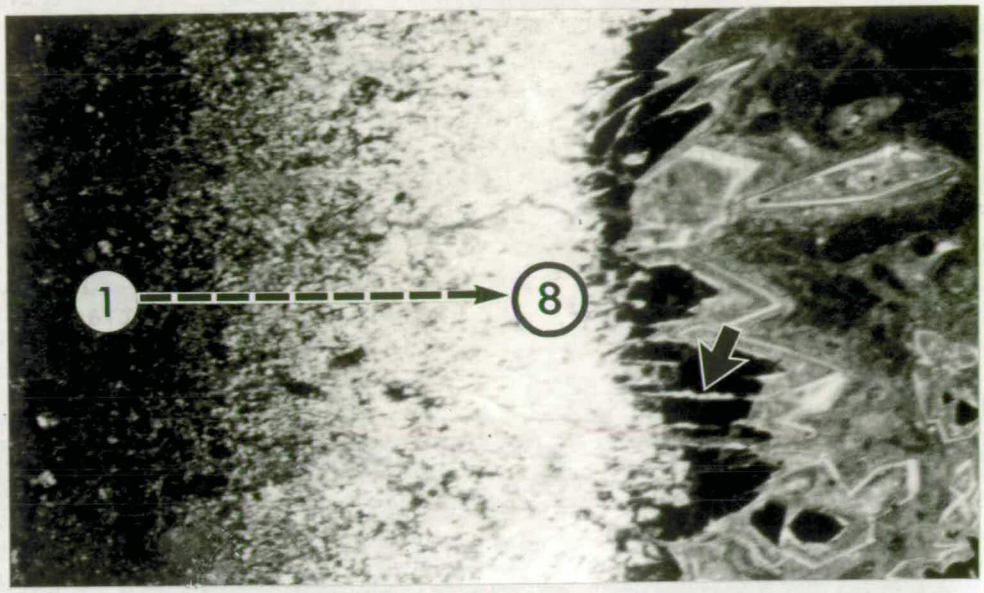

B

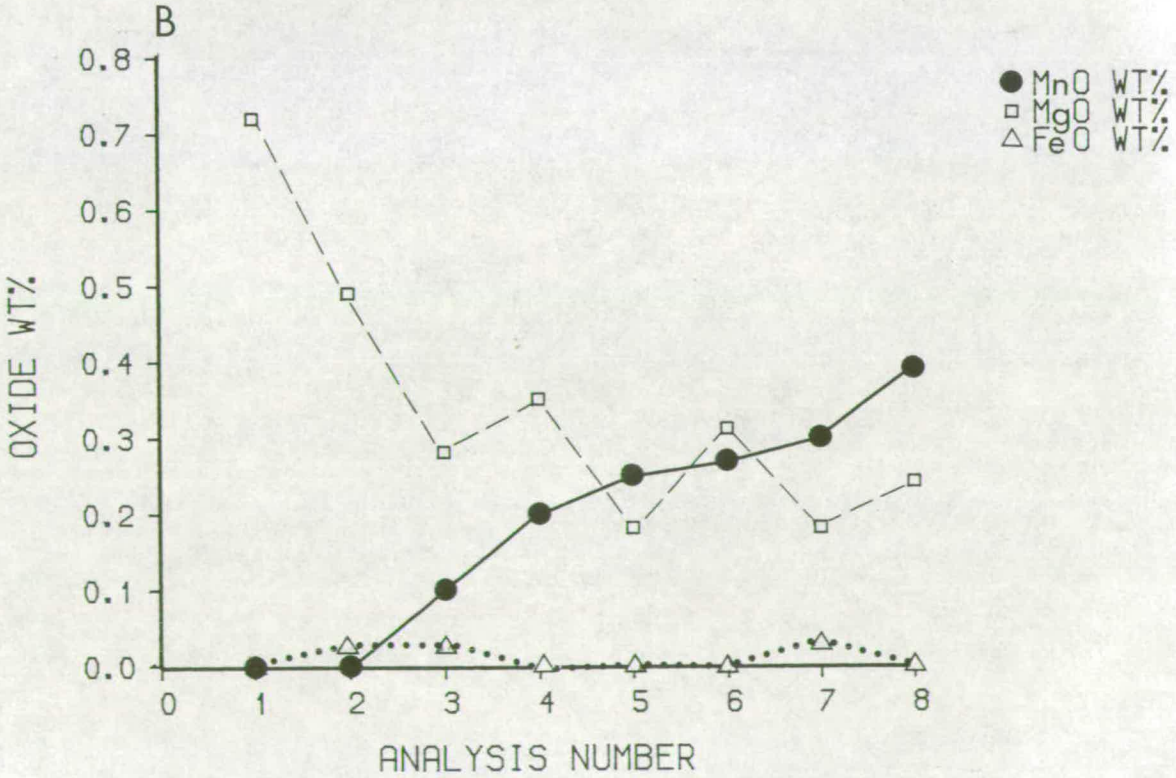

The degree of skeletal fabric retention is generally good in all cases, except for crinoids where preservation quality is highly variable. Some crinoid ossicles contain regions of different luminescence. The originally porous stereome is commonly filled with bright luminescent calcite, which may have been cement, while the rest of the grain is dull or non-luminescent. Rarely, small brick-red luminescent microdolomites occur in the stereome, and these may have a similar origin to those found in radiaxial fibrous calcite by Lohmann and Meyers (1977), i.e. products of the HMC-LMC transition. Edges of crinoid grains may also be preferentially recrystallised, as often are the cleavage planes which develop in these large single-crystal bioclasts. Although most crinoids in the bank facies are now non-ferroan calcite, staining shows that others are partially replaced by ferroan calcite.

Stable isotopic compositions of non-luminescent bioclasts are indistinguishable from those of Stage B cements (Fig. 7.7) which, along with the comparable staining and CL characteristics indicates that such allochems recrystallised while the pore fluids were still essentially oxic seawater.

17.2 TIMING AND ORDER OF RECRYSTALLISATION

17.2.1 CFC cement.

a). HMC-LMC transition

The original transition of the HMC fibrous precursor to CFC resulted in a substantial loss of Mg and must have involved a fluid phase (Bathurst 1975; Marshall & Ashton 1980). Non-luminescence and low concentrations of Fe^{2+} and Mn^{2+} indicate oxic porewaters (see Chapter 6&7). CFC cements retained an essentially marine isotopic composition which suggests recrystallisation took place while the pores still contained sea water (Hudson 1978; Marshall & Ashton 1980).

b). Diffuse fringes.

Most diffuse layers are non-ferroan calcite and have moderate to bright orange-yellow CL similar to that of Stage C and Stage D cements. Many diffuse fringes can be directly linked by hairline 'microveinlets' to void-filling Stage C and D cements, confirming that most of this 'secondary' recrystallisation occurred in the shallow subsurface after pore fluids had begun to turn anoxic. The Stage C and D cements were diachronous, and therefore the recrystallisation of CFC must also have been diachronous.

Some diffuse fringes are composed of ferroan calcite and therefore must have developed at deeper burial depths than the Stage C and Stage D equivalents. It is not uncommon to find more than one phase of 'secondary' recrystallisation in the CFC cements (and micrites) of this study. Recrystallisation and cementation are commonly coeval, and it is possible that all major changes in pore fluids produced both recrystallisation and cementation.

17.2.2 Drusy calcite cements

Recrystallisation of void-filling post-CFC cements was usually associated with the dissolution episodes which marked cement stage boundaries. This often meant that recrystallisation was primarily confined to cements which were temporally or stratigraphically adjacent, i.e. a cement stage was often only recrystallised by fluids from which the succeeding stage precipitated. A common example of this type of replacement resulted in the development of the complex replacement aggregates which tend to be associated with the ferroan calcite stages (see Chapter 9).

Of the deep burial fluids from which calcite cements precipitated, those of Stage N were the most aggressive. This consistently resulted in the development of marked dissolution surfaces and initiated significant recrystallisation of earlier cements along cleavage planes and intercrystalline boundaries.

17.2.3 Sediments

In common with CFC cements, the recrystallisation of most sedimentary grains took place during shallow burial diagenesis and was initiated by the non-ferroan calcite Stage B-D fluids, particularly those of C and D which indicate suboxic to sulphate reduction diagenetic zones (Chapter 7). However, recrystallisation was a continuous process, and all late diagenetic fluids potentially effected a degree of recrystallisation in all sediments. Cathodoluminescence, showing the presence of bioclasts in sparry or clotted micrite, provides good evidence of recrystallisation of former sediments. Of the bioclasts, only brachiopod shell material showed any consistency in CL and staining characteristics which could be interpreted as being representative of a particular stage in the diagenetic sequence in the Waulsortian facies. The non-luminescence of these bioclasts along with their characteristic marine stable isotope composition and consistently good primary fabric retention indicates that any recrystallisation had occurred while oxic seawater was the dominant pore fluid. It is possible that the brachiopods have actually undergone very little recrystallisation, as they were originally LMC and their non-luminescence indicates that no trace element substitution occurred. It is for these reasons that non-luminescent brachiopods have been seen as good material for isotopic analysis when attempting reconstructions of palaeo-seawater composition (see Chapter 7).

It has been suggested in various publications that certain fabrics are replaced more readily than others. Bathurst (1959) suggested an order of increasing resistance to replacement in Dinantian limestones, namely: micrite, peloids, dasycladacean algae, foraminiferida, ooids. Other authors have suggested orders of recrystallisation for skeletal grains (eg. Crickmay 1945; Schlanger 1964; Banner & Wood 1964). Jameson (1980) deduced an order based upon the CL characteristics of fossil components in a Dinantian limestone from the Midland Valley of Scotland. No such sequence of recrystallisation can be proposed for the Craven Basin Waulsortian as there is too much variation in luminescence characteristics of

individual fossil groups. Jameson (op. cit.) mentions similar variation within his samples but was still able to construct his generalised order of recrystallisation. Lasemi and Sandberg (1983) indicated that the fabrics and geochemistry of neomorphosed sediments (and therefore, presumably, their CL), is partially dependent upon the precursor mineralogy.

I would suggest that there are rather too many potential variables which may affect the susceptibility of sediments and their constituent grains to recrystallisation in ancient rocks. These include:

1. Original mineralogy and stability of the grain.
2. Mineralogy of surrounding grains.
3. Porosity-permeability characteristics of surrounding grains related to grain size, degree of sorting and degree of cementation.
4. Proximity of the grains to fluid reservoirs or conduits i.e. open cavities, fractures, stylolites.
5. Degree of cementation bounding fluid source areas. Cavities with thick isopachous cements may prevent diagenetic fluids from entering the surrounding sediment while those with little or no cement are easily penetrated.

I therefore do not propose any sequence of recrystallisation for the sediments in this study, except to confirm the views of several previous workers that brachiopods, because of their primary LMC composition, are least likely to show recrystallisation fabrics, and to add that most sediment and CFC recrystallisation was effected by early diagenetic fluids in the suboxic and sulphate reduction environments.

17.3 IMPLICATIONS OF NEOMORPHISM FOR CEMENT STRATIGRAPHY

Cement stratigraphy involves the recognition of a sequence of cement stages in which the oldest cements are usually nearest the primary substrate. Recrystallisation of the kind described above results in the development of crystals which assume an anomalous position within the cement stratigraphy, potentially leading to

misinterpretation of the diagenetic sequence. For example, failure to identify the replacive nature of textures such as the diffuse fringes in CFC described above could result in the effects of a single change in pore fluid composition being interpreted as two separate episodes; the replacive phase being assigned to an earlier diagenetic episode than the later cement phase. The replacive phases are, in effect, a repetition or reversal of the cement sequence. The multiple banding in Fig.17.1B could be interpreted as a multiple sequence of bright and dull luminescent cements, but in reality the bands are all related to a single recrystallisation phase which affected a non-luminescent CFC cement layer at some time after the cement was precipitated.

There is considerable variation in the degree of cement recrystallisation in the Waulsortian of the Craven Basin, both within and between buildups, although no systematic pattern could be discovered.

Failure to indentify the recrystallisation fabrics could result in the following types of misinterpretation of a regional cement sequence and diagenetic history:

a. Incorrect interpretation of diagenetic environments from CL, trace-element and isotopic characteristics of recrystallised material.

b. Misinterpretation of localised variations in cement stratigraphies (and therefore diagenetic environments and palaeoaquifer distributions), if variations in the degree of recrystallisation were wrongly assumed to be primary cement textures.

c. Failure to recognise real local variation in cement sequences if recrystallisation had masked the primary characteristics.

d. Incorrect identification of repetition within the cement sequence as a result of anomalous positioning of recrystallised material.

CONCLUSIONS

1. Recrystallisation, the neomorphic process of replacement without involving gross mineralogical change, affected all rock fabrics, at least to some degree, in the Craven Basin Waulsortian build-ups.

2. CFC cements are themselves a product of recrystallisation from HMC precursor to LMC. They were substantially recrystallised during later diagenesis, often totally, but usually in diffuse fringes along selective centripetal bands which probably reflect the primary growth fabric of the precursor fibrous calcite.

3. Development of the diffuse centripetal fringes in CFC was controlled by:
   a) presence of micrite horizons
   b) primary growth fabrics
   c) inherent variations in chemical composition.

4. Most diffuse fringes of CL in CFC were connected by dissolution-precipitation micro-veinlets to early diagenetic Stage C and Stage D void filling cements.

5. Post CFC cements were recrystallised via fluids of the stage which immediately post-dated their development (in a stratigraphical sense), leading to the development of complex crystal aggregates.

6. Neomorphism in micritic sediments was complex and often multi-phase. Despite difficulties in distinguishing neomorphism and cement at such fine grain sizes, ultra-thin sections indicate that all micrite has been neomorphosed/recrystallised. Aggrading neomorphism was common, and euhedral, compositionally-zoned pseudospar also developed.

7. Peloids generally show different luminescence to enclosing spar or micrite. In these cases, recrystallisation was selective, towards either the peloids or the interstitial material. It is possible that the peloids recrystallised after coexisting micrite as indicated by Bathurst (1959) when he studied these rocks. Recrystallisation of the M1 sediments often developed clotted micrite/spar textures of "structure grumeleuse" type.

8. Aragonitic mollusc shells and siliceous sponge spicules were dissolved during early diagenesis, leaving mouldic voids which became cement-filled. Of the other fossil grains, only brachiopods show consistent CL characteristics, and this may be because they were originally LMC and have undergone little or no recrystallisation. It is not possible to construct an order of recrystallisation for other bioclasts owing to the highly variable CL characteristics within individual fossil groups. Echinoderm material shows most CL variation and brachiopods least.

9. A range of variables may affect the degree of recrystallisation of grains in a sediment or cement sequence including: the nature, mineralogy and porosity-permeability characteristics of surrounding material; original mineralogy of grains; proximity to fluid reservoirs and conduits and the effectiveness of cement seals within them.

10. The products of recrystallisation can be confusing in cement stratigraphies because: they often occupy anomalous positions within the sequence; they may result in total loss of primary fabric, trace element and isotopic characteristics which lead to incorrect inferences on diagenetic environments; they may mask real variation in cement sequences on local or regional scales.

11. Recrystallisation may selectively replace and therefore highlight primary cement fabrics which would otherwise not be identifiable.

12. Cathodoluminescence is a valuable character for identifying neomorphic fabrics.

13. Most recrystallisation and neomorphic fabrics in CFC and sediments were effected by Stage B-D fluids during the period of early diagenesis which produced non-ferroan LMC. Recrystallisation was a continuous process and occurred to some degree in association with the development of most cement stages. Fluids effecting recrystallisation during early stages "soaked-out" from open voids, resulting in gradual decrease in recrystallisation away from the source.

14. The Waulsortian rocks of the Craven Basin are as much a product of neomorphism (recrystallisation) as they are a product of sedimentation and cementation.

SYNTHESIS

&

CONCLUSIONS

CHAPTER 18
SYNTHESIS: BURIAL HISTORY AND POROSITY EVOLUTION

18.1 BURIAL HISTORY and DIAGENETIC ENVIRONMENTS

18.1.1 Introduction

The major episodes of basin development, as deduced from the litho- and tectono-stratigraphy of the Craven Basin (Grayson & Oldham 1987; Gawthorpe 1987) are summarised below:-

a). Dinantian

The Tournaisian transgression produced an extremely thick, monotonous sequence of argillaceous and calcareous mudstones, heavily bioturbated and punctuated by algal oncolite horizons which indicate modertately shallow depths on the distal portion of a subsiding ramp. Subsidence more or less kept pace with sedimentation into the Chadian (Chatburn Limestone Formation), but this was followed by a phase of deepening (probably to near the photic limit), generating the Waulsortian complexes of the Clitheroe Lst. Fm. This area of continued subsidence and thick sedimentation, the Craven Deep (sensu Grayson & Oldham op. cit.), persisted for the remainder of the Dinantian and into the Namurian. Structurally, the Deep was already somewhat complex, including several mid-basin highs, represented by abnormally thin Dinantian sequences, possibly caused by small tilt blocks or half-grabens (Miller & Grayson 1982). As a result of tectonism during the late Chadian/early Arundian, this structure became modified by a series of NE-SW and NW-SE trending faults (Gawthorpe 1987). This was associated with submarine erosion and the development of local unconformities and debris flow deposits.

This period of tectonism marked the transition from carbonate ramp to slope sedimentation (Gawthorpe 1986).

A second phase of tectonism within the Dinantian occurred during late Asbian/early Brigantian times, resulting in the break-up of the

northern rim of the basin, allowing major clastic influxes, dominantly clays intercalated with turbiditic sandstones. This ended major carbonate sedimentation within the basin. (Gawthorpe 1986 op cit.).

b). Post-Dinantian

Deposition of Namurian fluvio-deltaics and Westphalian Coal Measures after the Dinantian, increased the thickness of the post-Waulsortian sediment pile to somewhere in the region of 3km. Further reactivation of the Hercynian structures during Upper Carboniferous (Stephanian) times resulted in major uplift and the development of the Ribblesdale Fold Belt (Gawthorpe 1987). Severe erosion occurred as a result of this uplift, reaching Mid-Dinantian sediments in some parts of the Craven Basin.

Burial then resumed with the deposition in the Permo-Trias of Zechstein marls and aeolian sands, the latter represented by small outliers resting on Chadian and other Dinantian beds.

Although the Hercynian orogeny had largely run its course by the end of the Permo-Triassic, movement on the Hercynide structures continued after this time, and during one late phase was associated with hydrothermal mineralisation. With the exception of Pleistocene boulder clays and Recent river sands and gravels, there are no post-Permo-Trias sediments in the Craven Basin. There is, however, evidence of continued tectonism during the Tertiary, particularly represented by intrusion of a single basaltic dyke.

18.1.2 Burial and Diagenetic trends

Having established the diagenetic history of the Waulsortian and adjacent facies in the Craven Basin, it remains to combine these observations and interpretations with the lithostratigraphy, and attempt an overview of the burial history of these rocks (Fig. 18.1). The curve for estimated depth of burial (Fig. 18.1) is based on the $\delta^{18}O$ values of successive cement stages. It must be stressed that it is the trend of this curve which is important. It was decided not to apply any correction to dolomite $\delta^{18}O$ values; firstly because the degree of correction that should be applied is uncertain and contro-

versial (see Chapter 11); secondly, because the correction would not affect the overall trend; and thirdly, because the estimated burial depths used as a guideline in Fig. 18.1 best fit the observed changes in thickness of the post-Waulsortian sediment pile when no correction is applied. The problems of relating $\delta^{18}O$, which is under temperature contol, to depth of burial in a sediment pile have already been discussed (Chapter 12). It is for those reasons that the burial depths indicated in Fig. 18.1 are merely a working estimate. However, the calculated burial curve is a good fit with lithostratigraphic data, and this gives confidence that it is indeed a reasonable representation of the burial history of the Waulsortian. In the absence of any precise constraint upon the timing of the cement stages, beyond the relationship of some of them to specific fracturing episodes, the time scale on Fig. 18.1 is an arbitrary one.

18.1.2.1 Shallow Burial Phase

The Waulsortian buildups in the Craven Basin were formed in the moderately deep-water marine environment, within the photic zone but below the level of storm-wave base (Lees & Miller 1985). This was the starting point for the subsequent diagenetic and burial histories of the deposits. Early dissolution episodes in the bank facies resulted in significant modification and volumetric increase in the primary void network. Incipient, but patchy, early cementation in the banks probably mechanically stabilised much of the sediment and prevented collapse of the pore system in those areas after the early dissolution phases. These two early diagenetic processes had a significant effect upon the nature of the original void system in the bank facies and, therefore, its subsequent diagenetic development.

Within the first few tens of metres of burial, diachronous cements developed, including isopachous fibrous calcite (Stage A), followed by scalenohedral calcites (Stages B-D), which represent pore fluid restriction and progressive anaerobiosis within the buildups. The Stage A, crypto-fibrous calcite (CFC) cements have characteristic Lower Carboniferous marine isotopic signatures and have been used as the reference to which all other isotopic values were compared.

Fig. 18.1 Burial history of the Craven Waulsortian.

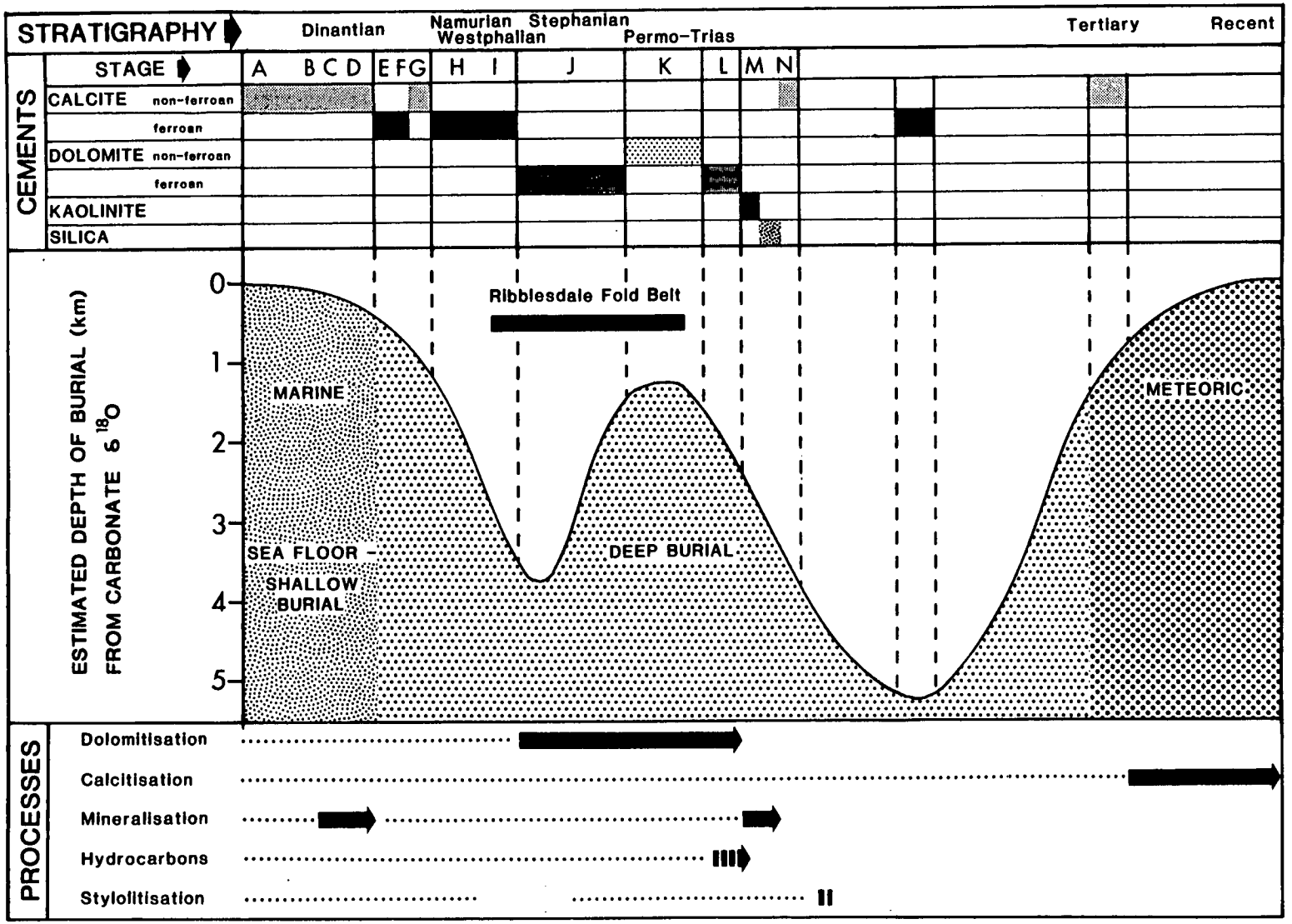

During this shallow burial phase, instability of some areas within the buildups caused by sediment collapse and dewatering, resulted in their fracturing and generation of neptunian dykes. Cavernous secondary voids were occasionally created by the hydrostatic processes accompanying formation of the neptunian dykes, which to some extent exploited existing primary void networks. The fluids associated with these dykes were often reducing, and led to the development of crustiform iron sulphides in some cavities (Fig. 18.1).

18.1.2.2 Deep burial phase

The first set of brittle fractures may have been related to tectonism and movements on major faults. However, these fractures are generally uncommon, particularly outwith the bank facies, and it is possible that they were related to a localised stress-field around the buildups developed as a result of their greater competence relative to peri-Waulsortian facies during compaction at depths probably in the region of hundreds of metres. The calcite cements precipitated within these fractures were ferroan, and probably reflected the onset of bacterial fermentation of organic matter in the sediments (Stages E and F).

A subsequent phase of fracturing was associated with dissolution followed by the precipitation of non-ferroan calcites of Stage G. There are indications from isotopic data that burial continued, but geochemical data show that the pore fluid conditions must have changed significantly. It is proposed that Stage G may reflect an influx of oxic fluids into the system (hence low Fe), possibly related to fault movements during the late Asbian/early Brigantian tectonism which concurrently produced debris flow deposits in some areas of the basin (e.g. Gawthorpe & Clemmey 1985). Buffering of pore fluid carbonate by the carbonate-rich Dinantian sediments may have masked any possible change in fluid source from the marine one existing so far. Despite lack of conclusive isotopic evidence for a change in source, an influx of meteoric waters at this time cannot be ruled out, and would certainly explain the evident dissolution and redox changes.

Burial and fracturing continued after Stage G, as indicated by further $\delta^{18}O$ depletion in the subsequent Stage H and I fracture-filling cements. A return to reducing conditions caused ferroan calcites to precipitate.

Stage I itself reflects another marked change in composition of the formation waters. A significant increase in Fe and Mg concentrations in this cement was probably related to clay mineral transformations at burial depths in the order of 2-4km (Fig. 18.1). This was accompanied by increased pressure dissolution effects, and the development of the first stylolites in the bank facies. It is proposed that Stages H to I were emplaced in structures related to fault movements during Namurian to Westphalian times.

18.1.2.3 Uplift phase

Clay mineral transformations during compaction continued to supply increasing amounts of Fe and Mg to the pore fluids, so that the next cements that precipitated were ferroan dolomites (Stage J). These were the first cements in the bank facies to truncate stylolites, and in fact the dolomite parent fluids exploited the pressure dissolution surfaces following their tectonic reactivation. The migration of these dolomitising fluids into the Waulsortian buildups caused locally extensive fabric-selective replacement and neomorphism. Stage J dolomite emplacement marked an hiatus in the burial curve in terms of $\delta^{18}O$ depletion of cements. The next cement (Stage K) was non-ferroan dolomite and was considerably enriched in $\delta^{18}O$ relative to Stage J. This $\delta^{18}O$ enrichment would be equivalent to approximately 2km of uplift. Furthermore, Stage K has a less stoichiometric composition than Stage J, which could also be indicative of shallower burial (Lumsden & Chimahusky 1980; and Chapter 11 above).

Uplift and erosion of a similar magnitude is known to have occurred during Upper Carboniferous (Stephanian) times in the Craven Basin, resulting in the Ribblesdale Fold Belt (Arthurton 1983, 1984). The Horrocksford Hall Thrust was initiated at this time. Veins containing Stages H-N were identified in the vicinity of this fault from the Chatburn Limestone in the Ribblesdale Cement Co.

quarry at Clitheroe. Also, low amplitude folds below the base of the buildup in Coplaw Quarry contain fracture sets with Stage H-L cements, indicating that these structures were also developed during the same period.

The exposed and folded Dinantian was then overlain by Permo-Triassic sediments representing marine (Zechstein) and terrestrial environments.

It is proposed, therefore, that the upward trend in the burial curve between Stage J and K in Fig. 18.1 represents the Stephanian uplift, and that the non-ferroan dolomite of Stage K is related to the downward influx of hypersaline fluids after the Zechstein incursion of the Permo-Trias, such as is represented by the marine Manchester Marls in adjacent areas.

18.1.2.4 Burial after the Permo-Trias.

Burial resumed with the deposition of the Permo-Trias sediments.

A new period of fracturing which reactivated the Hercynian faults occurred during this time. Cements precipitated in these fractures were the late ferroan dolomites of Stage L. These, like Stage J, are interpreted as deep burial dolomites, characteristic of burial temperatures within the oil window (50-160°C, cf. Radke & Mathis 1980). Indeed, towards the end of the dolomitisation episode, and for a time afterwards, small amounts of hydrocarbons migrated into the Waulsortian, primarily along stylolites, but no deposits of economic significance were formed as the former vuggy porosity of the buildups was already largely occluded by cement.

The next episode in the burial history involved the kaolinitisation of dolomite and the development of kaolinite cements (Stage M) along a new but poorly developed fracture system. It seems likely that kaolinitisation was a product of hydrothermal fluids, and that this heralded the beginning of the main phase of base-metal mineralisation in the Craven Basin.

The only consistent evidence of this late mineralisation in the Waulsortian buildups is the presence of replacive silica and silica cements at this point in the cement stratigraphy. Locally, however, galena, sphalerite, fluorite and barite deposits developed. This

mineralisation was associated with reactivation of Hercynian faults in the Craven Basin, and also developed new fracture sets parallel to the existing major structural trends in the basin (e.g. at Hall Hill). Evidence from areas adjacent to the Craven Basin shows that this mineralisation was probably post-Permo-Trias in age (Ineson et al. 1972).

Mineralised rock was then frequently cut by a subsequent fracture set which contained ferroan and non-ferroan calcite cements, culminating in Stage N. The $\delta^{18}O$ values for these cements suggest renewed burial after the Permo-Trias. The detailed cement stratigraphy cannot be extended beyond Stage N, but several different fracture sets which cross-cut and, therefore, post-date Stage N can be identified from isotopic analysis of vein-filling cements, and these give some important evidence about the remainder of the burial history.

Burial continued after Stage N to a maximum estimated depth of several kilometres (probably less than 6km). Some of the late veinlets cut a second set of stylolites which themselves truncate Stage N, and this stylolitisation reinforces the isotopic evidence of continued burial. Although no late Mesozoic and Tertiary sediments occur in the Craven Basin, some idea of their likely cover can be made by extrapolation from adjacent areas. A detailed study of released oil well data from Northern England and the west Midlands, conducted by R.F. Grayson (pers. com.) indicates that the post-Hercynian (post-Westphalian) sediment pile in the Craven Basin was probably in the order of 4km thick. This corresponds surprisingly well with the estimate of maximum burial derived from the $\delta^{18}O$ values of vein-filling cements in this study. Interpretation of the burial trend from isotopic data, however, is complicated by the recent discovery of increased geothermal gradients at certain "hot spots" across Europe after the Westphalian, one of which appears to include the Craven Basin (unpublished information communicated to me by R.F. Grayson). Such an abnormal geothermal gradient could have the affect of reducing the $\delta^{18}O$ calculation of burial depth derived from the late vein-fill cements. However, despite introducing more uncertainty as to the depth of burial, the trend is unaffected.

18.1.2.5 Tertiary erosion and meteoric diagenesis

The latest fracture-filling cement phase identified in the diagenetic sequence consists of brightly luminescent non-ferroan calcite which has $\delta^{18}O$ values indicating much shallower burial than previous vein-fill cements. A striking characteristic of these very late non-ferroan calcites is their depletion in $\delta^{13}C$, which suggests a recharge of the formation fluids by meteoric water (see Chapter 14), while their CL and staining response suggests more oxic conditions. It is proposed that these fractures developed during late Tertiary and Quaternary erosion of the area, uncovering the Waulsortian buildups and other Dinantian rocks in the Ribblesdale fold belt.

The only report of Tertiary tectonism in the Craven Basin concerns the intrusion of a single igneous dyke (Earp et al. 1961), and it is possible that this late fracture phase was associated with some related crustal extension originating in the Tertiary Volcanic centres of NW Britain.

The final episode in the burial history of the Waulsortian buildups involved the calcitisation of dolomite by near-surface oxidising meteoric fluids (see Chapter 15). This process is apparently taking place in exposed rocks in the Craven Basin today.

18.2 POROSITY EVOLUTION

Carbonate buildups of various kinds have long attracted attention from petroleum geologists because of their often high initial porosity and occurrence in argillaceous and carbonaceous peripheral facies which represent potential source-rocks. Buildups sometimes have a propensity to develop significant secondary porosity.

Using the framework of the cement stratigraphy established in this study, the opportunity was taken to obtain some estimates of the buildup porosity at various stages. However, the sample set used in this study was biased by the deliberate collection of large sparry areas or veins, and therefore any estimation of the bulk porosity of a given buildup from such samples would be grossly misleading.

A small-scale petrographic study was nevertheless undertaken in an attempt to quantify and compare the relative proportions of the total spar volume comprised by successive cement stages in bank, toe and off-bank facies.

Visual estimates were made from a representative sample of most microfacies variations in the study, comprising 35 stained thin sections and peels, noting the relative proportions of each cement present (Tables 18.1 and 18.2). The proportion of dolomite was included in these estimates in an attempt to quantify the extent of dolomitisation.

Toe and off-bank facies are lithologically more homogeneous than the banks, and, therefore, an estimate of the total spar volume (based on thin section area) in the rock was included for these facies in Table 18.2.

Cements were divided into easily identifiable packages based upon their staining characteristics and crystal habit:-

Stage A	CFC	Non-ferroan	Calcite
Stage B-D	Scalenohedral	Non-ferroan	Calcite
Stage E-F	Blocky	Ferroan	Calcite
Stage G	Blocky	Non-ferroan	Calcite
Stage H-I	Blocky	Ferroan	Calcite
Stage J-L	Rhombic/Saddle	Fe- and non-Fe	Dolomite
Stage N	Blocky	Non-ferroan	Calcite
Others	Kaolinite (Stage M), Silica		

Cathodoluminescence was not suitable for this purpose owing to the difficulty of defining some of the stage boundaries by CL alone, and the restricted field of view which could be examined at any one time without the aid of macrophotography. The stained sections and peels were observed using a binocular petrographic microscope with a zoom lens which gave much greater flexibility. Furthermore, most of the peels were of larger areas of sample than the thin sections, and therefore gave a more reliable estimation of cement proportions in the rock as a whole.

TABLE 18.1 ABUNDANCE OF CEMENT STAGES AND DOLOMITE AS PROPORTIONS OF TOTAL SPAR AREA.

BANK FACIES

SAMPLE	PROPORTION OF TOTAL SPAR (%)		PROPORTION OF POST-CFC AREA (%)							
	STAGE ⇨ A(CFC)	POST-CFC	B-D	E-F	G	H-I	N et al.	Others	Dolomite Rhomb	Dolomite Saddle
Ash 2	75	25	65	2	20	10	3	-	-	-
Ash 5	90	10	70	10	17	3	-	-	-	-
C21	43	57	5	20	60	10	5	-	-	-
C24	54	46	8	32	38	10	-	-	-	10
CX5	54	46	10	25	60	5	-	-	-	-
CX7	47	53	7	1	1	5	1	5	-	80
CH41	75	25	20	4	-	75	1	-	-	-
DG4	25	75	3	-	-	-	87	-	-	10
Du3	92	8	15	10	12	20	53	-	30	10
Du22	73	27	30	5	15	20	-	-	20	10
Du27	88	12	7	5	75	4	7	-	-	-
HA4	44	56	10	5	55	25	-	-	-	5
HG23	12	88	5	15	50	25	5	-	-	-
HN F1	73	27	69	5	10	15	1	-	-	-
IB F3	75	25	26	50	1	23	-	-	-	-
LK3	73	27	5	-	15	80	-	-	-	-
LK4	77	23	3	-	-	95	-	-	-	2
LM1	67	33	22	5	1	40	7	-	-	25
LM6	69	31	5	-	5	88	2	-	-	-
NLH13	93	7	5	-	-	75	20	-	-	-
SF3	25	75	2	2	41	55	-	-	-	-
SHX3	25	75	40	60	-	-	-	-	-	-
SU11	20	80	2	1	2	50	10	-	35	-
SU15	17	83	6	2	4	-	20	-	64	4
WW5	58	42	55	2	5	36	-	-	2	-
WW6	78	22	17	1	46	37	-	-	-	-
mean	59 ±25	41 ±25	19 ±21	10 ±15	21 ±23	31 ±30	9 ±19	-	7 ±15	5 ±15

TABLE 18.2 ABUNDANCE OF CEMENT STAGES AND DOLOMITE AS PROPORTIONS OF TOE AND OFF-BANK SPAR AREA.

TOE FACIES (No CFC present)

SAMPLE	Total spar (%)	CEMENT STAGES AS PROPORTION OF TOTAL SPAR (%) B-D	E-F	G	H-I	N et al.	Others	Dolomite Rhomb	Saddle
CX2	5	80	15	5	-	-	-	-	-
C24/2	15	57	40	2	1	-	-	-	-
WW3	10	22	65	-	12	-	-	-	1
WW4	15	60	30	5	3	-	-	-	2
mean	11±4	54±24	38±18	3±2	4±5	-	-	-	1±1

OFF-BANK FACIES (No CFC Present)

SAMPLE	Total spar (%)	CEMENT STAGES AS PROPORTION OF TOTAL SPAR (%) B-D	E-F	G	H-I	N et al.	Others	Dolomite Rhomb	Saddle
C40	15	32	60	7	1	-	-	-	-
CX5	2	30	70	-	-	-	-	-	-
IB22	2	10	60	-	10	-	20 (silica)	-	-
SM1	5	45	50	-	5	-	-	-	-
SH38	3	85	5	-	10	-	-	-	-
mean	5±5	41±25	49±23	1±3	5±4	-	4	-	-

Relative proportions of cement packages were estimate as a percentage of the total cement area.

Of the Stage A in the bank facies, the majority of the spar area was true cement although some inclusion-rich intergranular equivalents of CFC, for example in peloidal sediments, may have been replacements of interstitial micrite. Estimation of Stage A volume (area) was, therefore, confined to the unequivocal cements, mainly of the interconnected void network. This often accounted for upwards of 50% of the total spar area in the banks (Fig. 18.2A).

The percentage proportions of post-CFC cements in the bank facies were normalised to 100% in order to compare their pore-occlusion trend with those of the equivalent cements in the toe and off-bank facies where CFC did not develop (Fig. 18.2B). Finally, a cumulative spar percentage was plotted for bank, toe and off-bank facies in order to show the trend of pore-occlusion with time.

Comments

Before drawing any conclusions from the pore occlusion data presented in this section, it is important to emphasise the limitations of the data set.

1. Sampling bias was introduced in endeavouring to acquire fracture and cavity-fill material for cement stratigraphy studies, and therefore, calculations of overall original porosity volume could not be made for the extremely heterogeneous bank facies. The samples of toe and off-bank facies, however, are likely to give a more representative value for primary porosity.

2. The data set does not discriminate between spars filling primary porosity, and those in secondary (post-dissolution) pores. Nor does it account for the volume of internal sediments in the pore system.

3. Dissolution episodes occurred at most cement stage boundaries. The data set cannot reflect the degree of porosity rejuvenation which might have occurred as a result of the dissolution of spars by successive diagenetic fluids.

4. A significant proportion of the dolomites in this study were replacive. Only dolomites which occurred within void-fills were included in the data set, but whether they were cements or replacements could often not be determined. Furthermore, for those dolomites which were identified as replacements, it was not usually possible to identify which calcite stages had been dolomitised.

5. Estimation by visual means using standard comparison charts has been shown to have reasonable accuracy and repeatability for a given operator. Given the provisos noted above, it is felt that the figures produced are reasonable estimates, and certainly their trend is valid.

18.2.1 Trends and facies control

18.2.1.1. Stage A, CFC

The most obvious and striking difference between the bank and other facies was the significant role played by the Stage A (CFC) cements. Over 50% of the total porosity in the bank facies was occluded by these marine calcites (Fig. 18.2A), while none developed in toe and off-bank sediments.

The main contributing factors to the development of these cements in the bank facies were;

a) Early lithification and resistance to compaction.
b) Skeletal support of voids by sponges and fenestrate bryozoans.
c) Significant pre-CFC dissolution creating secondary porosity.
d) High degree of inter-connectivity in the void systems thus produced.

Fig. 18.2 Porosity Evolution

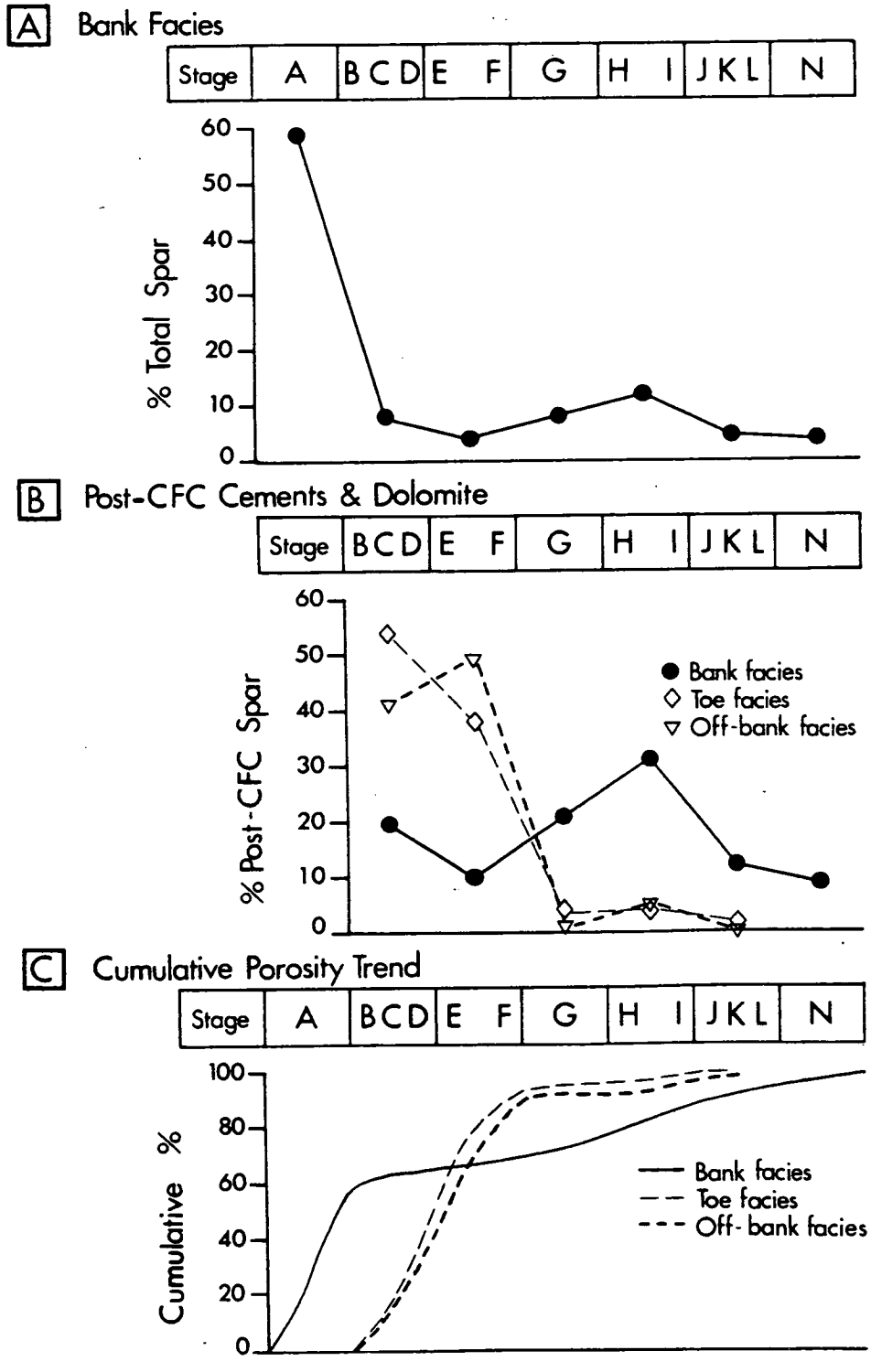

e) Possible influence on cement precipitation of micro-organisms specific to the banks

18.2.2. Post-CFC cements

Sediment grain size and the nature of the porespace were the main contols on the development of post-CFC cements. The main difference being that the banks had large interconnected void networks while the toe and off-bank porosity was mainly restricted to smaller intergranular and intragranular pores.

These factors controlled the migration of cementing fluids through the rocks, and the development of shallow burial diagenetic zones which effected the composition of early burial stages.

a). Stages B-D

The proportionately small volume of Stage B-D in the bank facies was mainly a product of the nature of the pore system.

The large size of many of the voids in the bank facies meant that the scalenohedral crystals would have been unlikely to fill the entire pore volume unless the banks had remained in the shallow burial environment for much longer. In toe and off-bank facies, however, the individual voids were much smaller, and therefore, crystals growing in from the walls would be more likely to occlude the entire void space. Most of the off-bank facies comprises bituminous, argillaceous bioclastic wackestones. The initial porosity-permeability characteristics of these sediments would probably have been poorer than the toe facies which, although consisting of finer-grained material, did contain some large pores. Accompanied with the high levels of organic matter in the off-bank it seems likely that reducing conditions would be reached earlier in that facies, allowing relatively less time for individual cement stages to develop. This suggests that Stages B-D might be expected to account for a smaller proportion of the total spar volume in off-bank relative to toe facies.

b). Stages E-F

Stages E and F were the first ferroan calcites in the cement stratigraphy, and indicate the onset of bacterial fermentation of organic matter in the sediment. They were also the first fracture-fed cements, although fracturing was not intense at this stage. (Chapter 9).

Stages E-F accounted for a greater relative proportion of the total spar volume in the off-bank than in other facies (Fig. 18.2B).

If the source of these cements had been purely from fracturing, then complementary trends would be expected for all facies so long as fundamental differences in primary sediment mineralogy had not occurred causing selective dissolution and secondary porosity development. There is no evidence from this study that such fundamental differences in primary sediment existed, except that the off-bank facies are more bituminous than toe and bank facies. It would appear, therefore, that the distribution of Stage E and F cements was not entirely controlled by fracturing in all facies.

In the off-bank facies, the relatively early attainment of reducing conditions is indicated from Stage B-D development. It is probable, therefore, that bacterial fermentation would have begun earlier (i.e. nearer to the surface) thus precipitating relatively greater volumes of Stage E-F cements in the off-bank facies. This in-turn indicates that Stages E-F were also diachronous.

In the bank facies, Stage E-F development was controlled by the development of a set of fractures. These were not very common and therefore, Stage E and F were not extensively developed in the bank facies. The fact that these fractures are even less common in the off-bank facies is further evidence of the localised control on Stage E-F development, and indeed, their diachronous nature.

c). Stage G

In the bank facies, Stage G was associated with significant porosity rejuvenation, and this is reflected in the relatively large volumes of Stage G cement in that facies. In the toe and off-bank facies, Stage G had only limited development (Fig. 18.B). This is

mainly related to the fracture origin of this cement stage and the nature of the pore systems in the different facies.

Over 90% of the porosity in toe and off-bank facies was occluded by Stages B-F, leaving little space for subsequent cement precipitation, as against 70% in the bank facies (Fig. 18.2C). Furthermore, there would have been a higher degree of interconnection in the pore system of the bank facies because of the nature of the original void network, and so the fracture-fed fluids would have had more opportunities to enter the remaining void space in the banks, than in the more isolated porosity of the toe and off-bank facies. The better connectivity of voids in the bank facies may also have allowed higher fluid flow rates which would have increased the effects of the dissolution episode and encouraged faster crystal growth rates in the subsequent Stage G cements.

d). Deeper burial (Stages H-N)

The porosity occlusion trends for all facies are similar for the remainder of the deep burial history of the rocks. An upward trend in pore occlusion occurred during Stage H-I, reflecting the fact that fracture frequency was increased during this stage, particularly with the development of microfacture swarms (Chapter 8).

e). Dolomitisation

Dolomitisation (and the precipitation of dolomite cement) was proportionately greater in the bank facies pore system than in other facies. This confirms the petrographic observation that outwith the bank facies, dolomite (Stages J-L) is almost entirely confined to fractures (Chapter 11). The contribution of dolomite stages to pore occlusion is uncertain because of the replacive nature of much of this mineral in the study samples.

18.2.3 Significance of cumulative porosity trends

The cumulative porosity curves mainly reflect the contrast in porosity styles between the bank and other facies.

The large dimensions of some of the voids which remained in the bank facies after CFC development meant that early burial cements were unlikely to fill the entire pore space. This left larger volumes of pore space for subsequent cementation. In the toe and off-bank facies, however, pore dimensions were smaller, and were therefore more likely to be completely occluded by earlier generations of cement. Hence, the majority of the pore space in the toe and off-bank facies was occluded by Stages B-F whereas the bank facies still maintained significant pore space until the dolomite cements of Stages J,K and L.

Dissolution episodes between cement stages were much more effective in the bank facies, and, therefore, secondary rejuvenation of porosity was probably another contributing factor in depressing the pore occlusion curve in that facies. This suggests that the amount of available porosity in the bank facies at any time during the burial history was less than the pore occlusion curve would suggest, except for those periods immediately prior to the precipitation of each cement stage.

This becomes important when considering the hydrocarbon reservoir potential of the bank facies during any period of its burial history. The pore occlusion curve in Fig. 18.2C, therefore, represents the maximum available pore space, and the actual values were probably much less.

By relating the pore occlusion curve to the burial history curve (Fig. 18.1), it is apparent that the majority of pore occlusion in the bank facies occurred before the end of the Westphalian, and probably earlier. In the toe and off-bank faices, over 90% of the original pore space had been cemented by the end of the Dinantian.

In his study of the Mid-Late Courceyan Waulsortian buildups of Eire, King (1984) concluded that most diagenesis was complete by the end of the Chadian, again indicating that large volumes of cement may develop in the banks over relatively short time periods.

As the majority of deep burial cements in the bank facies were sourced externally to the buildups via fractures from formation waters, the importance of fracturing in the cementation process is emphasised. Without these tectonic episodes, considerable volumes of porosity would have remained open in the bank facies, thus improving

its reservoir potential. The fact that fracturing did allow deep burial cementation to take place, meant that little porosity was available for the migration of hydrocarbons which took place after the Carboniferous. Only a few percent porosity was available in the bank facies when the bituminous off-bank sediments reached maturation depth i.e., the "oil window". This implies that only those Waulsortian buildups which did not pass into the deep burial zone for significant periods of time would be likely hydrocarbon reservoirs.

CHAPTER 19
CONCLUSIONS AND FUTURE WORK

Using a range of petrographic and geochemical techniques in an integrated approach, it has been possible to identify a cement stratigraphy, comprising Stages A-N, within the Waulsortian buildups of this study. Some of these stages can confidently be correlated throughout the Craven Basin.

By integrating the cement stratigraphy with evidence of fracturing, stylolitisation, mineralisation, hydrocarbon migration, dolomitisation and calcitisation, it has been possible to recognise the development of trends in diagenetic environments and porosity evolution, and to therefore suggest a burial/diagenetic history for the deposits ranging from their origin in Chadian (Lower Dinantian) times up to the present day.

In the absence of any consistent descriptive nomenclature for use in petrographic cement stratigraphy studies, a three-fold heirarchical sub-division is proposed, comprising:-

Stage — The primary unit of a cement stratigraphy which has a high degree of mineralogical or textural homogeneity, or is geochemically distinctive so that it can be distinguished from adjacent cements. Stages should be sufficiently well-developed to allow correlation between samples within a sample set. Stage boundaries are often unconformable.

Substage — A compositionally distinctive, conformable unit within a cement stage that is locally correlateable and commonly has internal heterogeneity, which may be in the form of sharply-defined banding (zones), or may be gradational.

Zone — The smallest individual unit normally observable in a cement crystal. Zones are conformable and essentially homogeneous but are often of limited correlateability, often being consistent only within a single crystal.

19.1 CEMENTATION AND DIAGENETIC HISTORY

The diagenesis of the Craven Waulsortian buildups occurred in three general environments: sea floor to shallow burial marine; deep burial; and moderate burial to near-surface meteoric.

19.1.1. Sea floor to shallow burial marine environments

The nature of the original (M1) sediment was a major factor in the early diagenetic development of the Waulsortian buildups. Local production of large volumes of lime mud, possibly by non-filamentous cyanobacteria, in association with post-mortem disintegration of skeletal organisms, resulted in mound-forms or buildups which were able to maintain steep depositional slopes. These buildups were able to resist early compaction whereas the surrounding peri-Waulsortian facies were not. The resistance of the bank facies to early compaction was a product of the high carbonate and very low clay content in the M1 sediment together with patchy incipient cementation.

Synsedimentary collapse of this partially lithified sediment resulted in the development of a complex system of cavities whose shape was often determined by the mechanical bridging effects of larger allochems, particularly fenestellid bryozoans. Sediment collapse was also responsible for the production of the characteristically mottled polymud bank facies sediments (sensu Lees 1964).

In the peri-waulsortian facies, bioclast contents and grain sizes were larger than in the banks, and there were greatly increased amounts of clays, often in shale bands. These factors, together with a lack of incipient cementation, allowed extensive compaction to

greatly reduce the primary porosity. Such variations in primary sediments resulted in the development of different styles of early diagenesis in the bank and off-bank facies.

19.1.1.1 Early dissolution episodes.

As noted by Miller (1986), two periods of dissolution in the bank sediments (the first of siliceous sponge spicules and the second of carbonate), pre-dated the development of the first recognisable cements. Although spicule dissolution also occurred in the peri-Waulsortian facies, it was much less common, and replacement of hyalosteliid and other siliceous spicules by later stages of diagenetic calcite or silica was the rule. Evidence of early carbonate dissolution is absent from the off-bank facies.

The dissolution episodes were probably caused by pH changes in the pore fluids relating to bacterial degredation of certain kinds of organic matter in the seidments (Birnbaum & Wireman 1984; Miller 1986).

19.1.1.2 Stage A cements

The first recognisable cements developed in the bank facies (Stage A) are absent from peri-Waulsortian sediments. They formed inclusion-rich isopachous to sub-isopachous layers which are often interlayered with marine internal sediments. Such features are characteristic of the marine (phreatic) diagenetic environment. The Stage A cement layers consist of mosaics of crystals of variable habit, but all contain strong palimpsest textures in the form of inclusions and extinction patterns which reflect the presence of a fibrous cement precursor. The term "Crypto-fibrous calcite" (CFC) is proposed for these cements.

Four basic types of CFC were observed in this study;

1. Botryoidal mosaic
2. Bladed mosaic
3. Irregular mosaic
4. Radiaxial calcite mosaic

Botryoidal mosaics are characteristic of Craven Phase D Waulsortian, but even these did not form in every cavity. However, where botryoidal mosaics did form, they were consistently the earliest CFC cements in the sequence. They were always either encrusted by micrite of biogenic origin or covered by geopetal sediment, indicative of development in a relatively open pore system, probably still connected to the surface of the buildups.

Lateral transitions between bladed, irregular and radiaxial CFC types, commonly occur within a single cement layer, independently of substrate, and often associated with changes in inclusion density. The radiaxial calcite crystals are usually the least turbid type within such lateral transitions, and generally contain lower levels of Mg than other CFC types or allochems such as crinoid ossicles which were originally high-Mg calcite (HMC). Cathodoluminescence often picks out subsequent recrystallisation textures in CFC, which follow the precursor fibrous cement fabrics, but CL alone cannot distinguish between different CFC types. It is concluded, therefore, that CFC cements are the product of a neomorphic transition from a fibrous precursor common to all CFC mosaics of this study, and that radiaxial fibrous calcite (RFC of Kendall & Tucker 1973) is an end-member of this process. Geochemical and isotopic data suggest that the precursor in these cases weas originally HMC, and that the recrystallisation process was effected by fluids of ambient marine water composition.

With the recent development of high magnification CL imagery on some microprobe machines, and the continued advances in strontium isotope and fluid inclusion studies, there is potential for future work to further investigate the nature of inclusions in CFC cements and so, the origins of the cements themselves.

The exclusive occurrence of CFC in the bank facies was apparently controlled by a variety of factors:-

a) the resistance of the banks to early compaction allowed the development of large voids in the sediments. These were subsequently enlarged and modified during pre-CFC dissolution episodes resulting in extensive interconnected void networks which allowed the circulation of large pore-fluid volumes, conducive to the precipitation of isopachous fibrous cement layers.

b) the possible influence on cementation of micro-organism populations which (like the inferred mud-producers of Lees & Miller, 1985) were exclusive to the bank facies.

c) the absence of the above factors from peri-Waulsortian facies resulted in a compacted sediment with restricted porosity-permeability characteristics which inhibited fibrous cement precipitation.

19.1.1.3 Stage B-D cements

The cements which immediately post-date CFC in the bank facies are equivalent to the first recognisable cements of the peri-Waulsortian facies. They are inclusion-rich scalenohedral, non-ferroan calcites which exhibit a characteristic 'black-bright-dull' CL sequence comprising Stages B, C and D respectively. Geochemical and isotopic analysis shows that these cements reflect changes in pore-fluid chemistry during progressive burial through oxic to suboxic and sulphate reduction zones in the shallow subsurface. The nature and development of these diagenetic zones in modern sediments infers that the cements which precipitated during the progressive anaerobiosis would have been diachronous. This, therefore, rules out the need to invoke the presence of laterally and vertically extensive lenses of oxic and reducing fluids during the shallow burial of the Waulsortian buildups and associated sediments. It also suggests that the develoment of such cements need not be indicative of extensive palaeoaquifers, but that they are more probably a reflection of similarities in the processes affecting the geochemical development of connate fluids in the marine environment during shallow burial (perhaps to several tens or even hundreds of metres depth). It is distinctly possible that Stage A cements were also diachronous and may, at least in part, be time-equivalents of the earliest cements in peri-Waulsortian facies (Stage B).

19.1.1.4 Sediment-filled fissures and neptunian dykes

The Craven Waulsortian buildups contain two types of metre-scale sediment-filled fractures;

a) Fissures

b) Neptunian dykes

a). Fissures opened onto erosion surfaces which mark the top of some buildups. The sediments which filled fissures are unlike the bank faices and appear to represent relict post-Waulsortian sea floor deposits which draped the buildups. They were localised phenomena and had little apparent significance in the diagenetic history of the buildups.

b). Neptunian dykes developed throughout the shallow-burial diagenetic history of the buildups. The develoment of such synsedimentary sediment-filled fractures is evidence of the inherent instability and patchy lithification of the Waulsortian buildups during early diagenesis. Although the banks must have been sufficiently lithified to allow fractures to develop, there must also have been significant volumes of unconsolidated sediment available to fill the dykes after collapse and sediment de-watering caused increase of hydrostatic pressure at depth within the buildups. Neptunian dykes may taper towards the buildup surface, indicating upward propagation of these fractures. Lamination of dyke sediments parallel to the fracture margins suggests that material was injected along the dykes, while the purity of these lime-muds confirms an intra-buildup origin (sediment from any postulated sub-Waulsortian source facies would be expected to contain more argillaceous material).

Neptunian dykes occasionally terminated in cavernous voids which contain complex multigenerational internal sediments, sourced from episodic pulses of dyke-sediment injection.

The same processes which effected neptunian dyke development were also active on the microscopic scale. These combined processes opened significant volumes of secondary porosity, although most was almost immediately filled by injected sediment, as were parts of the original void network accessed by the dykes. Furthermore, the fracturing of the buildups during neptunian dyke dilation probably induced many other fractures which were themselves subsequently filled by early diagenetic cements.

Neptunian dykes and associated microscopic features may truncate all early diagenetic cements (Stages A-D), but never any later cements. This constrains their development to that period of the diagenetic history prior to the first deep burial cements in the

sequence. Therefore, complete lithification of the Waulsortian buildups of the Craven Basin was not achieved in the shallow burial environment. Planes of weakness represented by dykes were subsequently re-activated intermittently during deep burial, allowing later diagenetic fluids to enter the buildups. Neptunian dykes were therefore of considerable importance in the diagenetic history of the Waulsortian buildups, and their influence has hitherto been overlooked.

19.1.2 Deep Burial environments

All cement stages following the diachronous Stage B-D cements can be related to phases of brittle fracturing in the Waulsortian facies, indicating a deep burial origin.

19.1.2.1 Stages E-I

The first deep burial cements (Stage E and F) were ferroan calcites, suggesting that the bank sediments had passed through the sulphate reduction zone into the zone of bacterial fermentation of organic matter (cf. Irwin et al. 1977).

A subsequent fracturing episode after further burial, possibly related to intra-Dinantian tectonism, allowed the influx of more oxic fluids which effected dissolution of earlier cements, and from which precipitated non-ferroan calcites of Stage G.

Stage H cements are ferroan calcites, and have similar trace-element composition to Stage F, while their $\delta^{18}O$ signature indicates continued burial after Stage G.

The subsequent Stage I cements were much more strongly ferroan than previous cements. The increase in Fe content was accompanied by an increase in Mg, supplied by clay mineral transformations during burial compaction. This increase in dissolved Mg^{2+} and Fe^{2+} in the formation waters heralded the onset of dolomitisation in the build-ups.

Stage I veinlets are the first fracture phase to post-date stylolites in both bank and off-bank facies. Cement stages prior to Stage I all show evidence of truncation by stylolites, although the effects of pressure dissolution were more prevelant in off-bank facies.

19.1.2.2 Dolomite (Stages J,K and L)

Dolomites were the first stages to exploit and truncate stylolites in the bank facies. All previous cement stages preceeded the development of stylolites in the Craven Waulsortian. Dolomite cements as such were not extensively developed in the Waulsortian facies. More commonly, dolomite developed as a neomorphic replacement of existing calcite spars and geopetal sediments.

Evidence for the recognition of cement versus replacement textures in the Craven Waulsortian is often equivocal. Dolomite cements largely comprised mosaics of saddle dolomite (Radke & Mathis 1980). They developed in fractures and cavity-fill cement sequences. Replacive dolomite fabrics were more varied, including (in order of relative abundance):-

i). Rhombic-"spar" and "geopetal" mosaics formed by selective dolomitisation of calcite spar and internal sediment respectively, and consisting of idiotopic to hypidiotopic rhombic crystals.

ii). Saddle dolomite formed by selective replacement of calcite spar, and including a rare form; porphyrotopic dolomite comprising individual rhombohedral saddle dolomite crystals which replaced calcite spar in veinlets but also extended into the sediment adjacent to the fractures.

iii). Isolated rhombs as a replacement of M1 sediments.

iv). Anhedral dolomite formed as a replacement of internal sediments, and occasionally of the CFC layers interbedded with geopetal sediments, comprising mosaics of irregular anhedral crystals.

v). Neomorphic dolomite (Gregg & Sibley 1984): saddle dolomite developed by recrystallisation of earlier rhombic dolomite mosaics.

A consistent sequence of three dolomite stages (J,K and L) was identified in both cements and replacements, that relates all dolomites to the same three diagenetic episodes.

Dolomitisation began during deep burial with the precipitation of Stage J ferroan dolomite. Dolomitising fluids were derived from

pressure dissolution of pre-existing carbonate and clay mineral transformations in the argillaceous limestones outwith the banks. These fluids entered the bank facies along fratures and reactivated stylolites.

The second stage of dolomitisation, Stage K, is characterised by strong brick-red to red-orange luminescence, and represented a major change in pore-fluid composition. Stage K dolomites are non-ferroan, suggesting that the formation waters had become oxic. Their isotopic composition and stoichiometry indicate a shallower burial depth than Stage J, and therefore the possibility of an influx of hypersaline brines. This was the main phase of replacive dolomitisation in the buildups.

The final episode in the dolomitisation of the Craven Waulsortian (Stage L) was associated with reactivation of pre-existing fault systems. Stage L cements were ferroan dolomites. Their relatively depleted $\delta^{18}O$ isotopic signature, and their association with the development of fracture sets, indicate a resumption of burial after Stage K.

19.1.2.3 Post-Dolomite Burial cements

The cement stratigraphy cannot be extended with confidence after the dolomite, Stages J-L. By this time, the vast majority of pore space in the buildups had been occluded by cement. Subsequent cement stages, of which there were many (precisely how many cannot be determined), were largely confined to widely-spaced veins and isolated void-fill sequences, so that they could not be integrated with sufficient confidence at the necessary scale for cement-stratigraphical correlation. However, this period was important for a variety of reasons:-

a). Localised lead-zinc mineralisation occurred after reactivation of the Hercynian structures in the Craven Basin. This period of mineralisation was heralded by the development of relatively uncommon, but distinctive, kaolinite cements (Stage M) and kaolinitisation of dolomite, along with wide scale silicification in many buildups and peri-Waulsortian facies.

b). At about the same time, small amounts of hydrocarbons migrated into the bank facies, having been sourced outwith the buildups in the bituminous shales and argillaceous limestones which comprise much of the Dinantian sequence in the Craven Basin. Stylolites formed the main migration pathways for hydrocarbons entering the buildups. Some stylolites were re-activated during post-dolomite tectonic episodes.

c). Isotopic analysis allowed the identification of several separate post-dolomite cement-filled vein sets. Many of these late cements, while often petrographically indistinguishable, cannot be related to a specific stage in the cement stratigraphy, although some are locally correlateable between a few buildups. With only one exception they record a period of continued burial and multi-phase reactivation of faults in the Craven basin. Although the precise relative timing of many of these episodes could not be established, one consistent post-mineralisation cement, Stage N, can be identified basin-wide. Its precipitation was preceeded by dissolution and small-scale secondary porosity development.

While the $\delta^{18}O$ values of the cements in this study show systematic trends relating to the burial history of the buildups (see 19.2 below), the $\delta^{13}C$ values for the sea-floor to deep burial calcites show remarkably little variation. Exceptions to this general rule are;

a). Stage C; where depletion in $\delta^{13}C$ indicates the onset of reducing conditions in the sediment during shallow burial.

b). Dolomites; which show a $\delta^{13}C$ range of 4°/₀₀, possibly reflecting precursor carbonate isotopic signatures in replacive forms or the effects of variable stages of organic matter decay in the sediment (cf. Pisciotto 1981).

Buffering of pore-fluid $\delta^{13}C$ with that of carbonate dissolving out of the rock body during diagenesis is the most likely reason for the limited $\delta^{13}C$ variation observed in the burial cements. Buffering of $\delta^{13}C$ was apparently less effective during later meteoric diagenesis in the buildups (19.1.3).

An opportunity for future work would be to isotopically constrain samples of individual cement stages relative to the margins of the buildups, i.e. relative to the source of externally-derived

burial diagenetic fluids, and so investigate any systematic buffering effects along likely fluid-migration pathways.

19.1.3 Nearsurface to moderate-burial meteoric environments

Two late-stage carbonate phases; one, a vein-filling calcite cement; the other, a calcitisation product after dolomite; had significantly different isotopic signatures to the rest of the diagenetic phases in the Waulsortian buildups. While $\delta^{18}O$ was enriched relative to other burial cements (indicating nearer-surface environments) $\delta^{13}C$ was significantly depleted, indicating an influx of meteoric fluids.

19.1.3.1 Late Fracturing

A late diagenetic fracture-filling calcite stage was identified in three separate buildups, and in each case was the latest vein-fed spar in the sequence. The non-ferroan calcites are brightly luminescent, indicative of oxic parent-fluids.

19.1.3.2 Calcitisation of dolomite

Dolomite occurring at outcrop in the Craven Basin Waulsortian (particularly ferroan dolomite) is usually a characteristic rusty orange-brown colour as a result of calcitisation at, or near, the present day surface. The products of calcitisation include finely disseminated geothite inclusions (which impart the brown colouration) and brightly luminescent non-ferroan calcite (which indicates oxic fluid conditions). Calcitisation often reached completion, but in most examples, at least some relict fragments of the precursor dolomite can be observed petrographically, especially with CL.

Calcitisation progressed along crystallographic or intercrystalline planes of weakness in the dolomite mosaics, but was also selective along compositional zones of highest iron content in ferroan dolomites. In most cases, dolomite textures and fabrics were largely preserved during the neomorphic transition.

Calcitised surface layers commonly occur on fresh rock samples broken from outcrop, while ferroan dolomite in borehole core material was not calcitised. This, along with many similar examples from the literature, is confirmation that the calcitisation is a near-surface phenomenon. The process is still in occuring in the present day meteoric environment of the Craven Basin.

19.2 BURIAL HISTORY AND POROSITY EVOLUTION

A curve of estimated burial depth was derived from the $\delta^{18}O$ values of successive cement stages. By relating certain of these cement stages to veins formed during structural episodes, and then to periods of burial or uplift as indicated by the lithostratigraphy, it was possible to associate parts of the estimated burial curve with major episodes of basin development, and therefore, to tentatively date the cement stratigraphy. Combined with the diagenetic history, these observations and interpretations allow the reconstruction of the burial history and porosity evolution of the Waulsortian buildups in the Craven Basin.

19.2.1 Burial History

The diachronous cements of Stages A-D developed within the first few tens, perhaps up to hundreds of metres of burial during Chadian times.

Burial continued after Stage D into the deep burial realm. All subsequent cements were associated with the development of brittle fracture sets.

The first deep burial cements (Stages E and F) were ferroan calcites formed within the zone of bacterial fermentation of organic matter, and are related to a phase of fracturing which may have resulted from localised stress fields developed around the more competent buildups.

Two periods of tectonic activity have been identified from the post-Waulsortian Dinantian sediments (Gawthrope 1987). The later of

these periods, which occurred in late Asbian-early Brigantian times, may have been influenced the development of oxic conditions in the pore fluids of the banks, causing dissolution, followed by the precipitation of non-ferroan Stage G cements.

Further burial, and a return to reducing conditions, resulted in the development of ferroan calcite Stages H and I, which formed at depths of a few kilometres, corresponding favourably to the known thickness of the post-Waulsortian Dinantian sediment pile in the Craven Basin. These cements were emplaced in fractures which, it is proposed, were related to fault movements during Namurian-Westphalian times. The first stylolites to affect the bank facies were also developed during this phase of the burial history.

The major change in pore-fluid composition which resulted in the first ferroan dolomite cements of Stage J, marked an hiatus in the burial curve which reflects the begining of the late Carboniferous (late Hercynian) uplift in the Craven Basin.

The next episode in the burial history is represented by non-ferroan dolomites of Stage K. They have more calcian stoichiometry than the ferroan dolomites, suggesting that they formed during shallower (although still moderately deep) burial, and this is supported by their relatively heavy $\delta^{18}O$ values which correspond to 1-2km of uplift relative to the preceeding dolomite and calcite cements. This order of uplift is comparable with the thickness of Carboniferous sediments which are known to have been removed during a period of severe erosion in the Craven Basin associated with the late Hercynian uplift. It is suggested that the Stage K fluids may have been sourced from the incursion of the hypersaline Zechstein Sea, during the Permo-Trias, which is recorded in sediments in areas adjacent to the Craven Basin.

The deposition of Permo-Trias sediments resumed burial of the Waulsortian buildups. Episodic reactivation of Hercynian faults occurred during this period. The earliest of these episodes resulted in the precipitation of Stage L, ferroan dolomites. In common with

Stage J, these are interpreted as deep burial dolomites, characteristic of burial temperatures within the oil-window (50-160°C). Indeed, small amounts of hydrocarbons migrated into the buildups along stylolites towards the end of the dolomitisation episode, and immediately afterwards.

During continued subsequent burial, kaolinite cements (Stage M) and kaolinitisation of dolomite occurred as a precursor to post-Permo-Trias lead-zinc mineralisation, which was primarily associated with reactivation of Hercynian structures in the basin.

Mineralisation was followed by several episodes of fracturing, each associated with the develoment of vein-filling calcite cements whose relative timing can only be determined, at best, on a local scale. The maximum burial depth indicated by the most depleted $\delta^{18}O$ value of all these vein-fill cements is approximately 6km. However, the time at which this maximum burial depth was achieved cannot be determined with any accuracy as these late cements are confined to infrequent and isolated fractures and cannot be integrated into the cement stratigraphy.

A locally-developed late-stage cement was emplaced within fractures that truncated all earlier diagenetic fabrics in the buildups in which it occurs. Isotopic evidence suggests that these cements developed at moderate burial depths from a meteoric source fluid. It is proposed that this marked change in formation-water chemistry represents the process of emergence which began in association with tectonic episodes related to Tertiary uplift.

As the Waulsortian buildups were returned to near-surface diagenetic environments during the late Tertiary-Quaternary, meteoric fluids percolating downwards began to selectively calcitise dolomite in all buildups and many other Dinantian facies of the Craven Basin. This process is continuing at the present-day surface and shallow subsurface in the basin, and marks the final episode in the burial history to date.

Further work involving isotopic analyses from cements in post-Waulsortian sediments and vein-fills, could assist in improving the constraints of the timing of cements within the Waulsortian buildups. However, this would require a very exhaustive sampling process.

19.2.2 Porosity Evolution

The present sample set was biased towards spar-rich areas of the sediments and, therefore, could not be used as an accurate representation of the volumetric evolution of the pore space, especially in the bank facies. Furthermore, the replacive nature of some sparry areas, particularly dolomites, added uncertainty to any estimates of former void space. However, significant differences were observed in the evolutionary trends of porosity occlusion between bank and off-bank facies.

The most striking of these differences concerned the development of void space during early diagenesis. The significant modification of the bank facies void network by early dissolution episodes was a major influence on the subsequent diagenesis of the buildups, while in off-bank facies, early compaction and the absence of early dissolution produced a more restricted pore system.

The subsequent Stage A cements, exclusive to the buildups, reduced the total porosity of that facies, in some areas, by over 50%. This still left significantly larger volumes of open voids in the bank facies compared to the peri-Waulsortian, so that the buildups became effective "sinks" for the migration of formation waters during subsequent deep burial episodes, a factor that is particularly noticeable with respect to dolomitisation, which was far more effective in the banks than in peri-Waulsortian facies.

The occlusion of pore space in the deep burial realm was largely controlled by the development of tectonic fracture sets which acted as the main conduits for diagenetic-fluid migration, although reactivation of stylolite seams provided extra migration pathways, especially during dolomitisation episodes.

Dissolution episodes also had a marked affect on the porosity evolution of the bank facies but were again less important in the peri-Waulsortian. Although such dissolution episodes did not cause extensive porosity rejuvenation, those occurring prior to the two non-ferroan deep burial calcite cements, Stages G and N (late Dinantian and post Permo-Triassic age respectively) were most significant. With these exceptions, the porosity evolution of both bank and off-bank facies was generally one of progressive pore occlusion, with no major episodes of secondary porosity development after early diagenesis.

In relation to the overall burial history curve, it is apparent that pore occlusion in all facies was largely completed before the end of the Dinantian, so presenting a poor prospect for reservoir potential during the migration of hydrocarbons which occurred after the Permo-Trias.

19.3 LIMITATIONS OF CEMENT STRATIGRAPHIES

Cement stratigraphies record a sequence of processes which reflect different diagenetic environments. However, the sequence is generally complex and never represented in a single example. It is therefore necessary to combine data from a wide range of samples and several analytical techniques in order to draw reliable conclusions. The distribution of diagenetic products is often irregular due to a combination of systematic reasons and randomness, so that adjacent areas within individual samples may exhibit different, but incomplete sequences (Schroeder 1986). In order to overcome some of these drawbacks, I have emphasised the need to use large individual thin sections, as well as a large total area of thin sections.

A variety of factors which affect the development of cement stratigraphies have been identified in the course of this study:-

(i) Pore geometry

One of the most critical factors affecting the construction of cement stratigraphy is the dimension and shape of the void into which the cements precipitate. Small pores are more likely to be completely filled by early cement stages, while in larger voids, the probability of total pore occlusion by a single cement generation is lessened, and the development of a sequence of several successive cement stages is more likely. Furthermore, voids with parallel walls are more likely to remain open to circulating pore fluids than are irregular-sided cavities which have narrow pore-throats that are more easily constricted by cementation.

(ii) Availability of pore space

The availability of pore space is related to the pore geometry and is another important factor in controlling the development of cement stratigraphies.

During the latter stages of the diagenetic history of the Craven Waulsortian, fracture-fed cements were unable to access much of the void networks because earlier cements had largely occluded the pore space, or had choked pore-throats, so restricting fluid circulation. As a result, an indeterminate number of cement stages (isotopic evidence suggests as many as 6) were not represented in any cement sequence. This illustrates the potential imperfections of diagenetic histories as interpreted from cement stratigraphies based only on a few, often small, void-fill sequences. With its large volumes of early void space, the bank facies is near ideal for cement stratigraphy. In peri-Waulsortian wackestones and grainstones the problem of available pore space is acute. Cement stratigraphies based on such lithologies alone would, at best, be incomplete.

(iii) Proximity to fluid pathways

Voids lying in close proximity to the migration-pathways of pore fluids were most likely to be accessed by those fluids from which cements subsequently precipitated. This was illustrated by two

examples in this study;

a). Stage A cements developed thick isopachous layers in those areas which were connected to the main void network in the Waulsortian bank facies, but were often absent from pores which were somehow disconnected from those networks, irrespective of the type of pore space. This resulted in the development of different cement sequences in some neighbouring and contemporaneous voids.

b). During deep burial diagenesis, all cement stages in the Craven Waulsortian were fracture-fed. Cements only precipitated in those areas of the void network which were accessed by the fractures. This produced disconformities in many cavity-cement sequences, and so introduced further complexities into the cement stratigraphy.

(iv) Dissolution

Dissolution episodes produce secondary porosity and thus affect cement stratigraphies in two ways:-

a). Dissolution may develop significant disconformities in cement stratigraphies, or in some cases may completely remove earlier cement stages, thus destroying parts of the diagenetic record. Furthermore, the effects of dissolution may vary widely from void to void so that adjacent cement sequences may have a dissimilar appearance.

b). Where dissolution develops new voids which are unrelated to the primary porosity (e.g. mouldic porosity), then the cement stratigraphy in adjacent primary and secondary void-fills may be completely different.

v) Protection of pore space

Some voids may be isolated from circulating pore waters, either by enveloping skeletal structure, insoluble micrite envelopes, or early incipient cements. Such porosity may remain uncemented for considerable time. This is particularly important with respect to

the relative timing of secondary mouldic porosity development. In the absence of any other confirmatory evidence, the timing of mould formation need not be coincident with the precipitation of the first cement in the subsequent void-fill sequence.

(vi) Neomorphism

In this study, a close relationship was observed between the processes of cementation and replacement. It is apparent that both may occur during the same diagenetic episode, sourced by the same fluids.

The development of replacive fringes which follow centripetal growth banding in CFC (Stage A) cements illustrates this point, and shows how confusion could arise when neomorphic products adopt spurious positions within cement stratigraphies. This could result in gross misinterpretation of diagenetic sequences.

Dolomite textures are perhaps the most equivocal of all, and require special attention to determine their origin and relative timing.

Although some neomorphic products can be related to specific cement stages, many others cannot. Selective neomorphism (including dolomitisation and calcitisation) of sediments, could well result in authigenic mineral phases which have no equivalent in the cement stratigraphy.

(vii) Diachronous cements

The identification of diachronous cements in this study has important implications for cement stratigraphy interpretations. Most importantly, it eliminates the need to invoke extensive fluid lenses and basin-wide aquifers to explain the development of cements which are not vein-fed but occur in great thicknesses of sediment. The recognition of the diachronous nature of such cements is also important in modelling pore fluid processes. Their existence shows that processes effecting changes in cement characteristics need not be related to major structural episodes or climatic change.

19.4 PROBLEMS IN ENVIRONMENTAL INTERPRETATIONS FROM CEMENTS

Throughout this study, the emphasis has been upon an integrated approach to the problems of interpreting cement origins. Several comments on individual techniques are warranted by my experience.

19.4.1 Stable Isotopes

The use of stable isotope analysis has been of enormous value to the diagenetic interpretations in this study. However, without becoming involved in the theoretical limitations of stable isotope studies, some practical problems were encountered during this study and are summarised below:-

i). The sample weights needed for the method employed in this study (min. 5mg) are unsuitable for many cement stratigraphy studies. Purity of the sample was difficult to ensure, and the large sample size meant that it was rarely possible to obtain enough material to run repeat analyses. Smaller sample weights (less than 1mg) are now used by most researchers involved in similar studies, and are to be recommended. The advent of the laser or ion probes may solve many of these problems.

ii). Investigation of intended isotopic samples with both CL and chemical staining should be standard practice. Impurities are often distributed throughout cement stages in a very subtle manner. The three-dimensional aspect of sampling requires careful consideration. Cement stages mapped-out on a 2-D sample surface may not persist with depth.

19.4.2 Cathodoluminescence

Direct interpretation of cement composition and diagenetic environments from CL alone is not advisable. In this study, cements of widely differing chemical composition often had subjectively indistinguishable CL characteristics.

Previous authors have attempted to define the limits of CL in calcite and dolomite with little consistency in the results (Pierson 1981; Frank et al. 1982; Fairchild 1983). More recently, ten Have and Heijnen (1985) showed that the levels of Mn^{2+} activator which are necessary to cause CL in calcite, may be as low as a few ppm. Machel (1985) has raised the possibility of trace amounts of rare earth elements acting as sensitisors to CL.

Clearly, the causes of CL in carbonates are far more complex than simple activator/quencher ratios, and require more detailed investigation with more accurate techniques than those employed in this study. The use of CL spectra is one possible approach to the problem, and is certainly a much-needed step in making comparisons between cement stages more objective.

For these reasons I have not attempted to define CL limits on the basis of geochemistry from my data set.

In general, I can confirm that the CL of natural calcites and dolomites in the Craven Waulsortian tend to reflect changes in concentrations of Mn^{2+}, Fe^{2+} and, to a lesser extent, Mg^{2+}, in that increasing Mn with constant Fe gives brighter CL while increased Fe with constant Mn gives duller CL. Magnesium tends to redden calcite luminescence, as reported by Sommer (1972). Similar observations have recently been made by Meyers and Grams (in press) who disputed Machel's contention that sensitisation was important, and maintained that CL in natural carbonates is largely a function of Mn and Fe concentrations. The debate will no doubt continue. It will only be resolved by a thorough study, undertaken in conjunction with a solid-state physicist, to investigate the precise causes of CL in natural carbonate cement sequences. Meanwhile, on the purely qualitative, petrographic level at which most carbonate studies are presently undertaken, there is little doubt that CL must continue to play an important role in unravelling diagenetic histories.

ACKNOWLEDGMENTS

Over the last three and a half years, Dr. John Miller has not only been a dedicated and enthusiastic supervisor, but he has also been an active participant in every aspect of this study. His assistance over the critical writing-up period has been especially valuable, and the final draft of this Ph.D was greatly enhanced by his excellent criticism.

I have also been fortunate in having Dr. Terry Scoffin as a joint-supervisor. Discussions with him on many subjects, academic and otherwise, have been most rewarding. I am also grateful for his criticism of the final draft of this thesis.

I am grateful to Mrs. Denise Wilson for typing the majority of this thesis, and also Mrs. Marcia Wright who assisted on several occasions. To all of the secretaries at the Grant Institute who, at one time or another, have had to cope with my numerous mundane requests, and have still managed to keep a brave face, I thank you..... No really!

Thanks are also due to Drs. Graham Shimmield and Julian Andrews for discussion and reviews of some of the chapters, and to Dr N. B. Price for assistance with some of the problems of diagenesis. Proof reading was kindly undertaken by Dr. Geoff Harris and Neil Pickard, while George Ross helped with diagrams and taxi service....Good ol' Soapy!

A special thanks to Les Oldham and Robin Grayson for guidance in the field, and for sharing with me, their vast combined knowledge of the Craven Basin. Their kind hospitality during one short visit to Lancashire is also appreciated, but I must admit that I did not appreciate any of their jokes. Other assistance in the field was kindly provided by Dr. Nick Riley (B.G.S.), Mr. Rob Gawthorpe (B.P.), Prof. Alan Lees (Louvain), and Mr. Connor McDermot (Irish Geol. Surv.)

On the technical side, I am grateful to all involved with the Electron Microprobe Unit at the Grant Institute, especially Drs. Peter Hill and Douglas Russell. Thin sections were made by Kenny Cameron and Bill Hamilton, under the watchful eye of Colin Chaplin and Mrs. Flo' Tullis. Jim Smith has also provided expertise and bad humour from the workshop, and latterly, Mr. David Priestley has also been very helpful. Assistance from all other technical staff,

is appreciated.

Mrs Diane Baty is owed special thanks for her excellent long-term assistance with photographic and drafting facilities.

I must also thank Dr. Tony Fallick and other staff at the Scottish Universities Research and Reactor centre who helped with isotope analyses, particularly Dr. Adrian Boyce for sulphur isotopes, Dr. Ward Scott for carbon and oxygen isotopes. A special thanks to Capt. Terry Donnely for his technical assistance and hospitality.

Prof. G.S. Boulton of the Grant Institute kindly made funds available for the colour plates.

This work was carried out under an N.E.R.C. studentship.

REFERENCES

AHR, W.H. 1973. The carbonate ramp: an alternative model. Trans. Gulf Coast Geol. Soc. 23: 221-225.

AISSAOUI, D.M., BUIGUES, D., PURSER, B.H. 1986a. Model of reef diagenesis: Mururoa Atoll, French Polynesia. In: Reef Diagenesis. J.H. Schroeder and B.H. Purser (eds). Springer-Verlag, Berlin: 27-52.

____, CONIGLIO, M., JAMES, N.P. & PURSER, B.H. 1986b. Diagenesis of a Miocene reef-platform: Jebel Abu Shaar, Gulf of Suez, Egypt. In: Reef Diagenesis. J.H. Schroeder and B.H. Purser (eds). Springer-Verlag, Berlin: 112-131.

AL-HASHIMI, W.S. and HEMINGWAY, J.E. 1973. Recent dedolomitization and the origin of the rusty crusts of Northumberland. Jour. Sed. Petrology, 43: 82-91.

ALLAN, J.R. & MATTHEWS, R.K. 1977. Carbon and oxygen isotopes as diagenetic and stratigraphic tools: surface and subsurface data, Barbados, West Indies. Geology 5: 16-20.

___ & _____ 1982. Isotopic signature associated with early meteoric diagenesis. Sedimentology 29: 797-817.

AMIEUX, P. 1982. La cathodoluminescence: méthode d'étude sédimentologique des carbonates. Bull. Centres. Rech. Explor.-Prod. Elf-Aquitane Pau, 6: 437-483.

AMIEUX, P., DUCREUX, J.L., JAUTÉE, E., & PAILLERET, P. 1983. Septarias en domaine continental dans le Stampian de la Limagne d'Allier (Issoire, Puy-de-Dôme). Rev. Sc. Nat. d'Auvergne 49: 7-18.

ANDERTON, R., BRIDGES, P.H., LEEDER, M.R. & SELLWOOD, B.W. 1979. A Dynamic Stratigraphy of the British Isles. A study in crustal evolution. George Allen & Unwin, London, 301pp.

ARTHURTON, R.S. 1983. The Skipton Rock Fault - an Hercynian wrench fault associated with the Skipton Anticline, Northwest England. Geol. Journal 18: 105-114.

____ 1984. The Ribblesdale Fold Belt, NW England - a Dinantian-early Namurian dextral shear zone. In: Variscan tectonics of the North Atlantic region. D.H.W. Hutton and D.J. Sanderson (eds). Spec. Pub. Geol. soc. London 14: 131-138.

BADIOZAMAN, K. 1973. The Dorag dolomitization model - Application to the Middle Ordovician of Wisconsin. Jour. Sed. Petrology 43: 155-161.

BANNER, F.T. & WOOD, G.V. 1964. Recrystallisation in microfossiliferous limestones. Geol. Journal 4: 21-34.

BATHURST, R.G.C. 1959. Diagenetic fabrics in some British Dinantian limestones. Liverpool Manchester Geol. Journal 2: 11-36.

____ 1964. The replacement of aragonite by calcite in the molluscan shell wall. In: Approaches to Paleoecology. J. Imbrie & N.D. Newell (eds). Wiley, New York 357-76.

____ 1966. Boring algae, micrite envelopes and lithification of molluscan biosparites. Geol. Journal 5: 15-32.

____ 1970. Problems of lithification in carbonate muds. Geologists Association Proceedings 81: 429-440.

____ 1975. Carbonate sediments and their diagenesis (2nd edition). Elsevier, Amsterdam, 658pp.

____ 1977. Ordovician Meiklejohn bioherm, Nevada. Geol. Mag. 114: 308-311.

____ 1980. Stromatactis - origin related to submarine-cemented crusts in Paleozoic mud mounds. Geology 8: 131-134.

____ 1982. Genesis of stromatactis cavities between submarine crusts in Palaeozoic carbonate mud buildups. J. geol. Soc. London 139: 165-181.

____ 1983. Neomorphic spar versus cement in some Jurassic grainstones: significance for evaluation of porosity evolution and compaction. J. geol. Soc. London 140: 229-237.

BEALES, F.W. 1971. Cementation by white sparry dolomite. In: Carbonate cements. O.P. Bricker (ed). Baltimore John Hopkins University Studies in Geology 19: 330-338.

____ & HARDY, J.L. 1980. Criteria for the recognition of diverse dolomite types with an emphasis on studies on host rocks for Mississippi Valley-Type ore deposits. In: Concepts and Modles of Dolomitization. D.H. Zenger, J.B. Dunham and R.L. Ethington. Soc. Econ. Paleontol. Mineral. Spec. Pub. 28: 197-213.

BERNER, R.A. 1981. Authigenic mineral formation resulting from organic matter decomposition in modern sediments. Fortschritte der Mineralogie 59: 117-135.

____ & MORSE, J.W. 1974. Dissolution kinetics of calcium carbonate in sea water, IV Theory of calcite dissolution. Amer. Jour. Sci. 274: 108-134.

BERRY, J.R. 1984. The sedimentology and diagenesis of the Asbian limestones of North Derbyshire. PhD. Thesis (Unpub.) Univ. Aberdeen.

BIRNBAUM, S.J. & WIREMAN, J.W. 1984. Bacterial Sulfate reduction and pH: Implications for early diagenesis. Chemical Geology 43: 143-149.

BJØRLYKKE, K. 1983. Diagenetic reactions in sandstones. In: Sediment diagenesis. A. Parker and B.W. Sellwood (eds). NATO ASI Series C 115: 169-213.

BLACK, W.W. 1958. The structure of the Burnsall-Cracoe area and its bearing on the origin of the Cracoe knoll-reefs. Proc. Yorks. geol. Soc. 31: 391-414.

BODINE, M.W. HOLLAND, H.D. & BORCSIK, M. 1965. Coprecipitation of manganese and strontium with calcite. In: Symposium on problems of postmagmatic ore deposition 11: Prague 401-406.

BÖGLI, A. 1964. Mischungskorrosion, ein betrag zum verkarstungsproblem. Erkunde 18: 83-92.

BRAND, U. 1982. The oxygen and carbon isotope composition of Carboniferous fossil components: sea water effects. Sedimentology 29: 139-147.

____ & VEIZER, J. 1980. Chemical diagenesis of a multi-component carbonate system - 1: trace elements. Jour. Sed. Petrology 50: 1219-1236.

____ & _____ 1981. Chemical diagenesis of a multicomponent carbonate system - 2: Stable isotopes. Jour. Sed. Petrology 51: 987-997.

BRICKER, O.P. 1971 (ed). Carbonate Cements. Baltimore, Johns Hopkins University studies in Geology 19.

BROWN, P.R. 1964. Petrgraphy and origin of some upper Jurassic beds from Dorset, England. Jour. Sed. Petrology 34: 254-269.

BARNES, H.L. (ed) 1979. Geochemistry of hydrothermal ore deposits (2nd edition). Wiley and Sons, New York.

BURNLEY, A.J., EDMONDS, W.M., GALE, I.N. 1984. Catalogue of Geothermal resources of the UK. BGS Borehole index No SD66. CLITHEROE MHD2 British Geol. Surv.

BURRUS, R.C. CERCONE, & HARRIS, P.M. 1985. Timing of hydrocarbon migration - Evidence from fluid inclusions in calcite cements, tectonics and burial history. In: Carbonate cements. N. Schneidermann and P.M. Harris (eds). Soc. Econ. Paleontol. Mineral. Spec. Pub. 36: 277-289.

BUXTON, T.M. & SIBLEY, D.F. 1981. Pressure solution features in a shallow burried limestone. Jour. Sed. Petrology 51: 19-26.

CARPENTER, A.B. 1980. The chemistry of dolomite formation I: the stability of dolomite. In: Concepts and Models of dolomitization. D.H. Zenger, J.B. Dunham and R.L. Ethington. Soc. Econ. Paleontol. Mineral. Spec. Pub. 28: 111-121.

____, TROUT, M.L. & PICKETT, E.E. 1974. Preliminary report on the origin and chemical evolution of Pb-Zn rich oil field brines in Central Mississippi. Econ. Geology 69: 1191-1206.

CAYEUX, L. 1935. Les roches sedimentaires de France; roche carbonatées: Paris, Masson, 463pp.

CERCONE, K.R. & LOHMANN, K.C. 1986. Diagenetic History of the Union 8 Pinnacle Reef (Middle Silurian), Northern Michigan, USA. In: Reef Diagenesis. J.H. Schroeder and B.H. Purser (eds). Springer-Verlag, Berlin: 381-398.

CHAFETZ, H.S. 1979. Petrology of CO_3 nodules from a Cambrian tidal inlet accumulation, Central Texas. Jour. Sed. Petrology 49: 215-222.

____ & FOLK, R.L. 1984. Travertines: Depositional morphology and the bacterially constructed constituents. Jour. Sed. Petrology 54: 289-316.

CHARSLEY, T.J. 1984. Early carboniferous rocks of the Swinden No.1 Borehole, west of Skipton. Rep. British Geological Surv. No16/1: 5-12.

CHOQUETTE P.W. 1968. Marine diagenesis of shallow lime-mud sediments: Insights from SO^{18} and SC^{13} data. Science 161: 1130-1132.

____ 1971. Late ferroan dolomite cement, Mississippian carbonates, Illinois Basin, USA. In: Carbonate cements, O.P. Bricker (ed). Baltimore, Johns Hopkins University studies in Geology no 19; 339-346.

____ & PRAY, L.C. 1970. Geologic nomenclature and classification of porosity in sedimentary carbonates. Bull. Am. Assoc. Petrol. Geologists 54: 207-250.

____ & STEINEN, R.P. 1980. Mississippian non-supratidal dolomite, Ste. Genevieve Limestone, Illinois basin: Evidence for mixed-water dolomitization. In: Concpets and models of dolomitization. D.H. Zenger, J.B. Dunham and R.L. Ethington. Soc. Econ. Paleontol. Mineral. Spec. Pub. 28: 163-196.

COLEMAN, M.L., CURTIS, C.D. & IRWIN, H. 1979. Burial rate a key to source and reservoir potential. World Oil 188: 83-92.

CONIGLIO, M. & JAMES, N.P. 1985. Calcified algae as sediment contributors to Early Palaeozoic limestones: Evidence from deep water sediments of the Cow Head Group, Western Newfoundland. Jour. Sed. Petrology 55: 746-754.

COOGAN, A.H. 1970. Measurements of compaction in oolitic grainstone. Jour. Sed. Petrology 40: 921-928.

COTTER, E. 1966. Limestone diagenesis and dolomitization in Mississippian carbonate banks in Montanna. Jour. Sed. Petrology 36: 764-774.

COWAN, P. 1980. Diagenesis of lime mud, Mississippian-age bioherms. Sacramento Mountains, New Mexico. MS Thesis (Unpub.) State Univ. of New York at Stony Brook.

____ & MEYERS, W.J. 1982. Diagenesis of lime mud, Mississian-age bioherms. Sacramento Mountains, New Mexico (abs). Bull. Amer. Assoc. Petrol. Geologists 66: 559-60.

CRICKMAY , G.W. 1945. Petrography of limestones. In: Geology of Lau, Fiji. H.S. Ladd and J.E. Hoffmeister (eds). Bernice P. Bishop Museum Bull 181: 211-250.

CROCKET, J.H. & WINCHESTER, J.W. 1966. Coprecipitation of zinc with calcium carbonate. Geochim. Cosmochim. Acta. 30: 1093-1109.

CULLIS, C.G. 1904. The mineralogical changes observed in the cores of the Funafuti borings. In: The Atoll of Funafuti. T.G. Bonney (ed). Roy. Soc. London: 393-240.

CURTIS, C.D. 1978. Possible links between sandstone diagenesis and depth related geochemical reactions occurring in enclosing mudstones. J. geol. Soc. London 135: 107-117.

CURTIS, R., EVANS, G., KINSMAN, D.J.J. & SHEARMAN, D.J. 1963. Association of dolomite and anhydrite in the recent sediments of the Persian Gulf. Nature 197: 679-680.

CZERNIAKOWKSI, L.A., LOHMANN, K.C. & WILSON, J.L. 1984. Closed-System marine burial diagenesis: isotopic data from the Austin Chalk and its components. Sedimentology 31: 863-877.

DAVIES, G.R. 1977. Former magnesian calcite and aragonite submarine cements in upper Palaeozoic reefs of the Canadian arctic: A summary. Geology 5: 11-15.

____ 1979. Dolomite reservoir rocks - Processes, controls, porosity development. In Geology of carbonate porosity. Am. Assoc. Petrol. Geologists Continuing Education Course Notes Series 11: C1-C17.

____ & KROUSE, H.R. 1975. Carbon and oxygen isotopic composition of Late Paleozoic calcite cements, Canadian Arctic Archipelago - Preliminary results and interpretaitons. Canada Geological Survey Paper 75-1 part B; 215-220.

DEGENS, E.T. & MOPPER, K. 1976. Factors controlling the distribution and early diagenesis of organic material in marine sediments. In: Chemical Oceanography 6. J.P. Riley and R. Chester (eds). Academic Press, London: 59-113.

DEGROOT, K. 1967. Experimental Dedolomitization. Jour. Sed. Petrology 37: 1216-1220.

DICKSON, J.A.D. 1965. A modified staining technique for Carbonates in thin section. Nature 205: 587.

____ 1966. Carbonate Identification and Genesis as Revealed by Staining. Jour. Sed. Petrology 36: 491-505.

____ 1980. Artificial colouration of fluorite by electron bomardment. Min. Mag. London 43: 820-822.

____ 1983. Graphical modelling of crystal aggregates and its relevance to cement diagenesis. Phil. Trans. Roy. Soc. London 309 465-502.

____ & COLEMAN, M.L. 1980. Changes in carbon and oxygen isotope composition during limestone diagenesis. Sedimentology 27: 107-118.

DUNNINGTON, H.V. 1954. Stylolite develoment post-dates rock induration. Jour. Sed. Petrology 24 27-49.

DUPONT, E. 1863. Sur le calcaire carbonifère de la Belgique et du Mainaut francais. Bull. Acad. roy. Belg., 2e série 15 86 et seq.

____ 1881. Sur l'origine des calcaires dévoniens de la Belgique. Bull. Acad. Roy. Sci. Belg. 3rd Ser. 2: 264-280.

DUPONT, H. 1969. Contribution à l'étude des Facies du Waulsortien de Waulsort. Mém. Inst. Geol. Univ. Louvain XXIV: 95-163.

DURNEY, D.W. & RAMSAY, J.G. 1973. Incremental strains measured by syntectonic crystal growth. In: Gravity and tectonics. K.A. De Jong and R. Scholten (eds). Wiley, New York: 67-96.

DYMOND, J., LYLE, M., FINNEY, B., PIPER, D.Z., MURPHY, K., CONARD, R., & PISIAS, N. 1984. Ferromanganese nodules from MANOP sites H, S and R - Control of mineralogical and chemical composition by multiple accretionary processes. Geochim. Cosmochim. Acta 48: 931-949.

EARP, J.R., MAGRAW, D., POOLE, E.G., LAND, D.H. & WHITEMAN, A.J. 1961. Geology of the country around Clitheroe and Nelson. Mem. Geol. Surv. UK London No 68, 346 pp.

ENOS, P. 1986. Diagenesis of Mid-Cretaceous Rudist Reefs, Valles Platform, Mexico. In: Reef Diagenesis. J.H. Schroeder and B.H. Purser (eds). Springer-Verlag, Berlin: 160-185.

EPSTEIN, S., BUCHSBAUM, R., LOWENSTAM, H.A. & UREY, H.C. 1953. Revised carbonate-water isotopic temperature scale. Geol. Soc. Am. Bull. 64: 1315-1326.

EVAMY, B.D. 1963. The application of chemical stain technique to a study of dedolomitization. Sedimentology 2: 164-170.

____ 1967. Dedolomitisation and the development of rhombohedral pores in limestones. Jour. Sed. Petrology 37: 1204-1215.

____ 1969. The precipitational environment and correlation of some calcite cements deduced from artificial staining. Jour. Sed. Petrology 39: 787-793.

____ & SHEARMAN, D.J. 1965. The development of overgrowths from echinoderm fragments. Sedimentology 5: 211-233.

____ & ____ 1969. Early stages in development of overgrowths on echinoderm fragments in limestones. Sedimentology 12: 317-322.

FAIRCHILD, I.J. 1980. Stages in a Precambrian dolomitization, Scotland: cementing versus replacement textures. Sedimentology 27: 631-650.

____ 1983. Chemical controls of cathodoluminescence of natural dolomites and calcites: new data and review. Sedimentology 30: 579-583.

FEAZEL, C.T. & SCHAZINGER, R.A. 1985. Prevention of Carbonate cementation in petroleum reservoirs. In: Carbonate Cements: N. Schneidermann and P.M. Harris (eds). Soc. Econ. Paleontol. Mineral. Spec. Pub. 36: 97-106.

FEWTRELL, M.D. & SMITH, D.G. 1980. Revision of the Dinantian Stratigraphy of the Craven Basin, N. England. Geol. Mag. 117: 37-49.

FLÜGEL, E. 1982. Microfacies analysis of limestones. Springer-Verlag, Berlin, 633pp.

FOLK, R.L. 1959. Practical petrographical classification of limestones. Bull. Amer. Assoc. Petrol. Geologists 43: 1-38.

____ 1965. Some aspects of recrystallization in ancient limestons. In: L.C. Pray and R.C. Murray (eds). Dolomitization and limestone diagenesis: a symposuim. Soc. Econ. Paleontol. Mineral. Spec. Pub. 13: 14-48.

____ 1973. Carbonate petrography in the post-Sorbian age. In: Evolving concepts in sedimentology. Johns Hopkins University studies in geology 21: 118-158.

____ 1974. The natural history of crystalline calcium carbonate: Effects of magnesium content and salinity. Jour. Sed. Petrology 44: 816-825.

____ & ASSERETO, R. 1974. Giant aragonite rays and baroque white dolomite in tepees, Traissic of Lombardy (abs). Am. Assoc. Petrol. Geologists. Prog. Ann. Meeting, San Antonio, Texas: 34-35.

____ & LAND, L.S. 1975. Mg/Ca ratio and salinity: Two controls over crystallization of dolomite. Bull. Am. Assoc. Petrol. Geologists 59: 60-68.

FRANK, J.R. 1981. Dedolomitization in the Taum Sauk Limestone (Upper Cambrian), southeast Missouri. Jour. Sed. Petrology 51: 7-18.

____, CARPENTER, A.B. & OGLESBY, T.W. 1982. Cathodoluminescence and composition of calcite cement in the Taum Sauk Limestone (Upper Cambrian), Southeast Missouri. Jour. Sed. Petrology 52: 631-638.

FREEMAN, T. 1971. Morphology and composition of an Ordovician vadose cement. Nature Phys. Sci. 233, 133-134.

FRIEDMAN, G.M. 1965. Terminology of crystallization textures and fabrics in sedimentary rocks. Jour. Sed. Petrology 35: 643-655.

____ 1968. The fabric of carbonate cement and matrix and its dependence on the salinity of water. In: Recent developments in Carbonate Sedimentology in Central Europe. G. Muller and G.M. Friedman (eds). Springer-Verlag, Berlin: 11-20.

____ 1974. Early diagenesis and lithification in carbonate sediments. Jour. Sed. Petrology 34: 777-813.

____ 1985. The problem of submarine cement in classifying reefrock: An experience in frustration. In: Carbonate Cements. N. Schneidermann & P.M. Harris (eds). Soc. Econ. Paleontol. Mineral. Spec. Pub. 36: 117-121.

____, AMIEL, A.J. & SCHNEIDERMANN, N. 1974. Submarine cementation in reefs: example from the Red Sea. Jour. Sed. Petrology 44: 816-825.

____, ALI, S.A. & KRINSLEY, D.H. 1976. Dissolution of quartz accompanying carbonate precipitation and cementation in reefs: example from the Red Sea. Jour. Sed. Petrology 46: 970-973.

FRITZ, P. & KATZ, A. 1972. The sodium distribution of dolomite crystals. Chem. Geology 10: 237-244.

FROELICH, P.N., KLINKHAMMER, G.P., BENDER, M.L., LEUDTKE, N.A., HEATH, G.R., CULLEN, D., DAUPHIN, P., HAMMOND, D., HARTMAN, B. & MAYNARD, V. 1979. Early Oxidation of organic matter in pelagic sediments of the eastern equatorial Atlantic: suboxic diagenesis. Geochim. Cosmochim. Acta 43: 1075-1090.

FRYKMAN, P. 1986. Diagenesis of Silurian bioherms in the Klinteberg Formation, Gotland, Sweden. In: Reef Diagenesis. J.H. Schroeder and B.H. Purser (eds). Springer-Verlag, Berlin: 399-423.

FUCHTBAUER, H. & HARDIE, L.A. 1976. Experimentally determined homogeneous distribution coefficients for precipitated magnesium calcites. Abstr. Ann. Progr. Meet. geol. Soc. Am. 877.

GAWTHORPE, R.L. 1986. Sedimentation during carbonate ramp-to-slope evolution in a tectonically active area: Bowland Basin (Dinantian), northern England. Sedimentology 33: 185-206.

____ 1987. Tectono-sedimentary evolution of the Bowland Basin, N. England, during the Dinantian. J. geol. Soc. London 144: 59-71.

____ & CLEMMEY, H. 1985. Geometry of submarine slides in the Bowland Basin (Dinantian) and their relation to debris flows. J. geol. Soc. Lodnon 142: 555-565.

GILES, R. & MARSHALL, J.D. 1986. Constraints on the development of secondary porosity in the subsurface: re-evaluation of processes. Marine and Petroleum. Geol. 3: 243-255.

GIVEN, R.K. & LOHMANN, K.C. 1985. Derivation of the original isotopic composition of Permian marine cements. Jour. Sed. Petrology 55: 430-439.

____ & _____, K.C. 1986. Isotopic evidence for the early meteoric diagenesis of the reef facies, Permian reef complex of west Texas and New Mexico. Jour. Sed. Petrology 56: 183-193.

GOLDBERG, M. 1967. Supratidal dolomitization and dedolomitization in Jurassic Rocks of Hamakhtesh Haqatan, Israel. Jour. Sed. Petrology 37: 760-773.

GRAYSON, R.F. & OLDHAM, L. 1987. A new structral framework for the Northern British Dinantian as a basis for oil, gas and mineral exploration. In: European Dinantian Environments. J. Miller, A.E. Adams and V.P. Wright (eds). Wiley and Sons, Chichester, New York: 33-60.

GREGG, J.M. & SIBBLEY, D.F. 1984. Epigenetic dolomitization and the origin of xenotopic dolomite texture. Jour. Sed. Petrology 54: 908-931.

GROVER, J.R.G. & READ, J.F. 1983. Palaeoaquifer and Deep Burial related cements defined by regional cathodoluminescent patterns, Middle Ordovician carbonates, Virginia. Bull. Am. Assoc. Petrol. Geologists 67: 1275-1303.

HALLEY, R.B. & HARRIS, P.M. 1979. Freshwater cementation of a 1,000 year-old oolite. Jour. Sed. Petrology 49: 969-988.

____ & SCHOLLE, P.A. 1985. Radiaxial Fibrous Calcite as early burial, open system cement: Isotopic evidence from Permian of China (abs). Bull. Am. Assoc. Petrol. Geologists 69: 261.

HANSHAW, B.B., BACK, W. & DEIKE, R.G. 1971. A geochemical hypothesis for dolomitization by ground water. Econ. Geology 66: 710-724.

HARRIS, P.M. (ed) 1983. Carbonate buildups - A core workshop. Soc. Econ. Paleontol. Mineral. Core Workshop No 4, Dallas, 593pp.

HARRISON, D.J. 1982. The limestone resources of the Craven Lowlands: description of parts of 1:50 000 Geological sheets 59,60,61,67,68 and 69. Miner. Assess. Rep. Inst. Geol. Sci. No 116.

HENRICH, R. & ZANKL, H. 1986. Diagenesis of Upper Traissic J.H. Schroeder and B.H. Purser (eds). Springer-Verlag Berlin: 245-268.

HEY, M.H. 1962. An index of mineral species and varieties arranged chemically (2nd edition). British Museum London 728pp.

HITCHON, B. 1977. Geochemical links between oil field and ore deposits and sedimentary rocks. In: Proc. forum on oil and ore in sediments. P. Garrard (ed). dept Geol. Imperial College London, England: 1-37.

HUDSON, J.D. 1977. Stable isotopes and limestone lithification. J. geol. Soc. London 133: 637-660.

____ 1978. Concretions, isotopes and diagenetic history of the Oxford clay (Jurassic) of central England. Sedimentology 25: 339-370.

ICHIKUNI, M. 1973. Partition of strontium between calcite and solution: effect of substitution of manganese. Chem. Geol. 11: 315-319.

ILLING, L.V. 1954. Bahaman calcareous sands. Bull. Amer. Assoc. Petrol. Geologists 38: 1-95.

INESON, P.R., RICHARDSON, R.T. & WOOD, G.H. 1972. A Baryte-Galena vein in the magnesian Limestone at Whitwell, Derbyshire. Proc. Yorks Geol. Soc. 39: 139-150.

IRWIN, H. 1980. Early diagenetic carbonate precipitation and pore fluid migration in the Kimmeridage clay of Dorset, England. Sedimentology 27: 577-591.

____, CURTIS, C. & COLEMAN, M. 1977. Isotopic evidence for source of diagenetic carbonates formed during burial of organic-rich sediments. Nature 269: 209-213.

JAMES, N.P. & CHOQUETTE, P.W. 1983. Diagenesis 6. Limestones - The sea floor diagenetic environment. Geoscience Canada 10: 162-180.

___ & ____ 1984. Diagenesis 9. Limestones - The meteoric diagenetic environment. Geoscience Canada 11: 161-193.

____, GINSBURG, R.N., MARSZALEK, D.S. & CHOQUETTE, P.W. 1976. Facies and fabric specificity of early sub-sea cements in shallow Belize (British Honduras) reef. Jour. Sed. Petrology 46: 523-544.

JAMESON, J. 1980. Depositional environments in the Petershill Formation, Bathgate, West Lothian. PhD Thesis (Unpub.) Edinburgh University.

JODRY, R.L. 1969. Growth and dolomitization of Silurian reefs, St Clair County, Michigan. Bull. Am. Assoc. Petrol. Geologists 52: 957-981.

KANARIS-SOTIRIOU, R., NEVES, R. & GIBB, F.G.F. 1986. Wall-rock silicification associated with fluorite veins in Carboniferous limestone at Butts Quarry, Derbyshire, England. Geol. Mag. 123: 569-579.

KAPLAN, I.R. 1983. Stable isotopes of sulphur, nitrogen and deuterium in Recent marine environments. In: Stable isotopes in geology. Soc. Econ. Paleontol. Mineral. Short Course No. 10: Chapter 2.

KASTNER, M. 1971. Authigenic feldspars in carbonate rocks. Am. Mineral. 56: 1403-1442.

KATZ, A. 1971. Zoned dolomite crystals. Jour. Geol. 79: 38-51.

KEITH, M.L. & WEBER, J.N. 1964. Carbon and oxygen isotopic composition of selected limestones and fossil. Geochim. Cosmochim. Acta 37: 1899-1908.

KELLER, W.D. 1978. SEM of kaolins collected from diverse environments of origin. Clays and Clay Minerals 24: 107-113.

KEMP, A.L.W. & THODE, H.G. 1968. The mechanism of the bacterial recution of sulphate and of sulphite from isotope fractionation studies. Geochim. Cosmochim. Acta 32: 71-91.

KENDALL, A.C. 1977. Fascicular-optic calcite: a replacement of bundled acicular carbonate cements. Jour. Sed. Petrology 47: 1056-1062.

____ 1985. Radiaxial fibrous calcite: A reappraisal. In: Carbonate cements. N. Schneidermann and P.M. Harris (eds). Soc. Econ. Paleontol. Mineral. Spec. Pub. 36: 59-77.

____ & TUCKER, M.E. 1973. Radiaxial fibrous calcite: a replacement after acicular calcite. Sedimentology 20: 365-389.

KERANS, C. HURLEY, N.F. & PLAYFORD, P.E. 1986. Marine Diagenesis in Devonian Reef Complexes of the Canning Basin, Western Australia. In: Reef Diagenesis. J.H. Schroeder and B.H. Purser (eds). Springer-Verlag, Berlin: 357-380.

KING, D.E. 1984. A diagenetic history of the Waulsortian limestones, eastern Midlands and Dublin Basin, Republic of Ireland. MS thesis (Unpub.) State Univ. of New York at Stoney Brook, 369pp.

KOCH, R. & SCHORR, M. 1986. Diagenesis of Upper Jurassic sponge-algal reefs in SW Germany. In: Reef diagenesis. J.H. Schroeder and B.H. Purser (eds). Springer-Verlag, Berlin: 224-244.

KREBS, W. 1969. Early void-filling cementation in Devonian fore-reef limestones (Germany). Sedimentology 12: 279-299.

LAND, L.S. 1970. Phreatic versus vadose meteoric diagenesis of limestones: eivdence from fossil water tables. Sedimentology 14: 175-185.

____ 1971. Submarine lithification of Jamaican reefs. In: Carbonate cements. O.P. Bricker (ed). Johns Hopkins University Studies in Geology 19: 59-62.

____ 1976. Early dissolution of sponge spicules from reef sediments, North Jamaica. Jour. Sed. Petrology 46: 967-969.

____ 1980. The isotopic and trace element geochemistry of dolomite: The state of the art. In: Concepts and models of dolomitization. D.H. Zenger, J.B. Dunham and R.L. Ethington (eds). Soc. Econ. Paleontol. Mineral. Spec. Pub. 28: 87-110.

____ & EPSTEIN, S. 1970. Late Pleistocene diagenesis and dolomitization north Jamaica. Sedimentology 14: 187-200.

____ & GOREAU, T.F. 1970. Submarine lithification of Jamaican reefs. Jour. Sed. Petrology 40: 457-562.

LASEMI, Z. & SANDBERG, P.A. 1983. Recognition of original mineralogy in micrites. (abs). Bull. Am. Assoc. Petrol. Geologists 67: 499-500.

LEES, A. 1964. The structure and origin of Waulsortian (Lower Carboniferous) "reefs" of west-central Eire. Phil. Trans. Roy. Soc. London B247: 483-531.

____ & MILLER, J. 1985. Facies variation in Waulsortian buildups, Part 2; Mid-Dinantian buildups from Europe and North America. Geol. Journal 20: 159-180.

____ HALLET, V. & HIBO, D. 1985. Facies variations in Waulsortian buildups, Part 1; A model from Belgium. Geol. Journal 20: 133-158.

LINDHOLM, R.C. & FINKLEMAN, R.B. 1972. Calcite staining: semiquantitative determination of ferrous iron. Jour. Sed. Petrology 42: 239-242.

LOGAN, B.W. & SEMENIUK, V. 1976. Dynamic metamorphism; processes and products in Devonian carbonate rocks. Canning Basin Western Australia. Geol. Soc. Australia Spec. Pub. 6: 138pp Sydney.

LOHMANN, K.C. & MEYERS, W.J. 1977. Microdolomite inclusions in cloudy prismatic calcites: a proposed criterion for former high magnesian calcites. Jour. Sed. Petrology 47: 1078-1088.

LONGMAN, M.W. 1980. Carbonate diagenetic textures from near surface diagenetic environments. Bull. Am. Assoc. Petrol. Geologists 64: 461-487.

____ & MENCH, P.A. 1978. Diagenesis of Cretaceous limestones in the Edwards aquifer system of south-central Texas: a scanning electron microscope study. Sedimentology Geology 21: 241-276.

LOVE, L.G., AL-KAISY, A.T.H. & BROCKLEY, H. 1984. Mineral and organic material in matrices and coatings of framboidal pyrite from Pennsylvanian sediments, England. Jour. Sed. Petrology 54: 869-876.

LOWENSTAM, H.A. 1961. Mineralogy, O^{18}/O^{16} ratios and strontium and magnesium contents of recent and fossil brachiopods and their bearing on the history of the fossil oceans. Jour. Geol. 69: 241-260.

LUMSDEN, D.N. & CHIMAUSKY, J.S. 1980. Relationship between dolomite nonstoichiometry and carbonate facies parameters. In: Concepts and models of dolomitization. D.H. Zenger, J.B. Dunham and R.L. Ethington (eds). Soc. Econ. Paleontol. Mineral. Spec. Pub. 28: 123-137.

MACINTYRE, I.G. 1977. Distribution of submarine cements in a modern Caribbean fringing reef, Galeta Point, Panama. Jour. Sed. Petrology 47: 503-516.

____ 1984. Extensive submarine lithification in a cave in the Belize Barrier Reef platform. Jour. Sed. Petrology 54: 221-235.

MACHEL, H.G. 1985. Cathodoluminescence in calcite and dolomite and its chemical interpretation. Geoscience Canada 12: 139-145.

MAGARA, K. 1976. Thickness of removed seidmentary rocks, paleopore pressure and palaotemperature southwestern part of Western Canada Basin. Bull. Am. Assoc. Petrol. Geologists 60: 554-565.

MARSHALL, J.D. 1981. Zoned calcites in Jurassic ammonite chambers: trace elements, isotopes and neomorphic origin. Sedimentology 28: 867-887.

____ 1982. Isotopic composition of displacive fibrous calcite veins: reversals in pore water composition trends during diagenesis. Jour. Sed. Petrology 52: 615-630.

____ & ASHTON, M. 1980. Isotopic and trace element evidence for submarine lithification of hardgrounds in the Jurassic of eastern England. Sedimentology 27: 271-289.

MATTER, A., DOUGLAS, R.G. & PERCH-NIELSON, K. 1975. Fossil preservation, geochemistry and diagenesis of pelagic carbonates from Shatsky Rise, Northwest Pacific. In: Larson et al., Init. Rep. Deep Sea Drilling Project 32: 980pp.

MATTES, B.W. & MOUNTJOY, E.W. 1980. Burial dolomitization of the Devonian Miette buildup, Jasper National Park, Alberta. In: Concepts and models of dolomitization. D.H. Zenger, J.B. Dunham and R.L. Ethington (eds). Soc. Econ. Paleontol. Mineral. Spec. Pub. 28: 259-297.

MATTHEWS, R.K. 1968. Carbonate diagenesis: equilibration of sedimentary mineralogy to the subaerial environment: coral cap of Barbados, West Indies. Jour. Sed. Petrology 38: 1110-1119.

____ 1974. A process approach to diagenesis of reefs and reef associated limestones. In: Reefs in time and Space. L.F. Laporte (ed). Soc. Econ. Paleontol. Mineral. Spec. Pub. 18: 234-256.

MAZZULLO, S.J. 1980. Calcite pseudospar replacive of marine acicular aragonite, and implications for aragonite cement diagenesis. Jour. Sed. Petrology 50: 409-422.

____ 1986. Mississippi Valley-type sulphides in Lower Permian Dolomites, Delaware Basin, Texas: Implications for basin evolution. Bull. Am. Assoc. Petrol. Geologists 70: 943-952.

MEYERS, W.J. 1974. Carbonate cement stratigraphy of the Lake Valley Formation, Mississippian, Sacramento Mountains, New Mexico. Jour. Sed. Petrology 44: 837-861.

____ 1978. Carbonate Cements: Their regional distribution and interpretaiton in Mississippian limestones of southwestern New Mexico. Sedimentology 25: 371-400.

____ 1980. Compaction in Mississippian skeletal limestones, southwestern New Mexico. Jour. Sed. Petrology 53: 231-242.

____ & LOHMANN, K.C. 1980. Geochemistry of regionally extensive calcite zones in Mississippian skeletal limestones, New Mexico. Bull. Am. Assoc. Petrol. Geologists (abs). 64: 750.

____ & ____ 1985. Isotope geochemistry of regionally extensive calcite cement zones and marine components in Mississippian limestones, New Mexico. In: Carbonate cements. N. Schneidermann and P.M. Harris (eds). Soc. Econ. Palaeontol. Mineral. Spec. Pub. 36: 223-239.

____, COWAN, P. & LOHMANN, K.C. 1982. Diagenesis of Mississippian skeletal limestones and bioherm muds, New Mesico. In: Symposium on the paleoenvironmental setting and distribution of the Waulsortian facies. K. Bolton, H.R. Lane and D.V. Le Mone (eds). El Paso Geol. Soc. and Univ. of Texas: 80-95.

MICHARD, G. 1968. Coprecipitation de l'ion manganeauz avec le carbonate de calcium. Comptes Rendus Acad. Sci., Paris, ser D 267: 1685-1688.

MILLER, J. 1973. Coignouina decora sp. nov. and Carbonocoryphe hahnorum sp. nov. (Trilobita) from a Visean fissure deposit near Clitheroe, Lancs. Geol. Mag. 110: 113-124.

____ 1986. Facies relationships and diagenesis in Waulsortian mudmounds from the Lower Carboniferous of Ireland and N. England. In: Reef Diagenesis. J.H. Schroeder and B.H. Purser (eds). Springer-Verlag, Berlin: 311-335.

MILLER J. (1988) Microscopial techniques II: In; M.E. Tucker (ed.), Techniques in Sedimentology. Blackwell.

____ & CLARKSON, E.N.K. 1980. The post-ecdysial development of the cuticle and the eye of the Devonian trilobite Phacops rana milleri Stewart 1927. Phil. Trans. Roy. Soc. London 288: 461-480.

____ & GRAYSON, R.F. 1972. Origin and structure of the Lower Visean "reef" limestones near Clitheroe, Lancashire. Proc. Yorks. geol. Soc. 38: 607-638.

____ & ____ 1982. The regional context of Waulsortian facies in Northern England. In: Symposium on the paleoenvironmental setting and distribution of the Waulsortian facies. K. Bolton, H.R. Lane and D.V. Le Mone (eds). El Paso Geol. Soc. and Univ. of Texas. 17-33.

MILLIMAN, J.D. 1974. Marine Carbonates. Springer-Verlag, New York, 375pp.

MIRSAL, I.A. & ZANKL, H. 1985. Some phenomenological aspects of Carbonate geochemistry. The control effect of transition metals. Geologische Rundschau 74: 367-377.

MISIK, M. 1971. Observations concerning calcite veinlets in carbonate rocks. Jour. Sed. Petrology 41: 450-460.

MOORE, C.H. 1985. Upper Jurassic subsurface cements: A case history. In: Carbonate Cements. N. Schneidermann and P.M. Harris (eds). Soc. Econ. Paleontol. Mineral. Spec. Pub. 36: 291-308.

____ & DRUCKMAN, Y. 1981. Burial diagenesis and porosity evolution, Upper Jurassic Smackover, Arkansas and Louisianna. Bull. Am. Assoc. Petrol. Geologists 65: 597-628.

M'RABET, A., NEGRA, M.H., PURSER, B.H., SASSI, S. & BENAYED, N. 1986. Micrite diagenesis in Senonian rudist build-ups in central Tunisia. In: Reef Diagenesis. J.H. Schroeder and B.H. Purser (eds). Springer-Verlag, Berlin: 210-223.

MUIR, M., LOCK, D. & VON DER BORCH, C. 1980. The coorong model for penecontemporaneous dolomite formation in the middle Proterozoic McArthur Group, Northern Territory Australia. In: Concepts and models of dolomitization. D.H. Zenger, J.B. Dunham and R.L. Ethington (eds). Soc. Econ. Paleontol. Mineral. Spec. Pub. 28: 51-67.

MURATA, K.J., FRIEDMAN, I. & MADSEN, B.M. 1967. Carbon-13 rich diagenetic carbonates in Miocene formations of California and Oregon. Science 156: 1484-1486.

MURRAY, R.C. 1960. Origin of porosity in carbonate rocks. Jour. Sed. Petrology 30: 59-84.

MURRAY, J.W., DILLARD, J.G., GIOVANOLI, R., MOERS, H. & STUMM, W. 1985. Oxidation of Mn(II): Initial mineralogy, oxidation state and ageing. Geochim. Cosmochim. Acta 49: 463-470.

NELSON, R.A. 1981. Significance of fracture sets associated with stylolite zones. Bull. Am. Assoc. Petrol. Geologists 65: 2417-2425.

NEUMANN, A.C., KOFOED, J.W. & KELLER, G.H. 1977. Lithoherms in the straits of Florida. Geology 5: 4-10.

NORTHRUP, D.A. & CLAYTON, R.N. 1966. Oxygen isotope fractionation in systems containing dolomite. Jour. Geol. 74: 175-196.

OGLESBY, T.W. 1976. A model for the distribution of manganese, iron and magnesium in authigenic calcite and dolomite cements in the upper Smackover Formation in eastern Mississippi. MS Thesis (Unpub.) Univ. of Missouri, Columbia, Mo. 122pp.

OLDERSHAW, A.E. & SCOFFIN, T.P. 1967. The source of ferroan and non-ferroan calcite cements in the Halkin and Wenlock limestones. Geol. Journal 5: 309-320.

PARK, W.C. & SCHOT, E.H. 1968. Stylolites; their nature and origin. Jour. Sed. Petrology 38: 175-191.

PARKINSON, D. 1926. The faunal succession in the Carboniferous Limestone and Bowland Shales at Clitheroe and Pendle Hill, Lancashire. Q. Jl. geol. Soc. Lond. 82: 188-249.

1950. Some features of the Lower Carboniferous reef limestones of Clitheroe, Lancashire. Geol. Mag. 87: 337-350.

1957. Lower Carboniferous reefs of northern England. Bull. Am. Assoc. Petrol. Geologists 41: 511-537.

1967. The Lower Carboniferous limestone knolls of Clitheroe, Lancashire. Geol. Mag. 104: 371-389.

PEDERSEN, T.F. & PRICE, N.B. 1982. The geochemistry of manganese carbonate in Panama Basin sediments. Geochim. Cosmochim. Acta 46: 59-68.

PHILCOX, M.E. 1963. Banded calcite mudstones in the Lower Carboniferous "reef" knolls of the Dublin basin, Ireland. Jour. Sed. Petrology 33: 904-913.

PHILLIPS, W.J. 1974. The development of vein and rock textures by tensile strain crystallization. J. geol. Soc. London 130: 441-448.

1986. Hydraulic fracturing effects in the formation of mineral deposits. Trans. Instn. Min. Metall. 95: B17-24.

PIERSON, B.J. 1981. The control of cathodoluminescence in dolomite by iron and manganese. Sedimentology 28: 601-610.

PINGITORE, N.R. Jr 1976. Vadose and phreatic diagenesis: processes, products and their recognition in corals. Jour. Sed. Petrology 46: 985-1006.

PISCIOTTO, K.A. 1981. Review of secondary carbonates in the Monterey Formation, California. In: The Monterey Formation and related siliceous rocks of California. R.E. Garrison and R.G. Douglas (eds). Soc. Econ. Paleontol. Mineral.: 273-283.

PLUMMER, L.N. 1975. Mixing of seawater with calcium carbonate ground water. Geol. Soc. Am. Memoir 142: 219-236.

POPP, B.N., ANDERSON, T.F. & SANDBERG, P.A. 1983. Importance of co-ordinating compositional and textural analyses limestone constituents (abs). Geol. Soc. Am. Bull. 15: 662.

_____, PODOSEK, F.A., BRANNON, J.C. ANDERSON, T.F. & PIER, J. 1986a. $^{87}Sr/^{86}Sr$ ratios in Permo-Carboniferous sea water from the analyses of well-preserved brachiopod shells. Geochim. Cosmochim. Acta 50: 1321-1328.

_____, ANDERSON, T.F. & SANDBERG, P.A. 1986b. Brachiopods as indicators of original isotopic compositions in some Paleozoic limestones. Geol. Soc. Am. Bull. 97: 1262-1269.

PRATT. B.R. 1982. Stromatolitic framework of carbonate mud mounds. Jour. Sed. Petrology 28: 261-273.

PRAY, L.C. 1958. Fenestrate bryozoan core facies, Mississippian bioherms, southwestern United States. Jour. Sed. Petrology 28: 261-273.

_____ 1960 Compaction in calcilutites. (abs). Geol. Soc. Am. Bull. 71: 1946.

_____ 1965. Clastic limestone dikes in Mississippian bioherms, New Mexico. Geol. Soc. Am. Spec. Paper 82: 154-155.

_____ 1969. Micrite and carbonate cement: genetic factors in Mississippian bioherms. Jour. Paleontology Abstr. 43: 895.

_____ 1982. Section II Clastic Dikes (abs). In: Symposium on the Palaeonevionmental setting and distribution of the Waulsortian facies. K. Bolton, H.R. Lane and D.V. Le Mone (eds). El Paso Geol. Soc. and Univ. of Texas: 157.

_____ & MURRAY, R.C. (eds). 1965. Dolomitization and limestone diagenesis. Soc. Econ. Palentol. Mineral. Spec. Pub. 13, 180pp.

PREZBINDOWSKI, D.R. 1985. Burial cementation - Is it important? A case study. Stuart city trend, South Central Texas. In: Carbonate Cements. N. Schneidermann and P.M. Harris (eds). Soc. Econ. Palentol. Mineral. Spec. Pub. 36: 241-264.

PURSER, B.M. & SCHROEDER, J.H. 1986. The diagenesis of reefs: A brief review of our present understanding. In: Reef diagenesis. J.H. Schroeder and B.M. Purser (eds). Springer-Verlag, Berlin: 424-446.

RADKE, B.M. & MATHIS, R.L. 1980. On the formation and occurrence of saddle dolomite. Jour. Sed. Petrology 50: 1149-1168.

REEDER, R.J. & PROSKY, J.L. 1986. Compositional sector zoning in dolomite. Jour. Sed. Petrology 56: 237-247.

RICHTER, D.K. & FUCHTBAUER, H. 1978. Ferroan calcite replacement indicates former magnesian calcite skeletons. Sedimentology 25: 843-860.

ROSS, R.J. JAONUSSON, V. & FRIEDMAN, I. 1975. Lithology and origin of Middle Ordovician calcareous mud mound at Mieklejohn Peak, Southern Nevada. US. Geol. Surv. Prof. paper. 871: 48pp.

SANDBERG, P.A. 1983. An oscillating trend in Phanerozoic non-skeletal carbonate mineralogy. Nature 305: 19-22.

1985. Aragonite cements and their occurrence in ancient limestone. In: Carbonate Cements. N. Schneidermann and P.M. Harris (eds). Soc. Econ. Paleontol. Mineral. Spec. Pub. 36: 33-57.

SCHLANGER, S.O. 1964. Petrology of the limestones of Guam. US. Geol. Surv. Prof. Papers, 403-D: 1-52.

& DOUGLAS, R.G. 1974. The pelagic ooze-chalk-limestone transition and its implications for marine stratigraphy. In: Diagnesis of Deep-sea biogenic sediments. G.J. van der Lingen (ed). Benchmark papers in Geology 40: 31-62.

SCHMIDT, V. & McDONALD, D.A. 1979. The role of secondary porosity in the course of sandstone diagenesis. In: Aspects of diagenesis. P.A. Scholle and P.R. Schluger (eds). Soc. Econ. Paleontol. Mineral. Spec. Pub. 26: 175-207.

SCHNEIDERMANN, N. & HARRIS, P.M. (eds). 1985. Carbonate cements. Soc. Econ. Paleontol. Mineral. Spec. Pub. 36, 379pp.

SCHOFIELD, K. & ADAMS, A.E. 1985. Burial dolomitization of the Woo Dale Limestones Formation (Lower Carboniferous) Derbyshire, England. Sedimentology 33: 207-219.

SCHOLLE, P.A. & HALLEY, R.B. 1985. Burial diagenesis: out of sight, out of mind! In: Carbonate Cements. N. Schneidermann and P.M. Harris (eds). Soc. Econ. Paleontol. Mineral. Spec. Pub. 36: 309-334.

SCHROEDER, J.H. 1986. Diagenetic diversity in Paleocene coral knobs from the Bir Abu El-Husein area S. Egypt. In: Reef Diagenesis. J.H. Schroeder and B.H. Purser (eds). Springer-Verlag, Berlin: p132-158.

SCHROEDER, J.H. & PURSER, B.H. (eds). 1986. Reef Diagenesis. Springer-Verlag, Berlin 455pp.

SHACKLETON, N.J. & KENNETT, J.P. 1975. Paleotemperature history of the Cenozoic and the initiation of Antarctic Glaciation: Oxygen and Carbon isotope analyses in DSDP sites 277, 279 and 281. In: Init. Rep. DSDP 29. J.P. Kennet, R.E. Houtz, et al. (eds). US Govt. Printing Office Washington DC: 743-755.

SHIMMIELD, G.B. & PRICE, N.B. 1986. The behaviour of molybdenum and manganese during early sediment diagenesis - offshore Baja California, Mexico. Marine Chemistry 19: 261-280.

SHINN, E.A. 1969. Submarine lithification of Holocene carbonate sediments in the Persian Gulf. Sedimentology 12: 109-144.

SIPPEL, R.F. & GLOVER, E.D. 1965. Structures in carbonate rocks made visible by luminescence petrography. Science 150: 1283-1287.

SJOBERG, E.L. & RICKARD, D.T. 1984. Calcite dissolution kinetics: Surface speciation and the origin of variable pH dependence. Chem. Geology 42: 119-136.

SOMMER, S.E. 1972. Cathodoluminescence of carbonates, 1. Characterization of cathodoluminescence from carbonate solid solutions. Chem. Geology 9: 257-273.

SORBY, H.C. 1879. The structure and origins of limestones. Proc. geol. Soc. London 35: 56-95.

STEINEN, R.P. 1978. On the diagenesis of lime mud: Scanning electron microscopic observations on subsurface material from Barbados, West Indies. Jour. Sed. Petrology 48: 1139-1148.

STONE, R.A. 1972. Waulsortian-type bioherms (Reefs) of Mississippian age, Central Bridger Range Montana. Montana Geol. Soc. 21st Annual Field Conference: 38-55.

STOW, D.A.V. & MILLER, J. 1984. 23. Mineralogy, petrology and diagenesis of sediments at site 530, southest Angola Basin. Init. Rep. Deep Sea Drilling Project 75: US Govt. Printing Office, Washington: 857-873.

SURDAM, R.C., BOESE, S.W. & CROSSLEY, L.J. 1984. The chemistry of secondary porosity. In: Clastic diagenesis. D.A. McDonald and R.C. Surdam (eds). Am. Assoc. Petrol. Geologists Memoir 37: 127-151.

TAYLOR, J.M.C. & ILLING, L.V. 1969. Holocene intertidal calcium carbonate cementation, Qatar, Persian Gulf. Sedimentology 12: 69-107.

TAYLOR, T.F. & SIBLEY, D.F. 1985. Petrographic and geochemical characteristics of dolomite types and the origin of ferroan dolomite in the Trenton Formation, Ordovician, Michigan Basin, USA. Sedimentology 33: 61-86.

ten HAVE, T. & HEIJNEN, W. 1985. Cathodoluminescence activation and zonation in carbonate rocks: an experimental approach. Geologie en Mijnbouw 64: 297-310.

TUCKER, M.E. 1983. Diagenesis geochemistry and origin of a Pre-Cambrian dolomite: The Beck Spring Dolomite of Eastern California. Jour. Sed. Petrology 53: 1097-1119.

TURNER, P., ASHWORTH, J.R. & ISKENDERIAN, F.A. 1982. Authigenic alloite in the Pendleside Formation (Dinantian) of Northern England. Geol. Mag. 119: 395-404.

VAN DER LINGEN, G.J. (ed). Diagenesis of deep sea biogenic sediments. Benchmark papers in geology 40, 385pp.

VAN LAER, P. & MONTY, C.L.V. 1984. The cementation of mud mound cavities by microbial spars. 5ème Congr. europ. Sedimentol., (abs), 30-31.

VEIZER, J. & HOEFS, J. 1976. The nature of O^{18}/O^{16} and C^{13}/C^{12} secular trends in sedimentary carbonate rocks. Geochim. Cosmochim. Acta 40: 1387-1395.

_____ & LEMIEUX, J., JONES, B., GIBLING, M. & SAVELLE, J. 1978. Palaeosalinity and dolomitisation of a Lower Palaeozoic carbonate sequence, Somerset and Prince of Wales Islands, Arctic Canada: Canadian Jour. Earth. Sci. 15: 1448-1461.

VIDETICH, P.E. 1985. Electron microprobe study of Mg distribution in recent Mg calcites and recrystallised equivalents from the Pleistocene and Tertiary. Jour. Sed. Petrology 55: 421-429.

VON GÜMBEL, C.W. 1868. Geognotische beschreibung des ostbayerischen Grenzgebirge. Gotha, 968pp.

WALKDEN, G.M. & BERRY, J.R. 1984a. Natural calcite in cathodoluminescence: crystal growth during diagenesis. Nature 308: 525-527.

____ & ____ 1984b. Syntaxial overgrowths in muddy crinoidal limestones: cathodoluminescence sheds new light on an old problem. Sedimentology 31: 251-267.

WALKER, G. 1985. Mineralogical applications of luminescence techniques. In: Chemical bonding and spectroscopy in mineral chemistry. F.J. Berry and D.J. Vaughan (eds). Chapman & Hall, London, New York, 325pp.

WALLS, R.A., MOUNTJOY, E.W. & FRITZ, P. 1979. Isotoic composition and diagenetic history of carbonate cements in Devonian Golden Spike reef. Alberta, Canada. Geol. Soc. Am. Bull. 90: 963-982.

____ & BURROWES, G. 1985. The role of cementation in the diagenetic history of Devonian reefs, Western Canada. In: Carbonate cements. N. Schneidermann and P.M. Harris (eds). Soc. Econ. Paleontol. Mineral. Spec. Pub. 36: 185-220.

WANLESS, H.R. 1979. Limestone response to stress: Pressure solution and dolomitization. Jour. Sed. Petrology 49: 437-462.

WEBER, J.N. 1964. Trace element composition of dolostones and dolomites and its bearing on the dolomite problem. Geochim. Cosmochim. Acta 28: 1817-1868.

____ 1967. Possible changes in the isotopic composition of the oceanic and atmospheric carbon reservoir over geologic time. Geochim. Cosmochim. Acta 31: 2343-2351.

WELTON, J.E. 1984. SEM Petrology Atlas. Methods in Exploration Series No. 4: Am. Assoc. Petrol. Geologists, (pub) Tulsa Oklahoma,
237pp.

WILSON, J.L. 1975. Carbonate facies in geologic history. Springer-Verlag, New York, 471pp.

WONG, P.K. & OLDERSHAW, A. 1981. Burial cementation in the Devonian, Kaybob Reef complex, Alberta, Canada. Jour. Sed. Petrology 51: 507-520.

WORONICK, R.E. & LAND, L.S. 1985. Late burial diagenesis, Lower Cretaceous Pearsall and Lower Glen Rose Formations, South Texas. In: Carbonate Cements. N. Schneidermann and P.M. Harris (eds). Soc. Econ. Paleontol. Mineral. Spec. Pub. 36: 265-275.

ZANKL, H. 1969. Structural and textural evidence of early lithification in fine grained carbonate rocks. Sedimentology 12: 241-256.

ZENGER, D.H. & DUNHAM, J.B. 1980. An introduction. In: Concepts and models of dolomitization. D.H. Zenger, J.B. Dunham and R.L. Ethington (eds). Soc. Econ. Paleontol. Mineral. Spec. Pub. 28: 1-9.

____, _____ & ETHINGTON R.L. (eds). 1980. Concepts and models of dolomitization. Soc. Econ. Paleontol. Mineral. Spec. Pub. 28, 320pp.

APPENDICES

APPENDIX 1A: COMPOSITION OF DOLOMITE STAGES
DUNNOW - LITTLE DUNNOW BUILDUP
(Mole % carbonate)

STAGE J

	CaCO3	MgCO3	FeCO3	MnCO3
1	55.65	42.66	1.59	0.10
2	55.79	41.90	2.17	0.14
3	54.88	43.27	1.68	0.18
4	58.93	38.25	2.63	0.20
5	59.70	37.33	2.74	0.23

STAGE K

1	54.86	44.91	0.06	0.18
2	56.04	43.77	0.08	0.11
3	61.97	37.86	0.04	0.14
4	60.52	39.28	0.00	0.21
5	60.14	39.60	0.08	0.18
6	58.20	41.50	0.13	0.17
7	60.33	39.02	0.49	0.16
8	63.11	35.99	0.64	0.26
9	59.86	38.85	1.09	0.20

STAGE L

1	55.97	38.54	5.34	0.15
2	56.72	36.89	6.22	0.17
3	57.39	39.01	3.46	0.15
4	60.20	35.00	4.45	0.36
5	55.99	34.99	8.75	0.26
6	53.71	36.95	9.22	0.13
7	56.50	32.37	10.92	0.21
8	60.52	31.75	7.53	0.21

APPENDIX 1B: DOLOMITE COMPOSITION: CRAVEN BASIN WAULSORTIAN BUILDUPS
(Mole % carbonate)

STAGE J: FERROAN DOLOMITE

Sample		CaCO3	MgCO3	FeCO3	MnCO3
DU 22	(1)	55.65	42.66	1.59	0.10
	(2)	55.79	41.90	2.17	0.14
	(3)	54.88	43.27	1.68	0.18
LDU 6	(1)	58.93	38.25	2.63	0.20
	(2)	59.70	37.33	2.74	0.23

STAGE K: NON-FERROAN DOLOMITE

Sample		CaCO3	MgCO3	FeCO3	MnCO3
SU F1	(1)	56.22	42.43	1.23	0.12
	(2)	55.93	43.42	0.51	0.15
SU 11	(1)	64.76	34.93	0.20	0.12
	(2)	56.69	42.45	0.75	0.12
	(3)	55.59	43.28	0.98	0.15
DU 22	(1)	54.86	44.91	0.06	0.18
	(2)	56.04	43.77	0.08	0.11
LDU 6	(1)	61.97	37.86	0.04	0.14
	(2)	60.52	39.27	0.00	0.21
	(3)	60.14	39.60	0.08	0.18
	(4)	58.20	41.50	0.13	0.17
	(5)	60.33	39.02	0.49	0.16
	(6)	63.11	35.99	0.64	0.26
	(7)	59.86	38.85	1.09	0.20

STAGE L: FERROAN DOLOMITE

Sample		CaCO3	MgCO3	FeCO3	MnCO3
CALW 1A	(1)	58.27	35.32	6.26	0.15
	(2)	57.21	36.07	6.59	0.14
	(3)	57.41	32.70	9.60	0.29
	(4)	57.30	32.02	10.52	0.16
	(5)	59.62	33.00	7.30	0.08
	(6)	57.61	33.73	8.50	0.16
	(7)	57.80	33.14	8.80	0.27
	(8)	57.52	32.59	9.83	0.05
	(9)	59.68	34.07	6.25	0.00
	(10)	61.55	34.44	3.90	0.11
	(11)	60.09	32.35	7.56	0.00
	(12)	60.75	31.82	7.32	0.11
	(13)	60.78	30.55	8.52	0.15
	(14)	60.83	30.06	9.07	0.04
	(15)	60.73	30.33	8.78	0.16

STAGE L: Cont.

Sample		CaCO3	MgCO3	FeCO3	MnCO3
	(16)	60.32	30.68	8.86	0.14
	(17)	60.42	31.74	7.72	0.13
	(18)	61.06	33.51	5.35	0.07
	(19)	61.61	34.73	3.57	0.10
	(20)	61.39	35.19	3.38	0.03
	(21)	60.35	32.03	7.50	0.12
	(22)	60.36	32.42	7.13	0.09
	(23)	61.04	29.76	9.17	0.03
	(24)	60.80	30.18	8.89	0.13
	(25)	60.64	29.66	9.54	0.17
	(26)	56.92	26.37	16.37	0.34
SH 50	(1)	54.37	35.82	9.66	0.15
	(2)	54.77	37.94	7.15	0.14
	(3)	56.22	37.00	6.51	0.27
	(4)	55.25	38.41	6.11	0.23
	(5)	54.29	39.16	6.43	0.13
	(6)	56.57	36.62	6.72	0.08
	(7)	55.52	37.17	7.08	0.23
	(8)	54.89	38.27	6.63	0.22
	(9)	55.83	37.08	6.97	0.12
	(10)	55.88	37.03	6.89	0.20
C	(1)	52.84	36.56	10.14	0.46
	(2)	53.01	36.63	9.91	0.45
	(3)	53.43	36.80	9.37	0.41
	(4)	57.35	30.58	11.62	0.46
	(5)	53.13	35.41	11.05	0.40
	(6)	53.61	37.01	8.95	0.43
	(7)	53.21	34.75	11.58	0.46
	(8)	53.16	33.97	12.33	0.54
SU 11	(1)	54.97	42.80	2.11	0.12
	(2)	61.57	36.04	2.03	0.35
DU 22	(1)	55.97	38.54	5.34	0.15
	(2)	56.72	36.89	6.22	0.17
	(3)	57.39	39.01	3.46	0.15
LDU 6	(1)	60.20	35.00	4.45	0.36
	(2)	55.99	34.99	8.75	0.26
	(3)	53.71	36.95	9.22	0.13
	(4)	56.50	32.37	10.92	0.21
	(5)	60.52	31.75	7.53	0.21
CH 30	(1)	54.21	36.24	9.34	0.21
	(2)	54.85	37.08	7.87	0.20
	(3)	54.59	37.40	7.83	0.18

APPENDIX 2

APPDENIDX 2A SAMPLE LOCALITY CODES FROM FIG. 1.1

WAULSORTIAN BUILDUPS

CODE	LOCALITY	GR:	CODE	LOCALITY	GR:
AF	Arbour Farm	620,408	LK	Long Knots	643,468
ASH	Ashnott	793,480	LM	Leagram Quarries	638,448
BP	Bellmanpark Quarry	760,427	NEW	Dobbers Quarry, Newsholme	847,519
C	Coplow Quarry	752,432	NLH	New Laund Hill	651,468
CA	Cow Ark borehole (BGS)	683,465	PW	Porters Wood	660,471
CAL	Old Calamine Mines	642,477	RI	The Ridge	774,432
CC	Clitheroe Castle	743,418	RS	Raven Scar Plantation	669,469
CH	Crow Hill road cut	767,431	SC	Scarnber	938,578
DG	Downham Green	788,449	SF	Crimpton pit, Spire Farm	679,468
Du-LDU	Dunnow-Little Dunnow	702,514	SH	Salthill Quarry	755,426
*F	Fogger	895,553	SP	Springs	804,443
GE	Gerna	788,435	SU	Sugarloaf Quarry	688,508
HA	Hammerton Hall	718,532	TN	Twiston Mill Quarry	808,443
**HC	Haw Crag	914,565	W	Worsaw Hill	776,436
HG	Heaning	687,506	WG	Withgill Quarry	709,410
HN-HOD	Knoll Wood	684,502	WH	Waddow Hall	735,429
IB	Ings Beck	815,448	WW	Hall Hill Qy., Whitewell	667,467
LH	Leach House Quarry	628,412			

PERI-WAULSORTIAN and OTHER FACIES

CODE	LOCALITY	BNGR:SD
CB	Clitheroe By-pass (A59) Chadian stratotype. Partly interbank	775,445
CHQ	Chatburn Quarries, Clitheroe. Chatburn Lst. Fm.	760,440
***LO/C	Raygill Quarry, Lothersdale. Mineralised Embsay Lst., Worston Shales Fm. (Harrison 1982, p24)	942,453
PE	Stream section, Pendle Hill. Holkerian-Namurian	775,408
TP	Townfield Plantation, Slaidburn. Interbank facies	706,526
SL	Interbank Facies near Sugarloaf buildup	675,510
SY	Sykes Quarries. Turbiditic shelf slope carbonates of Gawthorpe (1986)	628,519

* Samples courtesy of Dr J. Miller
** Samples courtesy of Professor A. Lees
*** Samples courtesy of Mr L. Oldham

APPENDIX 2B. DETAILED SAMPLE LOCALITIES AND FACIES.

All samples are thin sections unless otherwise stated.

WAULSORTIAN BUILDUPS.

Arbour Farm Quarry (AF).
Abandoned quarry 4 km NE of Longridge, Lancs. BNGR:SD 620,408.
Samples:AF 1-4, AFX 1-2; Bank facies cut by neptunian dykes.

Ashnott (ASH).
Scattered hillside outcrops and old workings 2.8km S of Newton, Lancs. BNGR:SD 793,480.
Samples: ASH 1-6; Bank facies. Some sheet spars.

Bellmanpark Quarry (BP).
Recently abandoned quarry 1.8km NE of castle, Clitheroe, Lancs. BNGR:SD 760,427.
Samples:
BP1-16; Bank Facies, including cavernous void-fill sediment and spar, some of which contains crustiform iron sulphides.
BP60; Mineralised slickenside material from fault zone. Contains fluorite.
BP17; Biosparite facies. Cap Beds Lithology.

Coplow Quarry (C,CX).
Abandoned quarry now used as tip by Ribblesdale Cement Co. from whom access must be granted. (Parts are S.S.S.I.). Quarry, 1km NE of town centre, Clitheroe, Lancs. BNGR:SD 752,432.
Samples:
C21-28; Bank facies.
C30-33; Lateral facies transition. Bank to crinoidal packstones from a small isolated buildup (1.5m x 0.5m) at the quarry entrance.
CX2-CX7; Vertical transition through sub-bank, peri-Waulsortian (CX2-4) to bank facies (CX5-7). Sample CX5 contains the boundary between bank and sub-bank facies (Fig. 1.4).
C40; Sub-Waulsortian facies from northern face of the quarry.
C50-55; Samples of veinlets running parallel to axial planes of fold sets in the northern face of the quarry. Stained peels only.

Cow Ark borehole No. 9, (CA) British Geological Survey, Edinburgh.
Only two thin sections were cut from this borehole material. BNGR:SD 6832,4647.
Samples:
CA1; Mineralised bank facies including galena and ferroan dolomite.
CA2; Bank facies. Cavity with dolomitised internal sediment.
Several stained peels were taken from veinlet and cavity-fill sequences throughout the bank facies.

Old Calamine Mines (CAL, CALW).
Abandoned workings near Dinkling Green, 2km NW of Whitewell, Lancs. BNGR:SD 642,477.
Samples:
CALW1-5; Small working at the western end of the low ridge which is an extension of Long Knots (see below) and is cut by the road leading to Whitmore Farm. Samples include bank facies and crinoidal packstone flank facies.
CAL10-18; Main calamine working. Samples of bank facies which are heavily dolomitised and subsequently calcitised in parts, adjacent to a fault plane which cuts through the working.

Clitheroe Castle (CC).
Town centre, Clitheroe, Lancs. Castle is built on a Waulsortian buildup BNGR:SD 743,418.
Samples: CC1, 2; Bank facies.

Crow Hill (CH).
Road cut on A59 and scattered hillside exposures, 1km S of Chatburn, Lancs. BNGR:SD 767,431.
Samples:
CH30, 40, 42-45 Bank facies.
CH31, 33 Neptunian dyke sediments.

Downham Green (DG).
Small knoll-shaped buildups, 0.75km NNE of the village of Downham, Lancs. BNGR:SD 788,449.
Samples:
DG5, 6 Bank facies.
DG4 Fibre veinlets cut calcitised dolomite in bank facies.

Dunnow (Great Dunnow) (Du).
Abandoned quarry 1.5km SW of Slaidburn, Lancs BNGR:SD 702,514.
Samples:
Du1-5, 20-22; Bank facies.
Du24-26; Facies transition from toe to bank core.
Du27,28; Crinoidal packstone layer 10cm thick which separates a lower buildup in the main quarry face from an overlying buildup in the small working behind the main quarry.
Du29 & Du30; From upper buildup, bank facies.

Little Dunnow (LDu).
Stream section 1.2km SW of Slaidburn, Lancs., along Dunnow Syke, and scattered outcrops across the hillside towards Bluebutts Farm on the B6478. BNGR:SD 705,516.
Samples:
LDu1-3; Bank facies.
LDu4, 5, 7; Interbank facies.
LDu6; Bank facies with dolomite cements, Stages J-L.

Gerna (GE).
Scattered outcrops over a small knoll-form buildup; 1km SE of Downham, Lancs. BNGR:SD 788,435. Of 20 samples thin sections of 7 were prepared (GE1,3,5,13,17,19,20) stained peels were examined from the remaining. Samples comprised toe and bank facies.

Hammerton Hall (HA).
Scattered field exposures east of track leading to Hammerton Hall BNGR:SD 718,532.
Samples:
HA1; Crinoidal Flank facies.
HA3; Mineralised flank near galena/silica vein.
HA4; Bank facies.

Hall Hill (WW).
Quarry, 1km E of Whitewell, Bowland, Lancs. BNGR:SD 667,467.
Samples:
WW1,17, 3,2,5-8; Vertical section through bank facies.
WW17; Sub-Waulsortian dune bedforms.
WW10,12,11,13; Lateral transition along bank bed increasing in thickness towards WW13.
WW14-16, 18-20; Bank facies.
WW31; Mineralised veinlet in bank facies containing silica, sphalerite and late ferroan calcite.

Heaning (HG).
Scattered field outcrops and abandoned quarries in a 2sq km area W of the hamlet of Heaning, 1km W of Newton-in-Bowland, Lancs BNGR:SD 687,506.
Samples:
HG 1-5; Interbank facies.
HG 6-9; Toe to bank facies.
HG10-14; Bank facies in the vicinity of water valve house (BNGR:SD 6895,5029).
HG15-17; Flank-interbank facies.
HG18-22; Bank and interbank facies (BNGR:SD 6902,5034).

Haw Crag (HC).
Natural exposures on hilltop 2km NW of Gargrave, N. Yorks. BNGR:SD 914,565. Seven half-stained thin sections supplied by Professor A Lees.

Ings Beck (IB).
Old mineral workings and natural exposures. Ings Beck was the ancient border between the Geordie kingdom of Northumbria and the heathen hoardes to the south, 3km E of Downham, Lancs. BNGR:SD 815,448.
Samples:
IB 1,2 & IBFI-F6; Bank facies.
IB7, F8; Interbank facies.
IB20-24;Interbank facies of Chatburn Limestone Formation from a small abandoned limestone quarry at the same locality.

Knoll Wood (HN, HOD).
Quarry 1km WSW of Newton-in-Bowland, Lancs. BNGR:SD 684,502 (Samples HN). Also, outcrops in River Hodder and small disused working on the south bank (Sample HOD).
Samples:
HN20, 23, 300; Bank facies. Waulsortian Phase D characteristic.
HOD 1; Bank facies.
Supplemented by stained peels of 15 bank facies samples with thin sections and hand specimens collected by Dr J Miller.

Leach House (LH).
Abandoned quarry at Leach House hamlet, 4.5km NE of Longridge, Lancs. BNGR:SD 628,412.
Samples:LH1,LH2. Bank facies.

Long Knots (LK).
Roadside exposure on a ridge-form which connects the Old Calamine mines (CAL) with the buildup complex of New Laund Hill (NLH, see below), 1.3km W of Whitewell, Lancs. BNGR:SD 643,468.
Samples: LK1-4; Bank facies.

Leagram (LM).
Large abandoned quarry. 1.2km NE of Leagram Hall, and 3km SE of Whitewell, Lancs. BNGR:SD 638,448.
Samples:
LM 1-9; Bank facies.
LM10, 11; Neptunian dyke sediments.

Newsholme (NEW).
Dobbers quarry (abandoned), on A682, 0.6km NE of Newsholme, Lancs. BNGR:SD 847,519.
Samples:
NEW 1, 2; Bank facies rich in fenestellid bryozoans.
NEW 7, 4-6; Toe-Bank transition.
NEW 8; Sub-Waulsortian bituminous shales.

New Laund Hill (NLH).
Natural exposures over 1sq km area of a large buildup complex, 0.6km W of Whitewell, Lancs. BNGR:SD 651,468.
Samples:
NLH 1, 2, 12-22; Bank facies.
NLH 3; Peloidal neptunian dyke-fill.

Porters Wood (PW).
Exposure in woods, 0.2km NE of Whitewell, Lancs. BNGR:SD 660,471.
Samples:
PW 1-3, 5; Bank facies containing microscopic neptunian fractures.
PW 4; Toe-flank facies.

The Ridge (RI).
Small abandoned quarry and natural exposures. An extension of the Crow Hill complex. West of A59, 0.9km SE of Chatburn, Lancs. BNGR:SD 774,432.
Samples: RI 1-5; Bank facies.

Raven Scar Plantation (RS).
Abandoned quarry and stream eexposures in a small plantation, NW of the road to Hall Hill, 1km E of Whitewell, Lancs. BNGR:SD 669,469.
Samples:
RS1, 2; Sub-Waulsortian shale and bitumenous, crinoidal limestone.
RS 3-7; Bank facies.
RS 8; Post-Waulsortian calcareous shale.

Scarnber (SC).
Abandoned workings, 3.3km NNE of Gargarave, N. Yorks. BNGR:SD 938,578.
Samples:
SC1, 2; Bank facies.
SC3; Interbank facies.
SC4; Toe-bank facies.

Spire Farm (SF).
Crimpton Pit, abandoned working near Spire Farm. On the Cow Ark to Newton road, 2km ESE of Whitewell, Lancs. BNGR:SD 679,468.
Samples: SF1-3; Bank facies.

Salthill (SH).
Abandoned Quarry, now an industrial estate, 1.5km NE of castle, Clitheroe, Lancs. BNGR:SD 755,426.
Samples:
SH4,30,35,37,50 SHF11; Bank facies.
SH1-3, 38, 44; Toe/Flank facies.
SHX 1-4; Vertical sequence through a small isolated buildup in the NW of the quarry from sub-Waulsortian to bank facies.
SH45; Neptunian dyke sediment (float).

Springs (SP).
Roadside outcrop 2km E of Downham, Lancs. BNGR:SD 804,443.
Sample: SP1; Bank facies.

Sugarloaf (Su).
Quarry in Knot or Sugarloaf Hill, 1km NNE of Dunsop Bridge, Bowland, Lancs. BNGR:SD 666,508.
Samples:
Su 1-9; Lateral transition from toe to bank facies.
Su 11, 15-17, F1; Bank facies.

Twiston (TN).
Twiston Mill Quarry (abandoned), 0.7km NNW of Twiston, Lancs. and 2.5km E of Downham, Lancs.
Samples: TN 1-4; Bank facies.

Worsaw Hill (W).
Natural exposure on large buildup complex, 1km SW of Downham, Lancs. BNGR:SD 776,436.
Sample: WX1; Bank facies.

Withgill (WG).
Abandoned mineral workings, 3.5km WSW of Clitheroe, Lancs. BNGR:SD 709,410.
Samples:
WG3, 6, 7; Bank facies.
WG2; Toe facies.
WG4, 5; Flank/Interbank facies.
WG8, 10-12; Mineralised bank-flank facies.

Waddow Hall (WH).
Natural exposures in the grounds of Waddow Hall (now a Girl Guide camp; permission must be acquired from the Hall. The word 'exposure' should be used with great care). On B6478, 1.3km NW of Clitheroe, Lancs BNGR:SD 735,429.
Samples:
WH1-3,10-12,14-17,19,WHF; Bank facies.
WH6, 20, 21; Interbank facies.

PERI-WAULSORTIAN and other facies.

Clitheroe by-pass (CB).
Road cut on A59, 0.5km NE of Chatburn, Lancs. Chadian stratotype. BNGR:SD 775,445.
Samples: CB1-5; Chatburn Limestone Formation. Bituminous, argillaceous limestones.

Chatburn Quarries (CHQ).
Working quarries (Ribblesdale Cement Company), Horrocksford, 1.5km NNW of the castle, Clitheroe, Lancs. BNGR:SD 760, 440.
Samples: CHQ-1.3;Chatburn Limestone Formation, argillaceous limestones and veins associated with the Horrocksford Hall thrust.

Raygill Quarry (LO/C).
Old mineral workings, 2km WSW of Lothersdale, N. Yorks, and 20km ENE of Clitheroe, Lancs. BNGR:SD 942,453.
Samples LO/C 1-3; Mineralised Embsay Lst, Worston Shales Fm. Calcite/sphalerite veins, provided by Mr L. Oldham.

Pendle Hill (PE)
Stream section through Holkerian-Namurian sediments on Pendle Hill, 3.5km ESE of Clitheroe, Lancs. BNGR:SD 775,408.
Samples:
PE1; Pendle Grit.
PE 2, 3, 4; Bowland Shales.
PE 5-7; Pendleside Limestone.

Townfield Plantation. (TP in Fig. 1.1, Samples: Misc.)
Abandoned quarry in small plantation,0.6km W of Slaidburn, Lancs. BNGR:SD 706,526.
Samples: Misc 5-7; Interbank facies.

Sugarloaf interbank facies (SL).
Natural exposures east of Sugarloaf buildup, 2km NE of Dunsop Bridge, Bowland, Lancs. BNGR:SD 675,510.
Samples:SL 1-3; Interbank facies.

Sykes Quarries (SY).
Abandoned quarries and old mineral workings. Trough of Bowland, 3.5km NW of Dunsop bridge, Bowland, Lancs. BNGR:SD 628,519.
Samples: SY 1-4; Turbiditic shelf slope carbonates, late Chadian-Arundian. (see Gawthrope, 1986).